



UNIVERSIDAD DE MÁLAGA

Tesis Doctoral

**DESARROLLO DE NUEVOS MODELOS
PARA LA FOTOVOLTAICA INTEGRADA EN
EDIFICIOS (BIPV) EN CIUDADES
SOSTENIBLES**

Luis Fernando Mulcué Nieto

Málaga, junio de 2020



UNIVERSIDAD
DE MÁLAGA

ANDALUCIA TECH
Campus de Excelencia Internacional

Escuela de Doctorado

DECLARACIÓN DE AUTORÍA Y ORIGINALIDAD DE LA TESIS PRESENTADA PARA OBTENER EL TÍTULO DE DOCTOR

D./Dña LUIS FERNANDO MULCUE NIETO

Estudiante del programa de doctorado INGENIERÍA MECÁNICA Y EFICIENCIA ENERGÉTICA de la Universidad de Málaga, autor/a de la tesis, presentada para la obtención del título de doctor por la Universidad de Málaga, titulada: "DESARROLLO DE NUEVOS MODELOS PARA LA FOTOVOLTAICA INTEGRADA EN EDIFICIOS (BIPV) EN CIUDADES SOSTENIBLES"

Realizada bajo la tutorización de MARIANO SIDRACH DE CARDONA y dirección de LLANOS MORA LÓPEZ (si tuviera varios directores deberá hacer constar el nombre de todos)

DECLARO QUE:

La tesis presentada es una obra original que no infringe los derechos de propiedad intelectual ni los derechos de propiedad industrial u otros, conforme al ordenamiento jurídico vigente (Real Decreto Legislativo 1/1996, de 12 de abril, por el que se aprueba el texto refundido de la Ley de Propiedad Intelectual, regularizando, aclarando y armonizando las disposiciones legales vigentes sobre la materia), modificado por la Ley 2/2019, de 1 de marzo.

Igualmente asumo, ante a la Universidad de Málaga y ante cualquier otra instancia, la responsabilidad que pudiera derivarse en caso de plagio de contenidos en la tesis presentada, conforme al ordenamiento jurídico vigente.

En Málaga, a 5 de JUNIO de 2020

Fdo.: *Luis Fernando Mulcue Nieto*

UNIVERSIDAD DE MÁLAGA

Departamento de Lenguajes y Ciencias de la Computación

Tesis Doctoral

DESARROLLO DE NUEVOS MODELOS PARA LA FOTOVOLTAICA INTEGRADA EN EDIFICIOS (BIPV) EN CIUDADES SOSTENIBLES

Autor:

LUIS FERNANDO MULCUÉ NIETO

Directora:

Dr. LLANOS MORA LÓPEZ

Tesis doctoral presentada en la
ESCUELA DE INGENIERÍAS INDUSTRIALES
de la
UNIVERSIDAD DE MÁLAGA
para la obtención del Grado de Doctor

Málaga, junio de 2020

D. Llanos Mora López, Catedrática del Dpto. de Lenguajes y Ciencias de la Computación, de la Universidad de Málaga, como Directora de la Tesis Doctoral.

"DESARROLLO DE NUEVOS MODELOS PARA LA FOTOVOLTAICA INTEGRADA EN EDIFICIOS (BIPV) EN CIUDADES SOSTENIBLES"

Presentada por D. Luis Fernando Mulcué Nieto en la ESCUELA DE INGENIERÍAS INDUSTRIALES de la UNIVERSIDAD DE MÁLAGA para la obtención del Grado de Doctor

Hace constar que dicha tesis queda avalada por los siguientes artículos de investigación:

1. "A novel methodology for the pre-classification of façades usable for the decisión of installation of integrated PV in Buildings: The case for equatorial countries".

Luis Fernando Mulcué-Nieto, Llanos Mora-López.

REVISTA: Energy, Volume 141, December 2017, Pages 2264-2276.

EDITORIAL: Elsevier.

FACTOR DE IMPACTO: 5.5

2. "Methodology to establish the permitted maximum losses due to shading and orientation in photovoltaic applications in buildings".

Luis Fernando Mulcué-Nieto, Llanos Mora-López.

REVISTA: Applied Energy, Volume 137, 1 January 2015, Pages 37-45.

EDITORIAL: Elsevier.

FACTOR DE IMPACTO: 8.4

3. "A new model to predict the energy generated by a photovoltaic system connected to the grid in low latitude countries".

Luis Fernando Mulcué-Nieto, Llanos Mora-López.

REVISTA: Solar Energy, Volume 107, September 2014, Pages 423-442.

EDITORIAL: Elsevier.

FACTOR DE IMPACTO: 4.7

En Málaga, a 6 de Febrero de 2020

Fdo: Llanos Mora López

Directora

*En honor al que era, el que es, y el que ha de venir,
el Señor Dios Todopoderoso.*

Resumen

La Integración Fotovoltaica en Edificios, más conocida como *Building Integrated Photovoltaics* (BIPV), consiste en reemplazar elementos constructivos como cubiertas, fachadas, ventanas, entre otros, por módulos solares fotovoltaicos. Su implementación a medio plazo es de vital importancia para garantizar la construcción de “Edificios de Energía Cero” (Zero Energy Buildings). Para permitir tal desarrollo, resulta vital promover la investigación en técnicas, modelos y estimación del recurso solar disponible. Por otra parte, a nivel mundial todavía es muy incipiente la regulación técnica que orientada hacia la optimización del rendimiento energético en BIPV. En este trabajo de investigación se crearon nuevos modelos, herramientas y propuestas de normas técnicas para ser implementadas en proyectos que involucren BIPV en ciudades sostenibles.

En la primera parte, se aborda la predicción de la energía generada por un sistema de BIPV. Como resultado de la investigación se desarrolló y validó una nueva expresión matemática, que puede ser usada en países ubicados en latitudes menores a 20 grados. Esto se logró mediante un análisis exhaustivo en diversas ciudades, de las pérdidas angulares, pérdidas por polvo, las pérdidas por temperatura, y las pérdidas de conversión DC-AC. El modelo obtenido permite estimar el Performance Ratio (PR) contando únicamente con 4 valores de entrada: La temperatura ambiente promedio de la localidad, la latitud, la inclinación, y la orientación del plano del módulo fotovoltaico. La ecuación tiene un alto grado de precisión, confina más de 40 ecuaciones en una sola, y su resultado es equivalente a realizar una simulación compleja, mediante un procesamiento computacional que implica más de 20.000 cálculos.

En la segunda parte se propuso una metodología para formular normas técnicas internacionales para la BIPV. El objetivo de esta normativa es establecer valores máximos permitidos para las pérdidas por sombreado y orientación en proyectos de BIPV, tomando como punto de partida a España. Así mismo, se realizó el caso de estudio para ciudades de Colombia, mediante un análisis comparativo.

Finalmente, se propone una metodología para la pre-clasificación de fachadas en edificios potencialmente útiles para usarlas en BIPV. Esta metodología se basa en la cantidad de radiación solar que incide anualmente sobre la superficie. Así mismo, se propone la asociación a un sistema de código de colores similar al usado en eficiencia energética de equipos, según el sistema de letras A-G. Mediante la integración de los modelos encontrados se propuso un procedimiento a usar como paso inicial en el proceso de diseño y dimensionado de proyectos BIPV, antes de calcular el potencial completo. Por lo tanto, facilitará el trabajo de arquitectos e ingenieros en ciudades sostenibles.

Abstract

Solar Photovoltaic Integration in Buildings, better known as Building Integrated Photovoltaics (BIPV), consists of replacing construction elements such as roofs, facades, windows, among others, with solar photovoltaic modules. Its medium-term implementation is of vital importance to ensure that all new constructions are "Zero Energy Buildings" (ZEB) [1]. Because of this, it is a growing reality worldwide, and its development involves the implementation of techniques, models and estimation of the available solar resource. On the other hand, few countries have technical regulations that allow optimizing performance and energy efficiency in photovoltaic integration in buildings. In this research work, new models, tools and proposals of technical standards were created that can be used for the development of the BIPV in sustainable cities.

This work it is divided in 3 parts. The first one concerns the prediction of the energy that a BIPV system can produce. The problem of calculating the electricity produced by a BIPV system is mainly reduced to determining its Performance Ratio value, PR. This is not trivial as the performance of a PV system depends on several factors such as the solar irradiation available in the geographical location of the facility, the weather, the orientation and tilt of the used surfaces, the appropriate design of the system and the quality of the components, among others. In order to solve this problem, different methods have been proposed to predict the influence of the different variables on the amount of the generated electricity. Some of them are analytical; for example, the methods proposed by Osterwald in 1986 [2], Araujo in 1982 [3], and Green in 1998 [4]; all of them allow us to estimate the temperature. Other procedures that include more variables have likewise been proposed, most of them are based on the use of artificial neuronal networks [5][6]. However, the majority of them are very complicated to be implemented, while others do not take into account the specific characteristics of the system. Another way that has been proposed to solve the aforementioned problem is to use a standard performance value of PR equal to 0.75 for any photovoltaic system [7], which is not appropriate as the specific variables of the place must be taken into account. For example, studies of PR in 8 countries have been reported, obtaining values that range between 0.42 and 0.81 [8]. This is coherent, as the performance of the photovoltaic modules depends on the ambient temperature of the place of the facility. Latitude likewise plays an important role, because of its effect on solar irradiation, which means that the power supplied to the entrance of the inverter may be very low within certain time periods reducing the DC-AC conversion efficiency.

Another important factor that prevents the use of a generalized PR for BIPV applications are the energy losses caused by the tilt and orientation of the generator plane. Their origin lies in the fact that sun light is reflected more when the angle of

incidence is small with respect to the surface. The losses due to dust and dirt also depend on this variable. Thus, the PR is expected to vary for a single building, due to the large amount of surfaces available to be used on roofs and frontages. According to what has been discussed, the large number of factors present makes it very difficult to forecast the performance of a photovoltaic facility. Therefore, it would be suitable to have a simple method that could be used by architects and engineers. This is very important as many countries need to expand photovoltaic solar energy. In Colombia, for example, non-grid connected areas, that is, places that are not connected to power grid by means of the Sistema de Interconexión Nacional (Colombian power grid) account for nearly 52% of national territory [9]. Furthermore, it is recommended to implement BIPV within the cities in order to obtain economic and environmental benefits.

In the first part of this research, the topic of the prediction of the energy generated by a photovoltaic system in BIPV is discussed. Therefore a new simple and reliable mathematical expression was developed, which can be used in low-latitude countries. This was achieved by a thorough analysis in different cities of angular and dirt losses, temperature losses, and DC-AC conversion losses. The obtained model allows estimating the Performance Ratio (PR) with only 4 input parameters: the average ambient temperature of the city, latitude, and the tilt and orientation angles of the plane of the photovoltaic generator. The equation has a high degree of precision, confines more than 40 equations into one, and its result is equivalent to performing a complex simulation using a computer algorithm that performed more than 20,000 operations. The following procedure is proposed to establish this simple expression of the PR for low latitude countries, even though it may be used to extend the model to other world regions, assigning the adjustment parameters appropriately to the results.

The amount of annual average irradiation that a surface receives according to its tilt and azimuth was first calculated. The method used to calculate the annual solar irradiation on tilted surfaces is described in detail below. Only the global solar irradiation on a horizontal surface, $G_{dm}(0)$, in 12 monthly average daily values, is initially known. Taking those as the baseline, each value was decomposed into diffuse $D_{dm}(0)$ and direct radiation $B_{dm}(0)$. The fact described by Liu and Jordan was here taken into account [10], according to which the relation between the clearness index K_{Tm} and the diffuse fraction of solar radiation K_{Dm} is independent on the latitude. The equation proposed by Page [11], and valid for latitudes between 40°N and 40°S, was taken to include the dependency on those parameters. Once the daily components of global radiation, $D_{dm}(0)$ and $B_{dm}(0)$, were obtained, their respective hourly values, $D_h(0)$ and $B_h(0)$ were calculated. This has been done by using the expressions proposed by Collares - Pereira & Rabl [12]. The following set was to calculate the hourly global irradiation on the surface of the generator $G_h(\beta,\alpha)$. Then it was used the three-component model, which has proven to be quite accurate [13], and establishes that the incident radiation is made up of direct $B_h(\beta,\alpha)$, diffuse $D_h(\beta,\alpha)$, and reflected $R_h(\beta,\alpha)$ radiation. There are more than 20 models in the literature to calculate the diffuse component on the tilted surface. The Hay-Davies isotropic model was selected,

as it stands out in different comparative studies for its high accuracy and simplicity [14][15][16][17]. In this, the diffuse radiation composed by two parts is considered; a circumsolar component $D_c(\beta, \alpha)$ that comes directly from the sun, and another isotropic component $D_i(\beta, \alpha)$ from the whole celestial semi-sphere. Both components have a statistical weighting according to the anisotropy index k_1 . To calculate the reflected component, or albedo, it was assumed that the ground is horizontal and infinite in extension, and it reflects the light isotopically. Finally, the hourly components of the hourly global irradiation were added in order to obtain the monthly daily average on a tilted surface. The annual average daily value $G_{da}(\beta, \alpha)$ was approximately equal to the mean of the monthly daily average values.

The angular losses and losses due to dirt were then calculated. With the corrected irradiance amount and the ambient temperature, the input power at each photovoltaic module was calculated [18], thus establishing the temperature losses. The losses in the inverter were then calculated using the equation of its performance characteristic curve [19]. The other types of losses were taken to be equal to the usual values [20]. Contour diagrams of the PR were then built according to the tilt and orientation of the generator. Each city has a different contour map, characterized by its average ambient temperature and its latitude. Therefore, it would be necessary to use the long procedure described every time the performance of a facility has to be calculated. In fact, the above is not technically viable for every photovoltaic project. This is the reason why many designers have decided to design with a "standard value" of PR equal to 0.75 when they want to predict the energy produced. Nevertheless, as already mentioned above, the PR values obtained may vary according to the city and the type of surface, so that using this practice could result in an error of over 45 % when calculating the annual electricity, in the worst case. Finally, a careful analysis of them was performed, and as result of this, we have proposed a simple equation that enables similar results to those obtained by means of the process set out in the above paragraph.

The objective of the research carried out was to find an equation that adjusted the selected contour maps. For this, we have observed that for a single PR, the point curve approximately describes a sum of two Gaussian functions. The scope and breadth of such functions varies with the latitude of the place. Furthermore, the values obtained for the PR of each level curve are characteristics of the average temperature of the place. In accordance with this, we propose the model to calculate the PR. Mathematical procedure used to obtain the model is described below.

The contour diagrams can be displayed as a level curve of a function $PR = f(\beta, \alpha, Ta, \varphi)$, depending on the tilt, azimuth, average temperature of the city, and the latitude. This fact has been taken into account to obtain the model. In particular, for a city, set the latitude and temperature, the relationship is $PR_{city} = f(\beta, \alpha)$. Thus, the i th level curve, $PR_{city} = \text{constant}$, is a sum of two Gaussian functions (because the slope of the curves for $\alpha = -180^\circ$ and $\alpha = 180^\circ$ is nearly horizontal, that means rapid exponential decay characteristic of this type of function).

The PR values range between 0.51 and 0.65. In total, the variation interval was greater than 20%, while it can be up to 15% for each city. These results disagree with the usual practice to always assign a single “standard” PR value to different location or types of surfaces. The results obtained in the model correspond to an average GCPS on fixed surfaces. However, it is possible to obtain higher PR values if it is assumed that the system is very well designed. The values of an “average” system should be used to calculate the annual energy produced in the location.

In order to evaluate the degree of accuracy of the PR model, two graphs were constructed. These graphs shows two PR contour diagrams, one was produced using the long and tedious described process, which uses over 40 equations, in a computer algorithm that performed over 20,000 operations, and the other was calculated using the proposed equation. The error made was below 1%. This error increases slightly with the temperature and latitude. For example, for Tegucigalpa–Guatemala ($\varphi = 14.1^\circ$); the error in the majority of the points is 3% or less. These results point out the excellent degree of accuracy of the proposed model, despite its simplicity.

Other significant result was a model to predict the temperature losses of a photovoltaic system, in function of the average temperature of the place. In order to check the validity of this expression in other countries different to the equatorial ones, the losses were calculated for tilts near to the optimum one. The results where compared to those obtained for more than 200 monitored real photovoltaic systems in Japan [21], Ireland [22] and Indonesia [23]. The obtained values are consistent with those reported for photovoltaic systems installed in homes. Therefore, the expression for temperature losses has universal validity. However, it is important to point out that these losses may be greater in the case of BIPV, if an appropriate ventilation of the modules is not taken into account in the final design.

In the second part of this work, a methodology to establish international technical standards for the BIPV is proposed. The objective of this regulation is to limit the losses due to shading and orientation of the construction surfaces, taking as reference the country of Spain. The case study is also carried out for Colombia, making a comparative analysis for different cities. In 1998, the International Electrotechnical Commission (IEC) published the IEC 61724 International Standard [24]. The annual energy produced for Photovoltaic Applications Connected to the Electricity Grid according this standard can be estimated using an equation. That relation includes the annual solar irradiance on the surface, taking into account the losses due to shading. In order to calculate this magnitude, it should be included both Irradiation Factor FI and the Shading factor FS, that limits the final energy in the field of the BIPV. However the IEC 61724 document does not refer to them and does not propose allowed limits. This is understandable as the solar resource is different in each region. Consequently, it is necessary to formulate criteria within each country. This part of the research proposes a simple methodology to carry that out.

The following procedure was proposed to establish the loss limits due to orientation and shading. It is valid for any country. As a convention, every city of the country to be studied (Colombia, as example) was named as "Place 2". "Place 1" refers to the benchmark country, in our proposal it is Spain (This country was taken as reference because it has a legislation that limit the losses for BIPV). The amount of annual average radiation that a surface receives according to its tilt and azimuth was first calculated. The maximum incident amount in Place 2 was then compared to the worst frontage in Place 1. The loss limit percentage due to orientation and tilt per city was thus obtained. This criterion is highly useful:

- a. The limits are not established universally, taking into account that the solar resource is different in each region. This fact is important as equal global irradiation percentages may correspond to very different solar irradiance values on the surfaces.
- b. The fact that the amount of solar energy received per square meter is aligned shows that the countries that receive greater annual radiation have a greater variety of architectural integration opportunities.

In contrast, if a universal percentage is adopted, no frontage could be used for BIPV in equatorial countries (taking Spain as the benchmark).

- c. It is more beneficial from the environmental and economic point of view. This is due to the fact that replacing construction materials with photovoltaic modules is more beneficial in countries with a high level of annual irradiance.

Taking the above into account, the diffuse fraction of the main cities of Spain was then calculated. The average value of the above parameter representing the country was then established, with the remaining fraction being direct radiation. This value was compared with the maximum stipulated according to the benchmark tables published by the CTE [25]. It was also necessary to estimate the maximum annual solar irradiance $G_a(\beta_{opt})$ (Place 2) and minimum amount of annual solar $G_{a,MIN}(90,0)$ that a frontage can receive (Place 1). For obtaining the first value, we propose to repeat the procedure set out by increasing the tilt angle β from 0° to 90° , taking $\Delta\beta = 1^\circ$ as the increase in each step and using azimuth equal to 0° for positive latitudes, and equal to 180° for negative latitudes (the generator is facing south). According to the CTE, the losses from orientation and tilt on any surface for BIPV cannot exceed 40% for fully integrated systems. This surface was named the worst permissible frontage. Then, this frontage was "transferred" to Place 2. To establish the maximum loss percentage on each surface, the benchmark of 100% was first established, that is, the maximum annual solar irradiance $G_a(\beta_{opt})$.

On the other hand, the fact that diffuse fraction is different in Place 1 (Spain) was taken into account when establishing losses from shading limits in Place 2 (Colombia). Thus, the loss limit percentage was equivalent to a fraction of maximum irradiance that can be physically lost from shading. The main idea consists of equaling that fraction for both places. For example, if a third of the maximum possible radiation could be lost in Spain, that same fraction would be kept in Colombia. Therefore, it was used an absolute variable to compare these two places. Finally, the benchmark tables were established for each city, which will be used as input for future regulations in Colombia. It was then supposed that there is a standard in the

benchmark country with maximum limits for losses from shading $L_{shading,MAX,1}$. In Spain, the CTE sets the limit at 20 % for BIPV. To transfer the equivalent of this percentage to Colombia, the equivalent fraction of this 20% was calculated, with respect to the permanent shading situation. In such a hypothetical case, the radiation no longer received would be equal to the direct radiation $B_a(0)$, plus the circumsolar diffuse radiation $D_{ac}(0)$; both measured on a horizontal surface.

Data used for this part the study have been obtained from RETScreen International [26], which is funded by Natural Resources Canada. This database is supported by 6700 land weather stations and by NASA satellites, which cover the whole of the planet's surface. Solar global radiation data have been obtained for 20 cities in Colombia. Moreover, data from the Atlas de Radiación Solar en España (Solar Radiation in Spain Atlas) [27], published by the Spanish State Meteorology Agency were used [28]. The diffuse fraction of the main cities of Spain and of cities of Colombia was calculated according to the proposed method.

As regards the loss limits due to shading, the limits in Colombia were lower than those allowed for Spain. This is due to the fact that Colombia has a greater diffuse radiation fraction than the European country. This is coherent when comparing the amount of irradiance that can be lost due to shading, that is, the sum of the circumsolar diffuse and direct components. This figure was lower in Colombia than in Spain, with 67% and 84%, respectively. In case of establishing a single loss limit percentage due to shading for the whole Colombia, this should be equal to 16%. In order to unify world criteria for BIPV, it would be very interesting to use this methodology in emerging countries within the field of photovoltaic solar energy. Furthermore, a different benchmark to Spain could be taken.

Finally, a methodology for the pre-classification of facades that are potentially useful for BIPV in buildings is proposed. This methodology is based on the amount of annual solar irradiation on the surface. Likewise, it is associated with a color code system similar to that used in equipment energy efficiency, according to the A-G letter system.

There are several studies to calculate the photovoltaic potential in broad area ranges. However, they do not allow the BIPV potential of a specific façade to be assessed easily and quickly, without using sophisticated software. To solve this problem we propose a new methodology for the pre-classification of façades, based on simple mathematical equations and data. That tool would facilitate the design work for architects and engineers. This initial estimation would be applied previously to the complete calculation of the solar potential in a façade of a building, and it does not include the urban form and shading factors. The main advantage of the proposal that is made in this work regarding previous works is the facility to pre-classify façades without the need to use complex software. Thus, the use of the proposed methodology will allow us to obtain this pre-classification in a very simple way. In addition, the fact of having both a simple mathematical expression and the proposed

methodology will contribute to the easy divulgation of concepts in BIPV at university level.

This research uses the irradiation factor in order to pre-classify the BIPV façades. A new model and the “Energetic Efficiency Rating” for facades are also proposed, which can be used for countries near to the earth's equator (between 15° S and 15°N). These user-friendly tools are very valuable for architects and engineers working on projects. In summary, pre-classification of facades in BIPV has several potential advantages. First, it allows architects and engineers to quickly assess possible energy efficiency in each facade. Therefore, it is possible to do rapid estimates of the incident solar irradiation, as well as the possible electricity produced by each surface. Second, it facilitates analyzing and optimizing the possible orientations of the building. Third, it helps the process of deciding which façades to use for BIPV. Finally, it can be a criterion to select properly the photovoltaic modules according to the efficiency of each facade, etc. For example, installing modules with higher performance in more efficient facades, will allow a faster return on investment.

The following procedure was proposed to establish the methodology for the pre-classification of facades. The first step was to calculate the BIPV potential by using the solar irradiation factor. One of the fields of BIPV is to guarantee an adequate yield from the facilities. In this area, Spain became a world benchmark when it published the Building Technical Code (CTE) in 2009. This document sets limits on the losses caused by spatial layout of the photovoltaic generator. These losses are inevitable due to the engineering and architectural considerations involved in the construction, which often mean it is impossible to locate the generator so that it maximizes the use of the incident solar radiation. The index named irradiation factor FI, has been proposed for characterizing these losses. This is defined as the annual incident irradiation factor for an orientation α and tilt of generator β , with respect to that received for optimum tilt and orientation [29]. Several countries have also used this simple tool on BIPV, such as England[30]-7, Switzerland[32], Germany, Australia [33] and the United States[34]. FI depends on β , α , the latitude and diffuse radiation fraction of the place.

When it comes to integrated photovoltaics in buildings, the FI graphs can be very useful for the following reasons. It is useful to estimate the photovoltaic potential of a city or a country, as it visually enables the maximum possible losses from the façades and roofs to be determined [35]. Also, it can be used in the technical regulations of a country in order to limit the solar gain losses regarding a photovoltaic generator integrated in a building. This is very important for the sector worldwide, as it limits the amount of modules used and consequently, it has a direct economic and environmental impact on the wholesale appropriation of the technology. This is the case of the CTE in Spain, and of a proposal previously published for a worldwide standard. In the case of a new building, it becomes a highly useful tool for the architectural design as it is an easy way to determine the percentage of solar energy

used by each surface. This fact introduces the sustainability concept as work criteria between the project architecture and engineering.

The following procedure was used to prepare the FI graphs. The amount of annual average radiation that a surface receives according to its tilt and azimuth was first calculated. The peak of the graph where the incident energy is maximum was then identified. This point is given a value of $FI = 1$, thus determining the rest of the graph. In order to determine the optimum surface, the above procedure was repeated by increasing the tilt angle β from 0° to 90° , taking $\Delta\beta = 1^\circ$ as the increase. The optimum tilt angle β_{opt} was thus determined by the surface area that captures the maximum annual irradiation. This calculation was performed for 20 cities of Colombia located between latitudes -4°S and 12°N . Once the annual maximum irradiation was obtained for a certain city, the procedure was repeated cyclically, so that the value of $G_{da}(\beta, \alpha)$ was obtained for each pair of coordinates (β, α) . In order to obtain a highly reliable graph, the point scan suggested by Cronemberger was performed, where tilt β ranged between 0° and 90° , taking $\Delta\beta = 5^\circ$ [35]; and the orientation α between -180° and 180° , taking $\Delta\alpha = 5^\circ$. All the possible configurations could thus be covered. Finally, the irradiation obtained at each point was divided between the maximum, to obtain $FI(\beta, \alpha)$ according to the definition of equation (2). The software used to plot FI was OriginPro 8.

The irradiation factor has values between 0.27 and 0.52 for the facades. This means that up to 73% of solar energy can be lost when installing photovoltaic modules on a vertical surface. For this reason it is necessary to have a pre-classification method, in order to choose the most efficient ones. In the case of the roofs, the losses from completely horizontal roofs can be disregarded for latitudes under 8°N , as the maximum is for San Andrés with 2%. This is coherent with the fact that Colombia is an equatorial country. For north-facing roofs, the losses range between 7% and 21%, in the case of Leticia and San Andrés. Performing a similar analysis to the above one for the 20 cities, we suggested using 5 cities as benchmark graphs of the irradiation factor. The error when adopting this criteria is a maximum of 4 %, the reason for which they would be convenient to use for future legislation regarding BIPV losses in Colombia.

The minimum radiation losses on façades were 48 % for east-west facing ones in cities near to the Equator. This fact was to be expected as the irradiation percentage on vertical surfaces in an equatorial country is minimum. This would indicate that future legislation should enable greater losses for this concept, with respect to the Spanish case. This would be explained by the fact that Colombia receives a greater annual amount of solar irradiation. For north-facing façades, the losses range between 57 % and 73 % in the case of Leticia and San Andrés. When south facing, the values range between 63 % and 54 % for Leticia and Barranquilla, respectively. In the case of east- or west-facing facades, the losses do not vary, as they are 48 %. The irradiation factor for the façades has values that range between 0.25 and 0.55. This means that the solar irradiation on those surfaces range between 25 % and 55% of

the amount on the optimum surface. The maximum FI values are for façades facing east-west, i.e., with azimuth values of -90° and 90° .

Based on these results, a novel model of the irradiation factor on BIPV façades was developed. It was found that, for same latitude, the FI curve approximately describes a sum of two Gaussian functions. The amplitude and location of such functions varies with the latitude of the place. Thus, an expression was obtained that only requires 2 input parameters. The first of them is the city where the photovoltaic system will be installed: latitude ϕ . The other characterizes the plane of the façade of the generator, with its orientation angle α . A graph was built in order to verify the degree of accuracy of the model. The mathematical surface calculated using the proposed equation shows a very good degree of adjustment, with a determination coefficient of $R^2 = 0.98$. Finally, the following is described to provide an idea of the work saved by using the proposed model to calculate FI. To establish the FI by a conventional method, it was necessary to use over 30 equations, in a computer algorithm that performed over 4000 operations. The proposed model avoids this procedure.

In order to validate the model, a comparison with FI values obtained by using the PVWATTS® web site [36] and the equation of the proposed model was done. That tool was developed by the National Renewable Energy Laboratory of United States NREL, and it is often used in photovoltaic projects. The validation procedure is described below. First, the city is selected in PVwatts®. Second, a system size was set at 1000Wp. Third, the system losses were set to a given value. The values of $\alpha = 0$, $\beta = \beta_{\text{opt}}$ are introduced. Fourth, the result for $G_a(\beta_{\text{opt}}, 0)$ was obtained. Fifth, the α values are introduced for the particular orientation to be studied. Seventh, a value of 90° is assigned to the angle β . As results, the values of $G_a(\beta_{\text{opt}}, 0)$ and $G_a(\beta, \alpha)$ were obtained. Then, FI is calculated with these values. Finally, the previous value was compared with that obtained using the equation of the proposed model. In general, the model works very well, and has the advantage that it does not need internet connection, like PVWatts® tool. PVWatts® does not work very well for sites where no weather stations are available, especially in locations outside the United States. For these reasons we consider that our model is very valuable to make rapid calculations, and to pre-classify facades in BIPV projects.

The following procedure was proposed to pre-classification a possible BIPV façade located in equatorial countries. First, define the latitude of the place ϕ and orientation α that characterize the façade of the building. Second, calculate the FI irradiation factor of the façade using the proposed model of FI. Third, establish the annual solar irradiation on the horizontal plane of the place $G_a(0)$, available on the radiation atlases. Fourth, calculate the solar irradiation on the optimum surface $G_a(\beta_{\text{opt}})$. Fifth, calculate the solar irradiation on the façade $G_a(90, \alpha)$. Sixth, use the obtained value of $G_a(90, \alpha)$ to classify the façade, according to the proposed "Energetic Efficiency Rating for façades". This classification is based on publications about the amount of solar irradiation that receives a facade in different places over the world, as mentioned in the introduction of this work. Finally, it is possible to conclude about the potential use of the façade for BIPV. Once the pre-classification of the potential

facades has been done, the architects and engineers can calculate the complete BIPV potential, including the shape and shading factors, by using a complex software.

The models developed in this thesis will serve as input to the design and sizing photovoltaic systems integrated into buildings by architects and engineers in sustainable cities.

The suggested procedure for using these tools in BIPV projects is listed below:

CHARACTERIZATION OF THE PROJECT:

1. Characterize the place where the installation will be carried out, determining its latitude, ambient temperature, diffuse fraction, and annual solar irradiation on a horizontal plane.
2. Characterize the different surfaces of the building that are potential to use BIPV, determining its orientation and tilt angles, and the values of potential useful areas.

DISCARD OF SURFACES:

3. Use the irradiance factor graphs to calculate orientation and tilt losses, using the procedure in section 3 of chapter 6.
4. Determine the maximum allowable shading and orientation losses at the site, using figures 8 and 9.
5. Discard surfaces with higher losses than allowed.

CALCULATION OF THE PRODUCED ENERGY:

6. Calculate the Performance Ratio for each façade, with the model obtained in section 3.1.5
7. Use expression (1) and the graphs of the irradiation factor to calculate the annual electrical energy that each surface would produce.

PRE-CLASSIFICATION OF FACADES WITH ENERGY EFFICIENCY:

8. Calculate the irradiation factor of each facade with equation (52).
9. Pre-classify the facades using the procedure explained in section 3.3.5, and order them according to energy efficiency.
10. Finally, the cost per kWp of each BIPV subsystem is evaluated, starting with those facades that have the best classification.

After this summary, the rest of the thesis is organized as follows. An introduction to the problem of determining the performance ratio is described in the first section. The second section presents the theory and literature review. The methodology is described in section third. The obtained results are presented and discussed in section fourth. The fifth, sixth, and seventh sections present the published scientific papers of this work. The eighth section summarizes the conclusions of the work. The ninth section lists the awards and honors obtained because of this research.

Agradecimientos

Agradezco a Dios, por darme el tiempo, la salud, y las capacidades para desarrollar este trabajo, así como mostrarme el camino.

También a mi esposa Kerly y mis hijos David y Neythan, por la comprensión que implica el tener que sacrificar su tiempo de familia.

Agradezco especialmente a la profesora Llanos Mora López y al profesor Mariano Sidrach, por servirme de gran apoyo a lo largo de este proceso de mi vida. Les debo mucho, desde el máster y mi tránsito por el doctorado. Gracias por su paciencia.

Finalmente, quiero agradecer a la Universidad de Málaga, por darme esta maravillosa oportunidad de estudiar este doctorado. Les estaré siempre agradecido.

Contenido

1. Introducción	19
1.1 El problema de estimar el PR en BIPV.....	21
1.2 Otros aportes de la investigación.....	23
2. Metodología	25
2.1 Metodología en los modelos y normas técnicas propuestas	27
2.1.1 Fuentes de los datos de irradiación y temperatura	27
2.1.2 Cálculo de la irradiación solar anual sobre superficies inclinadas.....	27
2.1.3 Obtención de la inclinación óptima	28
2.1.4 Mapas de contorno del factor de irradiación	28
2.2 Metodología para el modelo del PR en BIPV.....	28
2.2.1 Pérdidas por reflexión angular y suciedad.....	28
2.2.2 Aproximación de las pérdidas por temperatura	29
2.2.3 Obtención de las pérdidas en el inversor	30
2.2.4 Obtención de los demás tipos de pérdidas.....	31
2.2.5 Cálculo del Performance Ratio.....	31
2.3 Metodología para la normativa técnica sobre pérdidas en BIPV.....	32
2.3.1 Límites de pérdidas por orientación e inclinación.....	32
2.3.2 Límites de pérdidas por sombreado	32
2.4 Metodología para el modelo de preclasificación de fachadas	33
3. Resultados y discusión	35
3.1 Nuevo modelo para el PR en sistemas de BIPV ubicados en bajas latitudes	37
3.1.1 Resultados del Performance Ratio.....	37
3.1.2 Modelo del PR máximo según el tipo de sistema	38
3.1.3 Modelo propuesto para las pérdidas por temperatura.....	39
3.1.4 PR en función de la inclinación y orientación.....	39
3.1.5 Modelo propuesto para el Performance Ratio.....	40
3.1.6 Grado de precisión del modelo	42
3.1.7 Uso del modelo para la creación de la APP sobre edificios fotovoltaicos RAITSUN	43
3.2 Metodología propuesta para limitar las pérdidas por inclinación, orientación y sombreado en BIPV a nivel mundial	44
3.2.1 Pérdidas máximas permisibles por orientación e inclinación	44
3.2.2 Pérdidas máximas permisibles por sombreado	46
3.2.2 Propuesta para un estándar técnico mundial	48
3.3 Nuevo método para pre clasificar las fachadas potenciales en BIPV	50
3.3.1 Gráficos del factor de irradiación	50

3.3.2	<i>Modelo propuesto para el factor de irradiación en fachadas</i>	51
3.3.3	<i>Grado de precisión del modelo</i>	52
3.3.4	<i>Validación del modelo.....</i>	53
3.3.5	<i>Metodología propuesta para la pre-clasificación de fachadas en BIPV.....</i>	54
3.4	<i>Procedimiento propuesto para integrar los modelos y herramientas de esta investigación</i>	56
4.	<i>Nuevo modelo para el PR en sistemas BIPV</i>	57
5.	<i>Metodología propuesta para limitar las pérdidas por inclinación, orientación y sombreado en BIPV</i>	79
6.	<i>Nuevo método para pre clasificar las fachadas potenciales en BIPV</i>	91
7.	<i>Conclusiones.....</i>	107
8.	<i>Premios a la investigación</i>	113
9.	<i>Referencias</i>	153

Capítulo 1

Introducción

1.1. El problema de estimar el PR en BIPV

La ciudad sostenible del futuro debe atender de manera prioritaria el manejo de los recursos naturales, la mitigación de gases efecto invernadero (GEI) y otras formas de contaminación [37]. Un elemento vital de una ciudad es su consumo energético, el cual puede ser suplido por diversas fuentes, tanto renovables como no renovables. Con el fin de asegurar la sostenibilidad a largo plazo y mitigar los GEI, los gobiernos promueven cada vez más la implementación de la generación de electricidad mediante las energías renovables.

Entre las energías renovables, la energía solar fotovoltaica cada vez toma mayor protagonismo a nivel mundial [38]. Asimismo, debido a las restricciones espaciales características de las ciudades y para posibilitar la utilización de este tipo de energía, resulta imprescindible instalar módulos fotovoltaicos sobre las fachadas de las edificaciones. Debido a este hecho surgió un nuevo sector, denominado *Fotovoltaica Integrada a Edificios*, o BIPV, por sus siglas en inglés *Building Integrated Photovoltaics*. Este concepto implica reemplazar varios elementos constructivos como techos, fachadas, ventanas, muros cortinas, entre otros; por módulos fotovoltaicos. Se estima que para el año 2021 la potencia total instalada en proyectos BIPV será alrededor de 12 GW [39] a nivel mundial, con un valor total del sector en el mercado de unos 26 millones de dólares para el 2022 [40]. Por lo tanto cada vez más inversionistas y empresas de desarrollo tecnológico están involucrándose en la industria BIPV.

Una de las áreas de prioridad para la BIPV es optimizar soluciones desde los puntos de vista estético, financiero y técnico. En el aspecto técnico, una gran contribución de la BIPV es funcionar como fuente renovable para la construcción de Edificios de Energía Cero, o ZEB por sus siglas en inglés *Zero Energy Buildings* [1]. Con la intención de alcanzar este objetivo, resulta de gran importancia la predicción de la cantidad de energía que producirá la instalación, como insumo al balance neto de energía.

Teniendo esto en mente, surge la pregunta: ¿Cómo realizar una predicción confiable de la energía producida por un sistema fotovoltaico integrado arquitectónicamente a un edificio?

Parte de la respuesta es sugerida por la *Comisión Electrotécnica Internacional* (IEC), mediante la normativa IEC 61724-1 del año 2017 [24]. En este documento se propone una expresión equivalente a la siguiente, para calcular la producción de energía anual de Sistemas Fotovoltaicos Interconectados:

$$E_{PV} = \frac{G_a(\beta, \alpha) \cdot P_{peak} \cdot PR}{G_{STC}} \quad (1)$$

Donde $G_a(\beta,\alpha)$ corresponde a la irradiación solar incidente sobre el plano del generador fotovoltaico, P_{peak} es la potencia nominal instalada, PR el rendimiento global del sistema, denominado *Performance Ratio*, y G_{STC} tiene el valor de 1 kW/m^2 . Por lo tanto, si se conocen bien los parámetros $G_a(\beta,\alpha)$ y PR, se concluye que se puede predecir la cantidad de energía producida por un sistema fotovoltaico. $G_a(\beta,\alpha)$ se puede hallar mediante gráficos del denominado *Factor de Irradiación* (FI) [30],[32]. Sin embargo, para la obtención de estos diagramas se hace necesario el uso de complicados algoritmos que consisten en engorrosas ecuaciones. Es por este hecho que en el diseño, modelado, y predicción de energía de un sistema fotovoltaico, usualmente es necesario el uso de software especializado.

En cuanto a la determinación del PR en sistemas de BIPV, la tarea tampoco resulta trivial, ya que este parámetro es función de la radiación solar del lugar, el clima, el azimut e inclinación de las superficies, el diseño de la instalación, la calidad de fabricación de equipos y elementos, entre otros. Esta dificultad se acentúa en los sistemas fotovoltaicos integrados en edificios, donde la mayoría de veces no es posible maximizar la cantidad de radiación solar que incide sobre los módulos, debido a las restricciones espaciales de las superficies usadas. Con el objetivo de predecir el PR, en varios estudios se han desarrollado modelos matemáticos de las variables que inciden en la energía producida por la instalación. Entre los más conocidos de carácter analítico, y que se usan para hallar las pérdidas por temperatura, destacan los propuestos por Osterwald [2], Araujo [3] y Green [4]. También se han propuesto otros modelos basados en redes neuronales artificiales [5][6], que abarcan más variables. Sin embargo, la mayoría de éstos son muy engorrosos de implementar. Otros modelos son menos complejos, pero no consideran todos los factores propios del sistema.

Frente a lo anterior, un camino fácil y muy usado en la actualidad, es aproximar $\text{PR}=0.75$ para *cualquier sistema* [7]. A pesar de la popularidad de este procedimiento empírico, no resulta conveniente por que descarta las variables características de cada instalación. Como evidencia de ello se han reportado valores para PR entre 0.42 y 0.81 [8], a nivel global. Esto es lógico, ya que la eficiencia de los módulos fotovoltaicos depende de la temperatura ambiente. Otra variable que ejerce gran influencia es la latitud del lugar geográfico, ya que su efecto en la irradiación solar incidente hace que la potencia a la entrada del inversor tenga valores muy bajos durante de ciertos lapsos de tiempo, lo cual repercute en la eficiencia de conversión. Por si lo anterior fuera poco, la práctica de asignar una única cifra al PR queda totalmente descartada en aplicaciones de BIPV, ya que las pérdidas energéticas debidas a la inclinación y orientación de las superficies usadas pueden llegar a ser bastante diferentes. La razón principal para esto radica en las pérdidas por *reflexión angular*, o tipo Fresnel, que se originan debido a que luz solar se refleja más a pequeños ángulos de incidencia con respecto a la superficie del módulo fotovoltaico. A su vez, esta variable ocasiona diferentes valores de pérdidas por polvo y suciedad. Por todo lo anterior, resulta completamente coherente que el PR varíe para un mismo edificio, teniendo en cuenta la gran variedad de superficies posibles a utilizar en cubiertas y fachadas.

Como conclusión, la gran cantidad de factores mencionados hacen muy difícil el predecir el PR para proyectos BIPV. Por esto, sería muy conveniente que los arquitectos e ingenieros puedan disponer de métodos sencillos que generen valores confiables para el PR. La importancia de esto es vital, ya que debido al cambio climático resulta urgente la implementación de los edificios de energía cero, mediante la masificación de la BIPV a nivel mundial.

En la presente investigación se aborda esta problemática mediante la creación de modelos entendibles y confiables, que permiten predecir la cantidad de energía producida en sistemas fotovoltaicos integrados a edificios. Estos modelos resultan muy útiles no solo en la predicción correcta de la energía producida por el futuro sistema de BIPV, sino que a su vez se permiten calcular valores de referencia para la monitorización y mantenimiento futuro de la instalación.

Todos los aportes de esta investigación se centran en facilitar la implementación y masificación de proyectos de BIPV en sus etapas iniciales, promoviendo la generación de electricidad mediante energía solar fotovoltaica. Así, esperamos contribuir a la disminución de la huella de carbono y la mitigación de los GEI, como ejes centrales en la dimensión ambiental de las ciudades sostenibles del futuro.

1.2. Otros aportes de la investigación

La obtención del modelo para el PR permite estimar de una mejor manera la energía anual producida en edificios con BIPV ubicados en bajas latitudes. Así, cada superficie constructiva presenta una eficiencia energética, dada por la relación entre la electricidad producida y la irradiación solar incidente. Por lo tanto, también se propone un modelo de normas técnicas internacionales que limiten las pérdidas máximas permitidas por sombreado y orientación de las superficies constructivas. Este modelo de normativas se basó en diseñar un procedimiento para generalización del apartado BIPV, incluido en el *Código Técnico de la Edificación* o CTE de España.

Finalmente, se propone una metodología para la pre-clasificación de fachadas potencialmente útiles para emplearlas en BIPV. Para esto se asoció un sistema de código de colores similar al usado en eficiencia energética de equipos eléctricos, según el código de letras A-G.

Además de la creación del modelo para el PR y las propuestas de normas técnicas, se diseñaron herramientas para la etapa de diseño, las cuales pueden ser empleadas para el desarrollo de la BIPV en ciudades sostenibles. El procedimiento sugerido para usar estas herramientas en proyectos de BIPV se enuncia a continuación:

CARACTERIZACIÓN DEL PROYECTO:

1. Caracterizar el lugar donde se realizará la instalación, determinando su latitud, temperatura ambiente, fracción de difusa, e irradiación solar anual sobre plano horizontal.
2. Caracterizar las diferentes superficies del edificio que son potenciales para emplear BIPV, determinando sus ángulos de orientación e inclinación, y los valores de áreas útiles potenciales.

DESCARTE DE SUPERFICIES:

3. Usar los gráficos del factor de irradiación para calcular las pérdidas por orientación e inclinación, mediante el procedimiento de la sección 3 del capítulo 6.
4. Determinar los valores máximos permitidos de pérdidas por sombreado y orientación en el lugar, mediante el uso de las figuras 8 y 9.
5. Descartar las superficies con pérdidas mayores a las permitidas.

CÁLCULO DE LA ENERGÍA PRODUCIDA:

6. Calcular el Performance Ratio para cada fachada, con el modelo obtenido en la sección 3.1.5
7. Usar la expresión (1) y los gráficos del factor de irradiación para calcular la energía eléctrica anual que produciría cada superficie.

PRE-CLASIFICACIÓN DE FACHADAS CON LA EFICIENCIA ENERGÉTICA:

8. Calcular el factor de irradiación de cada fachada con la ecuación (52)
9. Preclasificar las fachadas mediante el procedimiento explicado en la sección 3.3.5, y ordenarlas según la eficiencia energética.
10. Finalmente, se procede a evaluar el costo por kWp cada subsistema BIPV, empezando por aquellas fachadas que tienen mejor clasificación.

Capítulo 2

Metodología

2.1. Metodología en los modelos y normas técnicas propuestas

La metodología general de la investigación consistió en tomar datos reales geográficos y climatológicos, y procesarlos mediante ecuaciones comúnmente usadas en el campo de la fotovoltaica. Luego, se procedió a analizar los resultados y crear los nuevos modelos y normativas. En los puntos 2.1.1 hasta 2.1.4 se describe la metodología común empleada en las tres publicaciones. Por otra parte, en las secciones 2.2 hasta 2.4 se describe de forma global la parte de la metodología específica que concierne a cada investigación particular. Para una descripción detallada se recomienda revisar cada publicación anexa en los capítulos 5 a 7.

2.1.1 Fuentes de los datos de irradiación y temperatura

Los datos de irradiación solar para las ciudades fue el *RETScreen International* [26], software de proyectos de energía renovable. Abarca a más de 6700 estaciones meteorológicas, así como datos de estimaciones satelitales de la NASA. En este primer paso se obtuvieron los valores de la irradiación solar global sobre superficie horizontal $G_{dm}(0)$, en 12 valores diarios medios mensuales.

2.1.2 Cálculo de la irradiación solar anual sobre superficies inclinadas

Cada uno de los datos diarios medios mensuales de $G_{dm}(0)$ se fraccionó a su vez en dos componentes: radiación difusa, $D_{dm}(0)$, y directa, $B_{dm}(0)$. Para esto se usó la aproximación de Liu y Jordan [10], que establece la independencia latitudinal de la relación entre el índice de claridad K_{Tm} y la fracción de difusa K_{Dm} . Se usó el modelo de Page [11], válido para latitudes entre 40°N y 40°S. Una vez calculadas las componentes diarias de la irradiación solar global, se calculó los valores horarios, $D_h(0)$ y $B_h(0)$. Para esto se usaron las ecuaciones propuestas por Collares-Pereira y Rabl [12]. A continuación se calculó la irradiación global horaria incidente en el plano del generador $G_h(\beta,\alpha)$, mediante *el modelo de las tres componentes*, que ha demostrado bastante exactitud [13]. Esta aproximación establece que la radiación incidente sobre una superficie con inclinación β y orientación α , está conformada por radiación directa, $B_h(\beta,\alpha)$, difusa, $D_h(\beta,\alpha)$, y reflejada, $R_h(\beta,\alpha)$. Para la obtención de $D_h(\beta,\alpha)$ hay más de 20 modelos reportados. Se empleó el modelo isotrópico de Hay-Davies [41], debido a su alta precisión y simplicidad [14][15][16][17]. Este modelo establece que la radiación difusa está compuesta por la suma de dos componentes: la circunsolar $D^c(\beta,\alpha)$, y la isotrópica $D^i(\beta,\alpha)$, provenientes directamente del sol y de toda la semiesfera celeste, respectivamente. Para el cálculo de $R_h(\beta,\alpha)$ se tomó la reflectividad del suelo como $\rho=0.2$ [42]. Finalmente, al realizar la sumatoria temporal de las componentes se obtuvo el valor diario medio anual de la irradiación solar, $G_{da}(\beta,\alpha)$, incidente en el plano del generador.

2.1.3 Obtención de la inclinación óptima

La secuencia anterior se iteró incrementando el valor de inclinación β desde 0° hasta 90° , a incrementos de $\Delta\beta=1^\circ$. El azimut se fijó igual a 0° o 180° , dependiendo si las ciudades estaban ubicadas en latitudes positivas o negativas, respectivamente. Al final del proceso, el ángulo óptimo de inclinación β_{opt} que maximiza la irradiación solar anual quedó definido por la condición:

$$G_{da}(\beta_{opt}) = \begin{cases} \max[G_{da}(\beta, 0)] & \phi \geq 0 \\ \max[G_{da}(\beta, \pi)] & \phi \leq 0 \end{cases} \quad (2)$$

Este cálculo se hizo para ciudades localizadas en latitudes entre -4°S y 12°N . El listado completo se encuentra en la tabla 5 del capítulo 4.

2.1.4 Mapas de contorno del factor de irradiación

Teniendo como insumo la irradiación máxima anual para una determinada ciudad $G_{da}(\beta_{opt})$, se iteró el procedimiento del punto 2.1.2 de forma cíclica. Por lo tanto, se obtuvo el valor de $G_{da}(\beta, \alpha)$ incidente sobre cada superficie de inclinación y orientación (β, α) . Con miras a obtener un gráfico con alto grado de precisión, se realizó el barrido de puntos sugerido por Caamaño [35], en el cual la inclinación β se varía entre 0° y 90° , y la orientación α entre -180° y 180° . Los incrementos para cada una de éstas fueron $\Delta\beta=5^\circ$ y $\Delta\alpha=5^\circ$. Así se logró abarcar todas las superficies físicamente posibles. Finalmente, se realizó el cociente entre la irradiación obtenida en cada punto y la irradiación máxima, obteniendo así el valor del factor de irradiación solar, $FI(\beta, \alpha)$.

2.2 Metodología para el modelo del PR en BIPV

2.2.1 Pérdidas por reflexión angular y suciedad

La irradiación global incidente en cada superficie fue corregida al incluir tanto las pérdidas por suciedad como las angulares, mediante el modelo de Martin-Ruiz [18]. Esta aproximación reproduce resultados reales [43] y establece que la irradiancia global horaria $G'_h(\beta, \alpha)$ sobre el módulo fotovoltaico está conformada por cuatro componentes: la radiación directa $B_h(\beta, \alpha)$, la difusa circunsolar $D^C_h(\beta, \alpha)$, la difusa isotrópica $D^I_h(\beta, \alpha)$, y la reflejada $R_h(\beta, \alpha)$; así:

$$G'_h(\beta, \alpha) = FT_B \cdot B_h(\beta, \alpha) + FT_B \cdot D^C_h(\beta, \alpha) + FT_D \cdot D^I_h(\beta, \alpha) + FT_R \cdot R_h(\beta, \alpha) \quad (3)$$

Donde FT_B , FT_D , FT_R corresponden a las transmitancias relativas, dividida cada una entre la transmitancia total a incidencia normal, y definidas por:

$$FT_B = 1 - \frac{\exp\left(-\frac{\cos\theta_s}{a_r}\right) - \exp\left(-\frac{1}{a_r}\right)}{1 - \exp\left(-\frac{1}{a_r}\right)} \quad (4)$$

$$FT_D = 1 - \exp\left\{-\frac{1}{a_r} \left[c_1 \left(\sin\beta + \frac{\pi - \beta - \sin\beta}{1 + \cos\beta} \right) + c_2 \left(\sin\beta + \frac{\pi - \beta - \sin\beta}{1 + \cos\beta} \right)^2 \right] \right\} \quad (5)$$

$$FT_R = 1 - \exp\left\{-\frac{1}{a_r} \left[c_1 \left(\sin\beta + \frac{\beta - \sin\beta}{1 - \cos\beta} \right) + c_2 \left(\sin\beta + \frac{\beta - \sin\beta}{1 - \cos\beta} \right)^2 \right] \right\} \quad (6)$$

Donde θ_s es el ángulo entre los rayos solares y la normal al plano considerado. Los parámetros a_r y c_2 dependen del grado de suciedad, y el valor de c_1 es $4/(3\pi)$. Estos valores se escogieron para un grado de suciedad medio, es decir, $T_{dirt}(0)/T_{clean}(0)=0.97$, según la siguiente tabla:

Tabla 1. Valores usuales de los parámetros a_r y C_2 para módulos de Silicio. Fuente: [44]

$T_{dirt}(0)/T_{clean}(0)$	a_r	C_2
1	0.17	-0.069
0.98	0.20	-0.054
0.97	0.21	-0.049
0.92	0.27	-0.023

Finalmente, al realizar la sumatoria de $G'_h(\beta, \alpha)$ para todos los días del año, se obtuvo la irradiación solar anual incidente $G'_a(\beta, \alpha)$. Por otra parte, para calcular la irradiación solar anual $G_a(\beta, \alpha)$ en ausencia total de pérdidas angulares, se fijaron los valores de FT_B , FT_D , FT_R iguales a 1. Así, pérdidas anuales por reflexión angular y suciedad se calcularon mediante la expresión [18]:

$$L_{angular} = 1 - \frac{G'_{da}(\beta, \alpha)}{G_{da}(\beta, \alpha)} \quad (7)$$

2.2.2 Aproximación de las pérdidas por temperatura

Se empleó el modelo cosenoideal de variación de la temperatura ambiente a lo largo del día [45], que tiene como parámetros de entrada las temperaturas medias mínimas T_{am} y máximas T_{aM} . En esta aproximación se consideran tres suposiciones básicas:

1. La temperatura mínima ocurre al amanecer, cuando el ángulo horario es igual al ángulo de salida del sol, $\omega = \omega_s$.
2. La temperatura máxima ocurre dos horas después del mediodía solar, cuando el ángulo horario es igual a $\pi/6$.
3. Durante el día la temperatura cambia en función con dos semicírculos de funciones cosenoidales, cuya variable independiente es el tiempo solar ω . Ver sección 4.4. del capítulo 4 para una descripción detallada de las ecuaciones.

Una vez obtenida la temperatura ambiente T_a y la irradiancia global incidente $G'_h(\beta, \alpha)$, la temperatura instantánea de trabajo del módulo quedó determinada en función de la temperatura de operación nominal $TONC$, mediante la expresión:

$$T_c = T_a + G'(\beta, \alpha) \frac{TONC - 20^\circ C}{800 W/m^2} \quad (8)$$

El siguiente paso fue determinar la potencia máxima de salida del generador mediante el modelo de Osterwald [2], el cual es ampliamente usado [20]:

$$P_{máx} = P_{máx, STC} \frac{G'(\beta, \alpha)}{G_{STC}} \left[1 + \gamma (T_c - 25^\circ C) \right] \quad (9)$$

Finalmente, las pérdidas instantáneas por temperatura se calcularon con la siguiente ecuación:

$$L_{temperatura, ins} = -\gamma (T_c - 25^\circ C) \quad (10)$$

2.2.3 Obtención de las pérdidas en el inversor

Para obtener la eficiencia instantánea del inversor de potencia nominal $P_{monimal}$, se tomaron las siguientes relaciones:

$$\eta_{inverter} = \frac{P_{output}}{P_{input}} = \frac{p_{in} - (b_0 + b_1 \cdot p_{in} + b_2 \cdot p_{in}^2)}{p_{in}} \quad (11)$$

$$p_{in} = \frac{P_{input}}{P_{nominal}} \quad (12)$$

Donde los parámetros $b_0=0.02$, $b_1=0.02$ y $b_2=0.07$ son característicos de un conjunto representativo de inversores del mercado [19]. Por lo tanto, las pérdidas de conversión DC-AC en el inversor quedaron determinadas por:

$$L_{inverter} = 1 - \frac{E_{AC}}{E_{DC}} = 1 - \frac{\int_{\tau} \eta_{inverter} \cdot P_{max} \cdot dt}{\int_{\tau} P_{max} dt} \quad (13)$$

Las integrales se realizaron para el período de tiempo τ , que a su vez fue totalizado anualmente.

2.2.4 Obtención de los demás tipos de pérdidas

Para determinar los otros tipos de pérdidas se tomaron valores típicos reportados:

- Las pérdidas originadas por la diferencia entre la potencia real y la nominal de los módulos, se tomaron iguales a 5%, o $L_{rating}=0.05$. Este valor es una buena aproximación si se supone que los módulos están seleccionados adecuadamente [20].
- Las pérdidas por desacople, ocasionadas por el sombreado parcial de los módulos y la dispersión de las propiedades eléctricas del conexionado en serie o paralelo, se aproximan iguales 3% o $L_{mismatch}=0.03$. Este valor corresponde al promedio de los valores típicos reportados [20].
- Las pérdidas por errores de seguimiento del punto de máxima potencia se tomaron iguales a 6%, o $L_{SPMP}=0.06$. Esta cifra se basa en reportes de más de 100 instalaciones fotovoltaicas [21].
- Las pérdidas óhmicas debidas al efecto Joule se tomaron iguales al 1%, o $L_{ohmic}=0.01$. Este valor corresponde al promedio de los reportados [46].
- Las pérdidas por sombreado se aproximan al 7%, o $L_{shading}=0.07$. Este valor es adecuado según reportes de investigaciones previas para sistemas sobre techo [21][47][48]. Sin embargo, cuando se trata de BIPV, las pérdidas pueden llegar muy diferentes entre un proyecto y otro. Por ejemplo, se reportan valores tan diferentes como 10% y 23%, para sistemas ubicados en diferentes lugares[49]. Por lo tanto, se sugiere evaluar detalladamente este concepto mediante software especializado que incluya todos los obstáculos del entorno. Así, al obtener un valor diferente de pérdidas por sombreado, se puede introducir en el modelo propuesto del PR, como un factor igual a $(1-L_{shading,real})/0.93$.

2.2.5 Cálculo del Performance Ratio

El PR se calculó a partir de las pérdidas energéticas en cada parte del generador, L_i . Por lo tanto, el Performance Ratio se obtuvo mediante la productoria de los rendimientos individuales:

$$PR = \prod_{i=1}^n (1 - L_i) \quad (14)$$

2.3 Metodología para la normativa técnica sobre pérdidas en BIPV

2.3.1 Límites de pérdidas por orientación e inclinación

Con el fin de establecer los límites de pérdidas por inclinación y orientación del plano del generador, se define como lugar 1 a un país que cuente con normatividad técnica en BIPV, por ejemplo España. Similarmente, se denomina lugar 2 a la ciudad de un país diferente a España, en el cual se quieren establecer límites de pérdidas.

El primer paso fue fijar como base la referencia del 100%, de valor idéntico a la irradiación anual máxima incidente posible, $G_a(\beta_{opt})$. Una vez obtenida $G_a(\beta_{opt})$ para cada ciudad, se calculó la mínima cantidad de irradiación que puede recibir una fachada en España, $G_{a,MIN}(90,0)$. Para este fin, según el Código Técnico de la Edificación de España, las pérdidas por azimut e inclinación en BIPV no pueden superar el 40%. A la superficie que se encuentra en éste límite se le denominó como la *peor fachada permisible*. A continuación esta fachada se “traslada” al nuevo país o lugar 2. Por lo tanto, el máximo límite para el lugar 2 queda determinado por:

$$L_{\beta,\alpha,MAX,2} = 100 \left(1 - \frac{G_{a,MIN,1}(90,0)}{G_{a,2}(\beta_{opt})} \right) \quad (15)$$

Donde los subíndices 1 y 2 se refieren a los lugares 1 y 2, respectivamente. El traslado de irradiación solar a un lugar diferente se hizo para asegurar que en el peor de los casos en ambos lugares, se reciba igual cantidad de irradiación solar. De esta forma, se pueden comparar las pérdidas permitidas por orientación e inclinación de ambos lugares.

2.3.2 Límites de pérdidas por sombreado

En el caso de los valores máximos de pérdidas por sombreado también se tomó como base el documento del Código Técnico de la Edificación de España CTE, como país referencia. El objetivo es “trasladar” este límite a ciudades un país diferente. El CTE propone un límite máximo de pérdidas en BIPV de 20%, con respecto a la situación hipotética de sombreado total. En tal caso, la radiación dejada que deja de incidir sobre el plano del generador sería igual a la radiación directa, $B_a(0)$, más la difusa circunsolar, $D_a^C(0)$. Por lo tanto, sólo se recibe la fracción solar de difusa isotrópica.

Dado que el parámetro físico solar que se ve directamente involucrado es la fracción de difusa, ésta se calculó para las diferentes ciudades del lugar 1 (España). La fuente para ello fue el *Atlas de Radiación Solar en España* [27], publicado por la Agencia Estatal de Meteorología [28]. Seguidamente se calculó el valor promedio de la fracción de difusa que representa al país, ya que el CTE propone un único valor de

límite de pérdidas por sombreado. Finalmente, el valor perdido de irradiación solar directa se comparó con el máximo contemplado en las tablas de referencia del CTE. Como resultado de esto, se encontraron los valores de $B_a(0)$ y $D_a^C(0)$ para el lugar 1.

Por lo tanto, para el lugar 1 se define que la fracción máxima de irradiación perdida, con respecto a la físicamente posible es:

$$f_{MÁX,losses,1} = \frac{L_{shading,MAX,1}}{100\% \left(\frac{B_{a,1}(0) + D_{a,1}^C(0)}{G_{a,1}(0)} \right)} \quad (16)$$

Donde $L_{shading,MAX,1}$ es el límite máximo de pérdidas por sombreado en el lugar 1, que en el caso de España es 20%.

Finalmente, la fracción máxima de irradiación solar perdida en el lugar 1 se igualó a su equivalente en el lugar 2. Por lo tanto, las máximas pérdidas por sombreado para el lugar 2 quedaron definidas mediante:

$$L_{shading,MAX,2} = 100\% \left(\frac{B_{a,2}(0) + D_{a,2}^C(0)}{G_{a,2}(0)} \right) f_{MÁX,losses,1} \quad (17)$$

2.4 Metodología para el modelo de preclasificación de fachadas

Primeramente se halló el factor de irradiación en las fachadas, $FI_{facades}$, mediante el cual se calcula la irradiación solar en la superficie $G_a(90,\alpha)$. Posteriormente se propuso un modelo matemático ajustando los datos, el cual fue validado mediante la herramienta de PVWatts®, diseñada por el NREL. Se escogió esta herramienta, ya que las últimas versiones presentan una presición aproximada del 2% [50]. Así mismo, es muy conocida entre los instaladores y empresas de América. La expresión matemática para $FI_{facades}$, se ajustó tomando como datos independientes la orientación de la superficie y la latitud del lugar.

Por último, con $G_a(90,\alpha)$, y tomando como referencia el rango de valores que puede recibir una facha a nivel mundial, se propuso un modelo de pre-clasificación de fachadas basado en la escala de valores de eficiencia energética, similar al de equipos eléctricos

Capítulo 3

Resultados y discusión

3.1. Nuevo modelo para el PR en sistemas de BIPV ubicados en bajas latitudes

3.1.1. Resultados del Performance Ratio

En la tabla 2 se listan los resultados obtenidos para el PR, tanto los máximos como los mínimos. Se puede apreciar que los valores se encuentran entre 0.51 y 0.65, lo cual implica una variación de más del 20%. Solo este hecho demuestra de forma contundente que no es adecuada la práctica de asignar un único valor “estándar” de 0.75 para el Performance Ratio en BIPV.

Tabla 2. PR mínimo y máximo para cada ciudad.

Ciudad	PR min	PR max
Bogotá	0,58	0,65
Pasto	0,58	0,65
Manizales	0,56	0,64
Popayán	0,56	0,63
Medellín	0,54	0,62
Cali	0,54	0,61
Tumaco	0,54	0,61
Villavicencio	0,54	0,61
Leticia	0,54	0,61
Cúcuta	0,53	0,60
Barrancabermeja	0,53	0,60
San Andrés	0,51	0,60
Neiva	0,54	0,60
Montería	0,53	0,60
Barranquilla	0,52	0,60
Valledupar	0,51	0,60

Cabe destacar que el PR máximo depende de la temperatura ambiente media de la ciudad. Esta funcionalidad se aprecia en la figura 1. 0.81. 0.63

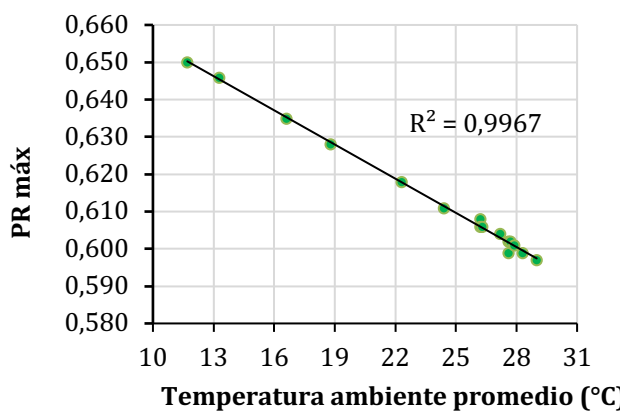


Fig. 1. Rendimiento máximo anual del sistema frente a la temperatura ambiente promedio.

La ecuación de regresión lineal que representa los datos es:

$$PR_{\max} = 0,686 - 0,0031 \text{ } ^\circ\text{C}^{-1} \cdot T_a \quad (18)$$

Esta ecuación se reescribió en términos de cada tipo pérdida energética del sistema, como sigue:

$$PR_{\max} = (1 - L_{\text{temp,max}})(1 - L_{\text{angular,min}})(1 - L_{\text{inverter,min}}) \prod_{i=1}^6 (1 - L_i) \quad (19)$$

Donde $L_{\text{temp,max}}$ son las pérdidas máximas por temperatura, correspondientes a pequeñas inclinaciones del generador. Estas están dadas por la ecuación:

$$L_{\text{temp,max}} = -\gamma (TOE_{\max} - 25 \text{ } ^\circ\text{C}) \quad (20)$$

Siendo TOE_{\max} la *temperatura de operación equivalente* máxima del generador durante todo el período considerado, ponderada por la irradiancia total [51]:

$$TOE = \frac{\int_{\tau} T_c \cdot G'(\beta, \alpha) \cdot dt}{\int_{\tau} G'(\beta, \alpha) \cdot dt} \quad (21)$$

Otro resultado interesante fue que la temperatura anterior depende directamente de la temperatura ambiente media de la ciudad:

$$TOE_{\max} = 1.12T_a + 15 \text{ } ^\circ\text{C} \quad (22)$$

3.1.2. Modelo del PR máximo según el tipo de sistema

En la tabla 3 se muestran dos aproximaciones para el valor máximo del Performance Ratio, según si el sistema fotovoltaico es promedio u óptimo. Esto depende principalmente de la aplicación de altos estándares en el diseño y la calidad de los equipos.

Tabla 3. Valores de pérdidas que aportan a PR_{\max} .

Término	Sistema promedio	Sistema óptimo	Situación
$L_{\text{angular,min}}$	0.04	0.03	Zonas lluviosas [18]
$L_{\text{inverter,min}}$	0.11	0.05	Muy buen inversor [45]
L_{rating}	0.05	0.03	Módulos excelentes [52]
L_{mismatch}	0.03	0.02	Módulos excelentes [20]
L_{SPMP}	0.06	0.02	Muy buen inversor [53]
L_{ohmic}	0.01	0.005	Sección del cableado [20]
L_{shading}	0.07	0.02	Pocos obstáculos [54]
$L_{\text{dirtiness}}$	0.03	0.02	Zonas lluviosas [18]

Según lo anterior, se puede definir una constante del sistema definida como k_{sist} , con valores de 0,662 y 0,820, para sistemas promedio y óptimo, respectivamente. Por lo tanto la ecuación (18) se modificó, así:

$$PR_{\max} = k_{sist} \cdot [1 + \gamma(1,12 \cdot T_a - 10^{\circ}\text{C})] \quad (23)$$

Es importante mencionar que los valores de PR en la tabla 2 fueron calculados para un sistema promedio. En el caso de sistemas óptimos, se obtienen rendimientos mínimos y máximos entre 0,63 y 0,81, respectivamente. Estas cifras abarcan valores de PR obtenidos para sistemas reales instalados [55], ya que tales instalaciones se ejecutan para valores de ángulos de inclinación óptimos. Con esto se valida parcialmente los resultados obtenidos.

3.1.3. Modelo propuesto para las pérdidas por temperatura

La expresión propuesta para hallar las máximas pérdidas por temperatura en sistemas BIPV es:

$$L_{temperature,\max} = -\gamma(1,12 \cdot T_a - 10^{\circ}\text{C}) \quad (24)$$

Con el fin de validar la anterior expresión, se compararon las pérdidas calculadas mediante la ecuación (24), con las pérdidas reportadas para sistemas reales. Los resultados obtenidos se muestran en la tabla 4. Se puede apreciar que el modelo tiene un alto nivel de predicción. Estas pérdidas son para el caso de un sistema promedio, donde los módulos tienen buena ventilación, por lo tanto representan las perdidas mínimas en sistemas BIPV con ventilación moderada.

Tabla 4. Valores de pérdidas por temperatura para generadores inclinados cerca a su ángulo óptimo.

Ciudad	País	Número de sistemas	Pérdidas medidas	Referencia	Pérdidas calculadas
Tokio	Japón	100	4%	[21]	4%
Dublín	Irlanda	1	0%	[22]	0%
Sukatani	Indonesia	101	8%	[23]	8%

3.1.4. PR en función de la inclinación y orientación

La ecuación (23) describe el PR en el caso de inclinaciones cercanas a la óptima, que maximizan la energía anual producida. Sin embargo, en el caso de los sistemas con BIPV se utilizan superficies orientadas e inclinadas en diversas direcciones. Esto puede dar lugar a un error hasta del 15% en el PR calculado, y por consiguiente en la energía anual.

Para entender mejor este efecto se graficaron mapas de contorno del Performance Ratio, en función de la inclinación y el azimut. Los resultados se muestran en las figura 2.

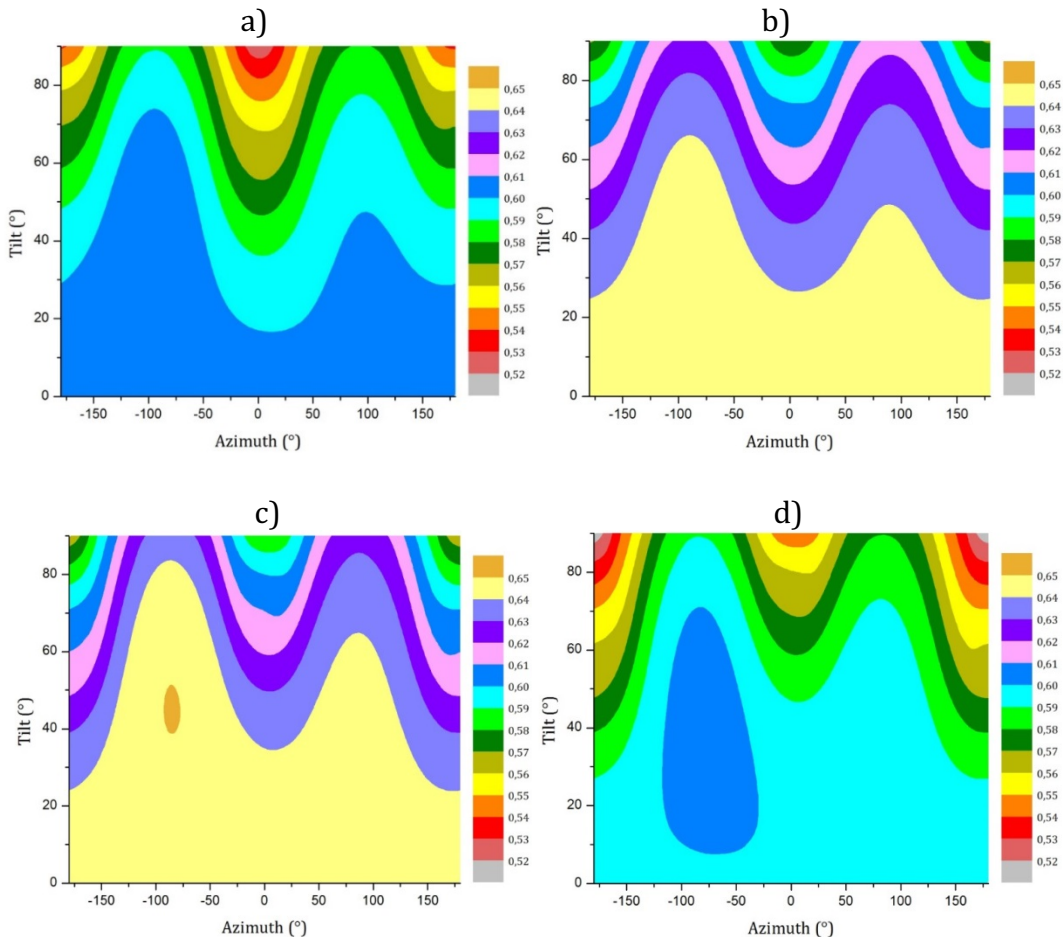


Fig. 2. Mapa de contorno de PR para a) Leticia ($\phi = -4.2^\circ$) b) Pasto ($\phi = 1.2^\circ$).
c) Bogotá ($\phi = 4.7^\circ$) d) Cúcuta ($\phi = 7.9^\circ$).

Se puede apreciar que todas las inclinaciones menores a 30° , es decir, todas las cubiertas tienen un PR igual al máximo. Así mismo, se presentan dos máximos de rendimiento, para las orientaciones de -90° y 90° . La principal causa de este comportamiento radica en que las pérdidas angulares y las de conversión son mínimas en las orientaciones en las direcciones este y oeste. El pico en $\alpha=-90^\circ$ es mayor que para $\alpha=90^\circ$, debido a que en las mañanas la temperatura ambiente es menor, lo cual disminuye las pérdidas. Esto mismo hecho causa la aparición de la región azul oscura en la figura 2.d.

3.1.5. Modelo propuesto para el Performance Ratio

Cada ciudad tiene un mapa de contorno para PR, según su temperatura ambiente y latitud. Por ello, si en un proyecto de BIPV se quiere predecir la cantidad de energía producida, basta con observar el PR en el mapa de contorno específico. Sin embargo, para obtener los gráficos es necesario emplear el tedioso procedimiento descrito en el punto 2.2. Esto no es viable técnicamente cuando se plantea un proyecto de BIPV.

Este es el motivo por el cual la comunidad ha optado por asignar un “valor estándar” de 0.75 al PR, para estimar la energía producida. Sin embargo, como ya se ha discutido, el adoptar esta práctica no resulta adecuado en el caso de BIPV, ya que los errores cometidos podrían llegar a ser hasta del 45%, en el peor de los casos.

Por lo tanto, resulta necesario desarrollar una ecuación que reproduzca de forma aproximada los mapas de contorno para el PR. Con este objetivo se tiene que, para un mismo PR, la gráfica tiene la forma aproximada a una suma de dos funciones gaussianas, cuya amplitud y ancho varían con la latitud. Además, hay un desplazamiento vertical de cada función, en función de la temperatura media de la ciudad. Por lo tanto, se ha propuesto el siguiente modelo para el cálculo del PR:

$$PR = 0,0011 \left(A_1 \cdot e^{-2\left(\frac{\alpha-\alpha_0}{W}\right)^2} + A_2 \cdot e^{-2\left(\frac{\alpha+90}{W}\right)^2} - \beta - 5 \right) + 0,117 \cdot PR_{\max} \quad (25)$$

Donde

$$A_1 = -1,1 \cdot |\varphi| + 60 \quad (26)$$

$$A_2 = -0,1 \cdot |\varphi| + 65 \quad (27)$$

$$W = -1,1 \cdot \varphi + 92 \quad (28)$$

$$\alpha_0 = -1,4 \cdot \varphi + 92 \quad (29)$$

Donde β corresponde a la inclinación, α al acimut y φ a la latitud, todos en grados sexagesimales.

Como conclusión importante, se propuso un modelo para calcular el Performance Ratio en sistemas de BIPV, y que requiere sólo 4 parámetros de entrada: La temperatura ambiente media, la latitud, la inclinación, y la orientación. Los pasos para usar la ecuación (25) se describen a continuación:

1. Calcular PR_{\max} con la ecuación (18).
2. Calcular PR mediante la ecuación (25). Si $PR > PR_{\max}$ entonces se tiene que $PR = PR_{\max}$. Si $PR < PR_{\max}$ entonces el PR es el obtenido con la ecuación.

3.1.6. Grado de precisión del modelo

Con el ánimo de verificar el grado de precisión del modelo, se construyó la figura 3. Se pueden apreciar dos diagramas de contorno del PR, el de la izquierda fue realizado mediante el extenso y complicado procedimiento explicado en el punto 2.2. El de la derecha fue elaborado usando el modelo propuesto en la ecuación (25). Así mismo, la figura muestra el porcentaje de error cometido, el cual es menor al 1% en la mayoría del gráfico.

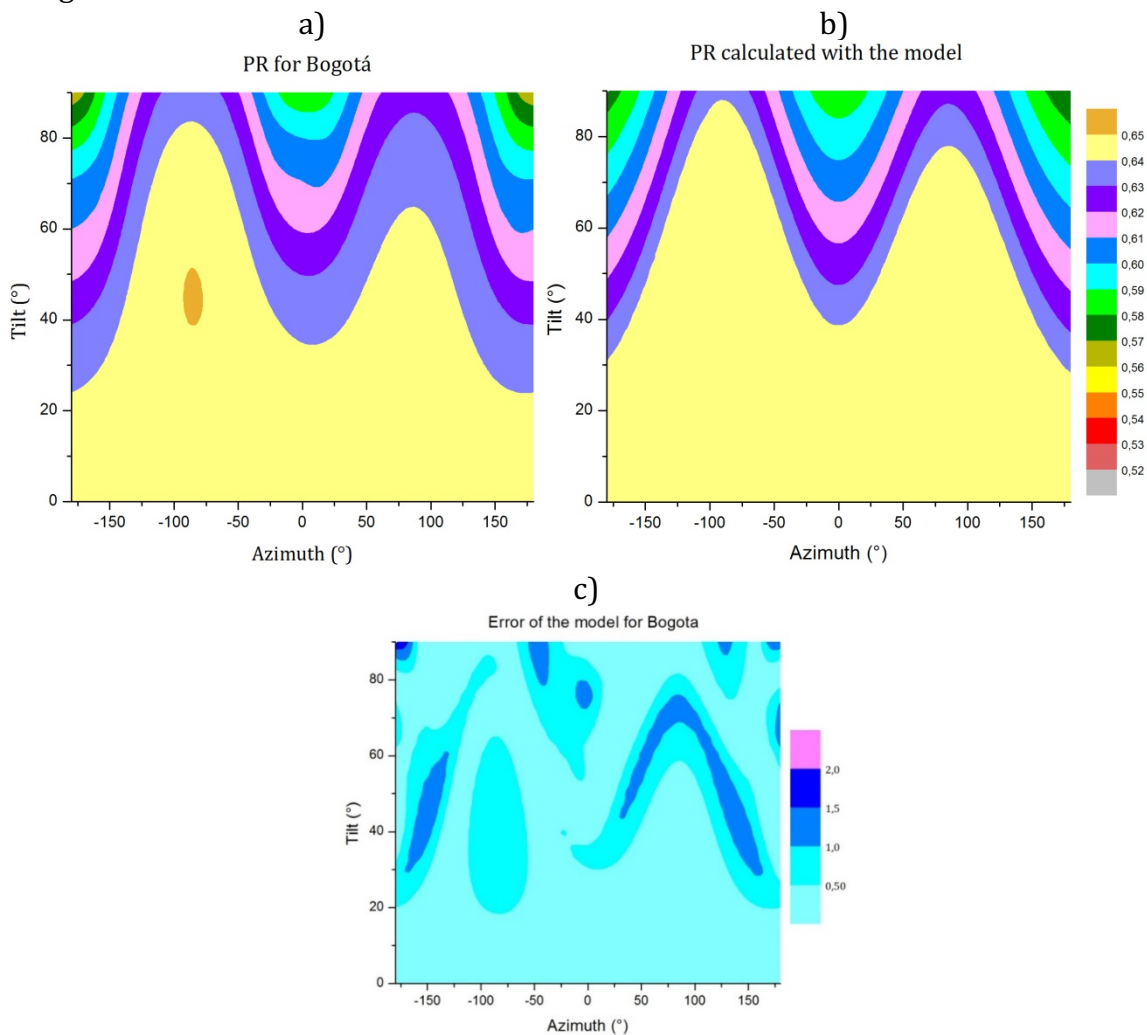


Fig. 3. PR para Bogotá. a) Obtenido con la simulación completa. b) Con el modelo propuesto. c) Porcentaje de error cometido

Como conclusión final, cabe destacar que emplear el modelo del PR de la ecuación (25) ahorra el tedioso trabajo de usar más de 40 ecuaciones, en más de 20.000 operaciones por computador. Consideramos que este modelo es una herramienta valiosa en proyectos de BIPV.

3.1.7. Uso del modelo para la creación de la APP sobre edificios fotovoltaicos RAITSUN

Con base en el modelo propuesto, se diseñó una APP llamada RAITSUN. Mediante esta APP se puede predecir la energía eléctrica y la rentabilidad que producirá un edificio que se rodee completamente de generadores solares, es decir, que use BIPV en sus fachadas y cubiertas. La versión beta es sólo para Colombia. La APP se desarrolló para Android. La interface de usuario se muestra en la figura 4.

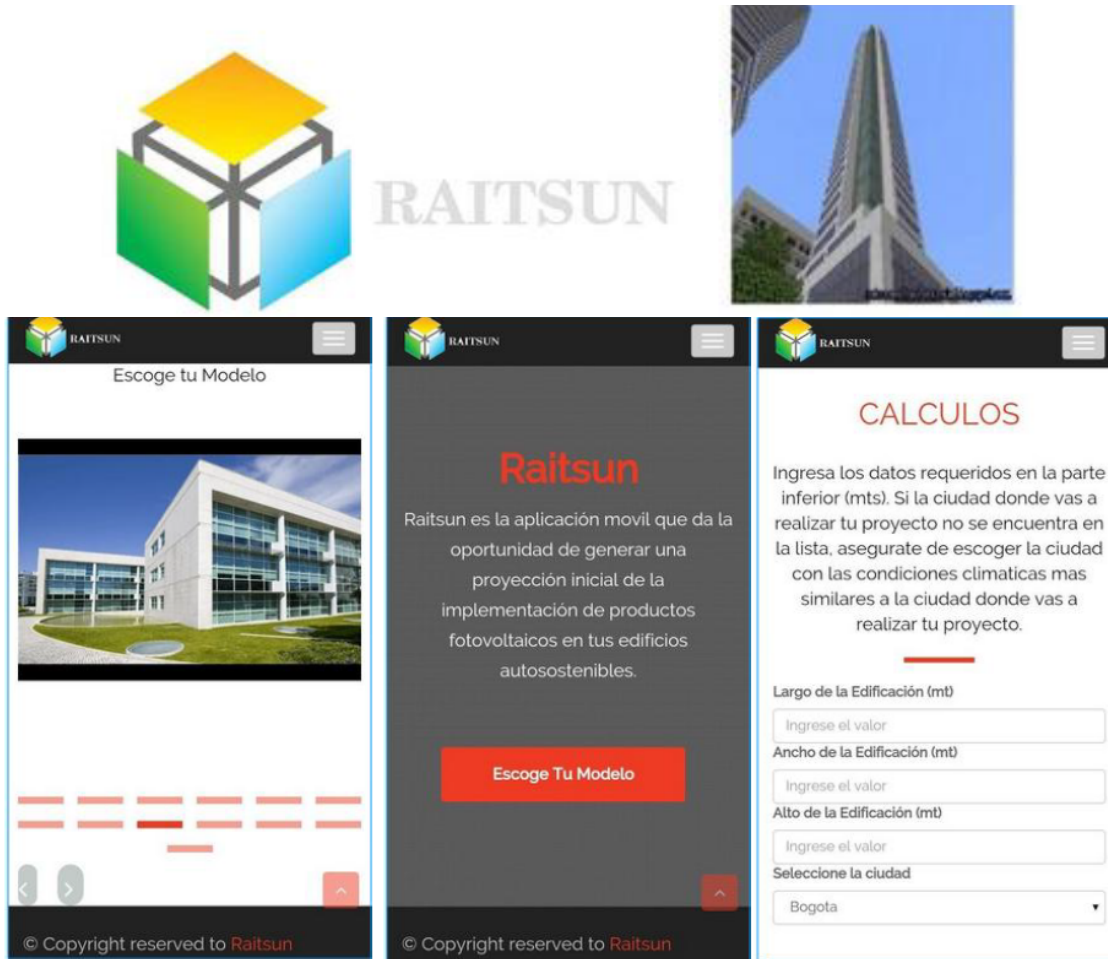


Fig. 4. Interface de usuario de la APP RAITSUN

3.2. Metodología propuesta para limitar las pérdidas por inclinación, orientación y sombreado en BIPV a nivel mundial

3.2.1. Pérdidas máximas permisibles por orientación e inclinación

Con el fin de proponer los límites de pérdidas por orientación e inclinación en BIPV, se encontró que la ciudad de España con menor irradiación solar anual es Bilbao, con 1292.1 kWh/m²año [27]. Así mismo, utilizando el gráfico de FI del CTE se encontró que 1520.1 kWh/m²año inciden sobre una superficie de inclinación óptima de esa ciudad. Por lo tanto, según el CTE, en esta localidad la *peor fachada aceptada* recibe el 60%, por lo cual $G_{a,\text{MIN},1}(90,0)=912.1 \text{ kWh/m}^2\text{año}$. Con esta irradiación se calcularon las máximas pérdidas permisibles para Colombia (caso de estudio). Los resultados se muestran en la tabla 5.

Tabla 5. Límites de pérdidas por inclinación y orientación.

Ciudad	$L_{\beta,\alpha,\text{MAX},2}$
Leticia	45%
Pasto	33%
Bogotá	42%
Cúcuta	48%
Barranquilla	53%

Con la tabla 5, y los gráficos del factor de irradiación de cada ciudad se graficó la figura 5. Las circunferencias concéntricas representan la inclinación del plano del generador, mientras que las líneas radiales se refieren al azimut. La región coloreada de verde cubre todas las posibles superficies de la edificación que cumplen con la norma propuesta, contrario a las que se encuentran en la región roja.

De las gráficas se deduce también que en algunas ciudades como Leticia, Pasto y Bogotá, es decir, cuando $\varphi \leq 7^\circ$ las fachadas no pueden usarse exclusivamente para BIPV. Sin embargo, se aclara que si el generador se distribuye una parte en fachada, y una parte en cubierta, se puede lograr el caso de que el porcentaje global de pérdidas esté dentro de los límites aceptables. Por otra parte, en las ciudades con latitudes mayores a 7° si existen fachadas con potencial para proyectos de BIPV. Entre más al norte esté la ciudad, mayor variedad de fachadas resultan permisibles.

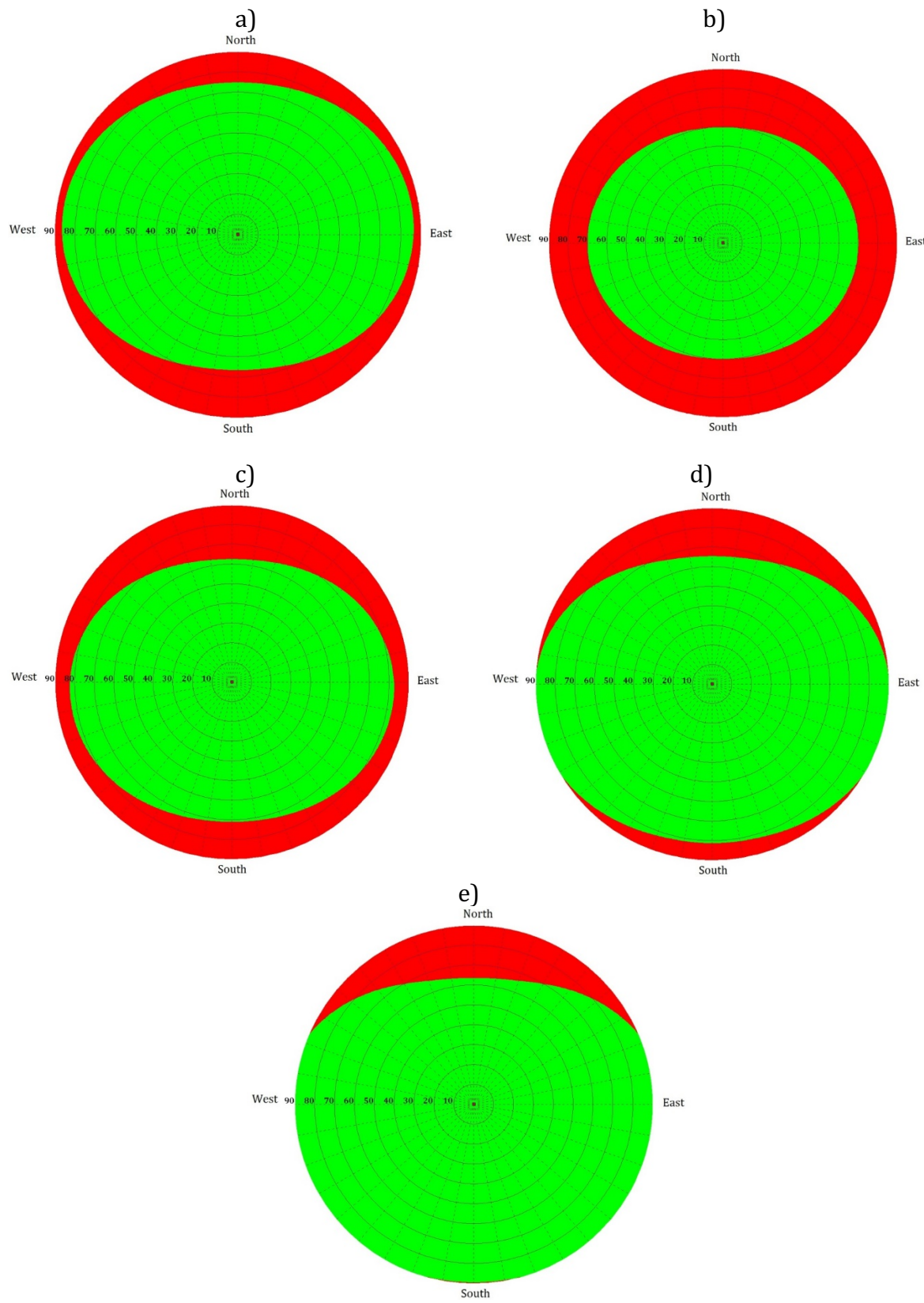


Fig. 5. Superficies posibles para a) Leticia ($\phi = -4,2^\circ$) b) Pasto ($\phi = 1,2^\circ$)
c) Bogotá ($\phi = 4,7^\circ$) d) Cúcuta ($\phi = 7,9^\circ$) e) Barranquilla ($\phi = 10,9^\circ$)

3.2.2. Pérdidas máximas permisibles por sombreado

En el caso de los límites de pérdidas por sombreado, se calculó la fracción de difusa en 54 ciudades de España. Los resultados se pueden apreciar en la figura 6, junto con el promedio del país, de 0.34.

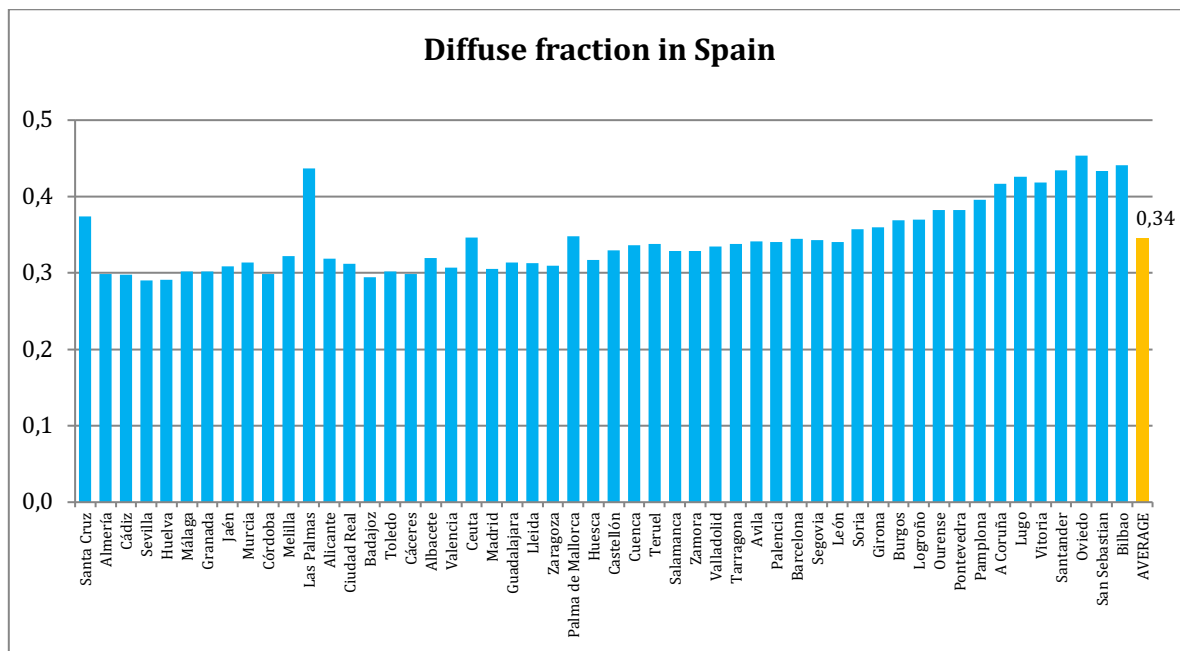


Fig. 6. Fracción de irradiación difusa para varias ciudades de España.

Por otra parte, según el CTE las pérdidas en el caso de sombreado total son del 84%. Esto implica que $B_{a,1}(0)=0.66G_{a,1}(0)$ y $D_{a,1}^C(0)=0.18G_{a,1}(0)$. Se deduce entonces que la fracción máxima de irradiación total fue de $f_{MAX,losses,1}=0.238$, correspondiente al 20% estipulado como pérdida.

En la figura 7 se muestra la suma de las componentes directa y difusa circunsolar para diferentes ciudades de Colombia (Lugar 2). Se puede observar que la variación es mayor que en España, razón por la cual se decidió proponer ciudades de referencia dentro del país. Por lo tanto, se calculó el promedio de las componentes para las ciudades dentro de la franja de latitudes que abarca cada ciudad referencia.

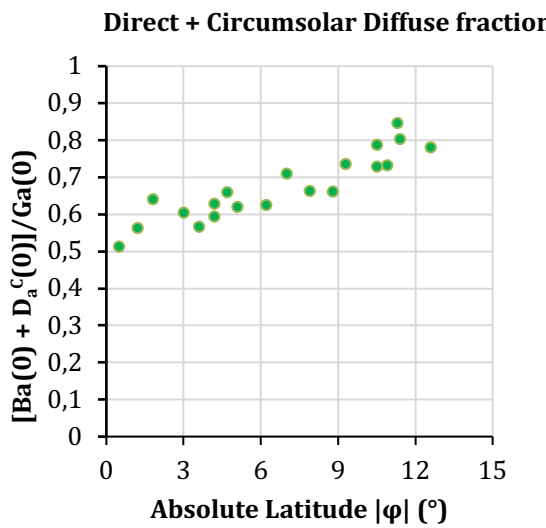


Fig. 7. Fracción de radiación directa más difusa circunsolar en función de la latitud.

En la tabla 6 se muestran los límites permisibles de pérdidas por sombreado, para el país de Colombia. En general, los valores son menores que los permitidos por el CTE de España. Esto se explica en el hecho de que Colombia tiene una mayor fracción de radiación difusa, y por lo tanto se puede perder una menor cantidad de radiación directa por sombreado. Se puede observar que los límites son muy similares en las ciudades de referencia, por lo cual cabe la posibilidad de considerar un único límite de 16% de pérdidas por sombreado para toda Colombia.

Tabla 6. Porcentajes máximos de pérdidas anuales por sombreado para Colombia.

Ciudad referencia	$L_{shading,MAX,2}$
Leticia	15%
Pasto	14%
Bogotá	15%
Cúcuta	16%
Barranquilla	18%

3.2.3 Propuesta para un estándar técnico mundial

Con el fin de proponer una expresión simple para hallar el límite de pérdidas debido a la orientación e inclinación para cualquier país, en la Figura 8 se representa este límite, en función la máxima irradiación solar anual del lugar. Se puede ver que los valores de esta variable oscilan entre 30% y 60%. Esta herramienta es de gran utilidad, ya que solo basta con ubicar el valor correspondiente a $G_a(\beta_{opt})$ de la ciudad, y asignar las pérdidas máximas correspondientes.

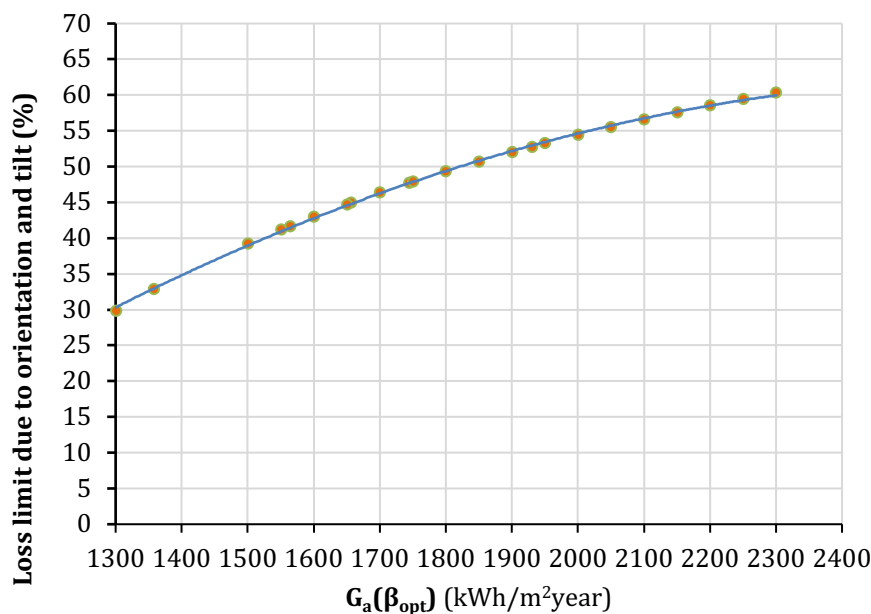


Fig 8. Límite de pérdidas debidas a la orientación e inclinación, contra la irradiación máxima anual de la ciudad..

Otra forma de hallar el valor exacto del límite es usar la siguiente expresión matemática, que corresponde a la misma ecuación (15), al reemplazar la irradiación solar anual de Bilbao:

$$L_{\beta,\alpha,MAX} = 100 \left(1 - \frac{1912.1}{G_a(\beta_{opt})} \right) \quad (30)$$

Del mismo modo, para encontrar una relación entre el límite de pérdidas debido al sombreado y la fracción difusa de la ciudad, se graficó la Figura 9. Se puede apreciar que sus cifras oscilan entre 10% y 25%, dependiendo del lugar.

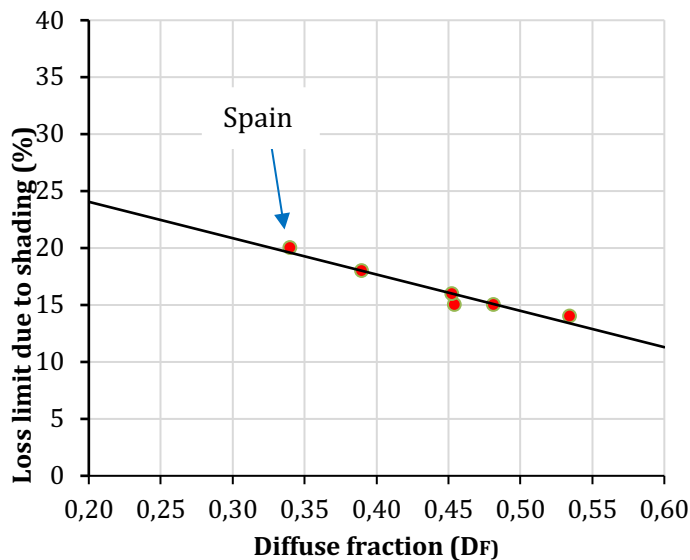


Fig 9. Límite de pérdidas debido al sombreado contra la fracción difusa de la ciudad.

Para calcular el valor exacto, se realizó una regresión lineal, resultando que los puntos establecen una relación de la siguiente manera ($R^2=0.943$):

$$L_{shading,MAX} = 31.907(0.951 - D_F) \quad (31)$$

En las figuras 8 y 9 se resume la propuesta de la norma técnica internacional. Estas herramientas son muy útiles para encontrar fácilmente las pérdidas máximas permitidas debido al sombreado, inclinación y la orientación de sistemas en BIPV. Sirven para futuras regulaciones en cualquier ciudad de un país, solo conociendo la fracción difusa y la irradiación máxima anual (G_a para $\beta=\beta_{opt}$). Este es un valioso insumo con miras a construir un futuro campo de eficiencia energética en BIPV.

3.3 Nuevo método para pre clasificar las fachadas potenciales en BIPV

3.3.1 Gráficos del factor de irradiación

Se graficó el FI para las diferentes ciudades. En las figuras 10 a 13 se muestran ejemplos para 4 ciudades.

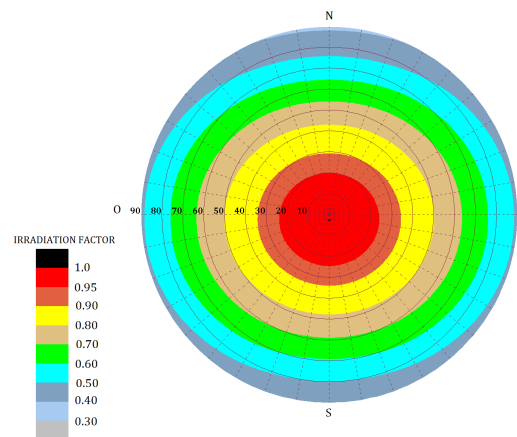


Fig. 10. Gráfico de FI para Cali ($\phi = 3.6^\circ$)

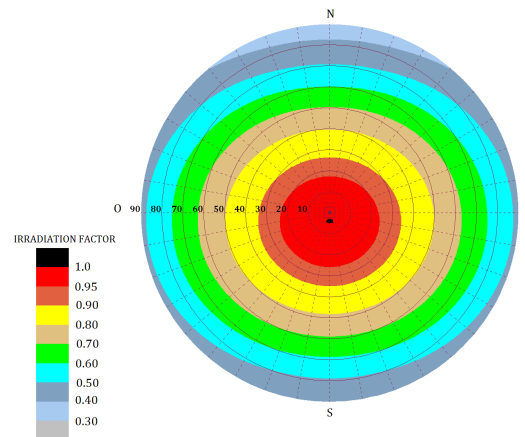


Fig. 11. Gráfico de FI Bogotá ($\phi = 4.7^\circ$)

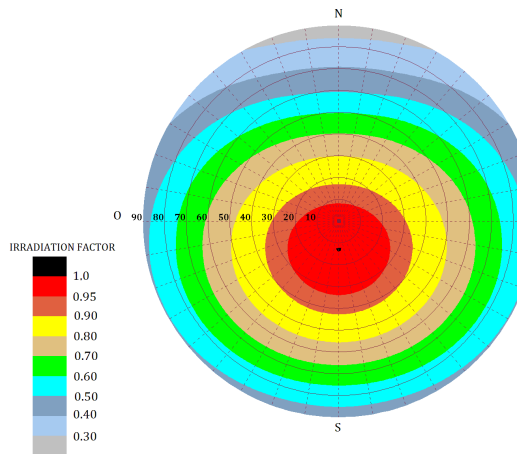


Fig. 12. Gráfico de FI para Barranquilla ($\phi = 10.9^\circ$)

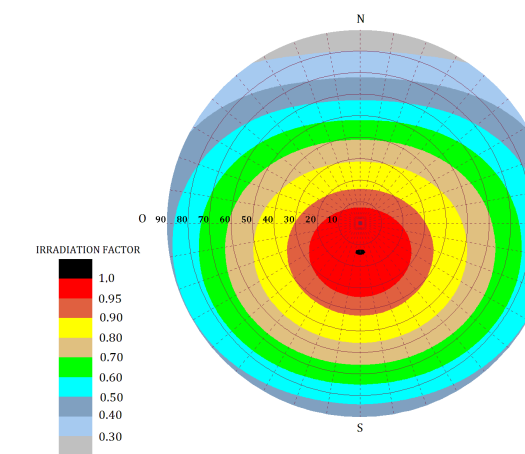


Fig. 13. Gráfico de FI San Andrés ($\phi = 12.6^\circ$)

Se puede observar que el factor de irradiación tiene valores entre 0.27 y 0.52 para las fachadas. Esto significa que se puede perder hasta el 73% de la energía solar al instalar módulos fotovoltaicos en una superficie vertical, en países de bajas latitudes. Por esta razón, es necesario contar con un método de preclasificación para elegir las fachadas más eficientes.

3.3.2 Modelo propuesto para el factor de irradiación en fachadas

La figura 14 muestra el factor de irradiación para las fachadas, en función del azimut y la latitud. Los máximos valores para FI se obtienen para fachadas orientadas en la dirección este-oeste, es decir, con un acimut de -90° y 90°, ya que se trata de ciudades de bajas latitudes.

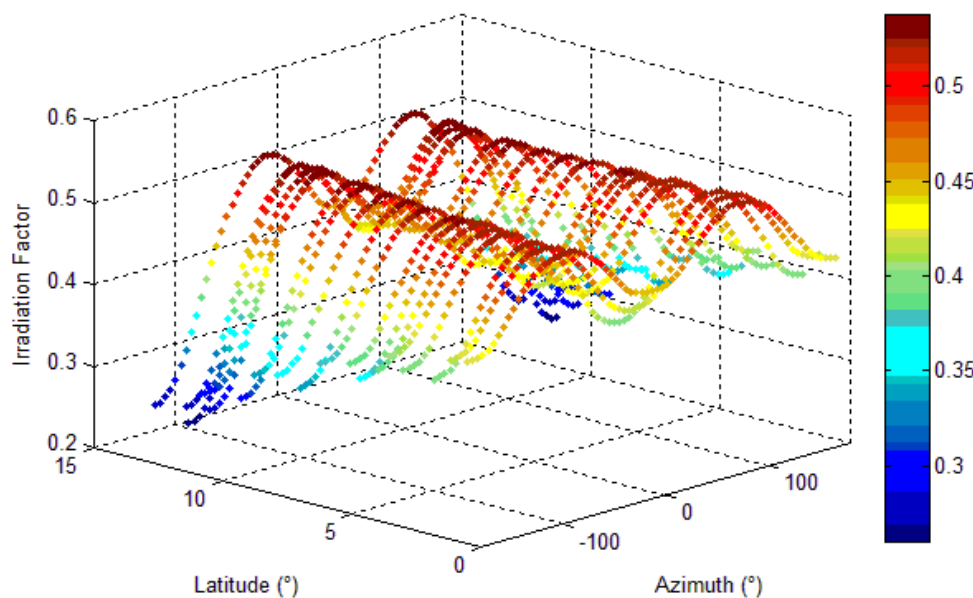


Fig. 14. Factor de irradiación para fachadas en función de la latitud y el azimut.

Con base en los datos de la figura 14 se desarrolló una expresión matemática. Se encontró que, para una misma latitud, la curva de puntos describe de forma aproximada una suma de dos funciones gaussianas. La amplitud y ubicación de tales funciones varía en función de la latitud del lugar. De acuerdo con esto, se propone el siguiente modelo para calcular el factor de irradiación en las fachadas:

$$FI_{facades} = A \cdot e^{-0.0002(\alpha - \alpha_0)^2} + A \cdot e^{-0.0002(\alpha + \alpha_0)^2} + 0.386 - 0.0127 \cdot |\varphi| \quad (52)$$

Donde

$$A = 0.1329 + 0.01413 \cdot |\varphi| \quad (53)$$

$$\begin{aligned} \alpha_0 &= 90 - 1.36 \cdot |\varphi| \\ |\varphi| &\leq 15^\circ \end{aligned} \quad (54)$$

Donde α es el ángulo de orientación de la fachada y ϕ la latitud de la ciudad, ambos en grados. Así, la expresión matemática obtenida solo requiere de dos parámetros de entrada. El primero de ellos es la ciudad donde el sistema fotovoltaico para BIPV será instalado: la latitud ϕ . El segundo caracteriza al plano de la fachada del generador, el ángulo de orientación α .

Es importante notar que para países ubicados en el hemisferio sur, el acimut cero se define como la dirección que apunta hacia el norte geográfico. Por lo tanto, la variable α en la ecuación del modelo se debe cambiar por $180-|\alpha|$ cuando se use en tales países.

3.3.3 Grado de precisión del modelo

La figura 15 fue construida con el fin de verificar el grado de precisión. Muestra los puntos obtenidos usando el largo y tedioso proceso descrito en la metodología, mientras que la superficie matemática fue calculada mediante el modelo propuesto. Se observa muy buen grado de ajuste, con un coeficiente de correlación de $R^2=0.98$. El error promedio cometido es aproximadamente igual al 5%.

Otra validación del modelo fue desarrollada mediante la reproducción de los resultados del factor de irradiación reportados para ciudades de Brasil [35], los cuales se ajustan con alto grado de exactitud.

Finalmente, se describe lo siguiente para tener una idea del ahorro en el trabajo al usar el modelo propuesto para calcular FI. Para establecer cada punto negro de la figura 28, fue necesario usar más de 30 ecuaciones, en un algoritmo computacional que desarrolló más de 4000 operaciones. Al contrario, sólo la ecuación (52) fue usada para generar la superficie matemática de la figura 15.

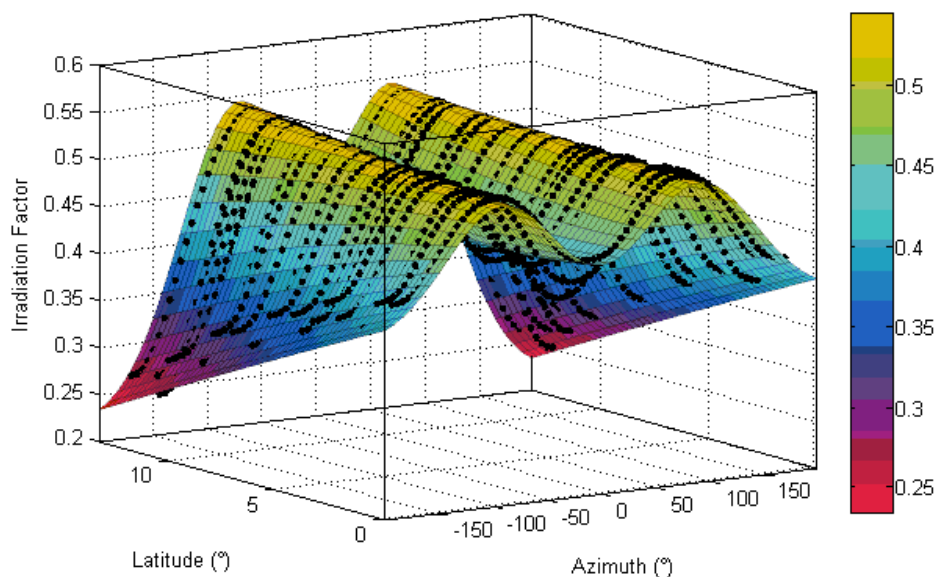


Fig. 15. Precisión del modelo para fachadas potenciales en BIPV .

3.3.4 Validación del modelo

Con el fin de validar el modelo, se realizó una comparación con los valores del FI obtenidos mediante el uso del sitio web PVWATTS® [36]. Esta herramienta fue desarrollada por el Laboratorio Nacional de Energía Renovable de NREL de Estados Unidos, y a menudo se usa en proyectos fotovoltaicos. Se escogió esta herramienta, ya que las últimas versiones presentan una precisión aproximada del 2% [50]. El procedimiento de validación se describe a continuación:

1. La ciudad se seleccionó en PVwatts®.
2. El tamaño del sistema se estableció en 1000Wp.
3. Las pérdidas del sistema se establecieron en un valor dado.
4. Se introducen los valores de $\alpha = 0$, $\beta = \beta_{\text{opt}}$
5. En los resultados se obtiene $G_a(\beta_{\text{opt}}, 0)$
6. Los valores α se introducen para la orientación particular a estudiar.
7. Se fija ser $\beta = 90^\circ$.
8. En los resultados se obtiene $G_a(\beta, \alpha)$
9. FI se calcula con la ecuación 1.
10. El valor anterior se compara con el obtenido usando la ecuación del modelo propuesto.

Los resultados se pueden ver en la figura 16. En general, el modelo funciona bastante bien, y tiene la ventaja de que no necesita conexión a internet, como la herramienta PVwatts®. El error promedio fue del 4% para Bogotá y 7% para Nicaragua. Esto podría indicar que el error se incrementa en función de la latitud. Por otra parte, PVwatts® no funciona muy bien para lugares donde no hay estaciones meteorológicas, especialmente en ubicaciones por fuera de Estados Unidos. Por estas razones consideramos que el modelo propuesto tiene mucho valor para realizar cálculos rápidos, y preclasificar fachadas en proyectos BIPV.

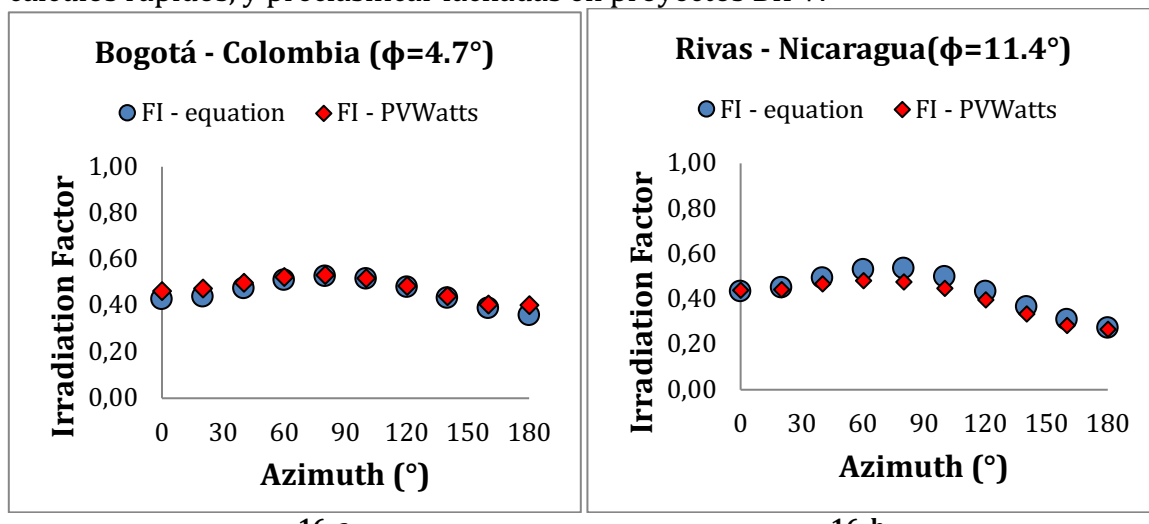


Fig. 16. Factor de irradiación calculado mediante el modelo propuesto, y el sitio web PVWatts®. a) El caso para Bogotá-Colombia. b. El caso para Rivas – Nicaragua.

3.3.5 Metodología propuesta para la pre-clasificación de fachadas en BIPV

El siguiente procedimiento propuesto se utilizará para clasificar previamente una posible fachada BIPV ubicada en países con bajas latitudes:

1. Definir la latitud del lugar ϕ y la orientación α , que caracterizan la fachada del edificio.
2. Calcular el factor de irradiación FI de la fachada usando la ecuación 52.
3. Establecer la irradiación solar anual sobre plano horizontal del lugar $G_a(0)$, disponible en los atlas de radiación.
4. Calcular la irradiación solar sobre la superficie óptima $G_a(\beta_{opt})$, usando la ecuación:

$$G_a(\beta_{opt}) = \frac{G_a(0)}{1 - 0,0015 \cdot |\phi| - 0,00007 \cdot |\phi|^2} \quad (55)$$

Donde ϕ es la latitud del lugar

5. Calcular la irradiación solar en la fachada $G_a(90,\alpha)$, usando la ecuación:

$$G_a(90,\alpha) = FI_{facades} \cdot G_a(\beta_{opt}) \quad (56)$$

6. Utilizar el valor obtenido de $G_a(90,\alpha)$ para clasificar la fachada, de acuerdo con la "Clasificación de eficiencia energética para fachadas en BIPV" en la figura 17. Esta clasificación se desarrolló con base en publicaciones sobre la cantidad de irradiación solar que recibe una fachada en diferentes lugares del mundo.

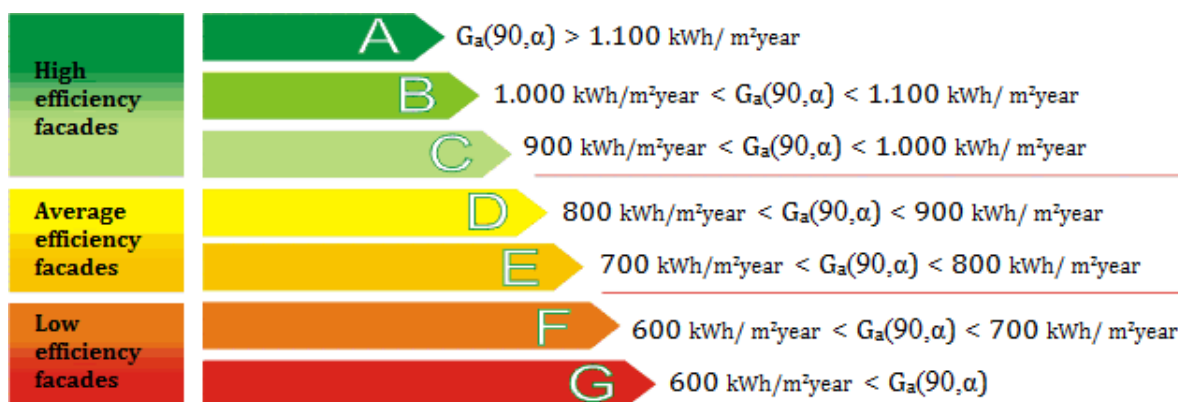


Fig. 17. Clasificación de eficiencia energética para fachadas en BIPV.

7. Concluir sobre el uso potencial de la fachada para BIPV.

Los resultados obtenidos cuando se utiliza la metodología propuesta para 8 ciudades en Colombia se muestran en la Tabla 7.

Tabla 7. Preclasificación de fachadas para 8 ciudades

Ciudad	Latitude φ (°)	β _{opt} (°)	G _a (β _{opt}) (kWh/m ² year)	G _{a,min} (90) (kWh/m ² year)	G _{a,max} (90) (kWh/m ² year)	Clasificación energética	de	eficiencia
Leticia	-4.2	4	1656	612,72	861,12	D	E	F
Pasto	1.2	0	1488	624,96	773,76		E	F
Cali	3.6	2	1495	612,95	777,4		E	F
Bogotá	4.7	4	1743	819,21	906,36	C	D	
Medellín	6.2	5	1643	624,34	854,36		D	E
Cúcuta	7.9	8	1746	611,1	907,92	C	D	E
Barranquilla	10.9	13	1942	582,6	1009,84	B	D	F
San Andrés	12.6	14	2078	561,06	1080,56	C	D	G

Una vez que se ha realizado la clasificación previa de las fachadas potenciales, los arquitectos e ingenieros pueden proceder a calcular el potencial BIPV completo, incluyendo los factores de forma y sombreado, utilizando un software especializado.

3.4 Procedimiento propuesto para integrar los modelos y herramientas de esta investigación

A continuación se describe el procedimiento sugerido para usar las herramientas y modelos desarrollados en la presente investigación doctoral, en proyectos de BIPV:

CARACTERIZACIÓN DEL PROYECTO:

1. Caracterizar el lugar donde se realizará la instalación, determinando su latitud, temperatura ambiente, fracción de difusa, e irradiación solar anual sobre plano horizontal.
2. Caracterizar las diferentes superficies del edificio que son potenciales para emplear BIPV, determinando sus ángulos de orientación e inclinación, y los valores de áreas útiles potenciales.

DESCARTE DE SUPERFICIES:

3. Usar los gráficos del factor de irradiación para calcular las pérdidas por orientación e inclinación, mediante el procedimiento de la sección 3 del capítulo 6.
4. Determinar los valores máximos permitidos de pérdidas por sombreado y orientación en el lugar, mediante el uso de las figuras 8 y 9.
5. Descartar las superficies con pérdidas mayores a las permitidas.

CÁLCULO DE LA ENERGÍA PRODUCIDA:

6. Calcular el Performance Ratio para cada fachada, con el modelo obtenido en la sección 3.1.5
7. Usar la expresión (1) y los gráficos del factor de irradiación para calcular la energía eléctrica anual que produciría cada superficie.

PRE-CLASIFICACIÓN DE FACHADAS CON LA EFICIENCIA ENERGÉTICA:

8. Calcular el factor de irradiación de cada fachada con la ecuación (52)
9. Preclasificar las fachadas mediante el procedimiento explicado en la sección 3.3.5, y ordenarlas según la eficiencia energética.
10. Finalmente, se procede a evaluar el costo por kWp cada subsistema BIPV, empezando por aquellas fachadas que tienen mejor clasificación.

Capítulo 4

Nuevo modelo para el PR en sistemas BIPV

Título:	A new model to predict the energy generated by a photovoltaic system connected to the grid in low latitude countries
Autores:	Luis Fernando Mulcué-Nieto, Llanos Mora-López.
Revista:	Solar Energy, Elsevier
Factor de impacto JCR:	4.7 - Q1
Año:	2014
Categoría:	Renewable Energy, Sustainability and the Environment
Publicación:	Volume 107, September 2014, Pages 423-442.
DOI:	10.1016/j.solener.2014.04.030



Available online at www.sciencedirect.com

ScienceDirect

Solar Energy 107 (2014) 423–442

**SOLAR
ENERGY**

www.elsevier.com/locate/solener

A new model to predict the energy generated by a photovoltaic system connected to the grid in low latitude countries

Luis Fernando Mulcué-Nieto ^{a,b,*}, Llanos Mora-López ^{b,c}

^a GIDTA Group, Research Group in Environmental and Technological Developments, Universidad Católica de Manizales, Carrera 23 No. 60 – 63, Manizales, Colombia

^b Universidad Internacional de Andalucía, Calle Severo Ochoa 16, 29590 Málaga, Spain

^c Department of Computer Languages and Sciences, ETSI Informática, Universidad de Málaga, Campus de Teatinos, 29071 Málaga, Spain

Received 24 February 2014; received in revised form 21 April 2014; accepted 22 April 2014

Available online 28 June 2014

Communicated by: Associate Editor Nicola Romeo

Abstract

The use of photovoltaic solar energy is a growing reality worldwide and its main objective is to meet electricity demand in a sustainable manner. The so-called Grid-Connected Photovoltaic Power Systems (GCPS) prevail in urban zones, together with Building-integrated Photovoltaics (BIPV); whose performance and energy efficiency depends on different factors. The main aspects include those related to the solar radiation available in the geographical location of the facility, the climate, the orientation and tilt of the used surfaces, the appropriate design of the system and the quality of the components. Therefore, several methods have been proposed to try to predict the influence of the aforementioned variables on the amount of electricity produced. However, the majority are very tedious to implement or do not take the specific characteristics of the system into account.

This paper proposes a simple and reliable expression, which can be used in low latitude countries. The case study is likewise performed for Colombia, with a comparative analysis for different cities of the angular losses and due to dirt, the losses due to temperature, the DC–AC conversion losses and the Performance Ratio of the system (PR).

© 2014 Elsevier Ltd. All rights reserved.

Keywords: Building-integrated Photovoltaics (BIPV); Performance Ratio (PR); Energy produced by a photovoltaic system; Performance of a photovoltaic system

1. Introduction

Photovoltaic solar energy is an excellent option to meet the energy demands of the world population, by means of generating electricity in a distributed manner (Pearce,

2002). Thousands of electricity generators have therefore been installed using this process around the world. The so-called Grid-Connected Photovoltaic Power Systems (GCPS) prevail in urban zones and they meet the energy needs of the building or housing unit, while the surplus electricity produced is injected into the grid.

On the other hand, installing photovoltaic panels on the surfaces of the buildings has become necessary due to the spatial and economic restrictions. This has led to a highly important and developed sector, Building-integrated Photovoltaics (BIPV), where different construction elements

* Corresponding author at: GIDTA Group, Research Group in Environmental and Technological Developments, Universidad Católica de Manizales, Carrera 23 No. 60 – 63, Manizales, Colombia. Tel.: +57 68782900x3300; fax: +57 68782937.

E-mail addresses: lmulcue@ucm.edu.co (L.F. Mulcué-Nieto), llanos@lcc.uma.es (L. Mora-López).

such as roofs, frontages or windows are replaced by photovoltaic modules.

One of the main goals in the field of BIPV is to achieve optimum aesthetic, economic and technical solutions, thus making sure that all the new constructions will be “Zero Energy Buildings” (ZEB) (Kanters and Horvat, 2012). In order to achieve this, it is vital to forecast the amount of electricity produced by the facility, so the net energy balance can be calculated. This calculation must be carried out in one of the design stages of the system.

In 1998, the *International Electrotechnical Commission* (IEC) published the IEC 61724 International Standard. This standard describes the recommendation for analysing the electrical performance of the photovoltaic systems. One of the characteristic parameters is the annual energy produced, which can be calculated using the following equation for Grid-Connected Photovoltaic Power Systems (The International Electrotechnical Commission (IEC), 1998):

$$E_{PV} = \frac{G_a(\beta, \alpha) \cdot P_{peak} \cdot PR}{G_{STC}} \quad (1)$$

where $G_a(\beta, \alpha)$ is the annual solar radiation on the generator surface, P_{peak} is the installed photovoltaic peak power, PR the annual yield of the facility known as the “Performance Ratio” and G_{STC} the solar irradiance under standard measurement conditions, equal to 1 kW/m^2 .

The $G_a(\beta, \alpha)$ value can be easily obtained by means of graphs of the so-called *Irradiation Factor* (FI) (Thomas, 2012; Roberts and Guariento, 2009). Therefore, the problem of calculating the electricity produced is mainly reduced to determining the PR value. Yet this task is not easy, as the performance depends on several factors such as the solar radiation available in the geographical location of the facility, the climate, the orientation and tilt of the used surfaces, the appropriate design of the system and the quality of the components, among others.

In order to solve the above problem, different methods have been put forward to predict the influence of different variables on the amount of electricity generated. Some of them are analytical, for example, those used by Osterwald (1986), Araujo et al. (1982) or Green (1998); which allow the temperature losses to be calculated. Other procedures have likewise been proposed that include more variables, based on artificial neuronal networks (Almonacid et al., 2009; Rodrigo et al., 2012). However, the majority of them are very tedious to implement, while others do not take into account the specific characteristics of the system.

Another way that has been proposed to solve the problem is to use a standard performance of $PR = 0.75$ for any photovoltaic system (Markvart and Castaner, 2003), which is not appropriate as the specific variables of the place must be taken into account. For example, studies of PR in 8 countries have been reported, obtaining values between 0.42 and 0.81 (Mondol et al., 2006). This is coherent, as the performance of the photovoltaic modules depends on

the ambient temperature of the place. Latitude likewise plays an important role, as its effect on solar irradiation means that the power supplied to the entrance of the inverter may be very low within certain time periods, thus reducing the DC–AC conversion efficiency.

Another important factor that prevents a generalised PR being used for BIPV applications are the energy losses caused by the tilt and orientation of the generator plane. Their origin lies in the fact that sun light is reflected more when the incidence angle is small with respect to the surface. The losses due to dust and dirt also depend on this variable. Thus, the PR is expected to vary for a single building, due to the large amount of surfaces available to be used on roofs and frontages.

According to what has been discussed, the large amount of factors present makes it very difficult to forecast the performance of the photovoltaic facility. It is therefore necessary to implement a simple method that can be used by architects and engineers. This is very important as many countries need to expand photovoltaic solar energy. In Colombia, for example, non-grid connected zones, that is, places that are not connected to electricity by means of the *Sistema de Interconexión Nacional* [Colombian power grid] account for nearly 52% of national territory (Senado de la República de Colombia, 2003). Furthermore, it is recommended to implement BIPV within the cities in order to obtain economic and environmental benefits.

This paper proposes a simple and reliable expression, which can be used in low latitude countries. The case study is likewise performed for Colombia, with a comparative analysis for different cities of the angular losses and due to dirt, the losses due to temperature, the losses of DC–AC conversion and the Performance Ratio of the system (PR). When carrying out this study, it is not only essential to correctly predict the energy produced by the future photovoltaic system, but it also provides a benchmark parameter to compare data from the monitoring system to be implemented with the estimated data in the design stage.

2. Loss factors in a grid-connected photovoltaic system

2.1. Losses due to dust and dirt

These are mainly due to the dust particles deposited on the glass surface of the photovoltaic module, which reduce light transmission to the solar cells. Generally, its impact is quantified in terms of the reduction in normal transmittance $T(0)$, with respect to what would have been obtained if the modules were completely clean. The typical values are set out in Table 1 (Luque and Hegedus, 2011), where $T_{dirt}(0)$ represents the transmittance of the normal incidence light when the surface is dirty, while $T_{clean}(0)$ implies that it is completely clean.

In keeping with the above, the losses from dirt can be calculated as:

Table 1

Usual values of normal incidence loss due to dirt on the modules. Source: [Luque and Hegedus \(2011\)](#).

Degree of dirt	$T_{dirt}(0)/T_{clean}(0)$	Losses (%)
None	1	0
Low	0.98	2
Medium	0.97	3
High	0.92	8

$$L_{dirtiness} = 1 - \frac{T_{dirt}(0)}{T_{clean}(0)} \quad (2)$$

It is important to note that Eq. (2) allows the normal incidence to be referred to, as when the incidence angle is different; the dust causes shadows of variable length on the surface. This fact must be taken into account regarding the angular losses.

2.2. Angular losses

The angular losses are determined for each surface, in other words, for each value pair (β, α) , where β is the tilt angle and α is the orientation with respect to the South (see Fig. 1).

Even though different expressions have been put forward to calculate the angular losses ([Preu, 1995](#); [Krauter and Grunow, 2006](#); [Engineers, 1978](#)), the Martin-Ruiz model ([Martin and Ruiz, 2001](#)) reproduces real results ([Zang and Wang, 2011](#)) and is relatively simple. The hourly global irradiance $G'_h(\beta, \alpha)$ incident on the module is made up by the contributions of the direct $B_h(\beta, \alpha)$, circumsolar diffuse $D_h^C(\beta, \alpha)$, isotropic diffuse $D_h^I(\beta, \alpha)$, and reflected $R_h(\beta, \alpha)$ radiation; thus:

$$G'_h(\beta, \alpha) = FT_B \cdot B_h(\beta, \alpha) + FT_B \cdot D_h^C(\beta, \alpha) + FT_D \cdot D_h^I(\beta, \alpha) + FT_R \cdot R_h(\beta, \alpha) \quad (3)$$

where FT_B , FT_D , FT_R are the relative transmittances, standardised by the normal incidence total transmittance and are calculated by means of the expressions:

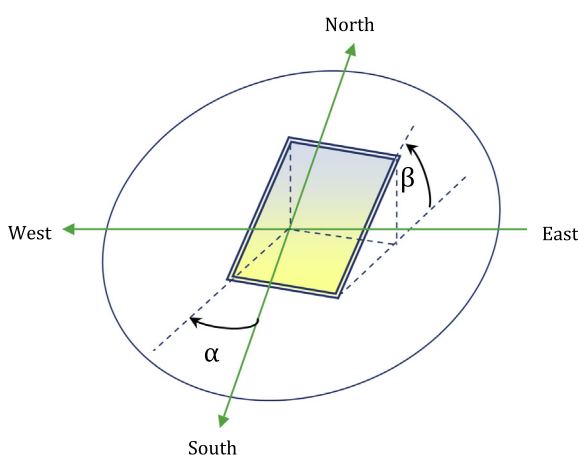


Fig. 1. Representation of the azimuth angle and orientation of a surface.

$$FT_B = 1 - \frac{\exp\left(-\frac{\cos \theta_s}{a_r}\right) - \exp\left(-\frac{1}{a_r}\right)}{1 - \exp\left(-\frac{1}{a_r}\right)} \quad (4)$$

$$FT_D = 1 - \exp\left\{-\frac{1}{a_r}\left[c_1\left(\sin \beta + \frac{\pi - \beta - \sin \beta}{1 + \cos \beta}\right) + c_2\left(\sin \beta + \frac{\pi - \beta - \sin \beta}{1 + \cos \beta}\right)^2\right]\right\} \quad (5)$$

$$FT_R = 1 - \exp\left\{-\frac{1}{a_r}\left[c_1\left(\sin \beta + \frac{\beta - \sin \beta}{1 - \cos \beta}\right) + c_2\left(\sin \beta + \frac{\beta - \sin \beta}{1 - \cos \beta}\right)^2\right]\right\} \quad (6)$$

where θ_s is the incident angle between the sun rays and the normal one for the plane in question, while a_r , y , c_2 are parameters of the degree of dirt and appear in [Table 2](#). The value of c_1 is $4/(3\pi)$ in all cases.

By calculating the sum of Eq. (3) for every day of the year, the annual solar irradiation incident on the generator $G'_a(\beta, \alpha)$ is obtained. In a similar way, if it is established that FT_B , FT_D , FT_R are equal to 1, the annual solar irradiation $G_a(\beta, \alpha)$ is obtained in the case of the total absence of angular losses. By comparing these two amounts, the annual angular losses are obtained:

$$L_{angular} = 1 - \frac{G'_a(\beta, \alpha)}{G_a(\beta, \alpha)} \quad (7)$$

Some annual angular loss values were calculated in European countries for the case of south-facing surfaces, resulting in values ranging between approximately 3% and 8%, depending on the tilt degree ([Martin and Ruiz, 2001](#)).

2.3. Losses due to differences with the nominal power

In the majority of the photovoltaic facilities, the installed real power differs from the nominal power stated by the manufacturer, under *standard test conditions* (STC). These conditions are defined as an incident irradiance of 1000 W/m^2 , temperature of the photovoltaic cell of 25°C , AM 1.5G standard spectrum.

This fact is due to each module having a manufacturing tolerance $\Delta P/P_{nom}$, defined as the percentage difference between the real power P_{real} and the nominal power P_{nom} . For example, values have been measured from 3% to 26% less in operating modules ([M. Drif et al., 2007](#); [Jahn and Nasse, 2007](#)).

Table 2

Usual values of the a_r and c_2 parameters for silicon modules. Source: [Luque and Hegedus \(2011\)](#).

$T_{dirt}(0)/T_{clean}(0)$	a_r	c_2
1	0.17	-0.069
0.98	0.20	-0.054
0.97	0.21	-0.049
0.92	0.27	-0.023

2004; Poissant and CanmetENERGY, 2009; Atmaram et al., 2008; Detrick et al., 2005; Carr and Pryor, 2004). Table 3 summarises some research showing the great dispersion of this parameter.

The high percentages reported may result in system performances of under 60% (Jahn and Nasse, 2004). However, recent studies have concluded that manufacturers are increasingly more responsible for this situation. Proof of this is the research carried out by *Solar America Board for Codes and Standards* (“Solar America Board for Codes and Standards (Solar ABCs),” 2013), where 9422 modules were reviewed, concluding that less than 0.7% of the total presented power under 97% of the nominal power (TamizhMani, 2011).

For a generator consisting of n modules equal to nominal power P_{nom} , losses due to differences with the nominal power L_{rating} are determined by:

$$L_{rating} = 1 - \frac{1}{n} \sum_{i=1}^n \frac{P_{real,i}}{P_{nom}} \quad (8)$$

where real $P_{real,i}$ represents the real power of the i th module.

If the modules are well selected, the losses due to differences with the nominal power can be estimated as being equal to 5% as a maximum (Almonacid et al., 2011).

2.4. Mismatch losses

When performing photovoltaic module parallel or serial connections, experience has shown that the total power of the system is not equal to the sum of the individual power. This energy deficit is attributed to the so-called *mismatch losses*, which are mainly caused by the partial shading of the generator and the dispersion of the electricity properties of the modules (Chouder and Silvestre, 2009).

The electric characteristics of each unit of the generator may vary due to the manufacturer's tolerance or degradation processes. The latter includes the degradation of the anti-reflective coating, the discoloration of the housing material, the degradation caused by light, hot points, and the mechanical breaking of the cell structure (Picault et al., 2010).

Due to the great many factors intervening in this aspect, there is no simple expression to predict this type of loss. However, there is research that has detected values up to 6% due to this concept (Baltus et al., 1997), while other

research indicates that they are between 2% and 4% (Almonacid et al., 2011).

2.5. Temperature losses

In the case of monocrystalline silicon modules, the output power drops by around 4% for each 10 °C increase in temperature (Luque and Hegedus, 2011). This is mainly due to the effect of the heating on the open circuit voltage of the photovoltaic cells.

The most common expression to calculate the maximum power that each module can deliver is the one proposed by Osterwald (1986), as it produces satisfactory results (Almonacid et al., 2011), despite its simplicity. This model uses the STC conditions as the benchmark:

$$P_{max} = P_{max,STC} \frac{G'(\beta, \alpha)}{G_{STC}} [1 + \gamma(T_c - 25)] \quad (9)$$

where P_{max} is the maximum power in W, $G'(\beta, \alpha)$ the incident irradiance on the surface in W/m^2 , $P_{max,STC}$ is the maximum power of the module in STC conditions in W, $G_{STC} = 1000 \text{ W/m}^2$, γ is the variation coefficient of the power peak with the temperature, and T_c the instantaneous temperature of the photovoltaic cells. The latter is given by:

$$T_c = T_a + G'(\beta, \alpha) \frac{TONC - 20}{800} \quad (10)$$

where T_a is the ambient temperature and $TONC$ is the nominal operating temperature of the cell, in other words, the one reached in normal incidence conditions under an irradiance equal to 800 W/m^2 and ambient temperature of 20 °C.

Pursuant to the above, the instantaneous temperature losses would be given by the difference between the real power P_{max} and the hypothetical power produced if the cells were working at 25 °C, resulting in:

$$L_{temperature,ins} = -\gamma(T_c - 25) \quad (11)$$

It can be seen that these losses depend on the temperature of the cells, in other words, of the ambient temperature and of the incident irradiance on the generator plane. In a similar way, they are determined for a time period by the expression proposed Caamaño Martín (1998):

$$L_{temperature} = -\gamma(TOE - 25) \quad (12)$$

where TOE is the *Equivalent Operating Temperature* of the generator in the period in question, weighted by the incident irradiance:

Table 3

Absolute percentage differences between the nominal power issued by the manufacturer and the real operating power of the modules.

Country	$ \Delta P/P_{nom} _{min} (\%)$	$ \Delta P/P_{nom} _{max} (\%)$	Reference
Spain	9	11	Drif et al. (2007)
Germany	5	26	Jahn and Nasse (2004)
Canada	6.5	23	Poissant and CanmetENERGY (2009)
USA	0	19.7	Atmaram et al. (2008), Detrick et al. (2005)
Australia	0.7	25.1	Carr and Pryor (2004)

$$TOE = \frac{\int_{\tau} T_c \cdot G'(\beta, \alpha) \cdot dt}{\int_{\tau} G'(\beta, \alpha) \cdot dt} \quad (13)$$

It can be seen that these losses are complex to evaluate for each system in particular, as they depend on the tilt and orientation of the generator, the incident irradiance on the plane of the generator (and therefore also on the angular losses) and the ambient temperature of the place. Typical values range between 5% and 15% (Almonacid et al., 2011).

2.6. Losses due to monitoring errors of the power maximum peak (PMP)

When the inverter cannot locate the optimal working point of the generator in the current curve–voltage, losses occur due to power being generated that is lower than expected. These losses depend on external and internal factors to the inverter, including (Jantsch, 1997):

- The PMP monitoring mechanism.
- The electrical characteristics of the generator.
- The incident irradiance and its irregularities.
- The ambient temperature.

Research conducted in 100 residential photovoltaic installations in Japan, by the Japanese monitoring programme, concludes that the average losses due to monitoring errors of the power maximum peak L_{SPMP} are of the order of 6% (Sugiura et al., 2003). This is consistent with data reported by the Spanish *Centre for Technological, Environmental and Energy Research* (CIEMAT) (“Centro de Investigaciones Energéticas, Medioambientales y Tecnológicas de España (CIEMAT),” 2013), with respect to which the standard values range between 4% and 6% for clear days and partially clouded days, respectively (Alonso-Abella and Chenlo, 2004).

2.7. Losses in the inverter due to DC–AC conversion

The DC–AC conversion efficiency of the inverters is the function, mainly, of the input power. However, it also affects the value of the input voltage and working temperature to a lesser extent. A frequently used model to describe this behaviour is the one proposed by Schmidt, according to which the instantaneous efficiency of the inverter is calculated by means of the equation (Jantsch et al., 1992):

$$\eta_{inverter} = \frac{P_{output}}{P_{input}} = \frac{P_{out}}{P_{out} + k_0 + k_1 \cdot P_{out} + k_2 \cdot P_{out}^2} \quad (14)$$

where

$$P_{out} = \frac{P_{output}}{P_{nominal}} \quad (15)$$

P_{input} is the instantaneous power at the input of the inverter in W, P_{output} is the instantaneous power at the output of the inverter in W, $P_{nominal}$ is the output nominal power of the

inverter at W, k_0 is the self-consumption loss coefficient, k_1 is the coefficient of losses proportional to the power and k_2 is the coefficient of losses proportional to the square of the power. Those parameters can be obtained of the efficiency curve of the inverter, provided by the manufacturer.

For simulation purposes, it is better to use an equivalent expression, but in terms of the input power:

$$\eta_{inverter} = \frac{P_{output}}{P_{input}} = \frac{p_{in} - (b_0 + b_1 \cdot p_{in} + b_2 \cdot p_{in}^2)}{p_{in}} \quad (16)$$

where

$$p_{in} = \frac{P_{input}}{P_{nominal}} \quad (17)$$

The values of the normally used coefficients are $b_0 = 0.02$, $b_1 = 0.02$, $b_2 = 0.07$; and are characteristics of the inverter type. These values match those of the Schmidt model $k_0 = 0.02$, $k_1 = 0.025$, $k_2 = 0.08$; and were calculated by choosing a representative sample of inverters existing on the markers (Jantsch et al., 1992).

The aforementioned expression enables the losses in the inverter to be calculated over a period of time τ :

$$L_{inverter} = 1 - \frac{E_{AC}}{E_{DC}} = 1 - \frac{\int_{\tau} \eta_{inverter} \cdot P_{max} \cdot dt}{\int_{\tau} P_{max} dt} \quad (18)$$

where E_{AC} is the energy generated at the output of the inverter, E_{DC} is the energy generated by the photovoltaic generator, and P_{max} is given by the Osterwald model (Osterwald, 1986), described above.

In a similar way to the temperature losses, the losses in the inverter depend on the tilt and orientation of the generator, the incident irradiance on the plane of the generator (and therefore also of the angular losses), the ambient temperature of the place, and of the inverter type. Therefore, they are very complex to assess as they are characteristics of the facility.

Conversion losses have been reported in a wide range. For example, some studies place them at around 13% (Mondol et al., 2006), 9.6–17.5% (Baltus et al., 1997), 6.3–16.8% (Alonso-Abella and Chenlo, 2004). However, they can be taken to be equal to 5% for very good inverters (Luque and Hegedus, 2011).

2.8. Ohmic losses in the cabling

The ohmic losses can be calculated approximately for a time period τ , by means of the expression:

$$L_{ohmic} = \frac{\sum_{i=1}^n \int_{\tau} I_i \cdot R_i^2 \cdot dt}{\int_{\tau} P_{max} dt} \quad (19)$$

where n represents the number of cables, I_i is the current that circulates in the i -th cable of electric resistance R_i , and P_{max} is given by the Osterwald model (Osterwald, 1986).

Usually, these losses fluctuate between 0.5% and 1.5% (Almonacid et al., 2011; Baltus et al., 1997), with 1% being an acceptable average value to be used.

2.9. Losses due to shading

The shading losses depend on the sun position, in other words, of the solar height Y_s , and the azimuth α . These coordinates are shown in Fig. 2.

When plotting Y_s against α for the whole year, the so-called *solar trajectory diagram* is obtained. When the diagram of the coordinates of the obstacles surrounding the solar panel is superimposed on this, the losses due to the shading can be calculated. One example of the aforementioned diagram is shown in Fig. 3, for the city of Bogota. The diagram of obstacles on the horizon appears in yellow.

Each one of the regions of Graph A1, A2, etc., represents a portion of the annual solar irradiation from the sun and that affects the photovoltaic system. Table 4, the so-called *benchmark table*, shows the percentage contributions of different regions. This matches a module tilted at 30° to horizon and south facing.

When multiplying the f_i fraction for the area covered by the obstacle, by the irradiance percentage of the region R_i , the losses due to shading in that portion of the graph are obtained. When all the contributions affected by the obstacles are totalled, the annual total losses due to shading in the system are obtained:

$$L_{shading} = \frac{1}{100} \sum_{i=1}^n f_i \cdot R_i \quad (20)$$

The current alternatives to calculate this type of loss are very complex, such as the photographic method proposed by Cellura et al. (2012), then improved (Orioli and Gangi, 2012). Some sites opt to do so with electronic appliances known as “fish eye”, designed for this purpose (Kenji et al., 2001).

Losses due to shading were measured in residential photovoltaic systems, that are on average 7% (Sugiura et al., 2003; Wittkopf et al., 2012), even though they may reach higher values (Nguyen and Pearce, 2012).

3. The Performance Ratio of the system

The performance of a photovoltaic system is quantified by means of the parameter called the “Performance Ratio” or PR, described above in Eq. (1). This parameter can be

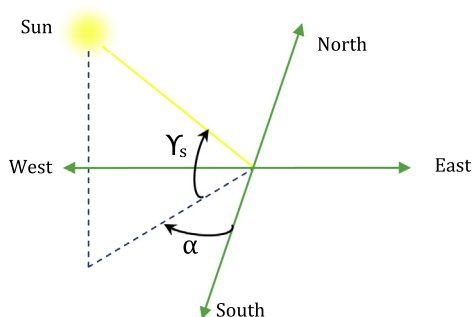


Fig. 2. Representation of the solar coordinates.

related with the different losses L_i set out above, by multiplying the respective performances, thus:

$$PR = \prod_{i=1}^n (1 - L_i) \quad (21)$$

It can be observed in the above equation that the PR of each specific GCPS is very complicated to calculate, if reliable results are to be obtained.

The main objective of this article is to provide a simple method, which is equivalent to calculating the aforementioned losses step by step. This procedure is very important to design BIPV applications, as the conditions of each geographical place (ambient temperature and latitude) and the surface type (orientation and tilt) characterise the PR.

4. Methodology

The following procedure is proposed to establish a simple expression of the PR for low latitude countries, even though it may be used to extend the model to other world regions, assigning the adjustment parameters appropriately to the results.

The amount of annual average radiation that a surface receives according to its tilt and azimuth was first calculated. The angular losses and due to dirt were then calculated. With the corrected irradiance amount and the ambient temperature, the input power at each photovoltaic module was calculated, thus establishing the temperature losses. The losses in the inverter were then calculated using the equation of its performance characteristic curve. The other types of losses were taken to be equal to the usual values described in Point 2.

Contour diagrams of the PR were then constructed according to the tilt and orientation of the generator for each city. Finally, a careful analysis of them was performed, in such a way that a simple equation was found that enables the results obtained by means of the process set out in the above paragraph to be reproduced.

The method used is described in detail below.

4.1. Obtaining temperature and irradiation data

The first step was to obtain global solar irradiance data for different cities in Colombia. The source to obtain this type of information was the website specialising in renewable energy projects called *RETScreen International* (Government of Canada, 2013), that is supplied by information from 6700 terrestrial meteorological stations and by NASA satellites. This step resulted in the 12 monthly average daily values of the global solar irradiation on the horizontal surface $G_{dn}(0)$.

Similarly, the temperature data were obtained from the website of the *World Meteorological Organisation* (“Organizzazione Meteorologica Mundial,” 2013), whose global climatology information is based on 30-year monthly measurements, between 1971 and 2000. Thus, the 12

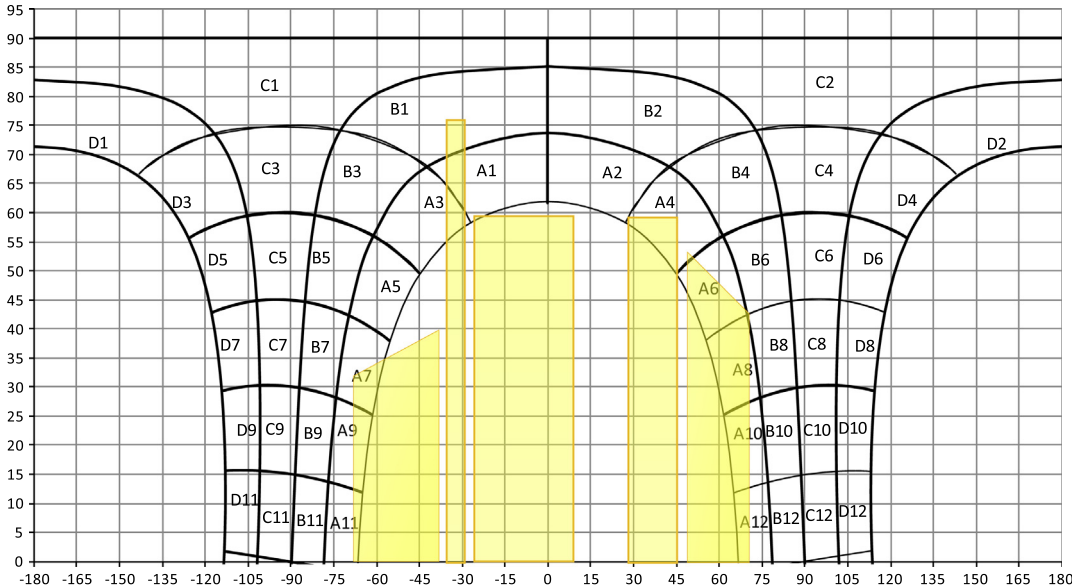


Fig. 3. Solar trajectory diagram used to calculate losses due to shading for the city of Bogota. The obstacle diagram is superimposed in yellow. (For interpretation of the references to colour in this figure legend, the reader is referred to the web version of this article.)

Table 4
Benchmark tables for a surface area with $\beta = 30^\circ$ and $\alpha = 0^\circ$.

Region	A	B	D	E
1	0.00	0.00	0.00	0.00
2	0.49	0.15	0.09	0.05
3	1.18	0.44	0.35	0.51
4	2.04	0.82	0.70	1.17
5	2.89	1.20	1.05	1.85
6	3.56	1.51	1.34	2.39
7	3.91	1.67	1.49	2.68
8	3.86	1.65	1.47	2.64
9	3.42	1.45	1.28	2.28
10	2.69	1.11	0.97	1.68
11	1.82	0.72	0.61	1.00
12	0.99	0.36	0.27	0.36
13	0.31	0.09	0.04	0.01
14	0.00	0.00	0.00	0.00

monthly average values of maximum and minimum temperature of each city were obtained.

4.2. Calculating the annual solar irradiance on tilted surfaces in Colombia

Taking the $G_{dm}(0)$ figures as the baseline, each value was decomposed into diffuse $D_{dm}(0)$ and direct $B_{dm}(0)$ radiation. The fact described by Liu and Jordan (1960) was taken into account, according to which the relationship between the clarity index K_{Tm} and the diffuse fraction K_{Dm} is independent of the latitude. The equation proposed by Page (1961), and valid for latitudes between 40°N and 40°S was taken as being dependent on those parameters:

$$K_{Dm} = 1 - 1.13K_{Tm} \quad (22)$$

where

$$K_{Dm} = \frac{D_{dm}(0)}{G_{dm}(0)} \quad (23)$$

$$K_{Tm} = \frac{G_{dm}(0)}{Bo_{dm}(0)} \quad (24)$$

With $Bo_{dm}(0)$ being the extra-terrestrial beam irradiance on a horizontal surface, obtained for day d_n of the month in which the dual value is equal to the monthly daily average. The equation to calculate it is (Luque and Hegedus, 2011):

$$Bo_{dm}(0) = \frac{24}{\pi} B_0 \varepsilon_0 (\omega_s \sin \delta \sin \phi + \cos \delta \cos \phi \sin \omega_s) \quad (25)$$

Here B_0 is the solar constant, ε_0 the correction factor of the eccentricity of the orbit of the earth, δ the solar declination angle according to Spencer (Spencer, 1971), ϕ the latitude of the place, and ω_s the sunrise angle; with all angles measured in radians.

The following was used for the direct radiation component:

$$B_{dm}(0) = G_{dm}(0) - D_{dm}(0) \quad (26)$$

Once the daily components were obtained of the global radiation, $D_{dm}(0)$ and $B_{dm}(0)$, their respective hourly values, $D_h(0)$ and $B_h(0)$ were calculated. This is performed using the expressions proposed by Collares-Pereira and Rabl (1979):

$$D_h(0) = r_d D_{dm}(0) \quad (27)$$

$$G_h(0) = r_g G_{dm}(0) \quad (28)$$

$$B_h(0) = G_h(0) - D_h(0) \quad (29)$$

where

$$r_d = \frac{\pi}{24} \left(\frac{\cos \omega - \cos \omega_s}{\sin \omega_s - \omega_s \cos \omega_s} \right) \quad (30)$$

$$r_g = r_d(a + b \cos \omega) \quad (31)$$

$$a = 0.409 + 0.5016 \sin(\omega_s - 1.047) \quad (32)$$

$$b = 0.6609 + 0.4767 \sin(\omega_s - 1.047) \quad (33)$$

The following step was to calculate the hourly global irradiance on the surface of the generator $G_h(\beta, \alpha)$. We therefore used the *three-component model*, which has proven to be quite accurate (Haberlin, 2012), and established that the incident radiation is made up of direct $B_h(\beta, \alpha)$, diffused $D_h(\beta, \alpha)$, and reflected $R_h(\beta, \alpha)$ radiation; thus:

$$G_h(\beta, \alpha) = B_h(\beta, \alpha) + D_h(\beta, \alpha) + R_h(\beta, \alpha) \quad (34)$$

The following equation was applied to calculate the direct radiation:

$$B_h(\beta, \alpha) = \left(\frac{B_h(0)}{\cos \theta_{zs}} \right) \cdot \max(0, \cos \theta_s) \quad (35)$$

With θ_s being the angle of incidence of the sun rays and the normal to the plane considered, and θ_{zs} the solar zenith angle, given by:

$$\begin{aligned} \cos \theta_s &= (\sin \phi \cos \beta - \text{sign}(\phi) \cos \phi \sin \beta \cos \alpha) \sin \delta \\ &\quad + (\cos \phi \cos \beta + \text{sign}(\phi) \sin \phi \sin \beta \cos \alpha) \\ &\quad \times \cos \delta \cos \omega + \cos \delta \sin \beta \sin \alpha \sin \omega \end{aligned} \quad (36)$$

$$\cos \theta_{zs} = \sin \delta \sin \phi + \cos \delta \cos \phi \cos \omega \quad (37)$$

In the above two equations, ω is the hour angle and is expressed in terms of time in hours, t_h :

$$\omega = \frac{(12 - t_h)}{12} \pi \quad (38)$$

The time interval Δt was taken to be equal to 0.25 h.

There are more than 20 models in the literature to calculate the diffuse component on the tilted surface. The Hay-Davies isotropic model (Hay, 1979), was selected, as it stands out in different comparative studies for its high accuracy and simplicity (Denegri et al., 2012; Noorian et al., 2008; Diez-Medivilla et al., 2005; Souza and Escobedo, 2013). This considers the diffuse radiation consisting of two parts, a circumsolar component $D^C(\beta, \alpha)$ which comes directly from the sun, and another isotropic component $D^I(\beta, \alpha)$ from the whole celestial hemisphere:

$$D_h(\beta, \alpha) = D_h^C(\beta, \alpha) + D_h^I(\beta, \alpha) \quad (39)$$

where

$$D_h^C(\beta, \alpha) = \frac{D_h(0)\kappa_1}{\cos \theta_{zs}} \cdot \max(0, \cos \theta_s) \quad (40)$$

$$D_h^I(\beta, \alpha) = D_h(0)(1 - \kappa_1) \frac{1 + \cos \beta}{2} \quad (41)$$

Both components have a statistical weighting according to the anisotropy index k_1 defined as:

$$\kappa_1 = \frac{B_h(0)}{B_0 \varepsilon_0 \cos \theta_{zs}} \quad (42)$$

To calculate the reflected component, or albedo, it is assumed that the ground is horizontal and infinite in extension, and it reflects the light isotropically:

$$R_h(\beta, \alpha) = \rho G_h(0) \left(\frac{1 - \cos \beta}{2} \right) \quad (43)$$

where ρ is the reflectivity of the ground, taken in general as $\rho = 0.2$.

4.3. Calculating angular losses and due to dirt

The global irradiation was corrected taking into account both the angular and losses due to dirt, by means of Eqs. (2)–(6). The main parameters of Tables 1 and 2 were selected for a medium degree of dirt, that is, $T_{dirt}(0)/T_{clean}(0) = 0.97$. As a result, the corrected hourly global irradiance was obtained $G'_h(\beta, \alpha)$.

4.4. Calculating the temperature losses

The ambient temperature varies during the day, but initially only two data were available: the minimum T_{am} and the maximum T_{aM} average temperature. To take this into account, a model was used which means:

- a. The minimum ambient temperature always occurs at dawn, that is, when $\omega = \omega_s$.
- b. The maximum ambient temperature takes place two hours after the solar midday, that is, when $\omega = \pi/6$.
- c. During the day, the ambient temperature varies according to two half-cycles of cosine functions, according to the solar time ω .

Thus, the expressions of this model are (Luque and Hegedus, 2011):

For $\omega_s < \omega < \pi/6$:

$$T_a = T_{am} + \frac{T_{aM} - T_{am}}{2} [1 + \cos(a\omega + b)] \quad (44)$$

where

$$a = \frac{\pi}{\omega_s - \pi/6} \quad (45)$$

$$b = -\frac{a\pi}{6} \quad (46)$$

For $\omega > \pi/6$:

$$T_a = T_{am} - \frac{T_{aM} - T_{am}}{2} [1 + \cos(a\omega + b)] \quad (47)$$

where

$$a = \frac{\pi}{\omega_s + 11\pi/6} \quad (48)$$

$$b = -\left(\pi + \frac{a\pi}{6} \right) \quad (49)$$

With each ambient temperature obtained and the corrected hourly global irradiance $G'_h(\beta, \alpha)$, the operating temperature of cell T_c was calculated using Eq. (10). TNOC was

taken to be equal to 46 °C, a typical value issued by the module manufacturers. With this value, and Eq. (9), the output maximum power P_{\max} was calculated. Thus, the temperature instantaneous losses were established by Eq. (11).

4.5. Calculating the losses due to the DC–AC conversion

With the power established in the above point and Eq. (16), the instantaneous efficiency of the inverter was calculated. To discover p_{in} , the nominal P_{nominal} power of the inverter is assumed to be equal to the peak power of the generator $P_{\max,STC}$. The output instantaneous power was then obtained. The total losses of the DC–AC conversion were thus calculated using Eq. (18).

4.6. Determining the other types of losses

With respect to the types of remaining losses, they were taken to be equal to the average values reported in the literature, as set out in Point 2 of this article: $L_{\text{rating}} = 0.05$, $L_{\text{mismatch}} = 0.03$, $L_{\text{SPMP}} = 0.06$, $L_{\text{ohmic}} = 0.01$, $L_{\text{shading}} = 0.07$.

4.7. Calculating the PR

The final Performance Ratio was calculated using Eq. (1). Therefore, the annual irradiation $G_a(\beta, \alpha)$ was given by means of the average of the monthly average daily values $G_{dm}(\beta, \alpha)$, multiplied by 365:

$$G_a(\beta, \alpha) = 365 \cdot \frac{1}{12} \sum_{n=1}^{12} G_{dm}(\beta, \alpha) \quad (50)$$

where the monthly average daily irradiation $G_{dm}(\beta, \alpha)$ was obtained by adding up the hourly components of the hourly global irradiation, during the representative day:

$$G_{dm}(\beta, \alpha) = \sum_{\text{day}} G_h(\beta, \alpha) \cdot \Delta t \quad (51)$$

On the other hand, the photovoltaic energy was given by:

$$E_{PV} = E_{AC}(1 - L_{\text{rating}})(1 - L_{\text{mismatch}})(1 - L_{\text{SPMP}}) \times (1 - L_{\text{ohmic}})(1 - L_{\text{shading}}) \quad (52)$$

where E_{AC} was calculated to a similar way to $G_a(\beta, \alpha)$, using the equations:

$$E_{AC} = 365 \cdot \frac{1}{12} \sum_{n=1}^{12} E_{AC,dm} \quad (53)$$

$$E_{AC,dm} = \sum_{\text{day}} \eta_{\text{inverter}} \cdot P_{\max} \cdot \Delta t \quad (54)$$

The procedure described in points 4.2–4.7 was repeated cyclically, so that the PR value was obtained for each pair of coordinates (β, α) , for the city in question. Tilt β varied

between 0° and 90°, taking $\Delta\beta = 5^\circ$; and tilt α between –180° and 180°, taking $\Delta\alpha = 5^\circ$. All the possible configurations could thus be covered.

Finally, the process was repeated for 16 cities of Colombia located between latitudes of –4°S and 12°N. Several other cities in Central America were also taken into account.

5. Results and discussion

5.1. Angular losses and due to dirt

The results of the angular losses for the 16 cities of Colombia are set out in Table 5. It can there be seen that the minimum values of this variable range between 4% and 5%, while the maximums are between 11% and 15%.

This behaviour differs slightly from the one reported for some cities of Europe (Martin and Ruiz, 2001), according to which the maximum losses were 8%, for 90° tilt. This can be explained by the fact that the south-facing frontages in equatorial countries receive less irradiation than those located in high latitudes.

It can also be seen from Table 5 that there is an approximate trend of a 1% increase in the maximum losses for each 3° of latitude. This is logical, as this type of losses can occur for north-facing vertical surfaces, which receive less irradiation as the latitude increases.

Fig. 4 was prepared to better understand the behaviour of the south-facing surface angular losses, according to their tilt angle.

It can be seen from Fig. 4 that the angular losses increase with the tilt. However, each curve really presents a minimum, which is given for the optimum angle that maximises the annual global irradiation. This trend can be better appreciated the greater the latitude of the place. In this case, it is San Andrés, whose minimum is approximately for 15°.

Table 5
Results obtained for the angular losses.

City	Latitude φ (°)	$L_{\text{angular min}} (\%)$	$L_{\text{angular max}} (\%)$
Leticia	–4.2	5	12
Pasto	1.2	5	11
Tumaco	1.8	4	12
Popayán	2.5	5	12
Neiva	3	5	12
Cali	3.6	5	12
Villavicencio	4.2	5	11
Bogotá	4.7	4	13
Manizales	5.1	5	12
Medellín	6.2	5	12
Barrancabermeja	0.5	4	14
Cúcuta	7.9	4	13
Montería	8.8	4	13
Valledupar	10.5	4	14
Barranquilla	10.9	4	14
San Andrés	12.6	4	15

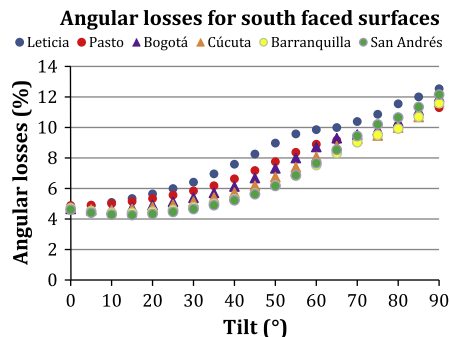


Fig. 4. Annual angular losses L_{angular} versus tilt angle β , for south-facing surfaces.

Fig. 5 was produced, which shows the case of north-facing surfaces, to establish the minimum and maximum losses on the roofs ($0 < \beta < 30^{\circ}$). When this is compared with Fig. 4, it can be concluded that the roofs will lose a minimum of 4% for angular concepts. Furthermore, the maximum losses do not exceed 8% when the roof is north facing. This is relatively good for the final performance of the system. The problem occurs with the frontages, where the losses drop from 11% to 15%.

In order to establish whether the frontage orientations enable the performance of the photovoltaic system to be increased, Fig. 6 was produced which shows the angular losses according to the azimuth. It can be seen that the optimum frontages are those facing east and west, with angular losses between 6% and 7% for San Andrés and Pasto, respectively. The reason for this is that the solar rays hit this type of surfaces more perpendicularly in countries near to the terrestrial equator.

5.2. Temperature losses

The results of the temperature losses are set out in Table 6. It can be seen that the minimum values of this variable range between -3% and 5% , which occur for high tilts. On the other hand, the maximum range between 2% and 11% and are obtained for surfaces that are slightly

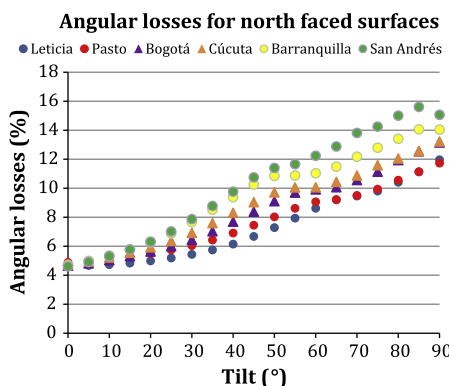


Fig. 5. Annual angular losses L_{angular} versus tilt angle β , for north-facing surfaces.

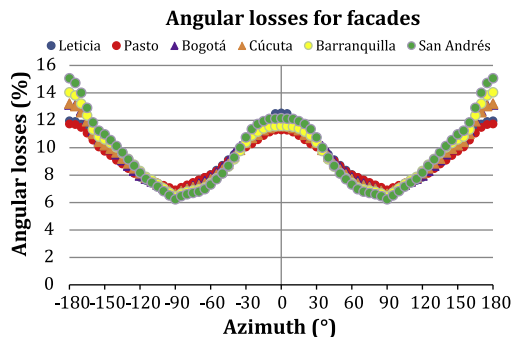


Fig. 6. Annual angular losses L_{angular} versus azimuth angle α , for different types of frontages.

tilted. The latter are approximately within the expected ranges (Almonacid et al., 2011). It can also be seen that the maximum losses tend to increase according to the average ambient temperature, which is logical. On the other hand, the losses within each city do not vary by approximately more than 5%.

Fig. 7 depicts the variation of the temperature losses for south-facing surfaces. It can be seen that they show a decreasing parabolic behaviour, according to the tilt. They can be assumed to be constant between 0° and 20° , and then decrease with the tilt, at the rate of 1% each 15° . This decrease is due to the annual solar irradiation received is lower for more vertical surfaces, which means that the cells heat less. Therefore, the frontages show the best temperature performances.

The cities of Pasto and Bogotá registered the lowest losses, around 2% for the roofs. However, it can be seen that they were negative for tilts over 50° . This means that a greater final performance than the theoretical once (STC) can be obtained, by the simple fact of using frontages in those cities.

Fig. 8, which shows the temperature losses according to the azimuth, was produced to establish which frontages are the optimum ones.

It can be observed that the optimum frontages are the north facing ones, while the west facing ones show the greatest losses. The reason for this is that the maximum ambient temperature is reached after midday, when the sun is in the west and the generators pointing in that direction therefore get hotter.

Fig. 9 was constructed in order to find a mathematical ratio between the average ambient temperature of the place and the maximum temperature losses. This represents the data for slightly tilted generators.

By performing a linear regression, the points establish the following relationship ($R^2 = 0.96$):

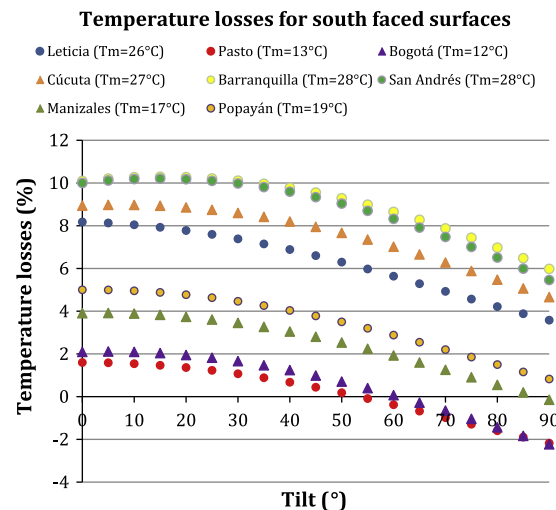
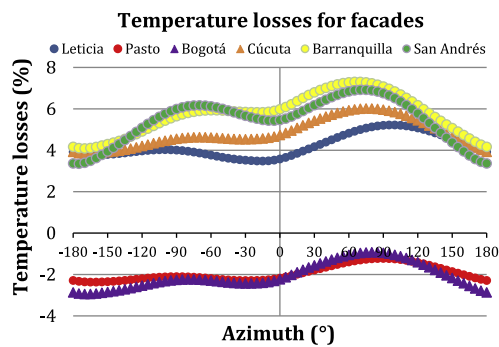
$$L_{\text{temperature,max}}(T_a) = 0.493T_a - 4.405 \quad (55)$$

This expression implies that for each 2°C increase in the average ambient temperature of the place, the maximum losses increase approximately by 1%. It can be concluded from this equation that there would be no losses for this concept for a city with an average temperature of 9°C .

Table 6

Maximum and minimum temperature losses for each city of Colombia.

City	Average T_a (°C)	$L_{temperature}$ min (%)	$L_{temperature}$ max (%)
Bogotá	11.7	-2.9	2.2
Pasto	13.3	-2.4	1.6
Manizales	16.6	-0.8	4.0
Popayán	18.8	0.4	5.1
Medellín	22.3	1.8	6.7
Cali	24.4	2.6	6.9
Tumaco	26.2	3.3	8.0
Villavicencio	26.2	3.4	8.0
Leticia	26.3	3.5	8.2
Cúcuta	27.2	3.8	9.1
Barrancabermeja	27.6	4.0	9.8
San Andrés	27.6	3.4	10.2
Neiva	27.7	4.2	8.8
Montería	27.9	4.1	9.5
Barranquilla	28.3	4.1	10.4
Valledupar	29	4.6	11.1

Fig. 7. Annual temperature losses $L_{temperature}$ versus tilt angle β , for south-facing surfaces.Fig. 8. Annual temperature losses $L_{temperature}$ versus azimuth angle α , for different types of facades.

By equalling Eqs. (12) and (60), the relationship between the maximum equivalent operating temperature and the ambient temperature can be found:

Temperature losses vs average ambient temperature

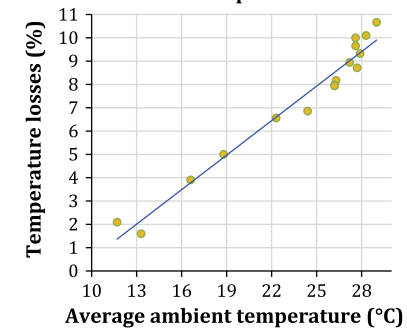


Fig. 9. Annual maximum temperature losses according to the average ambient temperature.

$$TOE_{max} = 1.12T_a + 15 \quad (56)$$

5.3. Losses in the inverter

Table 7 shows the values of the DC–AC conversion losses. It can be seen from there that its minimum value is approximately 11%, which is explained according to the choice of the parameters k_0 , k_1 , yk_2 , which characterise the efficiency curve of the inverter.

On the other hand, the maximum is between 19% and 22%. This indicates that as the surfaces are increasingly further tilted, the losses increase until they are the double.

The above behaviour for south-facing surfaces can be better seen in Fig. 10. Between $\beta = 0^\circ$ to $\beta = 40^\circ$ the DC–AC conversion losses can be considered to be approximately constant (11%). They tend to increase to 15% or 20% from that tilt onwards, depending on the latitude. It can also be seen that San Andrés registers fewer losses than Leticia, as the amount of solar irradiation received by this type of surfaces increases according to the latitude.

Table 7
DC–AC conversion maximum and minimum losses for each city of Colombia.

City	Average T_a (°C)	$L_{inverter}$ min (%)	$L_{inverter}$ max (%)
Leticia	-4.2	11.1	19.9
Pasto	1.2	11.2	18.8
Tumaco	1.8	10.1	19.1
Popayán	2.5	11.0	18.9
Neiva	3	11.2	19.9
Cali	3.6	11.4	20.0
Villavicencio	4.2	11.2	20.4
Bogotá	4.7	10.8	18.6
Manizales	5.1	11.0	19.1
Medellín	6.2	11.0	19.8
Barrancabermeja	0.5	10.8	20.0
Cúcuta	7.9	10.9	20.4
Montería	8.8	10.9	20.8
Valledupar	10.5	10.7	21.3
Barranquilla	10.9	10.8	21.4
San Andrés	12.6	10.7	21.9

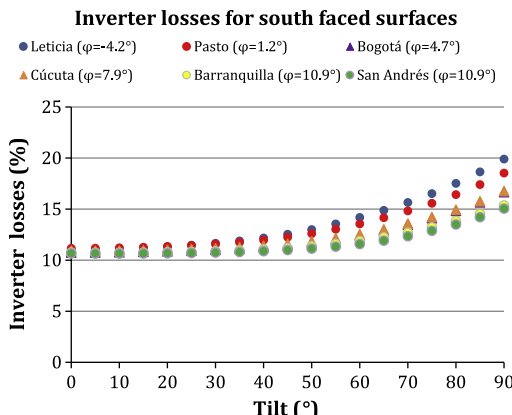


Fig. 10. Annual conversion losses $L_{inverter}$ versus tilt angle β , for south-facing surfaces.

Therefore, there will be greater power at the input to the inverter and greater efficiency.

The behaviour observed in the losses in the inverter (Fig. 10) is similar to the one exhibited by the angular losses (Fig. 4). This is explained by the fact of the stronger dependence on the efficiency of the inverter according to the input power. Pursuant to this, the losses will increase for north-facing surfaces as the tilt increases, more specifically to values between 19% and 22%. Similarly, the east- or west-facing frontages show lower losses than the others, around 13%.

5.4. System performance

Table 8 shows the maximum and minimum PR values, obtained for each city. The values range between 0.51 and 0.65. In total, the variation interval was greater than 20%, while it can be up to 15% for each city. These results are at odds with the usual practice to always assign a single “standard” PR value to different location or types of surfaces.

The maximum PR mainly strongly depends on the average ambient temperature of the place, degressively. This trend can be better appreciated on the regression line of Fig. 11, with a degree of adjustment of $R^2 = 0.9967$.

The straight line equation representing the data is:

$$PR_{max} = 0.686 - 0.0031 \cdot T_a \quad (57)$$

The above expression can be re-written in terms of the characteristic losses of each part of the system, as follows:

$$PR_{max} = (1 - L_{temp,max})(1 - L_{angular,min}) \times (1 - L_{inverter,min}) \prod_{i=1}^6 (1 - L_i) \quad (58)$$

Being

$$L_{temp,max} = -\gamma(TOE_{max} - 25) \quad (59)$$

$$TOE_{max} = 1.12T_a + 15 \quad (60)$$

Table 8

Maximum and minimum Performance Ratio for each city of Colombia. The data represent the performance of an “average” photovoltaic system.

City	Average T_a (°C)	Min PR	Max PR
Bogotá	11.7	0.58	0.650
Pasto	13.3	0.58	0.646
Manizales	16.6	0.56	0.635
Popayán	18.8	0.56	0.628
Medellín	22.3	0.54	0.618
Cali	24.4	0.54	0.611
Tumaco	26.2	0.54	0.608
Villavicencio	26.2	0.54	0.606
Leticia	26.3	0.54	0.606
Cúcuta	27.2	0.53	0.604
Barrancabermeja	27.6	0.53	0.602
San Andrés	27.6	0.51	0.599
Neiva	27.7	0.54	0.602
Montería	27.9	0.53	0.601
Barranquilla	28.3	0.52	0.599
Valledupar	29	0.51	0.597

Maximum PR vs average temperature of the city

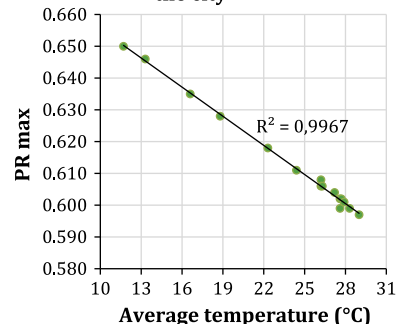


Fig. 11. Annual maximum performance of the system versus the average ambient temperature.

where the first 3 terms for PR_{max} were obtained by mean of simulation. It is important to note that the maximum temperature losses are used, as they are occur for small tilts, where the inverter and angular losses in turn are minimum. With respect to this type of surfaces, the gain in the performance of the system is up to 12% for angular concepts and 9% for conversion, for a total of 21%. On the other hand, 8% is lost by temperature. This joint performance results in a net gain of up to 13% in the PR.

5.5. Maximum values of the PR depending on the type of system

The results obtained in the model correspond to an average GCPS on fixed surfaces. However, it is possible to obtain higher PR values if it is assumed that the system is very well designed. These two situations are shown in Table 9, which sets out the loss figures to be used in Eq. (58), depending on the case.

Taking into account Table 9 and the equation for TOE_{max} , Eq. (58) may be simplified for practical purposes,

Table 9

Loss values to be used to calculate the PR_{max} .

Term	Significance	Average system	Optimum system	Status
$L_{angular,min}$	Angular losses in β optimum	0.04	0.03	Rainy areas (Martin and Ruiz, 2001)
$L_{inverter,min}$	Conversion losses in β optimum	0.11	0.05	Very good inverter (Luque and Hegedus, 2011)
L_{rating}	Module tolerance losses	0.05	0.03	Excellent modules (TamizhMani, 2011)
$L_{mismatch}$	Mismatch losses	0.03	0.02	Excellent modules (Almonacid et al., 2011)
L_{SPMP}	PMP monitoring losses	0.06	0.02	Very good inverter (Alonso-Abella and Chenlo, 2004)
L_{ohmic}	Ohmic losses in the cabling	0.01	0.005	Cable section (Almonacid et al., 2011)
$L_{shading}$	Losses due to shading	0.07	0.02	Few obstacles (Leloux et al., 2012)
$L_{dirtiness}$	Losses due to dirtiness	0.03	0.02	Rainy areas (Martin and Ruiz, 2001)
	Resulting factor k in the PR	0.662	0.820	

by introducing a constant k_{sist} that depends on the type of system, thus:

$$PR_{max} = k_{sist} \cdot [1 + \gamma(1.12 \cdot T_a - 10)] \quad (61)$$

where T_a is the average ambient temperature of the city in °C, and γ is the variation coefficient of the peak maximum power with the temperature. $\gamma = -0.0044 \text{ } ^\circ\text{C}^{-1}$ can be used for the crystalline silicon.

This equation reproduced the results obtained with a higher accuracy ($R^2 = 0.992$). In order to check the validity of this expression in countries other than equatorial ones, the temperature term was isolated and the losses were calculated for tilts near to the optimum one, thus:

$$L_{temperature,max} = -\gamma(1.12 \cdot T_a - 10) \quad (62)$$

The results obtained for some monitored real systems are shown in Table 10. Thus, the obtained values are consistent with those reported for photovoltaic systems installed in homes. Therefore the expression (62) has universal validity. However, it is important to stress that these losses may be greater in the case of BIPV, if an appropriate ventilation of the modules is not taken into account in the final design.

Fig. 12 was constructed to study the possible range of the maximum performance of the system according to the city. It can be appreciated that an optimum system can reach PR values between 0.74 and 0.81, depending on the type of city. Bogota is the city where the hypothetical system can best perform ($PR_{max} = 0.81$), while the lowest performance would be in Valledupar ($PR_{max} = 0.74$).

However, the values of an “average” system should be used to calculate the annual energy produced in the location.

5.6. PR variation with tilt and orientation

It is important to recall that Eq. (61) is used to calculate the PR in the case of tilts and orientation near to the

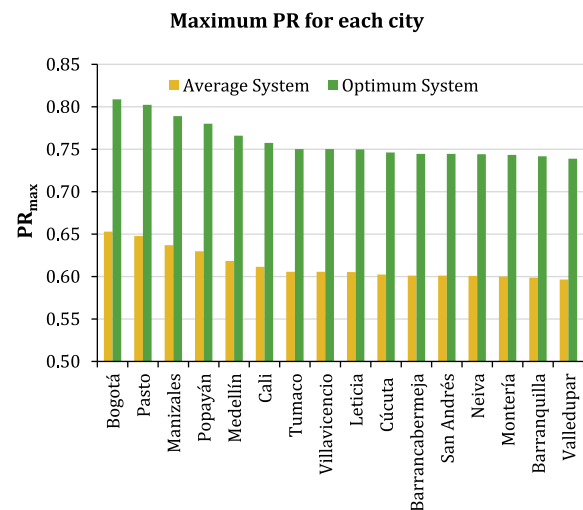


Fig. 12. Maximum annual performance of a generator for each city, according to the type of system.

optimum. However, its value can decrease by up to 15%, depending on the type of surface on which the modules are located. This behaviour implies its corresponding error when calculating the annual energy produced. The above can occur in the case of architectural integration (BIPV).

Taking this into account, PR contour maps were constructed according to the orientation and tilt for each city. Some of the results are set out for the cities of Leticia (Fig. 13), Pasto (Fig. 14), Bogota (Fig. 15), Cúcuta (Fig. 16), and Barranquilla (Fig. 17).

Figs. 13–17 show that all the surfaces tilted under 30°, regardless of their orientation, have a PR approximately equal to the maximum of that city. This implies that for the roofs, $PR = PR_{max}$ can be taken.

It can also be observed that there are two performance peaks in all the graphs for the approximate orientations

Table 10

Temperature loss values for generators tilted near to their optimum angle.

City	Country	Number of systems	Measured losses (%)	Benchmark	Calculated losses (%)
Tokyo	Japan	100	4	Sugiura et al. (2003)	4
Dublin	Ireland	1	0	Ayompe et al. (2011)	0
Sukatani	Indonesia	101	8	Reinders et al. (1999)	8

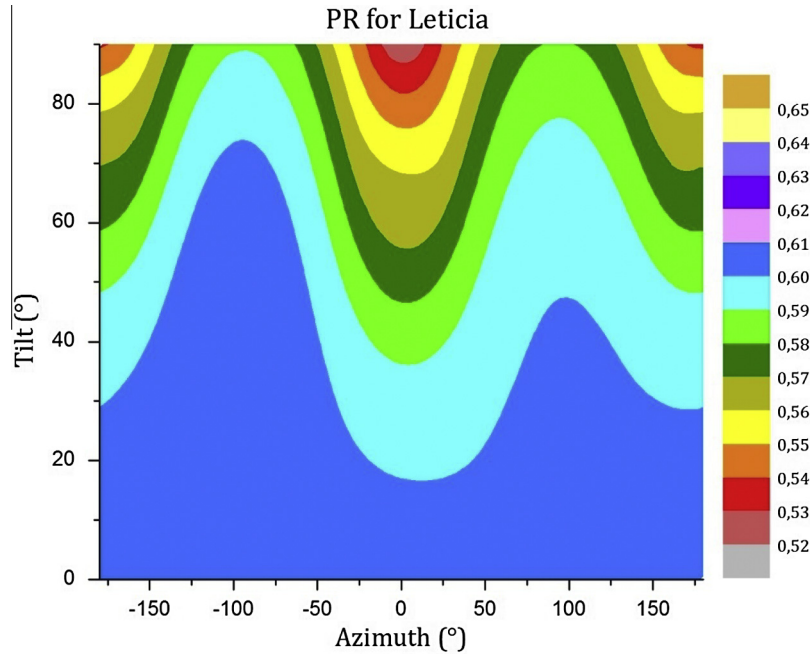


Fig. 13. PR graph for Leticia ($\varphi = -4.2^\circ$), according to the tilt and azimuth.

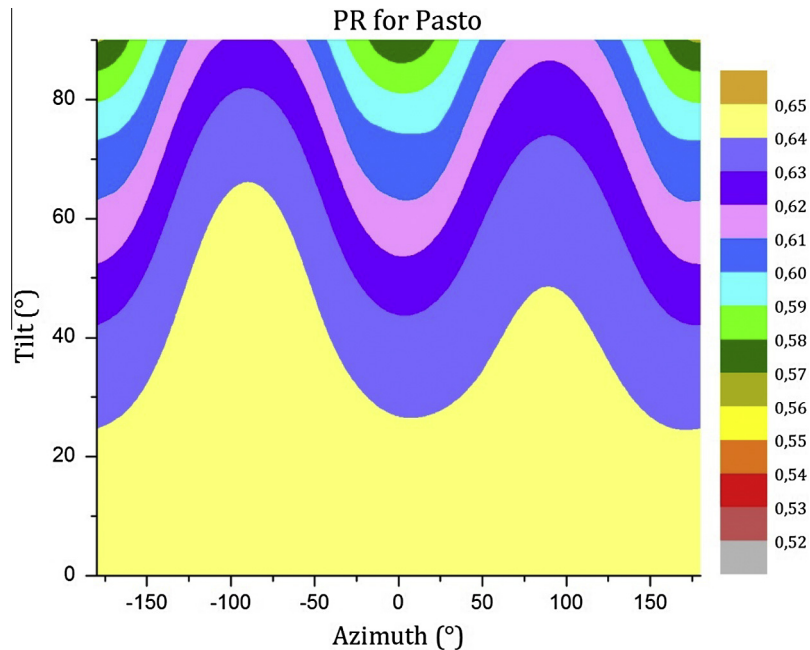


Fig. 14. PR graph for Pasto ($\varphi = 1.2^\circ$), according to the tilt and azimuth.

of -90° and 90° . This is due to the fact that both the angular and conversion losses are minimum for west- and east-facing surfaces. It can also be seen that the PR peak $\alpha = -90^\circ$ is greater than for $\alpha = 90^\circ$. The reason for this is that in the mornings, when the sun is in that orientation, the ambient temperature is lower, leading to smaller losses for this concept.

On the other hand, in cities located in negative latitudes, the lower performances are observed for south-facing

vertical generators ($\alpha = 0^\circ$). The opposite is observed for cities located above the equator line ($\alpha = 180^\circ$). That behaviour is logical due to the high inverter and angular losses in those cases.

5.7. Model proposed to calculate the PR

All the graphs obtained in this article are useful to carry out a detailed study of the losses in a future photovoltaic

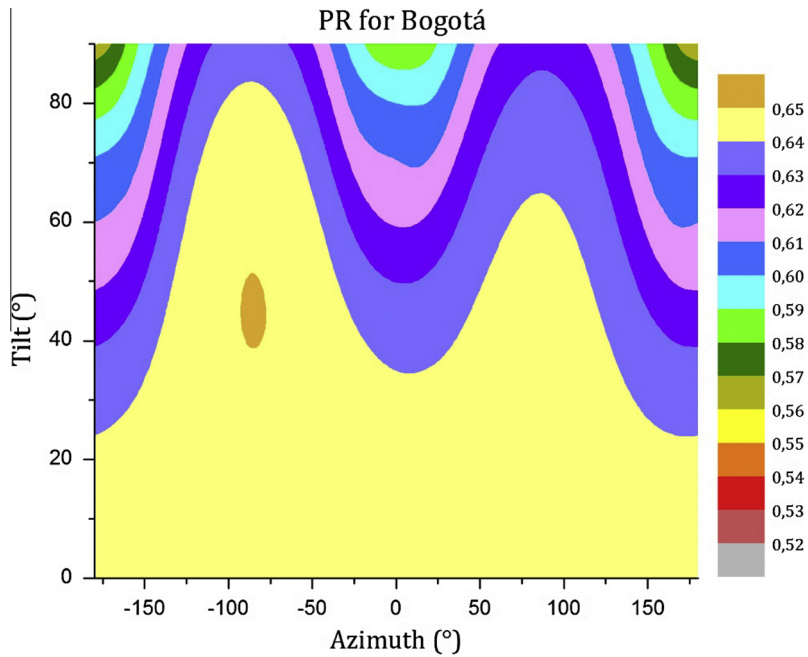


Fig. 15. PR graph for Bogota ($\varphi = 4.7^\circ$), according to the tilt and azimuth.

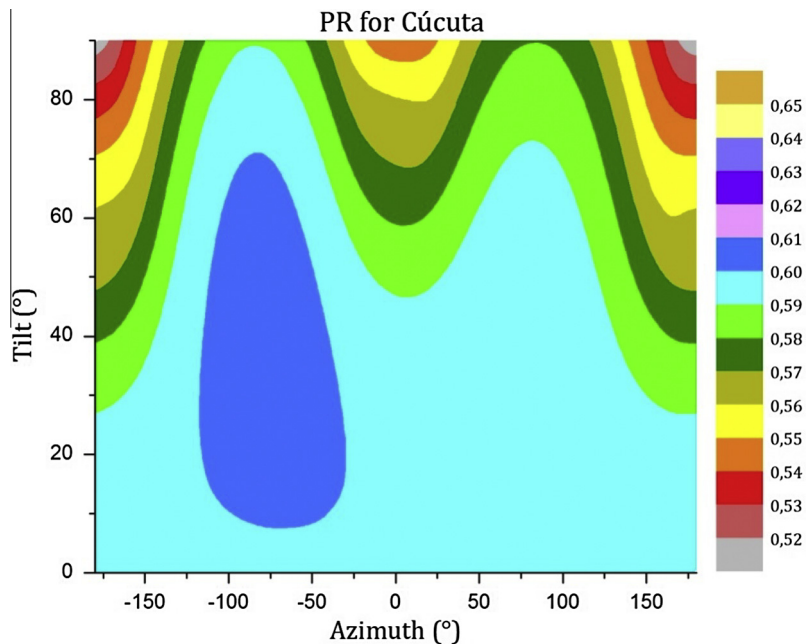


Fig. 16. PR graph for Cúcuta ($\varphi = 7.9^\circ$), according to the tilt and azimuth.

system. In particular, the contour maps in Figs. 13–17 allow the PR of the system to be identified visually. But each city has a different contour map, characterised by its average ambient temperature and its latitude. Therefore, it would be necessary to use the long procedure described in Point 4 each time that the aim is to predict the performance of a facility. In reality, the above is not technically viable when embarking on a photovoltaic project. This is the reason why many designers opt to design with a “standard value” of PR = 0.75 when they want to predict the

energy produced. Yet, as was shown above, the PR values obtained may vary according to the city and the type of surface, so that using this practice could result in an error of over 45% when calculating the annual electricity, in the worst of cases.

The proposal put forward to solve the problem was to find an equation that would adjust to the contour maps obtained. Reasoning in this showed that, for a single PR, the point curve approximately describes a sum of two Gaussian functions. The scope and breadth of such

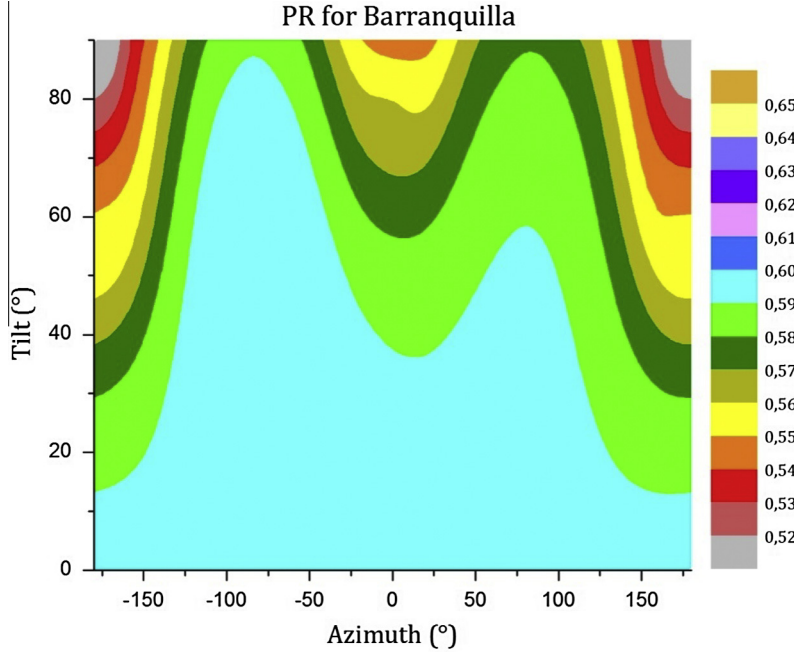


Fig. 17. PR graph for Barranquilla ($\varphi = -10.9^\circ$), according to the tilt and azimuth.

functions varies with the latitude of the place. Furthermore, the values obtained for the PR of each level curve are characteristics of the average temperature of the place. In accordance with this, we propose the following model to calculate the PR:

$$\text{PR} = 0.0011(A_1 \cdot e^{-2\left(\frac{\alpha-z_0}{W}\right)^2} + A_2 \cdot e^{-2\left(\frac{\alpha+90}{W}\right)^2} - \beta - 50) + 1.117 \cdot \text{PR}_c \quad (63)$$

where

$$A_1 = -1.1 \cdot |\varphi| + 60 \quad (64)$$

$$A_2 = -0.1 \cdot |\varphi| + 65 \quad (65)$$

$$W = -1.1 \cdot \varphi + 92 \quad (66)$$

$$\alpha_0 = -1.4 \cdot \varphi + 92 \quad (67)$$

$$\text{PR}_c = \text{PR}_{\max} + 0.0006 \cdot T_a - 0.017 \quad (68)$$

where β is the tilt angle, α the azimuth angle and φ the latitude of the city, all in degrees. T_a is the average ambient temperature of the city in °C.

The procedure to use Eq. (63) is the following:

- The value of PR_c is calculated using Eq. (68).
- The PR is calculated using Eq. (63). If $\text{PR} > \text{PR}_c$ then $\text{PR} = \text{PR}_c$ is taken as yield value. Otherwise, it is left the same as the one obtained.

Thus, an expression was obtained that only requires 4 input parameters. Two of them are for the city where the photovoltaic system will be installed: Ambient temperature T_a , and latitude φ . The other two characterise the surface type of the generator plane: Its tilt angle β , and orientation α .

5.8. Mathematical procedure used to obtain the model

The contour diagrams of Figs. 13–17 can be displayed as a level curve of a function $\text{PR} = f(\beta, \alpha, T_a, \varphi)$; this fact has been taken into account to obtain Eq. (63). In particular, for a city, set the latitude and temperature, the relationship is $\text{PR}_{\text{city}} = f(\beta, \alpha)$. Thus, the i th level curve $\text{PR}_{\text{city}} = \text{PR}_{ci}$ is a sum of two Gaussian functions (because the slope of the curves for $\alpha = -180^\circ$ and $\alpha = 180^\circ$ is nearly horizontal, indicating rapid exponential decay characteristic of this type of function). This curve can be expressed mathematically as follows:

$$\beta = \beta_{0i} + A_1 \cdot e^{-2\left(\frac{\alpha-z_0}{W}\right)^2} + A_2 \cdot e^{-2\left(\frac{\alpha+90}{W}\right)^2} \quad (69)$$

where A_1 , A_2 , W y α_0 are constant characteristics of the latitude of the city, so they were fitted by least squares (which was obtained $R^2 > 0.94$ in all cases).

Moreover, β_{0i} is the value of β in the far right and left i th level curve. By carefully observing the contour diagrams can be seen that each PR_{ci} corresponds to one β_{0i} , and both can be related by the expression:

$$\text{PR}_{ci} = -a \cdot \beta_{0i} + b \quad (70)$$

The slope a , and constant b , are calculated by least squares linear regression for each city ($R^2 > 0.96$ in all cases). As a result, it was observed that the value of a is approximately independent of the city, while the b value depends mainly on city PR_{\max} described by Eq. (57) ($R^2 = 0.96$). The latter parameter was the main contribution to the temperature dependence of the model, expressed in Eq. (68).

5.9. Degree of accuracy of the model

Fig. 18 was constructed in order to verify the degree of accuracy of the model. This graph shows two PR contour diagrams, one was produced using the long and tedious process described in Point 4, and the other was calculated using the proposed equation, both for the city of Bogota.

Likewise, **Fig. 19** shows the error percentage at each point of the graph. It can be seen how the error made is under 1%. This error increases slightly with the temperature and latitude. For example, for Tegucigalpa–Guatemala

($\varphi = 14.1^\circ$); the error in the majority of the point is 3% or less. These results indicate the excellent degree of accuracy of the proposed model, despite its simplicity.

Finally, the following is described to have an idea of the work saved by using Eq. (63) to calculate PR: To establish each point of the contour diagram of the left part of **Fig. 18**, it was necessary to use over 40 equations, in a computer algorithm that performed over 20,000 operations. On the contrary, only two equations were used at each point of the graph in the right of the same figure: that of PR_{\max} , Eq. (61), and the one proposed in our model, Eq. (63).

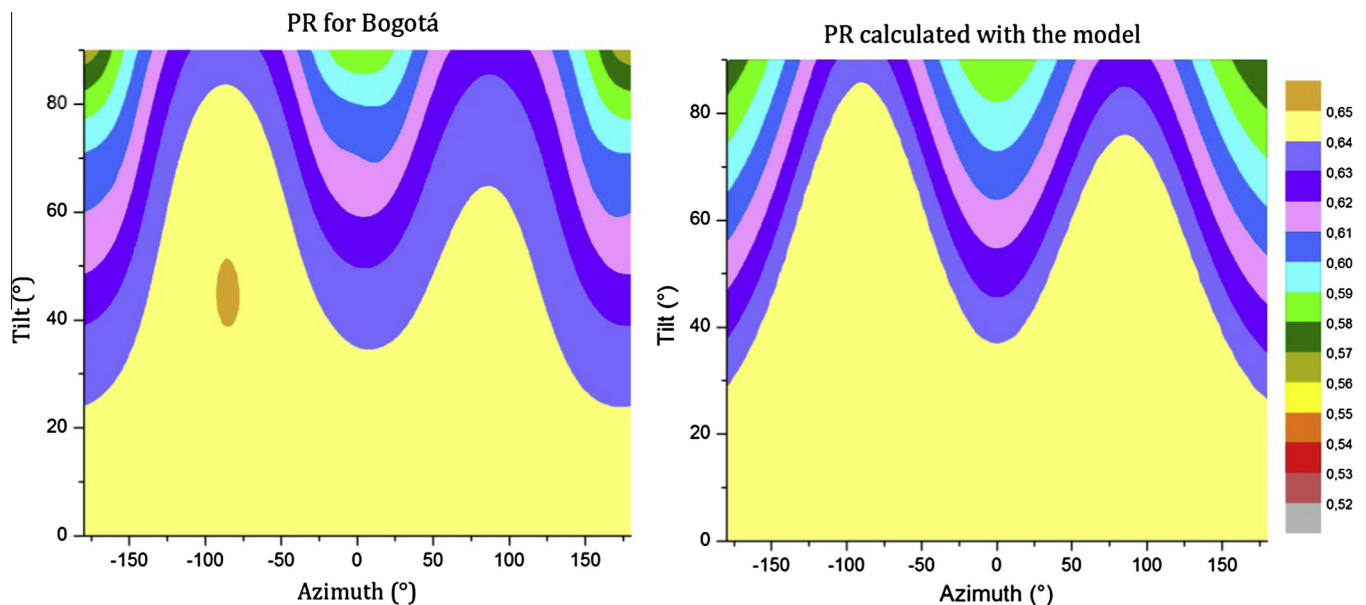


Fig. 18. Contours of the PR for Bogota, calculated by full simulation (Left) and by means of the proposed model (Right).

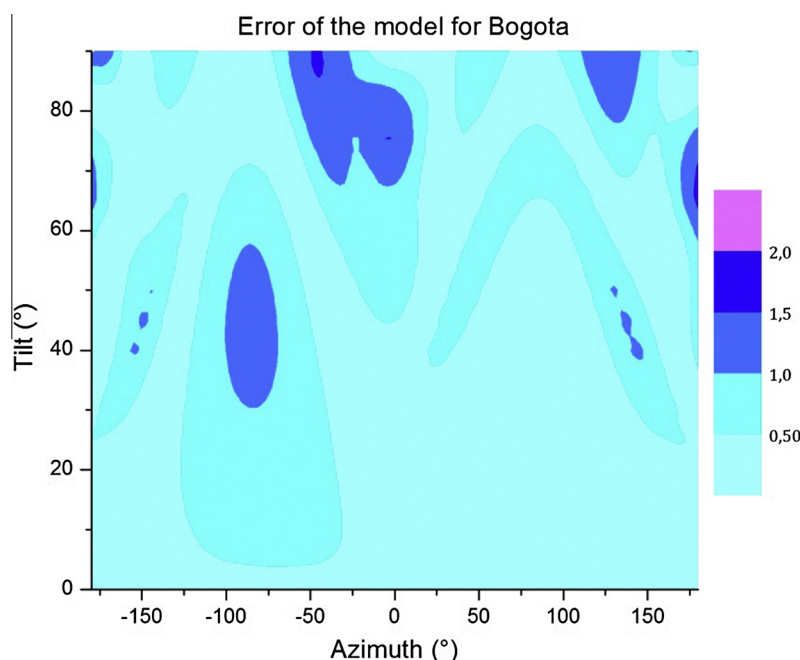


Fig. 19. Error percentage in the model proposed for the Bogota PR.

6. Conclusions

This paper analyses in detail the possible energy losses that impacted the performance of a photovoltaic system connected to the grid, placed in an equatorial country. The procedure was carried out for 16 cities of Colombia, for all the possible tilts and orientations of the generator plane.

The results showed that the angular losses were between 4% and 15%. It was also seen that there is an approximate trend of a 1% increase in the maximum losses for each 3° of latitude.

Maximum and minimum angular losses on the roofs were calculated, where it was found that they were between 4% and 8%. The optimum frontages are those facing east and west, with angular losses between 6% and 7% for San Andrés and Pasto, respectively.

With respect to the temperature losses, they were between -3% and 11%. However, they did not vary by over 5%, approximately, within each city. The maximum losses occurred for low tilts. It was also seen that the maximum losses tend to increase by 1% for each 2° in the average ambient temperature of the place. It was found that there are no losses for this concept for cities with average temperature of 9 °C. On the other hand, they were approximately constant on the roofs, and then decreased with the slope, on the basis of 1% each 15°, approximately. Therefore, the frontages provided better performances by temperature.

The cities of Pasto and Bogota registered the lowest losses by temperature, around 2% on the rooftops. There were negative for tilts over 50°, which means a final performance greater than the theoretical one can be obtained, simply by using frontages in those cities. It was also observed that that the optimum frontages were east facing.

It was found that the maximum equivalent operating temperature of the cells is nearly 15° higher than the ambient temperature. Furthermore an equation was proposed to calculate the maximum temperature losses in any country of the world. This was confirmed using monitored system data.

DC-AC conversion losses were between 11% and 22%. For south facing generators, they remained approximately constant between $\beta = 0^\circ$ and $\beta = 40^\circ$ (11%), to then increase to 15% or 20%, depending on the latitude. San Andrés registered fewer losses than Leticia, as the amount of solar irradiation received by this type of surfaces increases according to the latitude. The behaviour observed in the losses in the inverter was similar to the one exhibited by the angular losses. Therefore, the east- or west-facing frontages showed lower losses than the others, around 13%.

On the other hand, the performance of an “average system” in each city was estimated, with PR values of between 0.51 and 0.65 being found. Thus, the variation was over 20%, while it was up to 15% in each city. These results are at odds with the usual practice to assign a single “standard” PR value to different location or types of surfaces.

The maximum PR was mainly found for low tilts, and depends on the average ambient temperature of the place, degressively. This fact also allowed a highly accurate equation to be found that relate both variables, along with the losses of each element of the photovoltaic system. This equation allows an average GCPS to be distinguished from another very well-designed one, by introducing a constant known as k_{sist} . The result was that an optimum system in Colombia can reach PR values between 0.74 and 0.81, depending on the type of city.

All the surfaces tilted under 30°, regardless of their orientation, have a PR approximately equal to the maximum of that city. This implies that for the roofs, $PR = PR_{max}$ can be taken. Furthermore, the greatest performances of the frontages were for west- and east-facing surfaces.

Finally, a simple expression was proposed that allowed the PR to be estimated with just 4 input parameters: The average ambient temperature of the city, the latitude and the orientation and tilt angles of the plane of the photovoltaic generator. This model has a high degree of accuracy, and is equivalent to performing a complex simulation, according to the one seen in the methodology.

7. Future research

The proposed model can be extended to high latitude countries, but the parameters of the equation would need to be adjusted. Future researches in this field could include the analysis of the influence of ground conditions on the BIPV's surface temperature of PV cells.

We expect the results obtained in this study to be highly useful for architects and engineers involved in designing photovoltaic systems for BIPV in low latitude countries.

Acknowledgements

This research was carried out thanks to the support received by means of a grant from the Universidad Internacional de Andalucía for studies on the Official Master's in Technology of the Photovoltaic Solar Energy Systems. Also to the Faculty of Engineering and Architecture of the Universidad Católica de Manizales.

References

- Almonacid, F., Rus, C., Pérez, P.J., Hontoria, L., 2009. Estimation of the energy of a PV generator using artificial neural network. *Renew. Energy* 34, 2743–2750.
- Almonacid, F., Rus, C., Pérez-Higueras, P., Hontoria, L., 2011. Calculation of the energy provided by a PV generator. Comparative study: conventional methods vs. artificial neural networks. *Energy* 36, 375–384.
- Alonso-Abella, M., Chenlo, F., 2004. A model for energy production estimation of PV grid connected systems based on energetic losses and experimental data on site diagnosis. In: 19th European Photovoltaic Solar Energy Conference, Paris, pp. 2447–2450.
- Araujo, G.L., Sánchez, E., Martí, M., 1982. Determination of the two-exponential solar cell equation parameters from empirical data. *Sol. Cells* 5, 199–204.

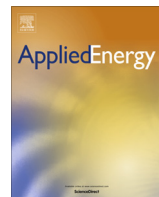
- Atmaram, G.H., TamizhMani, G., Ventre, G.G., 2008. Need for uniform photovoltaic module performance testing and ratings. In: 33rd IEEE Photovoltaic Specialists Conference, 2008. PVSC '08. Presented at the 33rd IEEE Photovoltaic Specialists Conference, 2008. PVSC '08, pp. 1–6.
- Ayompe, L.M., Duffy, A., McCormack, S.J., Conlon, M., 2011. Measured performance of a 1.72 kW rooftop grid connected photovoltaic system in Ireland. *Energy Convers. Manage.* 52, 816–825.
- Baltus, C.W.A., Eikelboom, J.A., Zolingen, R.J.C.V., 1997. Analytical monitoring of losses in PV systems. In: 14th European Photovoltaic Solar Energy Conference. Barcelona.
- Caamaño Martín, E., 1998. Edificios fotovoltaicos conectados a la red eléctrica: caracterización y análisis (PhD). E.T.S.I. Telecomunicación (UPM).
- Carr, A., Pryor, T., 2004. A comparison of the performance of different PV module types in temperate climates. *Sol. Energy* 76, 285–294.
- Cellura, M., Di Gangi, A., Orioli, A., 2012. A photographic method to estimate the shading effect of obstructions. *Sol. Energy* 86, 886–902.
- Centro de Investigaciones Energéticas, Medioambientales y Tecnológicas de España (CIEMAT), 2013. [WWW Document]. <<http://www.ciemat.es/>>.
- Chouder, A., Silvestre, S., 2009. Analysis model of mismatch power losses in PV systems. *J. Sol. Energy Eng.* 131, 024504–024504.
- Collares-Pereira, M., Rabl, A., 1979. The average distribution of solar radiation-correlations between diffuse and hemispherical and between daily and hourly insolation values. *Sol. Energy* 22, 155–164.
- Denegri, M.J., Raaijijk, C., Gallegos, H.G., 2012. Evaluación de diferentes modelos utilizados para la estimación de la radiación fotosintéticamente activa en planos inclinados. *Av. En Energ. Renov. Medio Ambiente* 16, 9–15.
- Detrick, A., Kimber, A., Mitchell, L., 2005. Performance evaluation standards for photovoltaic modules and systems. In: Conference Record of the Thirty-First IEEE Photovoltaic Specialists Conference, 2005. Presented at the Conference Record of the Thirty-first IEEE Photovoltaic Specialists Conference, 2005, pp. 1581–1586.
- Diez-Mediavilla, M., de Miguel, A., Bilbao, J., 2005. Measurement and comparison of diffuse solar irradiance models on inclined surfaces in Valladolid (Spain). *Energy Convers. Manage.* 46, 2075–2092.
- Engineers, A.S. of H., 1978. Refrigerating and Air-Conditioning, ASHRAE Standard Methods of Testing to Determine the Thermal Performance of Solar Collectors. ASHRAE.
- Government of Canada, 2013. N.R.C., RETScreen International. [WWW Document]. <<http://www.retscreen.net/>> (accessed 24.08.13).
- Green, M.A., 1998. Solar Cells: Operating Principles, Technology and System Applications. University of New South Wales.
- Haberlin, H., 2012. Photovoltaics: System Design and Practice. John Wiley & Sons, United Kingdom.
- Hay, J.E., 1979. Study of Shortwave Radiation on Non-horizontal Surfaces. *Atmospheric Environ. Serv. Report No.* 79–12.
- Jahn, U., Nasse, W., 2004. Operational performance of grid-connected PV systems on buildings in Germany. *Prog. Photovolt. Res. Appl.* 12, 441–448.
- Jantsch, M., Schmidt, H., Schmid, 1992. Results on the concerted action on power conditioning and control. In: 11th European Photovoltaic Solar Energy Conference. Montreux, pp. 1589–1592.
- Jantsch, M., Real, M., Haberlin, H., Whitaker, K., Blasser, G., Kremer, P., Verhoeve, C.W.G., 1997. Measurement of PV maximum power point tracking performance. In: Technical Committee 82: Photovoltaics. International Electrotechnical Commission, Barcelona.
- Kanters, J., Horvat, M., 2012. Solar energy as a design parameter in urban planning. *Energy Procedia* 30, 1143–1152.
- Kenji, O., Koichi, S., Kazuhiko, K., 2001. Shading loss analysis of PV systems using fisheye photography. *Pap. Tech. Meet. Front. Technol. Eng. IEE Jpn. FTE-01*, 23–28.
- Krauter, S., Grunow, P., 2006. Optical modelling and simulation of PV module encapsulation to improve structure and material properties for maximum energy yield. In: Conference Record of the 2006 IEEE 4th World Conference on Photovoltaic Energy Conversion. Presented at the Conference Record of the 2006 IEEE 4th World Conference on Photovoltaic, Energy Conversion, pp. 2133–2137.
- Leloux, J., Narvarte, L., Trebosc, D., 2012. Review of the performance of residential PV systems in France. *Renew. Sustain. Energy Rev.* 16, 1369–1376.
- Liu, B.Y.H., Jordan, R.C., 1960. The interrelationship and characteristic distribution of direct, diffuse and total solar radiation. *Sol. Energy* 4, 1–19.
- Luque, A., Hegedus, S., 2011. Handbook of Photovoltaic Science and Engineering, second ed. Wiley, United Kingdom.
- M. Drif, P.J.P., Aguilera, J., Almonacid, G., Gomez, P., de la Casa, J., Aguilar, J.D., 2007. Univer Project. A grid connected photovoltaic system of 200 kW p at Jaén University. Overview and performance analysis. *Sol. Energy Mater. Sol. Cells* 91, 670–683.
- Markvart, T., Castaner, L., 2003. Practical Handbook of Photovoltaics: Fundamentals and Applications. Elsevier.
- Martin, N., Ruiz, J.M., 2001. Calculation of the PV modules angular losses under field conditions by means of an analytical model. *Sol. Energy Mater. Sol. Cells* 70, 25–38.
- Mondol, J.D., Yohanis, Y., Smyth, M., Norton, B., 2006. Long term performance analysis of a grid connected photovoltaic system in Northern Ireland. *Energy Convers. Manage.* 47, 2925–2947.
- Nguyen, H.T., Pearce, J.M., 2012. Incorporating shading losses in solar photovoltaic potential assessment at the municipal scale. *Sol. Energy* 86, 1245–1260.
- Noorian, A.M., Moradi, I., Kamali, G.A., 2008. Evaluation of 12 models to estimate hourly diffuse irradiation on inclined surfaces. *Renew. Energy* 33, 1406–1412.
- Organización Meteorológica Mundial, 2013. [WWW Document]. <<http://wwis.aemet.es/>>.
- Orioli, A., Gangi, A.D., 2012. An improved photographic method to estimate the shading effect of obstructions. *Sol. Energy* 86, 3470–3488.
- Osterwald, C.R., 1986. Translation of device performance measurements to reference conditions. *Sol. Cells* 18, 269–279.
- Page, J., 1961. The estimation of monthly ea values of daily total short wave radiation on vertical and inclined surfaces from sunshine records for latitudes 40°N–40°S. In: Proc. UN Conf. New Sources Energy, vol. 4, pp. 378–390.
- Pearce, J.M., 2002. Photovoltaics—a path to sustainable futures. *Futures* 34, 663–674.
- Picault, D., Raison, B., Bacha, S., de la Casa, J., Aguilera, J., 2010. Forecasting photovoltaic array power production subject to mismatch losses. *Sol. Energy* 84, 1301–1309.
- Poissant, Y., CanmetENERGY, 2009. Field Assessment of novel PV module technologies in Canada. In: Presented at the Proc. 4th Canadian Solar Buildings Conference, Proc. 4th Canadian Solar Buildings Conference.
- Preu, R., 1995. PV-module reflection losses: measurement, simulation and influence on energy yield and performance ratio. In: Thirteenth European Photovoltaic Solar Energy Conference 1995. Proceedings, vol. 2, pp. 1465–1468.
- Reinders, A.H.M.E., Pramusito, Sudradjat, A., van Dijk, V.A.P., Mulyadi, R., Turkenburg, W.C., 1999. Sukatani revisited: on the performance of nine-year-old solar home systems and street lighting systems in Indonesia. *Renew. Sustain. Energy Rev.* 3, 1–47.
- Roberts, S., Guariento, N., 2009. Building Integrated Photovoltaics: A Handbook. Springer, Switzerland.
- Rodrigo, P., Rus, C., Almonacid, F., Pérez-Higueras, P.J., Almonacid, G., 2012. A new method for estimating angular, spectral and low irradiance losses in photovoltaic systems using an artificial neural network model in combination with the Osterwald model. *Sol. Energy Mater. Sol. Cells* 96, 186–194.
- Senado de la República de Colombia, 2003. Ley 855 de 2003. Definición de Zonas No Interconectadas al SIN.
- Solar America Board for Codes and Standards (Solar ABCs) [WWW Document], 2013. <<http://www.solarabcs.org/>>.

- de Souza, A.P., Escobedo, J.F., 2013. Estimates of hourly diffuse radiation on tilted surfaces in Southeast of Brazil. *Int. J. Renew. Energy Res.* IJRER 3, 207–221.
- Spencer, J.W., 1971. Fourier series representation of the position of the sun. *Search* 2 (5), 172.
- Sugiura, T., Yamada, T., Nakamura, H., Umeya, M., Sakuta, K., Kurokawa, K., 2003. Measurements, analyses and evaluation of residential PV systems by Japanese monitoring program. *Sol. Energy Mater. Sol. Cells* 75, 767–779.
- TamizhMani, G., 2011. Solar ABCs Policy Recommendation: Module Power Rating Requirements.
- The International Electrotechnical Commission (IEC), 1998. IEC 61724–1998, Photovoltaic system performance monitoring – Guidelines for measurement, data exchange and analysis.
- Thomas, R., 2012. *Photovoltaics and Architecture*. Taylor & Francis, London.
- Wittkopf, S., Valliappan, S., Liu, L., Ang, K.S., Cheng, S.C.J., 2012. Analytical performance monitoring of a 142.5 kWp grid-connected rooftop BIPV system in Singapore. *Renew. Energy* 47, 9–20.
- Zang, J., Wang, Y., 2011. Analysis of computation model of particle deposition on transmittance for photovoltaic panels. *Energy Procedia* 12, 554–559.

Capítulo 5

Metodología propuesta para limitar las pérdidas por inclinación, orientación y sombreado en BIPV

Título:	Methodology to establish the permitted maximum losses due to shading and orientation in photovoltaic applications in buildings
Autores:	Luis Fernando Mulcué-Nieto, Llanos Mora-López.
Revista:	Applied Energy, Elsevier
Factor de impacto JCR:	8.4 - Q1
Año:	2015
Categoría:	Energy Engineering and Power Technology
Publicación:	Volume 137, 1 January 2015, Pages 37-45.
DOI:	10.1016/j.apenergy.2014.09.088



Methodology to establish the permitted maximum losses due to shading and orientation in photovoltaic applications in buildings

Luis Fernando Mulcué-Nieto ^{a,b,c,*}, Llanos Mora-López ^{b,c}

^a GIDTA Group, Research Group in Environmental and Technological Developments – Universidad Católica de Manizales, Carrera 23 No. 60 – 63, Manizales, Colombia

^b Universidad Internacional de Andalucía, Calle Severo Ochoa, 16 29590 Malaga, Spain

^c Department of Computer Languages and Sciences, ETSI Informática, Universidad de Málaga, Campus de Teatinos, 29071 Malaga, Spain



HIGHLIGHTS

- We proposed a methodology to calculate the maximum losses permitted in BIPV.
- The procedure can be used for any country, taking another as baseline.
- The maxim allowed losses due to tilt and orientation was 53%.
- Only frontages cannot be used for BIPV at latitudes under 7°.
- The limits in shading for Colombia are lower than those for Spain.

ARTICLE INFO

Article history:

Received 27 March 2014

Received in revised form 23 September 2014

Accepted 28 September 2014

Available online 17 October 2014

Keywords:

Building-integrated photovoltaics (BIPV)

Performance ratio (PR)

Energy produced by a photovoltaic system

Performance of a photovoltaic system

ABSTRACT

Photovoltaic applications are implemented on a large scale in buildings, with a view to reducing global warming sustainably, as well as to meet energy demand. Thousands of electricity generators have been installed in this process around the world. However, very few countries have technical regulations that enable the energy efficiency and yield to be optimised in building-integrated photovoltaics (BIPV). On the other hand, all these normative should be a result of a serious study of the solar resource available in each region.

This paper proposes a methodology to establish technical standards in order to limit the losses due to shading and orientation of the constructed surface areas, where any country could be taken as benchmark. Colombia is also taken as a case study, by performing a comparative analysis for different cities.

© 2014 Elsevier Ltd. All rights reserved.

1. Introduction

Photovoltaic solar energy is an excellent option to cover the energy demands of the world population, by means of generating electricity in a distributed manner [1]. Two sectors of great importance and development are considered there: building-integrated photovoltaics (BIPV) and building-applied photovoltaics (BAPV). In the first, different construction elements such as roofs, frontages, windows are replaced by photovoltaic modules allowing modules having other functions in addition to being energy generators such as reducing the cooling load of the windows and concrete walls [2], while the second involves the already-constructed building.

Both the BIPV and the BAPV are the most elegant way of generating considerable fractions of urban electricity, as exclusive areas do not need to be dedicated to photovoltaic plant facilities [3]. Furthermore, their application in urban design is of vital importance to meet the European Union targets for 2020 [4], where it should be ensured there that all new constructions are “Zero Energy Buildings” (ZEB) [5].

One of the main targets in the field of BIPV is to attain optimum technical, economic and aesthetic solutions. Furthermore, other key factors to achieve their wide-scale implementation are the cutting of production costs, reducing the environmental impact and increasing the final efficiency of the system [6,7]. With respect to this last point, the design of the system plays a vital role in order to reduce possible losses, which can be due to angular and spectral response, temperature, low irradiance (orientation and shading), dirt and dust, Ohmic heating, module mismatch and different manufacturing tolerances.

* Corresponding author at: GIDTA Group, Research Group in Environmental and Technological Developments – Universidad Católica de Manizales, Carrera 23 No. 60 – 63, Manizales, Colombia. Tel.: +57 68782900x3300; fax: +57 68782937.

E-mail addresses: lmulcue@ucm.edu.co (L.F. Mulcué-Nieto), [\(L. Mora-López\).](mailto:llanos@lcc.uma.es)

In order to increase the energy yield, the amount of solar radiation impacting the generator needs to be maximised. However, that is not possible in the majority cases, due to engineering and architecture features of the building. For example, in countries near to the terrestrial equator, the house roofs receive a greater amount of irradiance per surface square meter than the frontages. On the other hand, replacing the construction material of a wall by a photovoltaic generator can be economically feasible. These facts raise the following question: To what point is it recommendable for photovoltaic to be on any surface of the building?

In 2009, Spain became one of the ground-breaking countries to answer the above question, when it published its *Código Técnico de la Edificación (Building Technical Code – CTE)* [8]. This document sets limits on the losses caused by shading and orientation of the photovoltaic generator. These regulations have been a highly successful contribution to spreading the architectural integration of photovoltaic in that nation. However, very few countries have technical regulations that enable the energy efficiency and yield to be optimised in the BIPV. On the other hand, all these normative should be a result of a serious study of the solar resource available in each region.

With respect to this, it should be pointed out that there is a need to establish criteria worldwide that enable joint projects to be developed, technological transfer of materials and inputs, to technically adapt the systems to each region and to reduce the environmental impact of the waste.

In the case of Colombia, it is estimated that the photovoltaic market sells approximately 300 kWp per year, mainly to isolated systems of the grid [9]. If this figure is extrapolated to the 30 years that the sector has been in the country, the total installed power would be around 9 MWp [10]. This figure is very low if the high levels of solar radiation available are taken into account. The national government is currently driving renewable energies, but, unfortunately, there is still no technical legislation that enables developments in the sector to be regulated.

This paper proposes a methodology to suggest technical standards in order to limit the losses due to shading and orientation of the photovoltaic applications on constructed surface areas, where Spain is taken as the benchmark. The paper is organised as follows: in Section 2, the different types of losses are characterised; in Section 3 the existing legislation is summarised; in Section 4 it is explained the proposed methodology; in Section 5, the results obtained with the proposed methodology are presented and discussed. Finally, in the last section the conclusions of the work are summarised.

2. Theory and calculations

2.1. Estimating solar irradiation on tilted surfaces

Any flat surface area, located in the northern hemisphere of the earth, is fully characterised by its tilt angle β over the ground and by the azimuth angle or orientation α with respect to the south. The amount of annual solar irradiance $G_a(\beta, \alpha)$ that the system receives is conditioned for each pair of values (β, α) .

We propose to estimate the solar irradiation on tilted surfaces using as input data the monthly average daily values on a horizontal surface, $G_{dm}(0)$. Taking those as the baseline, each value will be decomposed into diffuse $D_{dm}(0)$ and direct radiation $B_{dm}(0)$ using the expression proposed by Page [11], and valid for latitudes between 40°N and 40°S.

Once the daily components of global radiation, $D_{dm}(0)$ and $B_{dm}(0)$ are obtained, their respective hourly values, $D_h(0)$ and $B_h(0)$ are calculated using the expressions proposed by Collares and Rabl [12].

The following step is to calculate the hourly global irradiance on the surface of the generator $G_h(\beta, \alpha)$. We therefore use the *three-component model*, which has proven to be quite accurate [13], and establishes that the incident irradiance is made up of direct $B_h(\beta, \alpha)$, diffuse $D_h(\beta, \alpha)$, and reflected $R_h(\beta, \alpha)$ irradiance.

The Hay-Davies anisotropic model [14] is used for calculating the diffuse component on tilted surface, as it stands out in different comparative studies for its high accuracy and simplicity [15–18].

Finally, the components of the hourly global irradiance are totalled in order to obtain the monthly daily average on a tilted surface:

$$G_{dm}(\beta, \alpha) = \sum_{h=1}^{24} G_h(\beta, \alpha) \quad (1)$$

2.2. Losses due to orientation and tilting

In northern latitudes, the amount of annual solar irradiance is maximum when the photovoltaic module is orientated towards the south ($\alpha = 0$) and is tilted at an angle $\beta = \beta_{opt}$. For any latitude ϕ , this angle can be defined as:

$$G_a(\beta_{opt}) = \begin{cases} \max[G_a(\beta, 0)] & \text{if } \phi \geq 0 \\ \text{or} \\ \max[G_a(\beta, \pi)] & \text{if } \phi \leq 0 \end{cases} \quad (2)$$

Thus, the percentage of annual losses due to tilt and orientation can be calculated by:

$$L_{\beta, \alpha} = 100 \left(1 - \frac{G_a(\beta, \alpha)}{G_a(\beta_{opt})} \right) \quad (3)$$

Some authors [19,20] relate those losses using a highly useful concept, known as the *irradiance factor*, FI. The document entitled the *Pliego de Condiciones Técnicas de Instalaciones Aisladas de Red de España* [Spanish Technical Specification of Off-grid Facilities] [21], defines it as the incident annual radiation for an orientation α and tilt β generator, with respect to that received for optimum tilt and orientation $G_a(\beta_{opt}, 0)$:

$$G_a(\beta, \alpha) = FI(\beta, \alpha) \cdot G_a(\beta_{opt}, 0) \quad (4)$$

Therefore, Eq. (3) can be re-written as:

$$L_{\beta, \alpha} = 100(1 - FI) \quad (5)$$

FI depends on β , α , the latitude and diffuse radiation fraction of the place [13]. Therefore, given that the local climate conditions are characteristics of the site, the losses due to orientation and tilting cannot be unified in different places. Benchmark stations are therefore usually used to estimate FI in similar latitudes.

One example of the use of FI in a polar diagram is the one performed by Cronemberger et al. [22] who used this criterion to estimate the photovoltaic potential of roofs and frontages in Brazil. Brogren and Green [23] proposed an approach where the diagram was used in a rectangular shape by means of the PVSYST software. The analysis included in their research would allow building-integrated photovoltaic applications to be analysed in the city of Stockholm, Sweden.

Tilt and orientation can lead to the conclusion that some roof surfaces are unsuitable for installing photovoltaic systems. For instance, Lukac et al. [24] proposed a new method to evaluate the solar potential of a roof's surface. This method combines extracted urban topography from LiDAR data with measurements of global and diffuse solar irradiances.

With respect to the possible tilting and different shapes of the rooftops, Hachem et al. [25] conducted a study into the effect of those variables on the photovoltaic potential of houses in Canada. One of their conclusions was that the best frontage receives 1179 kW h/m² when it is south-facing.

2.3. Losses due to shading

As the sun moves through the sky, two angles, the sun height Υ_s , and the azimuth α , allow us to know its exact position. When plotting Υ_s against α for the whole year, the so-called *solar trajectory diagram* is obtained. When the diagram of the coordinates of the obstacles surrounding the solar panel is superimposed on this, the solar gain losses due to the shading can be calculated taking into account the shaded areas in this diagram and the relative contribution in terms of total annual energy for these areas. The relative total losses due to shaded areas, L_{shading} , are obtained as the sum of the relative losses in each shaded area. FS is the so-called *shading factor*, defined as the relationship between the real incident solar irradiance in the photovoltaic generator, and the ideal irradiance that the system will receive without shading [26].

On the other hand, the path diagram is then divided into 1 h interval to establish the benchmark tables. Several areas emerged from this division, each of which contains a set of days of the year between 2 specific hours. The sum of the circumsolar diffuse and direct irradiance components of each hour of the days is what can be lost from shading. When dividing the result by the annual irradiance, the fraction is obtained equivalent to the lost radiation percentage of region i :

$$R_i = \frac{\sum_j (B_j + D_j^C)}{G_a} \quad (6)$$

where the sum is calculated during the hours and days for the corresponding area of the diagram.

These two factors are related according to the expression:

$$L_{\text{shading}} = 100(1 - FS) \quad (7)$$

There are many articles that report studies into losses due to shading in BIPV, even though the majority of them only propose techniques for specific cases or assume that legislation already exists in that respect. For example, Cellura et al. [27] proposed a photographic method, that was subsequently improved [28], to estimate the effects of shading caused by surrounding obstructions. On the other hand, large losses due to shading can be present in claddings of buildings used for BIPV, depending on its azimuth and tilt [29].

Other quite interesting approach was taken by Nguyen Pearce [30], who developed a methodology based on satellite images to study global losses due to shading in the photovoltaic potential of a US city. This research concluded that the average energy losses for this concept in buildings are 25%. Loulas et al. [31] obtained similar results, when they conducted a detailed shadow study in a residential block in Greece. However, further research performed for the Canary Islands shows that it can reach up to 52%, according to Schallenberg-Rodríguez [32]. This corroborates the affirmation made by Brito et al. [33], that the greater the penetration of the photovoltaic modules on the roofs, the greater the importance the shading acquires.

3. International legislation

In 1998, the *International Electrotechnical Commission* (IEC) published the IEC 61724 International Standard. The annual energy produced for Photovoltaic applications Connected to the Electricity Grid according this standard can be estimated using the equation:

$$E_{PV} = \frac{G_{a,\text{real}}(\beta, \alpha) \cdot P_{\text{peak}} \cdot PR}{G_{\text{STC}}} \quad (8)$$

where P_{peak} is the installed photovoltaic peak power, PR the performance ratio or yield of the facility, G_{STC} the solar irradiance under standard measurement conditions, equal to 1 kW/m^2 , and $G_{a,\text{real}}$

(β, α) the annual solar irradiance on the surface, taking into account losses due to shading. Therefore, it can be written as:

$$G_{a,\text{real}}(\beta, \alpha) = FS \cdot G_a(\beta, \alpha) \quad (9)$$

when introducing Eq. (4), the former equation becomes:

$$G_{a,\text{real}}(\beta, \alpha) = FS \cdot FI \cdot G_a(\beta_{\text{opt}}, 0) \quad (10)$$

Both FI and FS limit the final energy in the field of the BIPV, however the IEC 61724 document does not refer to them and does not propose allowed limits. This is understandable as the solar resource is different in each region. Consequently, it is necessary to formulate criteria within each country. This paper proposes a simple methodology to carry that out.

4. Proposed methodology

The following procedure is proposed to establish the loss limits due to orientation and shading, it is valid for any country. The procedure is used in this work for different cities of Colombia.

As a convention, each of the cities of the country to be studied (Colombia) were named as "Place 2". "Place 1" refers to the benchmark country, Spain (This country was taken as reference due to have a legislation that limit the losses for BIPV).

The amount of annual average radiation that a surface receives according to its tilt and azimuth was first calculated. The maximum incident amount in Place 2 was then compared to the worst frontage in Place 1. The loss limit percentage due to orientation and tilt per city was thus obtained. This criterion is highly useful as:

- a. The limits are not established universally, taking into account that the solar resource is different in each region. This fact is important as equal global radiation percentages may correspond to very different solar irradiance values on the surfaces.
- b. The fact that the amount of solar energy received per square metre is aligned shows that the countries that receive greater annual radiation have a greater variety of architectural integration opportunities. In contrast, if a universal percentage is adopted, no frontage could be used for BIPV in equatorial countries (taking Spain as the benchmark).
- c. It is more beneficial from the environmental and economic point of view. This is due to the fact that replacing construction materials with photovoltaic modules is more beneficial in countries with a high level of annual irradiance.

On the other hand, the diffuse fraction is different in Place 1 (Spain) was taken into account when establishing losses from shading limits in Place 2 (Colombia). Thus, the loss limit percentage is equivalent to a fraction of maximum irradiance that can be physically lost from shading. The main idea consisted of equalising that fraction for both places. For example, if a third of the maximum possible radiation could be lost in Spain, that same fraction would be kept in Colombia. Therefore, it was used an absolute variable to compare these two places.

Finally, the benchmark tables were established for each city, which will be used as input for future regulations in Columbia.

4.1. Calculating the annual solar irradiation on tilted surfaces in Colombia

Only the global solar irradiation on a horizontal surface, $G_{dm}(0)$, in 12 monthly average daily values, is initially known. The methodology described in Section 2.1 has been used for obtaining the monthly daily average irradiation on a tilted surface.

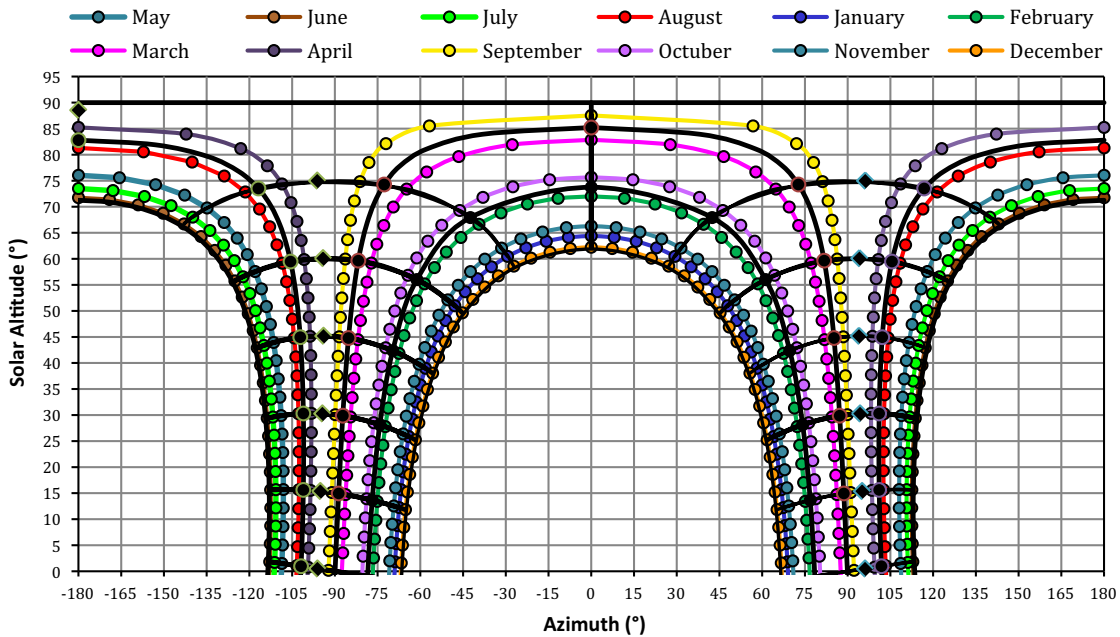


Fig. 1. Construction example of the solar path diagram for Bogotá.

Taking the above into account, the diffuse fraction of the main cities of Spain was then calculated. The average value of the above parameter representing the country was then established, with the remaining fraction being direct radiation. This value was then compared with the maximum stipulated according to the benchmark tables published by the CTE. This comparison is used to deduct the representative values of $B_a(0)$ and $D_{a,2}^C(0)$ for Place 1.

It is also necessary to estimate the maximum annual solar irradiance $G_a(\beta_{opt})$ (Place 2) and minimum amount of annual solar $G_{a,\text{MIN}}(90,0)$ that a frontage can receive (Place 1).

For obtaining the first value, we propose to repeat the procedure set out in Section 2.1 by increasing the tilt angle β from 0° to 90° , taking $\Delta\beta = 1^\circ$ as the increase and using azimuth equal to 0° for positive latitudes and equal to 180° for negative latitudes (the generator is facing south). Thus, Eq. (2) was used to establish the maximum annual irradiance.

According to the CTE, the losses from orientation and tilt on any surface for BIPV cannot exceed 40% for fully integrated systems. This surface was named the *worst permissible frontage*. Then, this frontage is “transferred” to Place 2. Therefore, the permissible percentage for Place 2 is:

$$L_{\beta,x,\text{MAX},2} = 100 \left(1 - \frac{G_{a,\text{MIN},1}(90,0)}{G_{a,2}(\beta_{opt})} \right) \quad (11)$$

where the subscripts 1 and 2 refer to places 1 and 2, respectively.

4.2. The loss limit percentage from shading

It was then supposed that there is a standard in the benchmark country with maximum limits for losses from shading $L_{\text{shading,MAX},1}$. The fraction to which this percentage corresponds, with respect to the physically possible maximum loss of irradiance is determined for Place 1 by:

$$f_{\text{MÁX,losses},1} = \frac{L_{\text{shading,MAX},1}}{100\% \left(\frac{B_{a,1}(0) + D_{a,1}^C(0)}{G_{a,1}(0)} \right)} \quad (12)$$

where subscript 1 indicates the irradiance of the baseline country, while $L_{\text{shading,MAX},1}$ was taken as 20%, pursuant to Spanish regulations for fully integrated systems.

The fraction of Eq. (12) was equalled to its equivalent in Colombia. Thus, the maximum losses from shading for Place 2 were calculated by means of:

$$L_{\text{shading,MAX},2} = 100\% \left(\frac{B_{a,2}(0) + D_{a,2}^C(0)}{G_{a,2}(0)} \right) f_{\text{MÁX,losses},1} \quad (13)$$

where subscript 2 indicates the irradiance of each city of Colombia.

The used method is described in detail below.

5. Results and discussion

Data used for this study have been obtained from RETScreen International [34], which is funded by Natural Resources Canada. This database is supported by 6700 land weather stations and by NASA satellites, which cover the whole of the planet's surface. Solar global radiation data have been obtained for 20 cities in Colombia. Moreover, data from the *Atlas de Radiación Solar en España* (*Solar Radiation in Spain Atlas*) [35], published by the Spanish State Meteorology Agency [36] were used.

The calculation described in Section 2.1 for obtaining global solar radiation in a tilted surface was performed for 20 cities of Colombia located between latitudes -4°S and 12°N .

5.1. Determining the loss limit percentage due to orientation and tilt

To establish the maximum loss percentage on each surface, the benchmark of 100% was first established, that is, the maximum annual solar irradiance $G_a(\beta_{opt})$.

In order to achieve the above objective, the procedure set out in Section 4.1 was used. $G_a(\beta_{opt})$ for each city of Colombia and the minimum amount of annual solar irradiance $G_{a,\text{MIN}}(90,0)$ that a frontage can receive in Spain have been calculated.

The permissible percentage for Place 2 has been estimated using Eq. (13).

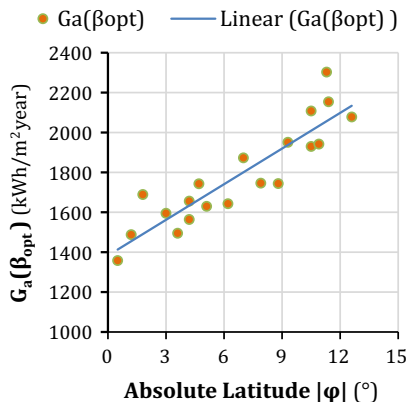
5.2. Calculation of the loss limit percentage from shading

The diffuse fraction of the main cities of Spain and of cities of Colombia was calculated according to the proposed method. The

Table 1

Annual maximum irradiance for each city of Colombia.

City	Latitude ϕ ($^{\circ}$)	$G_a(\beta_{opt})$ (kW h/m 2 year)
Leticia	-4.2	1656
Puerto Asís	0.5	1358
Pasto	1.2	1488
Tumaco	1.8	1689
Neiva	3	1595
Cali	3.6	1495
Villavicencio	4.2	1564
Bogotá	4.7	1743
Manizales	5.1	1630
Medellín	6.2	1643
Barrancabermeja	7	1873
Cúcuta	7.9	1746
Montería	8.8	1744
Sincelejo	9.3	1951
Cartagena	10.5	2108
Valledupar	10.5	1930
Barranquilla	10.9	1942
Santa Marta	11.3	2303
Maicao	11.4	2154
San Andrés	12.6	2078

**Fig. 2.** Maximum irradiance $G_a(\beta_{opt})$ versus absolute latitude $|\phi|$.

values of the maximum losses from shading for all cities were also calculated using Eq. (13).

In Spain, the CTE sets the limit at 20% for BIPV. To transfer the equivalent of this percentage to Colombia, the equivalent fraction of this 20% was calculated, with respect to the permanent shading situation. In such a hypothetical case, the radiation no longer perceived would be equal to the direct radiation $B_a(0)$, plus the circumsolar diffuse radiation $D_a^C(0)$; both measured on a horizontal surface.

5.3. Preparing the solar paths and benchmark tables

To produce the solar path diagram for each city located at latitude ϕ , the solar height and azimuth angles were estimated.

$$\sin \gamma_s = \sin \delta \sin \phi + \cos \delta \cos \phi \cos \omega \quad (14)$$

$$\cos \psi_s = \frac{\sin \gamma_s \sin \phi - \sin \delta}{\cos \gamma_s \cos \phi} [sign \phi] \quad (15)$$

These angles were used to prepare the path of each representative day of the month, for a total 12. The representative day is taken to be the one on which the irradiance equals the monthly daily average. For each day, the hour angle ω was calculated every 15 min. The graph obtained was divided into 4 portions that cover a range of months.

Table 2

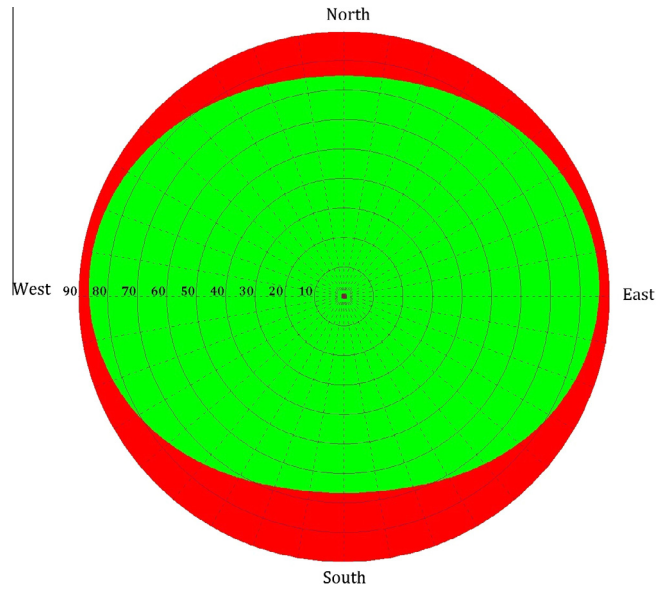
Benchmark cities and maximum irradiance values selected.

Benchmark city	Latitude range ϕ ($^{\circ}$)	$G_a(\beta_{opt})$ (kW h/m 2 year)
Leticia	$-4.2 \leq \phi < 0$	1656
Pasto	$0 \leq \phi < 4$	1358
Bogotá	$4 \leq \phi < 7$	1564
Cúcuta	$7 \leq \phi < 9$	1744
Barranquilla	$9 \leq \phi < 12.9$	1930

Table 3

Maximum annual loss percentages due to tilt and orientation.

Benchmark city	$L_{\beta,z,\text{MAX},2}$ (%)
Leticia	45
Pasto	33
Bogotá	42
Cúcuta	48
Barranquilla	53

**Fig. 3.** Possible surfaces for Leticia ($\phi = -4.2^{\circ}$).

Approximately, the procedure for obtaining the diagrams explained before can be abbreviated by taking Fig. 1 into account.

It can here be seen that the lower central region of the graph comprises 4 months: November, December, January and February. Therefore, the sum of Eq. (6) is approximately:

$$\sum_j (B_j + D_j^C) \approx 30 \sum_{\text{Nov,Dec,Jan,Feb}} (B_{hm} + D_{hm}^C) \quad (16)$$

where the definition of the representative day of the month has been used. Thus, B_{hm} and D_{hm} were the hourly components of this day in the region i . Taking this into account, the irradiance percentage of region R_i was calculated by means of:

$$R_i = \frac{\sum_{\text{months in the region}} (B_{hm} + D_{hm}^C)}{\sum_{\text{all months}} G_{dm}} \quad (17)$$

The above equation was also used to produce the benchmark tables on surfaces with typical orientations and tilting. To establish the number of tables to be prepared, it was taken into account that the plane was within the limits allowed by orientation and tilt.

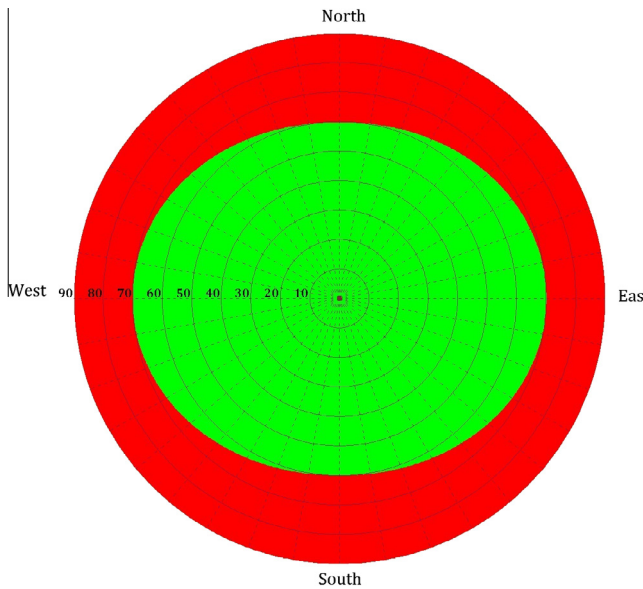


Fig. 4. Possible surfaces for Pasto ($\phi = 1.2^\circ$).

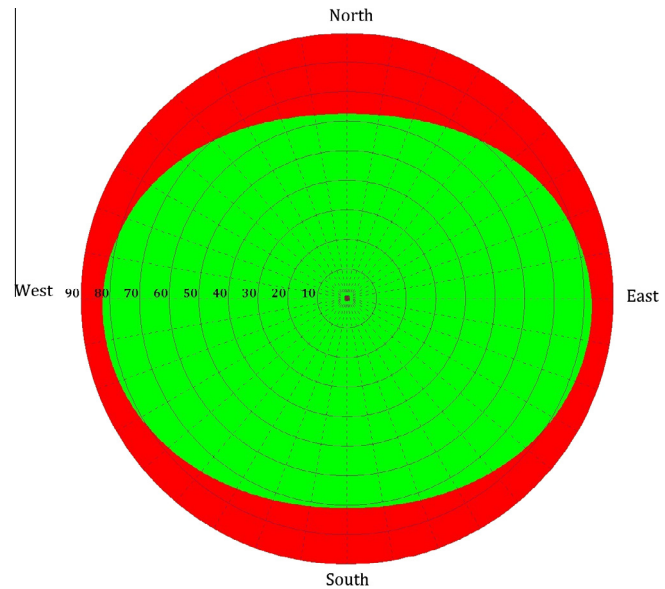


Fig. 5. Possible surfaces for Bogotá ($\phi = 4.7^\circ$).

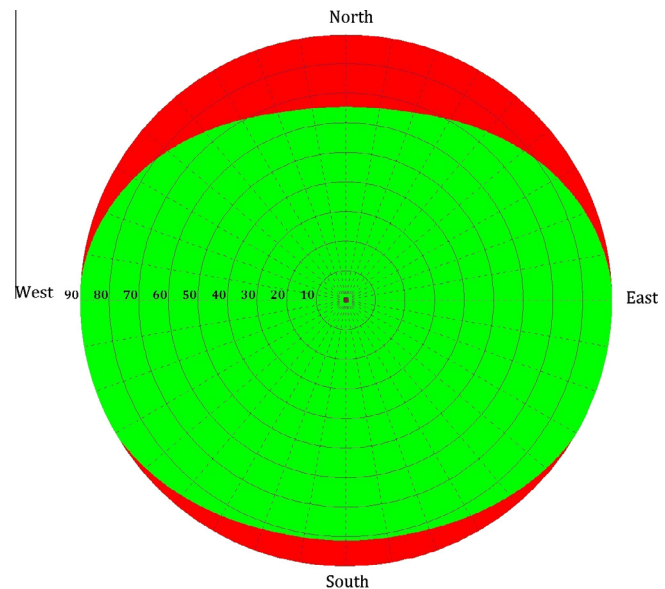


Fig. 6. Possible surfaces for Cúcuta ($\phi = 7.9^\circ$).

5.4. Maximum irradiation and selection of benchmark cities

The results of the annual maximum irradiation for the 20 cities of Colombia are set out in Table 1. It can be seen that $G_a(\beta_{opt})$ increases with the absolute latitude of the place. This is consistent with the irradiance maps of the *Atlas de Radiación Solar de Colombia* [37].

The difference between the maximum and minimum value of Table 1 was 945 kW h/m²/year, and is equal to 45% of the highest irradiance. This broad range means that it is necessary to regroup the data into benchmark cities, which facilitates the losses allowed for orientation and tilt being approximately uniform in each region. In this respect, Table 1 data are depicted in Fig. 2.

By performing a linear regression, the points establish a relation as follows:

$$G_a(\beta_{opt}) = 59.58|\phi| + 1383.2 \quad (18)$$

This expression implies that for each 3° of latitude, the maximum solar irradiance received increases approximately by 8%. On other hand, in a previous article, we proposed 5 benchmark cities, so that the irradiance factor FI does not vary significantly. Table 2 list the benchmark cities, along with the irradiance value $G_{a,2}(\beta_{opt})$ used in Eq. (13). The latter is selected so that reception not under the minimum irradiance quantity allowed in Spain will be guaranteed on the frontage of each sub-group.

5.5. Loss limits due to orientation and tilt

In order to establish the maximum losses due to orientation and tilt, Bilbao, with 1292.1 kW h/m² year, was determined to be the city of Spain that receives the lowest amount of annual solar irradiance on horizontal surface [35]. With this information and using the FI irradiance factor of the CTE, the irradiance for the optimum tilt was calculated to 1520.1 kW h/m² year. In this respect, the worst permissible frontage of Place 1 receives a minimum of 60%, in other words, $G_{a,\text{MIN},1}(90,0) = 912.1$ kW h/m² year.

The above value and the data of Table 2 were used to calculate the maximum permissible losses for Colombia. The results are set out in Table 3.

The previous limits imply that there is a limited set of surfaces for BIPV. In order to establish visually what they would be, all the planes that receive an irradiation percentage higher than the

established one are expressed graphically in Figs. 3–7. In those graphs, the tilt was represented as the concentric circumferences, while the azimuth was indicated with the radial lines; each of them at intervals of 10°. If the coordinates of the surface are within the region shown in green¹, the surfaces meets the standards, otherwise it is shown in red.

It can be seen from the graphs that there is a great variety of surfaces that comply with the calculated limits. Practically all types of roofs can be used, a fact that is logical for an equatorial country. However, in Leticia, Pasto and Bogotá, in other words, at absolute latitudes under 7°, only frontages cannot be used for BIPV. The above is true in the case that the generator is only located on the frontage, but a part may be simultaneously on the roof, so that the global loss percentage is within the limits.

¹ For interpretation of color in Figs. 3–7, the reader is referred to the web version of this article.

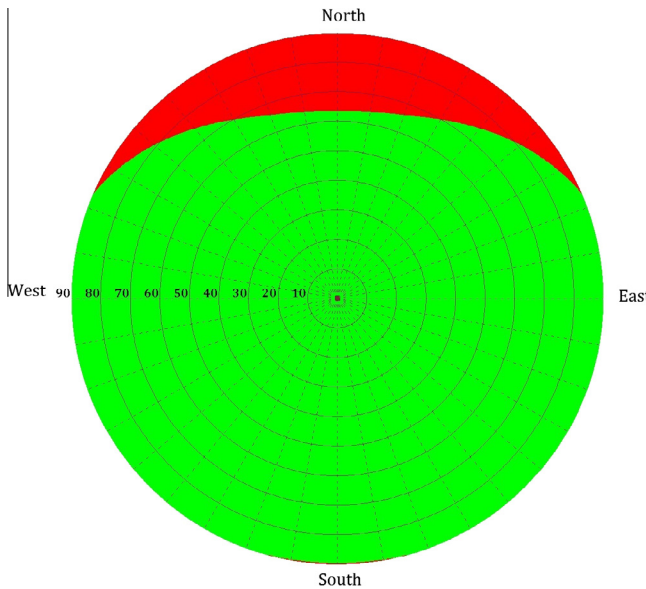


Fig. 7. Possible surfaces for Barranquilla ($\phi = 10.9^\circ$).

For latitudes over 7° , the diagram opens up, indicating the existence of frontages with photovoltaic potential. For example, frontages with azimuth between 60° and 90° , both to the east and to the west, are allowed for Cúcuta. Barranquilla is the one that allows the greatest variety, as practically any frontage with $-110^\circ \leq \alpha \leq 110^\circ$ is adequate.

5.6. Loss limits due to shading

To calculate the maximum losses due to shading, the diffuse fraction of 54 cities of Spain was first calculated. The results are shown in Fig. 8, where it can be seen that the average is 0.34. This means that 66% of the global irradiance is direct.

On the other hand, according to the Spanish CTE, the losses in the case of total shading would be approximately 84%. The above facts implies that there has to be $B_{a,1}(0) = 0.66G_{a,1}(0)$ and $D_{a,1}^c(0) = 0.18G_{a,1}(0)$ for Place 1. Therefore, it was established that the fraction corresponding to the legally-established 20% was $f_{\text{MAX,losses},1} = 0.238$.

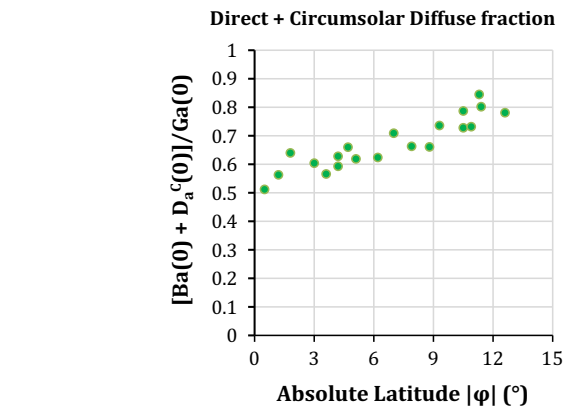


Fig. 9. Circumsolar diffuse and direct irradiation fraction for different cities of Colombia.

Fig. 9 likewise shows the sum of the fractions of circumsolar diffuse and direct components for the 20 cities of Colombia. It can be appreciated that the data fluctuation is greater than in Spain, which is the reason for working with benchmark cities. Thus, the average of the components was obtained for the cities within the range of latitudes that cover each benchmark city.

Table 4 shows the maximum permissible losses due to shading, calculated for Colombia. In general, the limits are lower than those allowed in Spain. This is due to the fact that Colombia has a greater diffuse radiation fraction, therefore there is a lower amount of direct irradiance that can be lost by shading.

The closeness of the values of Table 4 raises the possibility of establishing a single loss limit percentage for the whole of Colombia, in which case this should be 16%.

5.7. Solar paths and benchmark tables

The solar path diagrams were prepared for the benchmark cities. In particular, the minimum point of the diagram at midday varied from 70° to 55° . This ratifies the need for a single diagram not to be taken for Colombia. Likewise, between each benchmark city, there is a maximum displacement of 3° in the diagram, which is acceptable when locating the coordinates of obstacles that cause shadows.

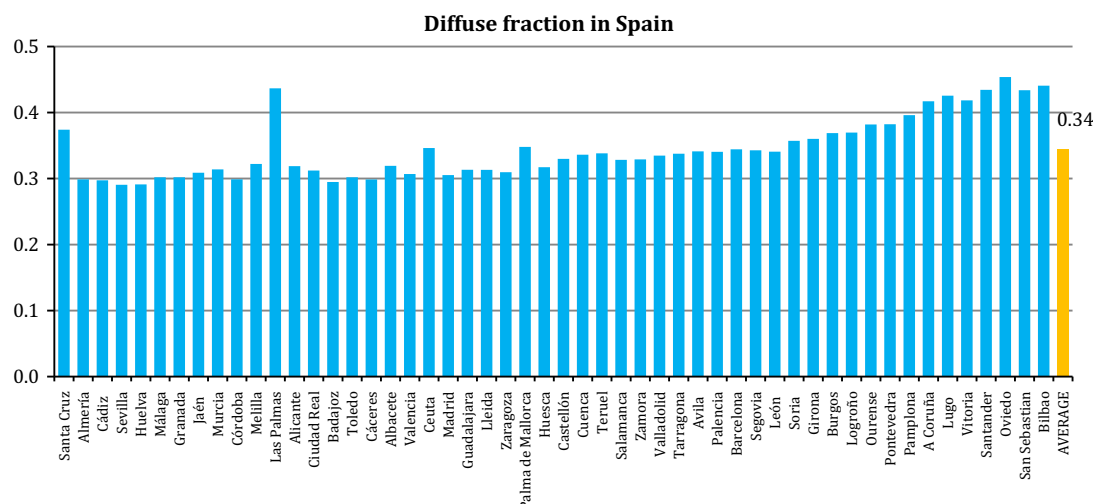


Fig. 8. Diffuse irradiation fraction for several Spanish cities.

Table 4
Maximum percentages of annual losses due to shading.

Benchmark city	$L_{\text{shading,MAX},2}$ (%)
Leticia	15
Pasto	14
Bogotá	15
Cúcuta	16
Barranquilla	18

There is a benchmark table for each of the path diagrams. These are not shown in this work due to their large extension and due to they will be published in a future regulation about photovoltaic applications for BIPV in Colombia.

5.8. Proposal for a future technical standard for Colombia

Fig. 10 summarises the results of the permissible limits for the losses due to orientation and shading in Colombia, and these could be taken as reference for equatorial countries. It is important to know that the total losses were calculated by taking half of the maximums due to shading, as the CTE stipulates. These should be used in a future technical standard in Colombia.

With respect to the maximum total losses permitted, it can be seen that the city of Pasto is the most restricted, with 40%. This is due to the proximity of its latitude to the Equator and, therefore, the lower quantity of irradiance received. On the other hand, the city with the greater margin of possibilities was Barranquilla with 62%. The reason for this is the high annual solar irradiation that it receives, together with the nearby cities.

The maximum value allowed in losses due to tilt and orientation was obtained for the city of Barranquilla (53%). In contrast, Pasto obtained the minimum with 33%. This performance is explained by the fact that regions with greater solar resource have greater flexibility for BIPV. Compared to the Spanish technical standard, Colombia was shown to have more possibilities of surfaces for BIPV.

In a similar way to what happened with the maximum losses due to orientation and tilting, Pasto showed the lower permissible limit in losses due to shading (14%). In contrast, the maximum was registered in Barranquilla with 18%. This implies that for Colombia, in general, the further away a city is from the Equator line, the greater the losses will be allowed for both concepts.

With respect to Spain, it can be concluded that Leticia, Cúcuta and Barranquilla exceeds it in terms of solar resource, as the total permitted losses are greater than the 50% stipulated in the CTE. This result is very important for the BIPV worldwide, as it implies that regions with greater solar resource have greater architectural

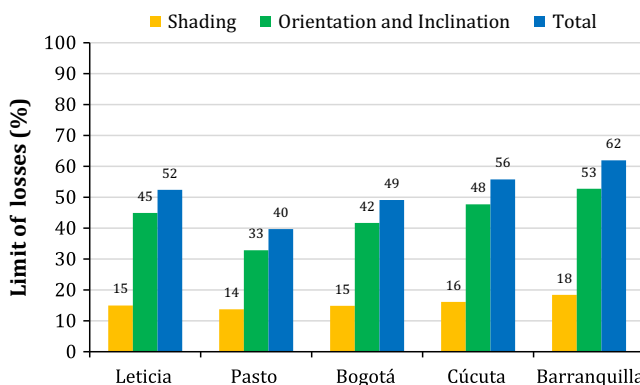


Fig. 10. Limit losses allowed for each benchmark city.

integration possibilities. The above allows greater equity when comparing the energy yield of two buildings located in different regions. The main reason for accepting this is that the greater the solar irradiance available, the higher the economic return for the photovoltaic.

5.9. Proposal for a worldwide technical standard

In order to propose a simple expression to calculate the loss limit due to orientation for any country, in Fig. 11 Eq. (11) was depicted for usual values of annual maximum irradiation. It can there be seen that the values of this variable range between 30% and 60%. According to this, only by locating the value corresponding to $G_a(\beta_{opt})$ of the city, it can be easily determined the maximum loss limit by this concept.

Similarly, to find a relation between the loss limit due to shading and the diffuse fraction D_F of the city, Fig. 12 was drawn. It can be appreciated that its figures range between 10% and 25%, depending on the place.

By performing a linear regression, the points establish a relation as follows ($R^2 = 0.943$):

$$L_{\text{shading,MAX}} = 31.907(0.951 - D_F) \quad (19)$$

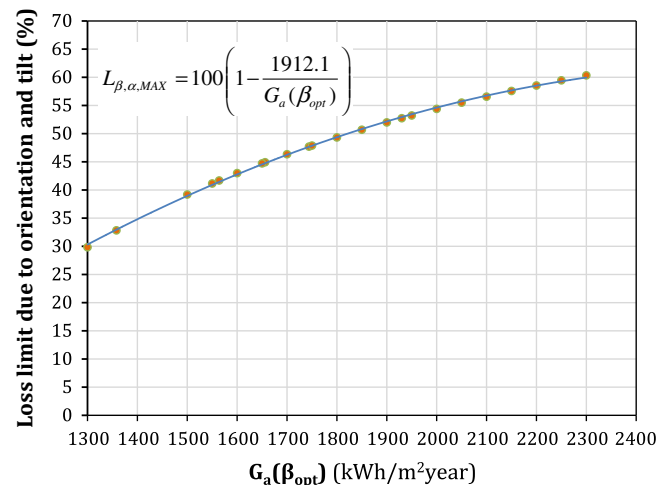


Fig. 11. Loss limit due to orientation and tilt against the annual maximum irradiation of the city.

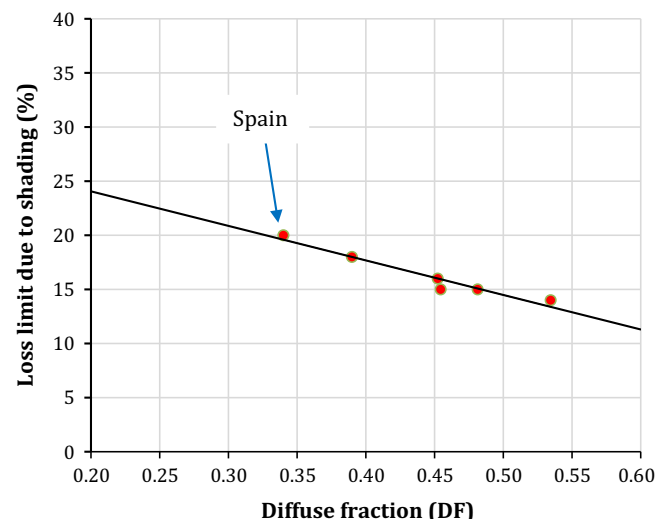


Fig. 12. Loss limit due to shading against the diffuse fraction of the city.

In Eq. (19) and Fig. 11 is summarised the process described in Section 4. These tools are very useful to find easily the maximum losses allowed due to shading and orientation for future regulations in any city of a country, only by knowing the diffuse fraction and the annual maximum irradiation (G_a for $\beta = \beta_{opt}$).

6. Conclusions

A methodology has been proposed to calculate the maximum losses permitted due to orientation and shading, in photovoltaic applications integrated in buildings (BIPV). The procedure can be used for any country, taking another country as a baseline that has a technical standard in that respect.

The methodology used showed that, for Colombia, the maximum annual global irradiance $G_a(\beta_{opt})$ increases with the absolute latitude of the place. For each 3° of latitude, the increase is approximately 8%, therefore it was proposed using 5 benchmark cities to address the whole country. This criterion enables the permissible shading limits to be approximately uniform in each region. Although practically all types of roofs in Colombia can be used, frontages cannot be used for BIPV at latitudes under 7° .

As regards the loss limits due to shading, the limits in Colombia are lower than those allowed for Spain. This is due to it having a greater diffuse radiation fraction than the European country. This is coherent when comparing the amount of irradiance that can be lost due to shading, that is, the sum of the circumsolar diffuse and direct components. This figure was lower in Colombia than in Spain, with 67% and 84%, respectively. In case of establishing a single loss limit percentage due to shading for the whole Colombia, this should be equal to 16%.

In order to unify world criteria for BIPV, it would be very interesting to use this methodology in emerging countries within the field of photovoltaic solar energy. Furthermore, a different benchmark to Spain could be taken.

Acknowledgements

This research was carried out thanks to the support received by means of a postgraduate grant from the Universidad Internacional de Andalucía. Also to the Faculty of Engineering and Architecture of the Universidad Católica de Manizales for providing different resources to make this publication possible.

Finally, we would like to thank the Spanish Institute for Energy Diversification and Savings (IDAE) to allow access to the images and tables of the CTE.

References

- [1] Pearce JM. Photovoltaics — a path to sustainable futures. *Futures* 2002;34:663–74. [http://dx.doi.org/10.1016/S0016-3287\(02\)0008-3](http://dx.doi.org/10.1016/S0016-3287(02)0008-3).
- [2] Sun L, Lu L, Yang H. Optimum design of shading-type building-integrated photovoltaic claddings with different surface azimuth angles. *Appl Energy* 2012;90(1):233–40. <http://dx.doi.org/10.1016/j.apenergy.2011.01.062>.
- [3] dos Santos IP, Rüther R. The potential of building-integrated (BIPV) and building-applied photovoltaics (BAPV) in single-family, urban residences at low latitudes in Brazil. *Energy Build* 2012;50:290–7. <http://dx.doi.org/10.1016/j.enbuild.2012.03.052>.
- [4] Jelle BP, Breivik C. State-of-the-art Building Integrated Photovoltaics. *Energy Procedia* 2012;20:68–77. <http://dx.doi.org/10.1016/j.egypro.2012.03.009>.
- [5] Kanters J, Horvat M. Solar energy as a design parameter in urban planning. *Energy Procedia* 2012;30:1143–52. <http://dx.doi.org/10.1016/j.egypro.2012.11.127>.
- [6] Jelle BP, Breivik C. The path to the Building Integrated Photovoltaics of tomorrow. *Energy Procedia* 2012;20:78–87. <http://dx.doi.org/10.1016/j.egypro.2012.03.010>.
- [7] Sadineni SB, Atallah F, Boehm RF. Impact of roof integrated PV orientation on the residential electricity peak demand. *Appl Energy* 2012;92:204–10. <http://dx.doi.org/10.1016/j.apenergy.2011.10.026>.
- [8] Gobierno de España. Código Técnico de la Edificación – HES Ahorro de Energía – Contribución Fotovoltaica Mínima de Energía Eléctrica; 2009.
- [9] Guerrero EC, Escoria JD. El sector solar fotovoltaico en el caribe colombiano: análisis técnico y de mercado. *Sci Tech* 2012;2:87–91.
- [10] Rodríguez Murcia H. Desarrollo de la energía solar en Colombia y sus perspectivas. *Revista Ingeniería* 2008;83–9.
- [11] Page J. The estimation of monthly ea values of daily total short wave radiation on vertical and inclined surfaces from sunshine records for latitudes 40°N–40°S. *Proc UN Conf New Sources Energy* 1961;4:378–90.
- [12] Collares-Pereira M, Rabl A. The average distribution of solar radiation-correlations between diffuse and hemispherical and between daily and hourly insolation values. *Sol Energy* 1979;22:155–64. [http://dx.doi.org/10.1016/0038-092X\(79\)90100-2](http://dx.doi.org/10.1016/0038-092X(79)90100-2).
- [13] Haberlin H. Photovoltaics: system design and practice. United Kingdom: John Wiley & Sons; 2012.
- [14] Hay JE. Study of shortwave radiation on non-horizontal surfaces. Atmospheric Environment Service, Report No 79–12; 1979.
- [15] Denegri MJ, Raaijijk C, Gallegos HG. Evaluación de diferentes modelos utilizados para la estimación de la radiación fotosintéticamente activa en planos inclinados. *Avances Energías Renovables Medio Ambiente* 2012;16:9–15.
- [16] Noorian AM, Moradi I, Kamali GA. Evaluation of 12 models to estimate hourly diffuse irradiation on inclined surfaces. *Renew Energy* 2008;33:1406–12. <http://dx.doi.org/10.1016/j.renene.2007.06.027>.
- [17] Diez-Medivilla M, de Miguel A, Bilbao J. Measurement and comparison of diffuse solar irradiance models on inclined surfaces in Valladolid (Spain). *Energy Convers Manage* 2005;46:2075–92. <http://dx.doi.org/10.1016/j.enconman.2004.10.023>.
- [18] de Souza AP, Escobedo JF. Estimates of hourly diffuse radiation on tilted surfaces in Southeast of Brazil. *Int J Renew Energy Res (IJRER)* 2013;3:207–21.
- [19] Thomas R. Photovoltaics and architecture. London: Taylor & Francis; 2012.
- [20] Roberts S, Guariento N. Building Integrated Photovoltaics: a handbook. Switzerland: Springer; 2009.
- [21] Instituto para la Diversificación y Ahorro de la Energía de España. Pliego de Condiciones Técnicas de Instalaciones Aisladas de Red (Instalaciones de Energía Solar Fotovoltaica); 2009.
- [22] Cronemberger J, Caamaño-Martín E, Sánchez SV. Assessing the solar irradiation potential for solar photovoltaic applications in buildings at low latitudes – making the case for Brazil. *Energy Build* 2012;55:264–72. <http://dx.doi.org/10.1016/j.enbuild.2012.08.044>.
- [23] Brogren M, Green A, Hammarby Sjöstad—an interdisciplinary case study of the integration of photovoltaics in a new ecologically sustainable residential area in Stockholm. *Sol Energy Mater Sol Cells* 2003;75:761–5. [http://dx.doi.org/10.1016/S0927-0248\(02\)00133-2](http://dx.doi.org/10.1016/S0927-0248(02)00133-2).
- [24] Lukáč N, Žlaša D, Seme S, Žalík B, Štumberger G. Rating of roofs' surfaces regarding their solar potential and suitability for PV systems, based on LiDAR data. *Appl Energy* 2013;102:803–12. <http://dx.doi.org/10.1016/j.apenergy.2012.08.042>.
- [25] Hachem C, Athenitis A, Fazio P. Parametric investigation of geometric form effects on solar potential of housing units. *Sol Energy* 2011;85:1864–77. <http://dx.doi.org/10.1016/j.solener.2011.04.027>.
- [26] Tomori T, Otani K, Sakuta K, Kurokawa K. On-site BIPV array shading evaluation tool using stereo-fisheye photographs, In: Conference record of the twenty-eighth IEEE photovoltaic specialists conference, 2000; 2000. pp. 1599–602. doi:10.1109/PVSC.2000.916204.
- [27] Cellura M, Di Gangi A, Orioli A. A photographic method to estimate the shading effect of obstructions. *Sol Energy* 2012;86:886–902. <http://dx.doi.org/10.1016/j.solener.2011.12.018>.
- [28] Orioli A, Gangi AD. An improved photographic method to estimate the shading effect of obstructions. *Sol Energy* 2012;86:3470–88. <http://dx.doi.org/10.1016/j.solener.2012.07.027>.
- [29] Sun L, Lu L, Yang H. Optimum design of shading-type building-integrated photovoltaic claddings with different surface azimuth angles. *Appl Energy* 2012;90:233–40. <http://dx.doi.org/10.1016/j.apenergy.2011.01.062>.
- [30] Nguyen HT, Pearce JM. Incorporating shading losses in solar photovoltaic potential assessment at the municipal scale. *Sol Energy* 2012;86:1245–60. <http://dx.doi.org/10.1016/j.solener.2012.01.017>.
- [31] Loucas NM, Karteris MM, Pilavachi PA, Papadopoulos AM. Photovoltaics in urban environment: a case study for typical apartment buildings in Greece. *Renew Energy* 2012;48:453–63. <http://dx.doi.org/10.1016/j.renene.2012.06.009>.
- [32] Schallenberg-Rodríguez J. Photovoltaic techno-economic potential on roofs in regions and islands: the case of the Canary Islands. Methodological review and methodology proposal. *Renew Sustain Energy Rev* 2013;20:219–39. <http://dx.doi.org/10.1016/j.rser.2012.11.078>.
- [33] Brito MC, Gomes N, Santos T, Tenedório JA. Photovoltaic potential in a Lisbon suburb using LiDAR data. *Sol Energy* 2012;86:283–8. <http://dx.doi.org/10.1016/j.solener.2011.09.031>.
- [34] N.R.C. Government of Canada. RETScreen international. <<http://www.retscreen.net/>>; 2013.
- [35] Sancho Ávila JM, Riesco Martín J, Jiménez Alonso C, Sánchez de Cos Escuin MC, Montero Cadalso J, López Bartolomé M. Atlas de radiación solar en España, Red Radiométrica Nacional. AEMET; 2012.
- [36] Agencia Estatal de Meteorología – AEMET. Gobierno de España, <<http://www.aemet.es/>>; 2013.
- [37] Ministerio de Minas y Energía, Unidad de Planeación Minero Energética (UPME), Ministerio de Ambiente, Vivienda y Desarrollo Territorial, Instituto de Hidrología, Meteorología y estudios ambientales (IDEAM), Bogotá: Atlas de Radiación Solar de Colombia; 2005.

Capítulo 6

Nuevo método para pre clasificar las fachadas potenciales en BIPV

Título:	A novel methodology for the pre-classification of façades usable for the decisión of installation of integrated PV in Buildings: The case for equatorial countries
Autores:	Luis Fernando Mulcué-Nieto, Llanos Mora-López.
Revista:	Energy, Elsevier
Factor de impacto JCR:	5.5 - Q1
Año:	2017
Categoría:	Electrical and Electronic Engineering
Publicación:	Volume 141, December 2017, Pages 2264-2276.
DOI:	10.1016/j.energy.2017.11.150



A novel methodology for the pre-classification of façades usable for the decision of installation of integrated PV in buildings: The case for equatorial countries

Luis Fernando Mulcué-Nieto^{*}, Llanos Mora-López

Departamento de Lenguajes y Ciencias de la Computación, ETSI Informática, Universidad de Málaga, Campus de Teatinos, 29071, Malaga, Spain

ARTICLE INFO

Article history:

Received 4 July 2017

Received in revised form

21 October 2017

Accepted 26 November 2017

Available online 5 December 2017

Keywords:

Building-integrated photovoltaics (BIPV)

Optimal façade

Irradiation factor (IF)

ABSTRACT

Building-integrated photovoltaics (BIPV) is a growing reality worldwide and its development involves implementing techniques to log and estimate the solar resources available. In this paper an easy methodology for the pre-classification of façades in BIPV projects has been described. This step is previous to the calculation of the complete solar potential in a building, and don't include the shape and shading factors. The proposed methodology covers the development of a new model that allows the irradiation factor (IF) to be estimated on façades with only 2 input parameters: the latitude of the place and the azimuth angle of the photovoltaic generator. The necessary tools to assess the "Energetic Efficiency Rating" for BIPV facades are provided, as an initial stage to be applied by architects and engineers.

© 2017 Elsevier Ltd. All rights reserved.

1. Introduction

Building-integrated photovoltaics (BIPV) is a growing reality worldwide and its development involves implementing techniques to log and estimate the solar resources available. That estimation is commonly named the BIPV potential, which can be classified according to the availability of data, regional characteristics, spatial resolution and the methodology used [1]. Furthermore, it is necessary to differentiate between four different types of photovoltaic potential [2]:

- *Theoretical potential*: All the available solar irradiation in a geographical region, based on its climate and without taking into account any type of technical or geographical limitations [3,4].
- *Geographical potential*: The fraction of the theoretical potential that is useable, i.e., due to the area and shape of the building. This potential also includes the shading factor because of the urban form and the natural topography [5,6].
- *Technical potential*: The irradiation that is technically usable also taking the efficiency of the photovoltaic modules, and other

equipment into account [7,8]. The technical potential of BIPV has been addressed by the analysis of the energy and exergy of the BIPV elements integrated with the coating of the building, which is known as building-integrated photovoltaic-thermal, BIPVT, [9–12]. Different BIPV products have already been developed, as described in Refs. [13,14].

- *Economic potential*: The proportion of the economically usable technical potential from a macroeconomic perspective [15].

Research into geographical potential is reviewed below, with an emphasis on façades in BIPV as this is the approaches related to the proposal of this paper.

Several models have been proposed to estimate the BIPV geographical potential in a specific place. Brito et al. [16] put forward a 3D solar model. The procedure that they used was LiDAR (Light Detection and Ranging) data analysis using the ArcGIS Solar Analyst tool. LiDAR is recommended at city and district level, [17,18]. Molin et al. [19] analysed the photovoltaic potential according to the electricity demand for Linkoping in Sweden. Basically, they used GIS data, Ecotect and PVsyst programmes. Esclapes et al. [20] generated 3D maps from different solar irradiance data sources and cadastral mapping. They concluded that for Spain the most suitable facades for BIPV are those with approximate orientation of 30°.

By contrast, the "Potential for BIPV" report by the International Energy Agency (IEA) [21], mentions that the architectural

* Corresponding author.

E-mail addresses: lfulcuen@unal.edu.co (L.F. Mulcué-Nieto), llanos@lcc.uma.es (L. Mora-López).

suitability factor and the safety of the installed systems need to be taken into account. The methodology used by IEA to assess the BIPV potential is based on a statistical method, working on the assumption that there is 0.4 m^2 of roof and 0.15 m^2 of façade for each 1 m^2 of floor area. This method has little resolution compared to the models based on LiDAR and similar.

As can be appreciated, LiDAR technology and statistical methods are very valuable to estimate the BIPV potential in cities where the buildings are already built. It follows then that when the project is just at the design stage, a methodology that allows the BIPV potential on façades to be rapidly assessed is missing. One possible direction to address the problem is to measure the performance of vertically situated modules, as was it the case in the research reported in Ref. [22]. However, such a procedure is not economically viable to be performed for each specific project. It can therefore be concluded that simulation methods are needed to predict the solar irradiation on the hypothetical surfaces, before to take in to account the landscape.

The studies with greater spatial resolution, but which are computationally more complex, are those where each surface of a specific building is independently assessed. Such an approach was undertaken by Cronemberger et al. for Brazil [23].

The aforementioned studies calculate the photovoltaic potential in broad area ranges. However, they do not allow the BIPV potential of a specific façade to be assessed easily and quickly, without using sophisticated software. To solve this problem we propose a new methodology for the pre-classification of façades, based on simple mathematical equations and data. That tools would facilitate the design work for architects and engineers [24]. This initial estimation would be applied previous to the complete calculation of the solar potential in a façade of a building, and it don't include the urban form and shading factors. The main advantage of the proposal that is made in this work regarding previous works is the facility to preclassify façades without the need to use complex software. Thus, the use of the proposed methodology will allow to obtain this preclassification in a very simple way. In addition, the fact of having both a simple mathematical expression and the proposed methodology will contribute to the easy divulgation of concepts in BIPV at university level.

This research uses the irradiation factor in order to pre-classify the BIPV façades. A new model and the "Energetic Efficiency Rating" for facades are also proposed, which can be used for countries near to the earth's equator (between 15° S and 15° N). These user-friendly tools are very valuable for architects and engineers working on projects. In summary, pre-classification of facades in BIPV has several potential advantages:

- It allows architects and engineers to quickly assess possible energy efficiency in each facade. Therefore, it is possible to make rapid estimates of the incident solar irradiation, as well as the possible electricity produced by each surface.
- It facilitates analyzing and optimizing the possible orientations of the building.
- It helps the process of deciding which façades to use for BIPV.
- It can be a criterion to select properly the photovoltaic modules according to the efficiency of each facade, etc. For example, installing modules with higher performance in more efficient facades, will allow a faster return on investment.

After this introduction, the rest of the paper is organized as follows. The solar irradiation factor and the BIPV are described in the second section. The third section presents the theory and calculations. The proposed methodology for the pre-classification of façades is described in section fourth. Experimental data used to check the proposed methodology are described in section fifth. The

obtained results are presented and discussed in section sixth. Finally, the last section summarizes the conclusions of the work.

2. The solar irradiation factor and the BIPV potential

One of the fields of BIPV is to guarantee an adequate yield from the facilities. In this area, Spain became a world benchmark when it published the *Building Technical Code* (CTE) in 2009 [25]. This document set limits on the losses caused by spatial layout of the photovoltaic generator. These losses are inevitable due to the engineering and architectural considerations involved in the construction, which often mean it is impossible to locate the generator so that it maximises the use of the incident solar radiation. The index named irradiation factor FI , has been proposed for characterizing these losses. This is defined as the annual incident radiation factor for an orientation α and tilt of generator β , with respect to that received for optimum tilt and orientation. Several countries have also used this simple tool on BIPV, such as England [26,27], Switzerland [28], Germany, Australia [29] and the United States [30].

FI depends on β , α , the latitude and diffuse radiation fraction of the place [31]. An example of the FI diagram, used for BIPV in Spain [25], can be seen in Fig. 1.

When it comes to integrating photovoltaics in buildings the FI graphs can be very useful for the following reasons:

- a. It is useful to estimate the photovoltaic potential of a city or a country, as it visually enables the maximum possible losses from the façades and roofs to be determined. An example of this was performed by Cronemberger et al. for Brazil in Ref. [23].
- b. It can be used in the technical regulations of a country in order to limit the solar gain losses regarding a photovoltaic generator integrated in a building. This is very important for the sector worldwide, as it limits the amount of modules used and consequently, it has a direct economic and environmental impact on the wholesale appropriation of the technology. This is the case of the CTE in Spain, and of a proposal previously published for a worldwide standard [32].
- c. In the case of a new building, it becomes a highly useful tool for the architectural design as it is an easy way to determine the percentage of solar energy used by each surface [7]. This fact introduces the sustainability concept as work criteria between the project architecture and engineering.

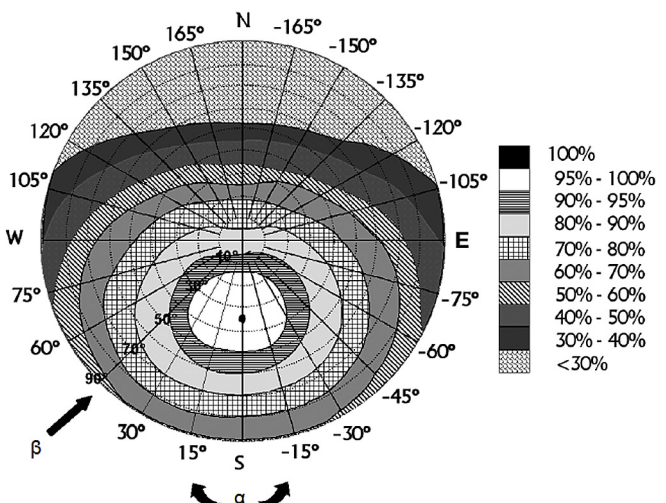


Fig. 1. Graph of the irradiation factor for Spain BIPV projects [25].

This paper seeks to provide a detailed methodology for the pre-classification of facades through the irradiance factor.

The paper is organized as follows. The theory and calculations are described in Section 3. The methodology for preparing the *irradiation factor* graphs is described in Section 4. The fifth section presents the experimental data used for this study. The results are presented and discussed in Section 6. Finally, the conclusions of the work are summarized in Section 7.

3. Theory and calculations

3.1. Irradiation factor concept

Any flat surface of a photovoltaic generator is fully characterised by two angles: tilt β of the modules with respect to the ground and by its azimuth or orientation α with respect to the south. The annual solar irradiation $G_a(\beta, \alpha)$ that influences this area is different from the one on the horizontal surface $G_a(0)$. Therefore, it is necessary to introduce a factor that allows the first amount to be calculated, once the second is established. This is known as the *annual global irradiation factor on a horizontal surface*, FI_h [31]:

$$G_a(\beta, \alpha) = FI_h(\beta, \alpha) \cdot G_a(0) \quad (1)$$

Other authors [28,33] work with a similar parameter, that in turn, the document entitled *Pliego de Condiciones Técnicas de Instalaciones Aisladas de Red de España* [Spanish Technical Specifications for Off-grid Facilities] [34] simply calls *irradiation factor*, FI . This is defined as the annual incident radiation factor for an orientation α and tilt β generator, with respect to that received for optimum tilt and orientation $G_a(\beta_{opt}, 0)$:

$$G_a(\beta, \alpha) = FI(\beta, \alpha) \cdot G_a(\beta_{opt}, 0) \quad (2)$$

The equivalence between those factors can be determined from the above two equations, thus:

$$FI_h(\beta, \alpha) = \frac{FI(\beta, \alpha)}{FI(0)} \quad (3)$$

Where $FI(0)$ is the radiation on a horizontal surface. It can be deducted from Equation [3] that with a $FI(\beta, \alpha)$ graph, it is possible to calculate FI_h quickly and easily, and therefore, the total incident irradiation on any photovoltaic module. This factor contributes in a simple way to calculate the daily average energy produced by the BIPV system, according to the equation:

$$E_{PV} = \frac{G_{dm}(\beta, \alpha) \cdot P_{peak} \cdot PR}{G_{STC}} \quad (4)$$

where P_{peak} is the installed photovoltaic peak power, PR the yield of the facility that can be easily determined by the Mulcue-Nieto and Móra-López model [7], G_{STC} the solar irradiance under standard measurement conditions, equal to 1 kW/m^2 , and $G_{dm}(\beta, \alpha)$ the annual average daily solar irradiation on the surface, calculated using the equation:

$$G_{dm}(\beta, \alpha) = FI_h(\beta, \alpha) \cdot G_{dm}(0) \quad (5)$$

In the above equation, $G_{dm}(0)$ is the annual average daily solar irradiation on a horizontal surface, that is usually easily obtained from weather stations or databases obtained from satellite images. Note that the relation between Equations (1) and (5) is approximately $G_a(\beta, \alpha) = 365 G_{dm}(\beta, \alpha)$.

3.2. Annual solar irradiation on tilted surfaces

Only the global solar irradiation on a horizontal surface, $G_{dm}(0)$, in 12 monthly average daily values, is initially known. Taking those as the baseline, each value was decomposed into diffuse $D_{dm}(0)$ and direct radiation $B_{dm}(0)$. The fact described by Liu and Jordan [35] was here taken into account, according to which the relation between the clarity index K_{Tm} and the diffuse fraction K_{Dm} is independent from the latitude. The equation proposed by Page [36], and valid for latitudes between 40°N and 40°S was taken as dependency on those parameters:

$$K_{Dm} = 1 - 1.13K_{Tm} \quad (6)$$

where:

$$K_{Dm} = \frac{D_{dm}(0)}{G_{dm}(0)} \quad (7)$$

$$K_{Tm} = \frac{G_{dm}(0)}{B_{dm}(0)} \quad (8)$$

With $B_{dm}(0)$ being the extraterrestrial beam irradiation on a horizontal surface, obtained for day d_n of the month in which the daily value, equal to the monthly daily average. The equation to calculate it is [37]:

$$B_{dm}(0) = \frac{24}{\pi} B_0 \varepsilon_0 (\omega_s \sin \delta \sin \varphi + \cos \delta \cos \varphi \sin \omega_s) \quad (9)$$

where:

$$B_0 = 1367 \frac{W}{m^2} \quad (10)$$

$$\varepsilon_0 = 1 + 0.033 \cos\left(\frac{2\pi d_n}{365}\right) \quad (11)$$

$$\begin{aligned} \delta &= 0.006918 - 0.399912 \cos \Gamma + 0.070257 \sin \Gamma \\ &\quad - 0.006758 \cos(2\Gamma) + 0.0000907 \sin(2\Gamma) \\ &\quad - 0.002697 \cos(3\Gamma) + 0.00148 \sin(3\Gamma) \end{aligned} \quad (12)$$

$$\Gamma = 2\pi \left(\frac{d_n - 1}{365} \right) \quad (13)$$

$$\omega_s = \arccos(-\tan \varphi \tan \delta) \quad (14)$$

With B_0 being the solar constant, ε_0 the correction factor of the eccentricity of the orbit of the earth, δ the solar declination angle according to Spencer [38], Γ the daily angle, φ the latitude of the place, and ω_s the sunrise angle; with all the angles measured in radians.

The following was used for the direct radiation component:

$$B_{dm}(0) = G_{dm}(0) - D_{dm}(0) \quad (15)$$

Once the daily components of global radiation, $D_{dm}(0)$ and $B_{dm}(0)$ were obtained, their respective hourly values, $D_h(0)$ and $B_h(0)$ were calculated. This involved using the expressions proposed by Collares – Pereira & Rabl [39]:

$$D_h(0) = r_d D_{dm}(0) \quad (16)$$

$$G_h(0) = r_g G_{dm}(0) \quad (17)$$

$$B_h(0) = G_h(0) - D_h(0) \quad (18)$$

where:

$$r_d = \frac{\pi}{24} \left(\frac{\cos \omega - \cos \omega_s}{\sin \omega_s - \omega_s \cos \omega_s} \right) \quad (19)$$

$$r_g = r_d(a + b \cos \omega) \quad (20)$$

$$a = 0.409 + 0.5016 \sin(\omega_s - 1.047) \quad (21)$$

$$b = 0.6609 + 0.4767 \sin(\omega_s - 1.047) \quad (22)$$

The following set was to calculate the hourly global irradiation on the surface of the generator $G_h(\beta, \alpha)$. We therefore used the *three-component model*, which has proven to be quite accurate [31], and establishes that the incident radiation is made up of direct $B_h(\beta, \alpha)$, diffuse $D_h(\beta, \alpha)$, and reflected $R_h(\beta, \alpha)$ radiation; thus:

$$G_h(\beta, \alpha) = B_h(\beta, \alpha) + D_h(\beta, \alpha) + R_h(\beta, \alpha) \quad (23)$$

The following equation was applied to calculate the direct radiation:

$$B_h(\beta, \alpha) = \left(\frac{B_h(0)}{\cos \theta_{zs}} \right) \cdot \max(0, \cos \theta_s) \quad (24)$$

With θ_s being the angle of incidence of the sun rays and the normal to the plane considered, and θ_{zs} the solar zenith angle, given by:

$$\begin{aligned} \cos \theta_s &= (\sin \varphi \cos \beta - \text{sign}(\varphi) \cos \varphi \sin \beta \cos \alpha) \sin \delta \\ &\quad + (\cos \varphi \cos \beta + \text{sign}(\varphi) \sin \varphi \sin \beta \cos \alpha) \cos \delta \cos \omega \\ &\quad + \cos \delta \sin \beta \sin \alpha \sin \omega \end{aligned} \quad (25)$$

$$\cos \theta_{zs} = \sin \delta \sin \varphi + \cos \delta \cos \varphi \cos \omega \quad (26)$$

In the above two equations, ω is the hour angle and is expressed in terms of time in hours, t_h :

$$\omega = \frac{(12 - t_h)}{12} \pi \quad (27)$$

There are more than 20 models in the literature to calculate the diffuse component on the tilted surface. The Hay-Davies isotropic model [40] was selected, as it stands out in different comparative studies for its high accuracy and simplicity [41–44]. In this, the diffuse radiation composed by two parts is considered; a circumsolar component $D_h^C(\beta, \alpha)$ that comes directly from the sun, and another isotropic component $D_h^I(\beta, \alpha)$ from the whole celestial semi-sphere:

$$D_h(\beta, \alpha) = D_h^C(\beta, \alpha) + D_h^I(\beta, \alpha) \quad (28)$$

where:

$$D_h^C(\beta, \alpha) = \frac{D_h(0)\kappa_1}{\cos \theta_{zs}} \cdot \max(0, \cos \theta_s) \quad (29)$$

$$D_h^I(\beta, \alpha) = D_h(0)(1 - \kappa_1) \frac{1 + \cos \beta}{2} \quad (30)$$

Both components have a statistical weighting according to the anisotropy index κ_1 defined as:

$$\kappa_1 = \frac{B_h(0)}{B_0 e_0 \cos \theta_{zs}} \quad (31)$$

To calculate the reflected component, or albedo, it is assumed that the ground is horizontal and infinite in extension, and it reflects the light isotropically:

$$R_h(\beta, \alpha) = \rho G_h(0) \left(\frac{1 - \cos \beta}{2} \right) \quad (32)$$

where ρ is the reflectivity of the ground, taken in general as $\rho = 0.2$.

Finally, the hourly components of the hourly global irradiation were totalled in order to obtain the monthly daily average on a tilted surface:

$$G_{dm}(\beta, \alpha) = \sum_{h=1}^{24} G_h(\beta, \alpha) \quad (33)$$

The annual average daily value $G_{da}(\beta, \alpha)$ is approximately equal to the mean of the monthly daily average values.

4. Methodology

The following procedure to prepare the FI graphs. The amount of annual average radiation that a surface receives according to its tilt and azimuth was first calculated. The peak of the graph where the incident energy is maximum was then identified. This point is given a value of FI = 1, thus determining the rest of the graph.

4.1. Determining the optimum surface

The above procedure was repeated by increasing the tilt angle β from 0° to 90° , taking $\Delta\beta = 1^\circ$ as the increase. The azimuth was kept equal to 0° for positive latitudes, which means that the generator is facing south. On the contrary, it was set as 180° for negative latitudes. The optimum tilt angle β_{opt} was thus determined by the surface area that captures the maximum annual irradiation:

$$G_{da}(\beta_{opt}) = \begin{cases} \max[G_{da}(\beta, 0)] & \varphi \geq 0 \\ \max[G_{da}(\beta, \pi)] & \varphi \leq 0 \end{cases} \quad (34)$$

This calculation was performed for 20 cities of Colombia located between latitudes -4°S and 12°N .

4.2. Preparing the graph of the irradiation factor

Once the annual maximum irradiation was obtained for a certain city, the procedure of point 2.2 was repeated cyclically, so that the value of $G_{da}(\beta, \alpha)$ was obtained for each pair of coordinates (β, α) . In order to obtain a highly reliable graph, the point scan suggested by Cronemberger [23] was performed, where tilt β ranged between 0° and 90° , taking $\Delta\beta = 5^\circ$; and the orientation α between -180° and 180° , taking $\Delta\alpha = 5^\circ$. All the possible configurations could thus be covered.

Finally, the irradiation obtained at each point was divided between the maximum, to obtain FI(β, α) according to the definition of equation (2). The software used to plot FI was OriginPro 8. The steps involved are shown in the flowchart of Fig. 2a.

Even though the FI data were obtained for the aforementioned 20 cities, only the graphs for 8 of them are included in this article and will be used as a benchmark to perform calculations for regions at similar latitudes. These cities are shown in Fig. 2b.

5. Experimental data

The first step was to obtain global solar radiation data for different cities in Colombia. The source to obtain this type of information was the website specialising in renewable energy

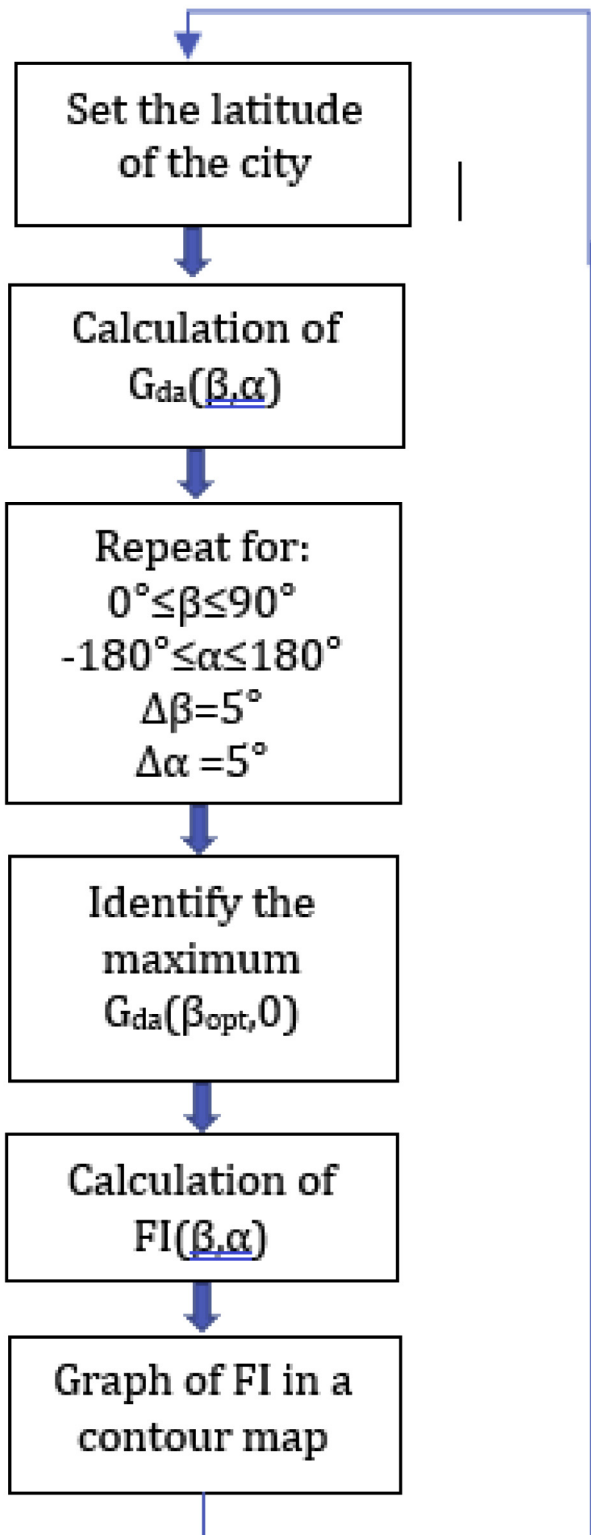


Fig. 2a. Flow chart used to draw FI graphs.



Fig. 2b. Location of the 8 cities for which the irradiation factor is plotted. Image used with the permission of the IGAC [45].

values from 22 years of data [47].

6. Results and discussion

6.1. Graphs of the irradiation factor and benchmark cities

FI was plotted for the following cities: Leticia (Fig. 3), Pasto (Fig. 4), Cali (Fig. 5), Bogotá (Fig. 6), Medellín (Fig. 7), Cúcuta (Fig. 8), Barranquilla (Fig. 9) and San Andrés (Fig. 10).

In Figs. 3–10 it can be observed that the irradiation factor has values between 0.27 and 0.52 for the facades. This means that up to 73% of solar energy can be lost when installing photovoltaic modules on a vertical surface. For this reason it is necessary to have a preclassification method, in order to choose the most efficient ones.

In the case of the roofs, the losses from completely horizontal roofs can be disregarded for latitudes under 8°N, as the maximum is for San Andrés with 2%. This is coherent with the fact that Colombia is an equatorial country. For north-facing roofs, the losses range between 7% and 21%, in the case of Leticia and San Andrés.

It can be seen that the FI graph for Pasto is very similar to the one for Cali, except for when the generator is facing completely southwards or northwards, where the maximum error committed may be 3%. It is therefore proposed to use the one for Pasto for latitudes between 0 and 4°N.

Performing a similar analysis to the above one for the 20 cities, we suggested using those listed in Table 1 as benchmark graphs of the irradiation factor. The error committed when adopting this criteria is a maximum of 4%, the reason for which they would be convenient to use for future legislation regarding BIPV losses in Colombia.

projects called *RETScreen International* [46], which is funded by Natural Resources Canada. This database is supported by 6700 land weather stations and by NASA satellites, which cover the whole the planet's surface. The data resolution is 0.3%, according to the Atmospheric Science Data Center of NASA, and correspond to average

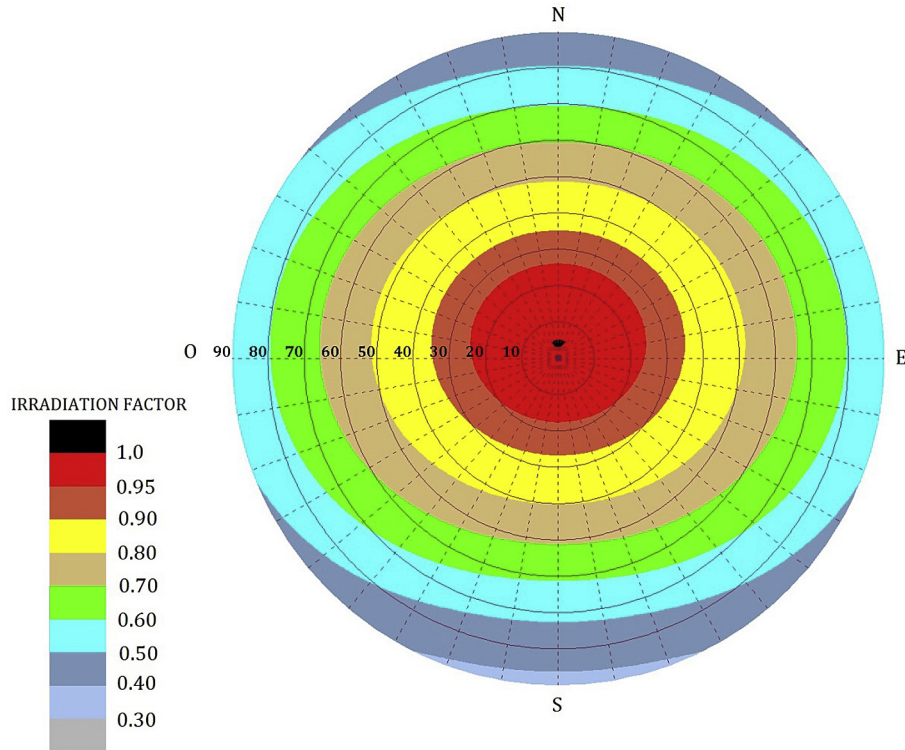


Fig. 3. Fl graph for leticia ($\phi = -4.2^\circ$).

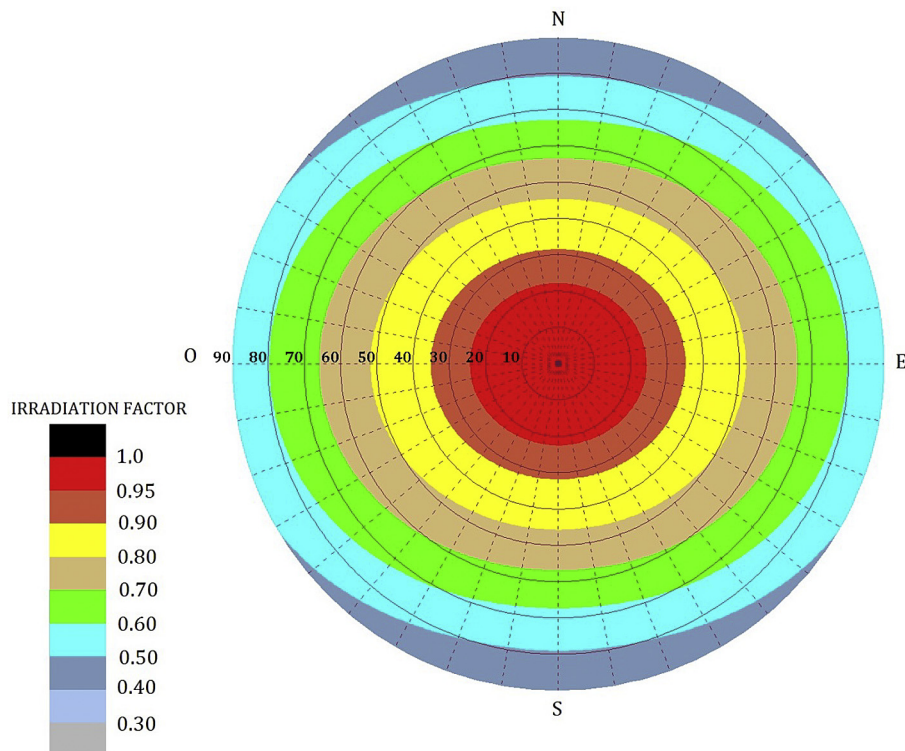


Fig. 4. Fl graph for pasto ($\phi = 1.2^\circ$).

6.2. Radiation losses on façades

Fig. 11 shows the radiation losses on façades. It should be noted

that the minimums were 48% for east-west facing ones in cities near to the Equator. This fact was to be expected as the irradiation percentage on vertical surfaces in an equatorial country is

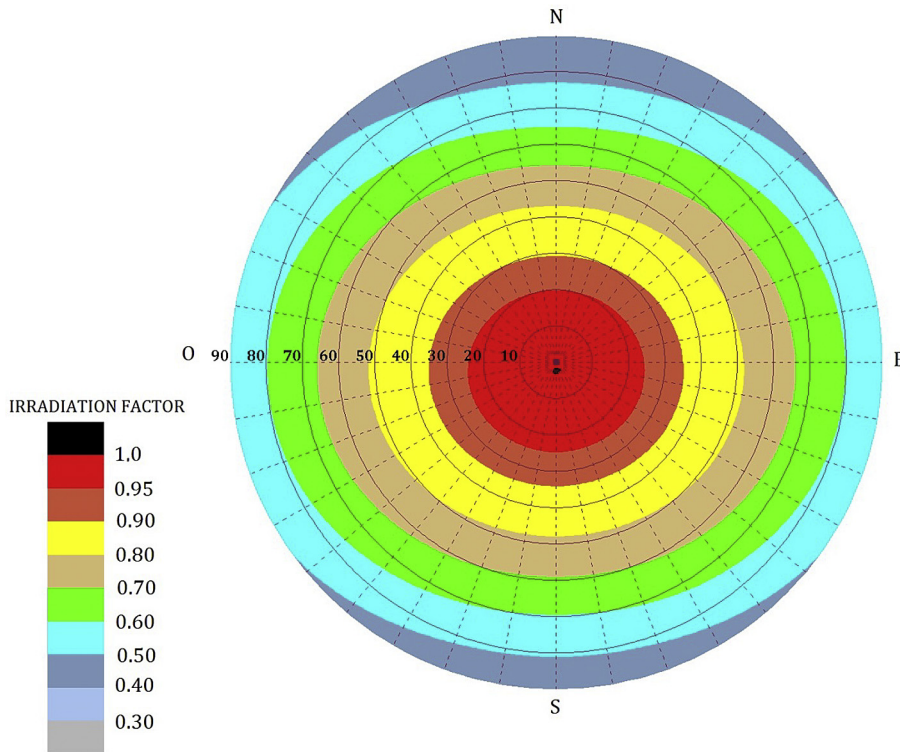


Fig. 5. FI graph for cali ($\phi = 3.6^\circ$).

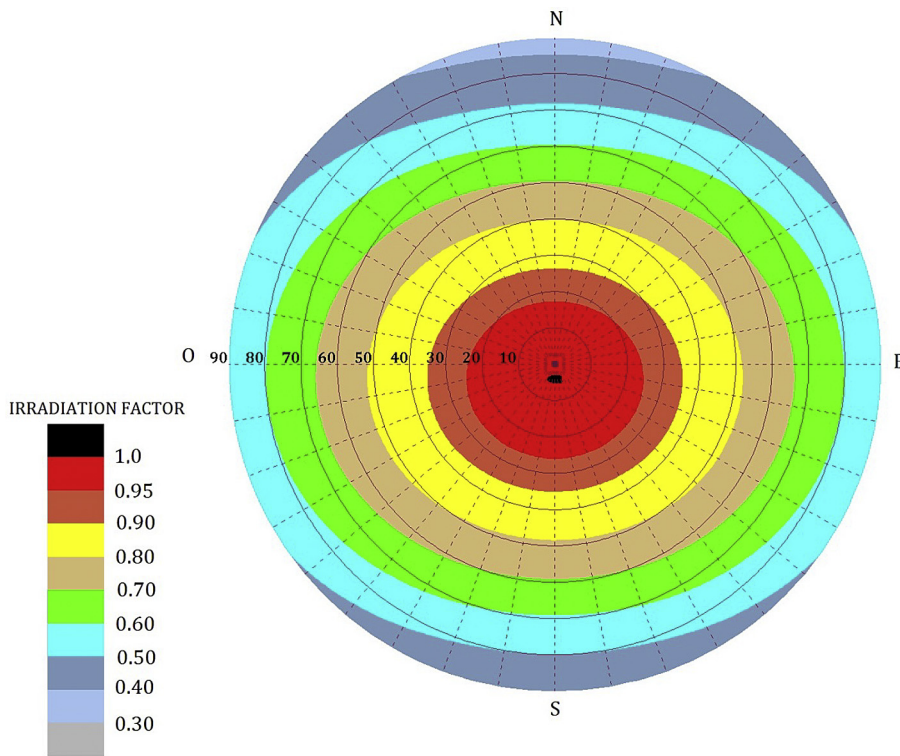


Fig. 6. FI graph for bogotá ($\phi = 4.7^\circ$).

minimum. This would indicate that future legislation should enable greater losses for this concept, with respect to the Spanish case. This would be justified by the fact that Colombia receives a greater

annual amount of solar irradiation.

For north-facing façades, the losses range between 57% and 73% in the case of Leticia and San Andrés. When south facing, the values

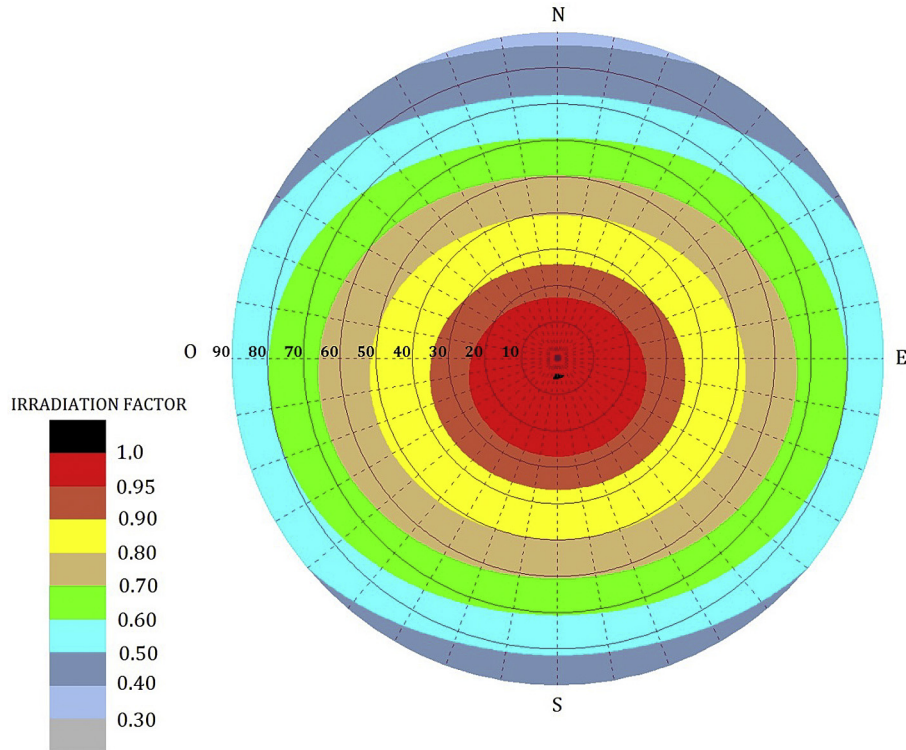


Fig. 7. Fl graph for medellín ($\phi = 6.2^\circ$).

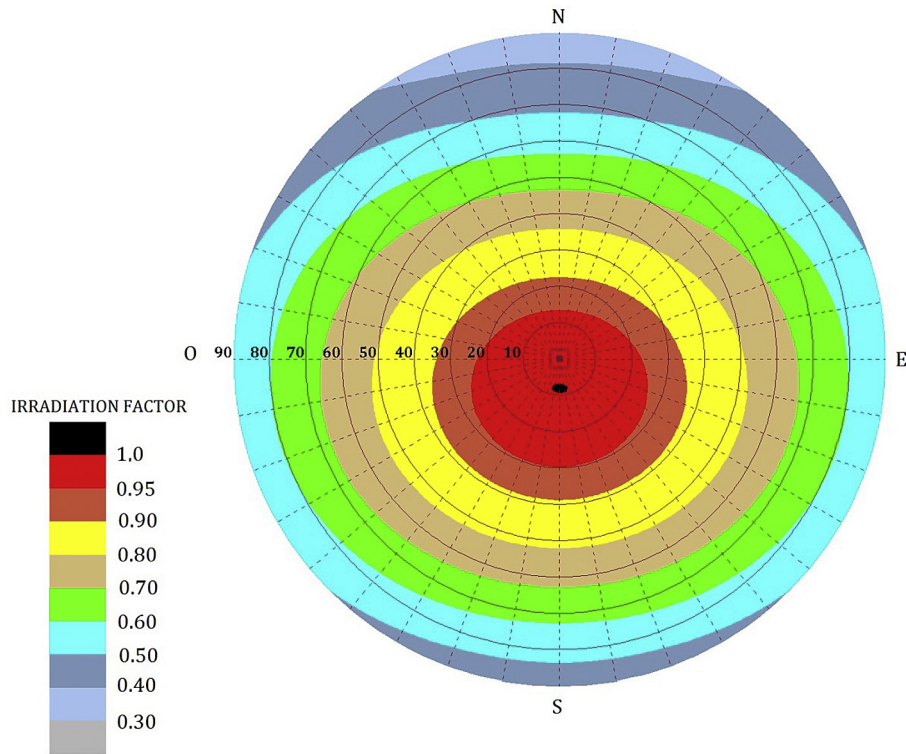


Fig. 8. Fl graph for cúcute ($\phi = 7.9^\circ$).

range between 63% and 54% for Leticia and Barranquilla, respectively. In the case of east- or west-facing facades, the losses do not vary, as they are 48%.

6.3. Novel model of the irradiation factor on BIPV façades

Fig. 12 shows the irradiation factor for the façades, according to

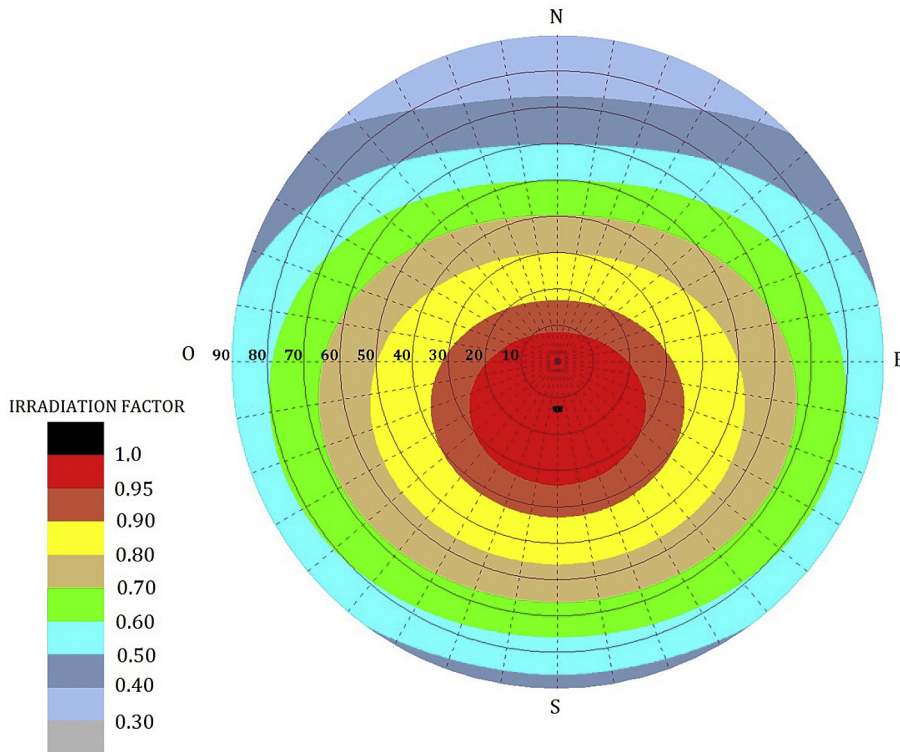


Fig. 9. FI graph for barranquilla ($\phi = 10.9$).

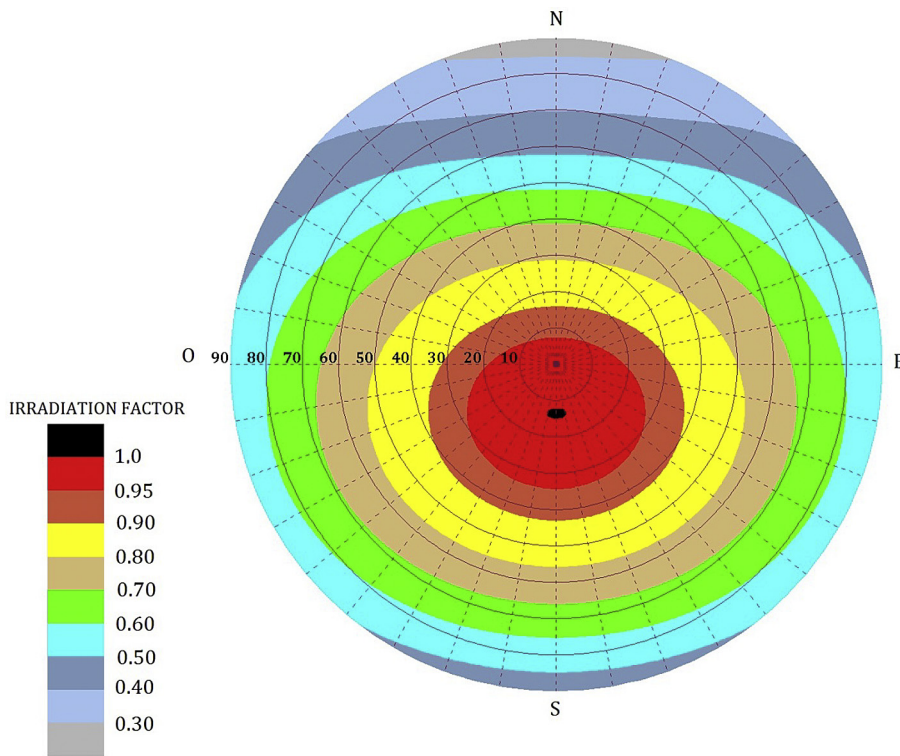


Fig. 10. FI graph for san andrés ($\phi = 12.6^\circ$).

the azimuth and latitude. The values used can be seen to range between 0.25 and 0.55. This means that the solar irradiation on those surfaces range between 25% and 55% of the amount on the

optimum surface. The maximum FI values are for façades facing east-west, i.e., with azimuth values of -90° and 90° .

Based on the data of Fig. 12 was developed a mathematical

Table 1

Proposed Graphs of the irradiation factor to be taken as benchmarks for Colombia.

Benchmark city	Latitude range ϕ ($^{\circ}$)
Leticia	$-4.2 \leq \phi < 0$
Pasto	$0 \leq \phi < 4$
Bogotá	$4 \leq \phi < 7$
Cúcuta	$7 \leq \phi < 9$
Barranquilla	$9 \leq \phi < 12.9$

expression. It was found that, for same latitude, the point curve approximately describes a sum of two Gaussian functions. The amplitude and location of such functions varies with the latitude of the place. In accordance with this, we propose the following model to calculate the irradiation factor on façades:

$$FI_{facades} = A \cdot e^{-0.0002(\alpha-\alpha_0)^2} + A \cdot e^{-0.0002(\alpha+\alpha_0)^2} + 0.386 - 0.0127 \cdot |\phi| \quad (35)$$

where

$$A = 0.1329 + 0.01413 \cdot |\phi| \quad (36)$$

$$\alpha_0 = 90 - 1.36 \cdot |\phi|, |\phi| \leq 15^{\circ} \quad (37)$$

Where α is the azimuth angle and ϕ is the latitude of the city, all in degrees. Thus, an expression was obtained that only requires 2 input parameters. The first of them is the city where the photovoltaic system will be installed: latitude ϕ . The other characterises the plane of the façade of the generator, with its orientation angle α .

It should be noted that for countries in the southern hemisphere, the zero azimuth is defined as the direction pointing towards the geographic north. Therefore, the variable α in Equation (35) must be changed by $180 - |\alpha|$.

6.4. Degree of accuracy of the model

Fig. 13 was constructed in order to verify the degree of accuracy of the model. It shows the points obtained using the long and tedious process described in Point 3, and the mathematical surface

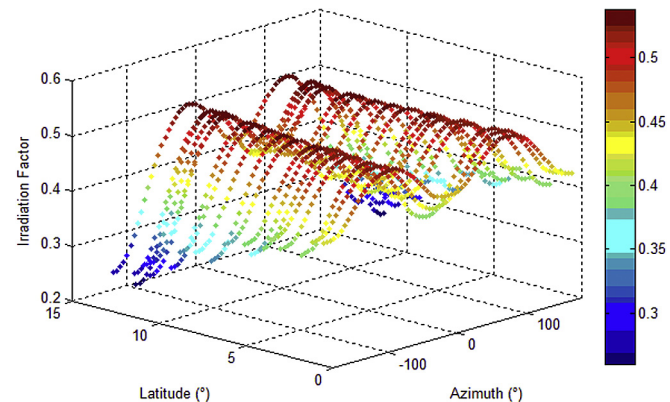


Fig. 12. Irradiation factor for façades according to latitude and azimuth.

calculated using the proposed equation. A very good degree of adjustment can be observed with a determination coefficient of $R^2 = 0.98$.

Another validation of the model was performed by means of reproducing the irradiation factor results reported for cities of Brazil [23], which are adjusted with great accuracy.

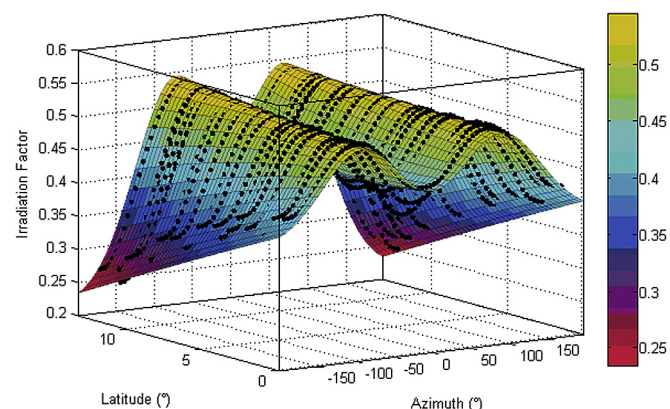


Fig. 13. Precision of the model for BIPV potential in façades.

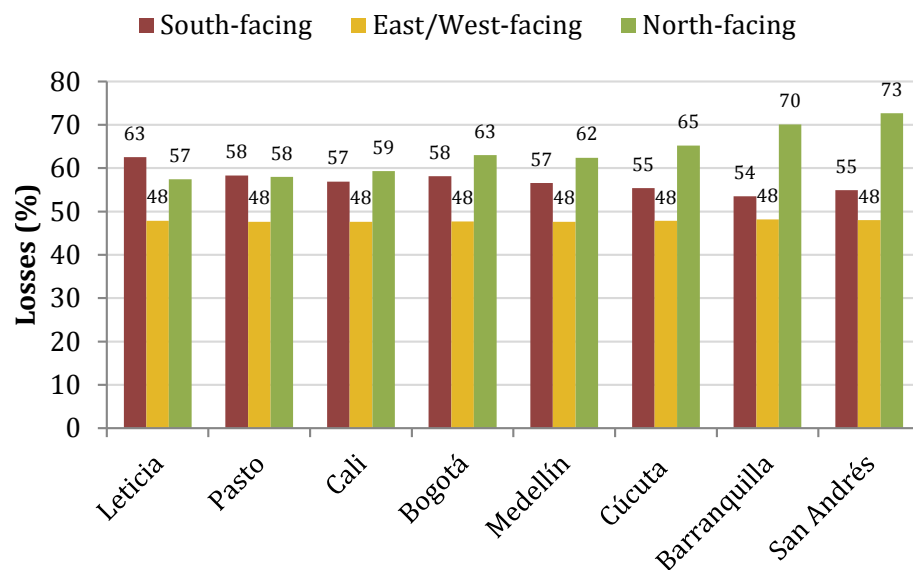


Fig. 11. Maximum losses on façades.

Finally, the following is described to provide an idea of the work saved by using Equation (35) to calculate FI. To establish each black point of the diagram in Fig. 13, it was necessary to use over 30 equations, in a computer algorithm that performed over 4000 operations. To the contrary, only Equation (35) was used for the mathematical surface of Fig. 13.

6.5. Validation of the model

In order to validate the model, a comparison with FI values obtained by using the PVWATTS^R web site [48] and equation (2) was done. This tool was developed by the National Renewable Energy Laboratory of United States NREL, and it is often used in photovoltaic projects.

The validation procedure is described below:

1. The city is selected in PVwatts.
2. A system size was set at 1000Wp.
3. System losses were set to a given value.
4. The values of $\alpha = 0$, $\beta = \beta_{opt}$ are introduced.
5. In the results $G_a(\beta_{opt}, 0)$
6. The α values are introduced for the particular orientation to be studied.
7. Let be $\beta = 90^\circ$.
8. In the results $G_a(\beta_{opt}, 0)$
9. In the results $G_a(\beta, \alpha)$
10. FI is calculated with equation (2).
11. The previous value is compared with that obtained using equation (35) of the proposed model.

The results can be seen in Fig. 14. In general, the model works very well, and has the advantage that it doesn't need internet connection, like PVWatts tool. PVWatts does not work very well for sites where no weather stations are available, especially in locations outside the United States. For these reasons we consider that our model is very valuable to make rapid calculations, and to pre-classify facades in BIPV projects.

6.6. Proposed methodology for pre-classification of BIPV façades

The following procedure will be used to pre-classification a possible BIPV facade located in equatorial countries:

1. Define the latitude of the place ϕ and orientation α that characterise the facade of the building.

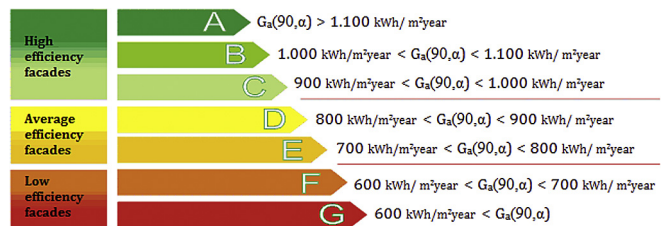


Fig. 15. Energetic Efficiency Rating for façades.

7. Conclude about the potential use of the façade for BIPV.
2. Calculate the FI irradiation factor of the façade using Equation (35).
3. Establish the annual solar irradiation on the horizontal plane of the place $G_a(0)$, available on the radiation atlases.
4. Calculate the solar irradiation on the optimum surface $G_a(\beta_{opt})$, using equation:

$$G_a(\beta_{opt}) = \frac{G_a(0)}{1 - 0.0015 \cdot |\phi| - 0.00007 \cdot |\phi|^2} \quad (38)$$

where ϕ is the latitude of the place.

5. Calculate the solar irradiation on the façade $G_a(90, \alpha)$, using the equation:

$$G_a(90, \alpha) = FI_{facades} \cdot G_a(\beta_{opt}) \quad (39)$$

6. Use the obtained value of $G_a(90, \alpha)$ to classify the façade, according to the "Energetic Efficiency Rating for façades" in Fig. 15. This classification is based on publications about the amount of solar irradiation that receives a facade in different places of the world, as mentioned in the introduction of this paper.

The obtained results when the proposed methodology is used for the 8 cities are shown in Table 2.

Once the pre-classification of the potential facades have been done, the architects and engineers can proceed to calculate the complete BIPV potential, including the shape and shading factors, by using a complex software.

7. Conclusions

A simple expression was proposed that allowed the FI

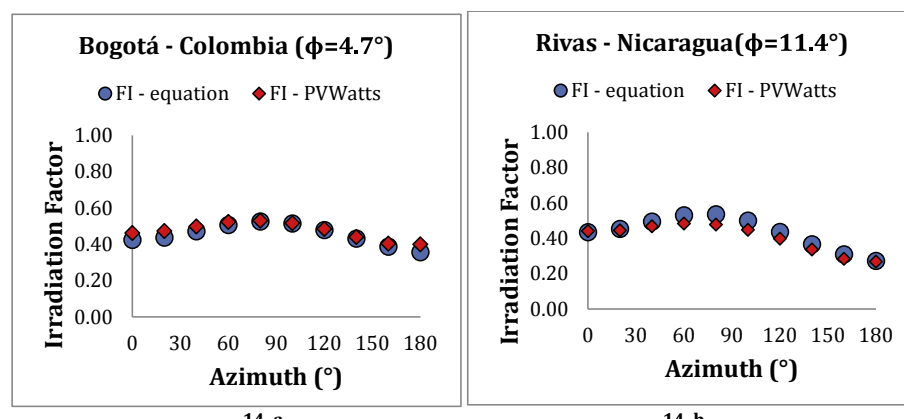


Fig. 14. Irradiation factor calculated by the proposed model, and by PVWatts web site. a) The case for Bogotá-Colombia. b) The case for Rivas – Nicaragua.

Table 2

Optimum tilt angles and annual maximum irradiation for each city.

City	Latitude φ (°)	β_{opt} (°)	$G_a(\beta_{\text{opt}})$ (kWh/m ² year)	$G_a,\text{min}(90)$ (kWh/m ² year)	$G_a,\text{max}(90)$ (kWh/m ² year)	Energy Efficiency Rating
Leticia	-4.2	4	1656	612.72	861.12	D E F
Pasto	1.2	0	1488	624.96	773.76	E F
Cali	3.6	2	1495	612.95	777.4	E F
Bogotá	4.7	4	1743	819.21	906.36	C D
Medellín	6.2	5	1643	624.34	854.36	D E F
Cúcuta	7.9	8	1746	611.1	907.92	C D E F
Barranquilla	10.9	13	1942	582.6	1009.84	B C D E F G
San Andrés	12.6	14	2078	561.06	1080.56	B C D E F G

irradiation factor on façades to be estimated with just two input parameters: the latitude and the azimuth angle of the photovoltaic generator. This model is highly accurate and it is equivalent to performing a complex simulation that uses over 30 equations, and 4000 operations. The equation was satisfactorily validated by using PVWATTS^R web site. Moreover, the proposed expression can also be used for educational purposes, as it will allow quick calculations without the need to use commercial software.

Finally, an easy methodology for the pre-classification of façades in BIPV projects in equatorial countries has been described. This includes a new proposal of “Energetic Efficiency Rating” for BIPV facades. We hope this procedure can be used as the initial step in the design process of BIPV projects, before of calculating the complete BIPV potential. Therefore, it will make easier the work of architects and engineers.

Acknowledgements

We acknowledge the Universidad de Málaga and Junta de Andalucía (grant no. P11-RNM-7115) for financial support.

References

- [1] Assouline D, Mohajeri N, Scartezzini J-L. Quantifying rooftop photovoltaic solar energy potential: a machine learning approach. *Sol Energy* Jan 2017;141:278–96.
- [2] Mainzer K, Fath K, McKenna R, Stengel J, Fichtner W, Schultmann F. A high-resolution determination of the technical potential for residential-roof-mounted photovoltaic systems in Germany. *Sol Energy* Jul. 2014;105:715–31.
- [3] Olatomiwa L, Mekhilef S, Shamshirband S, Mohammadi K, Petković D, Sudheer C. A support vector machine–firefly algorithm-based model for global solar radiation prediction. *Sol Energy* May 2015;115:632–44.
- [4] Ramli MAM, Twaha S, Al-Turki YA. Investigating the performance of support vector machine and artificial neural networks in predicting solar radiation on a tilted surface: Saudi Arabia case study. *Energy Convers Manag* Nov 2015;105:442–52.
- [5] Mavromatis G, Orehounig K, Carmeliet J. Evaluation of photovoltaic integration potential in a village. *Sol Energy* Nov. 2015;121:152–68.
- [6] Yuan J, Farnham C, Emura K, Lu S. A method to estimate the potential of rooftop photovoltaic power generation for a region. *Urban Clim* Sep. 2016;17:1–19.
- [7] Mulcué-Nieto LF, Mora-López L. A new model to predict the energy generated by a photovoltaic system connected to the grid in low latitude countries. *Sol Energy Sep.* 2014;107:423–42.
- [8] Evola G, Margani G. Renovation of apartment blocks with BIPV: energy and economic evaluation in temperate climate. *Energy Build Oct.* 2016;130(Supplement C):794–810.
- [9] Debbarma M, Sudhakar K, Baredar P. Comparison of BIPV and BIPVT: a review. *Resour-Effic Technol Sep.* 2017;3(3):263–71.
- [10] Debbarma M, Sudhakar K, Baredar P. Thermal modeling, exergy analysis, performance of BIPV and BIPVT: a review. *Renew Sustain Energy Rev Jun.* 2017;73(Supplement C):1276–88.
- [11] Shukla AK, Sudhakar K, Baredar P. Exergetic analysis of building integrated semitransparent photovoltaic module in clear sky condition at Bhopal India. *Case Stud Therm Eng Sep.* 2016;8(Supplement C):142–51.
- [12] Shukla AK, Sudhakar K, Baredar P. Exergetic assessment of BIPV module using parametric and photonic energy methods: a review. *Energy Build May* 2016;119(Supplement C):62–73.
- [13] Shukla AK, Sudhakar K, Baredar P. Recent advancement in BIPV product technologies: a review. *Energy Build Apr.* 2017;140(Supplement C):188–95.
- [14] Shukla AK, Sudhakar K, Baredar P. A comprehensive review on design of building integrated photovoltaic system. *Energy Build Sep.* 2016;128(Supplement C):99–110.
- [15] Lukáč N, Seme S, Dežan K, Žalík B, Štumberger G. Economic and environmental assessment of rooftops regarding suitability for photovoltaic systems installation based on remote sensing data. *Energy Jul.* 2016;107:854–65.
- [16] Brito MC, Gomes N, Santos T, Tenedório JA. Photovoltaic potential in a Lisbon suburb using LiDAR data. *Sol Energy Jan.* 2012;86(1):283–8.
- [17] Caamaño-Martín E, et al. Solar potential calculation at city and district levels. 2012, p. 675–85.
- [18] Martínez-Rubio A, Sanz-Adán F, Santamaría-Peña J, Martínez A. Evaluating solar irradiance over facades in high building cities, based on LiDAR technology. *Appl Energy Dec.* 2016;183:133–47.
- [19] Molin A, Schneider S, Rohdin P, Moshfegh B. Assessing a regional building applied PV potential – spatial and dynamic analysis of supply and load matching. *Renew Energy Jun.* 2016;91:261–74.
- [20] Esclapés J, Ferreiro I, Piera J, Teller J. A method to evaluate the adaptability of photovoltaic energy on urban façades. *Sol Energy Jul.* 2014;105(Supplement C):414–27.
- [21] Potential for building integrated photovoltaics. Int Energy Agency IEA 2002;7. IEA PVPS Task.
- [22] Chatzipanagi A, Frontini F, Virtuani A. BIPV-temp: a demonstrative building integrated photovoltaic installation. *Appl Energy Jul.* 2016;173:1–12.
- [23] Cronemberger J, Caamaño-Martín E, Sánchez SV. Assessing the solar irradiation potential for solar photovoltaic applications in buildings at low latitudes – making the case for Brazil. *Energy Build Dec.* 2012;55:264–72.
- [24] Cheng CL, Chan CY, Chen CL. Empirical approach to BIPV evaluation of solar irradiation for building applications. *Renew Energy Jun.* 2005;30(7):1055–74.
- [25] España Gobierno de. Código Técnico de la Edificación – HE5 Ahorro de

- Energía – contribución Fotovoltaica Mínima de Energía Eléctrica. 2009.
- [26] Thomas R. Photovoltaics and architecture. London. Taylor & Francis; 2012.
- [27] für Sonnenenergie DG. Planning and installing photovoltaic systems: a guide for installers. London: Earthscan: Architects and Engineers; 2008.
- [28] Roberts S, Guariento N. Building integrated photovoltaics: a handbook. Switzerland: Springer; 2009.
- [29] Prasad DK, Snow DM. Designing with solar power: a source book for building integrated photovoltaics (BiPV). Australia: Images Publishing; 2005.
- [30] P. E. G. J. Kiss, Building-integrated photovoltaic designs for commercial and institutional structures: a sourcebook for architects. DIANE Publishing.
- [31] Haberlin H. Photovoltaics: system design and practice. United Kingdom: John Wiley & Sons; 2012.
- [32] Mulcué-Nieto LF, Mora-López L. Methodology to establish the permitted maximum losses due to shading and orientation in photovoltaic applications in buildings. Appl Energy Jan. 2015;137:37–45.
- [33] Thomas R. Photovoltaics and architecture. London. Taylor & Francis; 2012.
- [34] Instituto para la Diversificación y Ahorro de la Energía de España. Pliego de Condiciones Técnicas de Instalaciones Aisladas de Red (Instalaciones de Energía Solar Fotovoltaica). 2009.
- [35] Liu BYH, Jordan RC. The interrelationship and characteristic distribution of direct, diffuse and total solar radiation. Sol Energy Jul. 1960;4(3):1–19.
- [36] Page J. The estimation of monthly ea values of daily total short wave radiation on vertical and inclined surfaces from sunshine records for latitudes 40°N–40°S. Proc U.N Conf New Sources Energy 1961;4(598):378–90.
- [37] Luque A, Hegedus S. Handbook of photovoltaic science and engineering. second ed. United Kingdom: Wiley; 2011.
- [38] Spencer JW. Fourier series representation of the position of the sun. Search 1971;2(5):172.
- [39] Collares-Pereira M, Rabl A. The average distribution of solar radiation—correlations between diffuse and hemispherical and between daily and hourly insolation values. Sol Energy 1979;22(2):155–64.
- [40] Hay JE. Study of shortwave radiation on non-horizontal surfaces. Atmos Environ Serv 1979;(79–12). Report No 79–12.
- [41] Denegri MJ, Raichijk C, Gallegos HG. Evaluación de diferentes modelos utilizados para la estimación de la radiación fotosintéticamente activa en planos inclinados. Av En Energy Renov Medio Ambiente 2012;16:9–15.
- [42] Noorian AM, Moradi I, Kamali GA. Evaluation of 12 models to estimate hourly diffuse irradiation on inclined surfaces. Renew Energy Jun. 2008;33(6):1406–12.
- [43] Diez-Mediavilla M, de Miguel A, Bilbao J. Measurement and comparison of diffuse solar irradiance models on inclined surfaces in Valladolid (Spain). Energy Convers Manag Aug. 2005;46(13–14):2075–92.
- [44] de Souza AP, Escobedo JF. Estimates of hourly diffuse radiation on tilted surfaces in Southeast of Brazil. Int J Renew Energy Res IJRR Mar. 2013;3(1):207–21.
- [45] Instituto geográfico agustín codazzi - igac. 29-Aug-2013. <http://www.igac.gov.co/igac>.
- [46] N. R. C. Government of Canada, RETScreen international. 24-Aug-2013 [Online]. Available: <http://www.retscreen.net/>. <http://www.retscreen.net/> [Accessed 24 Aug 2013].
- [47] National Aeronautics and Space Administration, NASA. Surface meteorology and solar energy. 2015 [Online]. Available: <https://eosweb.larc.nasa.gov/cgi-bin/sse/sse.cgi?skip@larc.nasa.gov+s01+s06#s06> [Accessed 20 Apr 2015].
- [48] PVWatts calculator. [Online]. Available: <http://pvwatts.nrel.gov/>. [Accessed 19 Jun 2017].

Capítulo 7

Conclusiones

Conclusiones

- Se propuso un nuevo modelo para calcular las pérdidas máximas por temperatura en sistemas de BIPV, en cualquier país del mundo. Este modelo fue validado mediante datos de sistemas monitorizados a nivel mundial.
- Mediante simulación, se calculó el Performance Ratio de sistemas BIPV ubicados en ciudades de baja latitud, considerando todas las superficies posibles. Se encontró que el PR tiene una variación de más del 20% entre diferentes ciudades, mientras que dentro de una misma edificación puede variar hasta en un 15%. Estos resultados ratifican que la práctica generalizada de asignar siempre un mismo valor de $PR=0.75$ a sistemas fotovoltaicos no resulta adecuada para dimensionar sistemas de BIPV, ya que esto induciría en el peor de los casos a cometer errores hasta del 45%.
- Se propuso una expresión matemática para calcular el Performance Ratio en sistemas de BIPV, teniendo como base sólo 4 variables de entrada: La temperatura ambiente media, la latitud, la inclinación y la orientación de la superficie usada. Este modelo probó tener un alto grado de precisión, y su uso evita realizar cálculos computacionales complejos, de más de 40 ecuaciones y 20.000 operaciones.
- Se desarrolló una nueva metodología para establecer los límites de pérdidas por inclinación, orientación y sombreado, en sistemas de BIPV. Con esta metodología se pueden elaborar normas técnicas para cualquier país del mundo, teniendo como referencia a otro país que cuente con una norma técnica en BIPV.

- Según cálculos realizados de pérdidas máximas por orientación e inclinación para diferentes ciudades, se evidencia que lugares con valores mayores de irradiación solar, cuentan con más flexibilidad para la BIPV. Tomando como base a la norma técnica de España, CTE, se mostró que países ubicados en bajas latitudes tienen más posibilidades de superficies para destinar a BIPV.
- Al obtener los límites de pérdidas máximas por sombreado, las ciudades de Colombia presentan valores menores que los establecidos para España en el CTE. La razón principal para esto es que Colombia tiene mayores valores de fracción de difusa, en comparación al país europeo.
- Se propuso un modelo matemático que permite estimar el factor de irradiación FI en fachadas con solo dos parámetros de entrada: la latitud del lugar y el ángulo de acimut del generador fotovoltaico. Este modelo es altamente preciso y evita realizar una simulación compleja que utiliza más de 30 ecuaciones y 4000 operaciones. La ecuación se validó satisfactoriamente mediante el uso del sitio web PVwatts^R. Además, la expresión propuesta también se puede utilizar con fines educativos, ya que permitirá realizar cálculos rápidos sin la necesidad de utilizar software comercial. Así mismo, esta ecuación se puede usar en lugares donde PVwatts no funciona bien, especialmente en ubicaciones fuera de Estados Unidos.
- Se ha propuesto una metodología fácil para la clasificación previa de fachadas en proyectos BIPV en países ecuatoriales. Esto incluye una nueva propuesta de "*Clasificación de Eficiencia Energética*" para fachadas BIPV, según un código de colores similar a la eficiencia de equipos eléctricos, de letras A-G.
- Mediante la integración de los modelos encontrados se propuso un procedimiento a usar como paso inicial en el proceso de diseño de proyectos BIPV, antes de calcular el potencial completo. Por lo tanto, facilitará el trabajo de arquitectos e ingenieros en ciudades sostenibles.

Conclusions

- It was found that the maximum equivalent operating temperature of the cells was about 15 ° higher than the ambient temperature. Likewise, a new equation was proposed to calculate the maximum temperature losses in any country of the world. This was validated using data from monitored systems worldwide.
- The performance of an “average photovoltaic system” in each city was estimated, finding PR values that vary by more than 20%, while within each city it was up to 15%. These results go against the usual practice of always assigning the same “standard” value of $PR = 0.75$ to different locations or types of building surfaces.
- A simple mathematical expression was proposed, which allows estimating the PR with only 4 input parameters: the average ambient temperature of the city, latitude, and the tilt and orientation angles of the photovoltaic generator plane. This model has a high degree of precision, and is equivalent to performing a complex simulation, using algorithms with more than 40 equations and 20,000 operations.
- A methodology was proposed to calculate the maximum losses allowed by orientation and shading, in BIPV systems. The procedure can be used for any country, starting with another country that has a technical standard in this regard.
- According to calculations of maximum losses due to orientation and inclination for different cities, it was evident that places with greater solar resources have greater flexibility for BIPV. In comparison to the technical

norm of Spain, it was shown that countries located in low latitudes have more variety of surfaces to allocate to BIPV.

- Regarding the limits of shading losses, in Colombia the limits are lower than those allowed for Spain. This is because it has a greater fraction of diffuse radiation than the European country.
- A mathematical model was proposed that allows estimating the irradiation factor FI on facades, with only two input parameters: the latitude of the place and the azimuth angle of the photovoltaic generator. This model is highly accurate and is equivalent to performing a complex simulation that uses more than 30 equations and 4000 operations. The equation was successfully validated through the use of the PVwatts^R website. In addition, the proposed expression can also be used for educational purposes, as it allows quick calculations without the need of use commercial software. Also, this equation can be used in places where PVwatts^R does not work well, especially in locations outside the United States.
- An easy methodology has been proposed for the previous classification of facades in BIPV projects of equatorial countries. This includes a new "Energy Efficiency Rating" proposal for BIPV facades.
- By integrating the models found, a procedure was proposed to be used as an initial step in the design process of BIPV projects, before calculating the full potential. Therefore, it will facilitate the work of architects and engineers in sustainable cities.

Capítulo 8

Premios a la investigación

1. Finalista en ECO-LÓGICAS "Concurso Latinoamericano y Caribeño en Energías Renovables"

Brasil, Octubre de 2015

Organizadores:

Instituto para el desarrollo de las Energías Alternativas IDEAL - Brasil.

<https://institutoideal.org/es/>

Organización Latino Americana de Energía, OLADE – Ecuador

<http://www.olade.org/>

DESCRIPCIÓN: La investigación fue seleccionada como una de las 10 mejores, en el "Concurso Latinoamericano y Caribeño en Energías Renovables y en Eficiencia Energética", edición 2015. El concurso se organiza por parte del "Instituto para el desarrollo de las Energías Alternativas-IDEAL, de Brasil. El trabajo que se presentó se titula: "*Nuevos aportes al diseño de edificios fotovoltaicos para ciudades sostenibles*", y será publicado y distribuido en bibliotecas públicas de América Latina y el Caribe. Ver los anexos que se encuentran después de los artículos publicados.

2. Premio Nacional Grupo de Energía de Bogotá

Bogotá, Noviembre de 2014

Organizador:

Grupo Energía Bogotá (GEB)

<https://www.grupoenergiabogota.com/>

DESCRIPCIÓN: La investigación fue seleccionada como una de las 3 mejores, dentro de la categoría maestría. El concurso se organiza por parte del Grupo Energía Bogotá (GEB), que es una multilateral líder en el sector de energía eléctrica y gas natural que tiene presencia en Colombia, Perú, Guatemala y Brasil. Se participó con el trabajo: "*Desarrollo de herramientas para el dimensionado y simulación de sistemas fotovoltaicos en Colombia*".

3. BECA IMP (International Mentor Program) Programa de mentoría de la Universidad de Harvard

Málaga, Noviembre de 2016

Organizador:

International Mentorship Foundation for the Advancement of Higher Education (IMFAHE)

<http://www.imfahe.org/es>

DESCRIPCIÓN: Se obtuvo beneficio del Programa Internacional de Asesoramiento (IMP) 2016-2017. Se aplicó a realizar un posdoctorado a la Universidad de Stanford, y se recibió aceptación académica. Actualmente se está en espera de gestión de proyecto para financiar la estancia.



**Concurso Latinoamericano de Monografías
sobre Energías Renovables y Eficiencia Energética**

Patrocinio



Eco_Lógicas

Concurso Latinoamericano de Monografías
sobre Energías Renovables y Eficiencia Energética

Trabajos Seleccionados



Quito - Ecuador
2016

Eco_lógicas
Concurso Latinoamericano de Monografías sobre Energías
Renovables y Eficiencia Energética 2015
Trabajos seleccionados / Instituto para el Desarrollo de Energías
Alternativas en Latinoamérica / Organización Latinoamericana de
Energía – Quito, Ecuador

236 p.

ISBN: 978-9978-70-11-9



COMISIÓN ORGANIZADORA

Mauro Passos - Instituto IDEAL
Fátima Martins - Instituto IDEAL
Gabrielle Bittelbrun - Instituto IDEAL
Andressa Braun - Instituto IDEAL
Lourdes Pillajo - OLADE

COMISIÓN CIENTÍFICA Y EVALUADORA

1. Sandra Garzón
Universidad de La Salle
Bogotá, COLOMBIA
2. Roberto Lamberts y su equipo de especialistas conformado por 5 personas.
Universidad Federal de Santa Catarina
Florianópolis, BRASIL
3. Rodrigo Flora Calili
Pontificia Universidad Católica
Río de Janeiro, BRASIL
4. Reinaldo Castro Souza y su equipo de especialistas conformado por 5 personas.
Pontificia Universidad Católica
Río de Janeiro, BRASIL
5. Fundación Bariloche y su equipo de especialistas conformado por 6 personas.
Buenos Aires, ARGENTINA
6. Ing. Enrique Riegelhaupt
Red Mexicana de Bioenergía AC
México
7. Fernando Luiz Cyrino Oliveira, D.Sc.
Industrial Engineering Department.
Pontifical Catholic University of Rio de Janeiro, Brazil

COMISIÓN JUZGADORA

Instituto para el Desarrollo de Energías Alternativas en Latinoamérica. IDEAL
Organización Latinoamericana de Energía, OLADE

COMISIÓN EDITORIAL

Marcelo Ayala
Jefe de Comunicación

Alex Romero
Diagramación

Peter Newton
Gabriela Martinez
Heidi
Traducción

OLADE es la organización política y de apoyo técnico que contribuye a la integración, al desarrollo sostenible y a la seguridad energética de la región, asesorando e impulsando la cooperación y la coordinación entre sus Países Miembros.

Bajo ese esquema OLADE ha creado espacios en donde se ha forjado alianzas con la academia con el fin de incentivar la investigación en las áreas de energías renovables y eficiencia energética, a través del fortalecimiento de las capacidades en programas en modalidad virtual, semipresencial y presencial. La Capacitación Energética Regional (CAPEV) de OLADE ha jugado un rol sumamente importante y reconocido en la región, tanto es así que durante el año 2015 se obtuvo más de 7000 funcionarios de los ministerios y secretarías de energía capacitados de los 27 países miembros de América Latina y el Caribe. Así también OLADE a través de la plataforma de redes técnicas del Sector Energético de América Latina y el Caribe (Expertos en Red) ha incentivado el diálogo e intercambio entre especialistas para el apoyo en el análisis y toma de decisiones de los expertos, los gobiernos y los demás actores del sector energético.

A lo anterior se ha sumado el Concurso Ecológicas, una iniciativa fomentada por el Instituto IDEAL de Brasil y ejecutada con el apoyo de la Organización Latinoamericana de Energía OLADE. A través de esta alianza con OLADE, el concurso en su primera edición de ejecutarlo en conjunto 2013/2014 obtuvo la participación de 12 países miembros de OLADE: Argentina, Brasil, Chile, Colombia, Cuba, El Salvador, México, Nicaragua, Panamá, Paraguay, Perú y Uruguay.

En la edición 2014/2015 se presentaron 42 trabajos provenientes de 9 países miembros de OLADE: Argentina, Brasil, Chile, Colombia, Guatemala, México, Paraguay, Perú y Uruguay. Estos trabajos fueron evaluados por el staff de Instructores de Capacitación de OLADE, el cual está conformado por alrededor de 100 especialistas pertenecientes a Universidades y Centros de Investigación del más alto nivel de la región. Luego de una evaluación exhaustiva se seleccionó un ganador en la categoría de Energías Renovables y uno en la categoría de Eficiencia Energética, aportando de esta manera al compromiso con el conocimiento, la sostenibilidad y la integración de la región.

A través de la publicación de este libro, el Instituto IDEAL y OLADE quieren extender su felicitación y reconocimiento a los estudiantes y profesores que participaron en esta edición del concurso, por su dedicación y su aporte a lograr una matriz energética limpia y sostenible.

Fernando Ferreira

Secretario Ejecutivo de OLADE

ENERGÍAS RENOVABLES

- < BRASIL > DESARROLLO DE UN INVERSOR TRIFÁSICO NO AISLADO PARA CONEXIÓN DE SISTEMAS FOTOVOLTAICOS EN LA RED PÚBLICA DE ENERGIA ELÉCTRICA 11
JULIAN CEZAR GIACOMINI
- < BRASIL > PRODUCCIÓN DE ENERGÍA ELÉCTRICA POR FUENTE EÓLICA EN RÍO GRANDE DEL NORTE 35
LUZIENE DANTAS DE MACEDO
- < CHILE > ESTIMADOR DE LA ENERGÍA DISPONIBLE PARA EL BANCO DE BATERÍAS DE UNA MICRO-RED BASADA EN ENERGÍAS RENOVABLES 55
CLAUDIO DANILO BURGOS MELLADO
- < COLOMBIA > NUEVOS APORTES AL DISEÑO DE EDIFICIOS FOTOVOLTAICOS PARA CIUDADES SOSTENIBLES 83
LUIS FERNANDO MULCUE NIETO
- < MÉXICO > DESARROLLO DE UN SISTEMA AUTÓNOMO DE EMERGENCIA MÓVIL PARA PURIFICAR AGUA 109
DULCE KRISTAL BECERRA PANIAGUA

EFICIENCIA ENERGÉTICA

- < BRASIL > MÉTODO DE APOYO EN LA TOMA DE DECISIONES PARA EL MEJORAMIENTO DE LA EFICIENCIA ENERGÉTICA EN EDIFICACIONES RESIDENCIALES 131
ARTHUR SANTOS SILVA
LAIANE SUSAN SILVA ALMEIDA
- < BRASIL > LA INFLUENCIA DE LOS USUÁRIOS SOBRE LOS SISTEMAS DE ILUMINACIÓN NATURAL Y ARTIFICIAL: CASO DE ESTUDIO AULAS DE LA ESCUELA DE ARQUITECTURA DE LA UFMG 155
CAMILA CAMPOS GONÇALVES
- < BRASIL > EFICIENCIA ENERGÉTICA EN EL PLANEAMIENTO DEL SECTOR ELÉCTRICO ENFOCADO A LAS EMISIONES DE CO² 173
LUIZ FILIPE ALVES CORDEIRO
- < BRASIL > APROVECHAMIENTO ENERGÉTICO DE RESÍDUOS SÓLIDOS URBANOS: CASO DE ESTUDIO EN EL MUNICIPIO DE ITANHAÉM-SP. 187
LUIZ HENRIQUE TARGA GONÇALVES MIRANDA
- < BRASIL > GESTIÓN POR EL LADO DE LA DEMANDA Y SISTEMAS FOTOVOLTAICOS CONECTADOS A LA RED COMO RECURSOS ENERGÉTICOS: UN ESTUDIO DE CASO DE LA INDUSTRIA ELÉCTRICA NICARAGÜENSE. 207
CARLOS GERMÁN MEZA GONZÁLE

NUEVOS APORTES AL DISEÑO DE EDIFICIOS FOTOVOLTAICOS PARA CIUDADES SOSTENIBLES

LUIS FERNANDO MULCUE NIETO
Orientación: profesor LLANOS MORA LÓPEZ

RESUMEN

En Latinoamérica los sistemas fotovoltaicos son todavía escasos. Son muy pocas las normativas técnicas que permiten integrar arquitectónicamente los generadores a los edificios, y no hay métodos que faciliten un desarrollo riguroso del sector. En esta investigación se crearon modelos y normativas que pueden ser empleados para el desarrollo de la Fotovoltaica Integrada a Edificios (*Building Integrated Photovoltaics - BIPV*), en Latinoamérica y el mundo.

La estructura de la investigación se dividió en dos partes: En la primera parte se propuso una metodología para establecer normas técnicas a nivel mundial. Este avance permite limitar las pérdidas energéticas debidas al sombreado y orientación de las superficies constructivas, de tal forma que los edificios sean *energéticamente eficientes* en la etapa de diseño. En la segunda parte, se trata el tema de la predicción de la energía generada por un edificio con tecnología tipo BIPV. Para esto se desarrolló modelo simple y confiable, que permite estimar el rendimiento global o *Performance Ratio (PR)* del sistema, con sólo 4 parámetros de entrada: La temperatura ambiente media de la ciudad, la latitud, y los ángulos de inclinación y orientación del plano del generador fotovoltaico. Este modelo tiene un alto grado de precisión, y evita el realizar una simulación compleja con más de 20.000 operaciones. Por último, se realizó el análisis de las pérdidas angulares y por suciedad, las pérdidas por temperatura, las pérdidas de conversión DC-AC, y el Performance Ratio del sistema (PR) para varias ciudades de Colombia. Con todos estos resultados se pueden tomar decisiones en la realización de proyectos con edificios auto-sostenibles, también llamados "*edificios energía cero*". El principal objetivo fue aportar de forma significativa al modelo de la *ciudad sostenible* del futuro.

PALABRAS CLAVE: Edificios Fotovoltaicos, Energía producida por un sistema fotovoltaico, Fotovoltaica integrada a edificios

INTRODUCCIÓN

La energía solar fotovoltaica es una excelente opción para cubrir las demandas energéticas de la población mundial, mediante la generación de electricidad de forma distribuida (1). Por consiguiente, se han instalado miles de generadores de electricidad a lo largo del planeta. En las zonas urbanas predominan los denominados Sistemas Fotovoltaicos Conectados a Red (SFCR), que suplen las necesidades energéticas del edificio o casa, mientras que el exceso de electricidad producida es inyectado a la red eléctrica.

Por otra parte, debido a las restricciones económicas y espaciales, se ha hecho necesario instalar los paneles fotovoltaicos sobre las superficies de los edificios. Esto ha dado lugar a un sector de gran importancia y desarrollo: La fotovoltaica integrada a edificios (BIPV), donde varios elementos constructivos como cubiertas, fachadas, ventanas, entre otros, son reemplazados por módulos fotovoltaicos. En la figura 1 se muestra un ejemplo de diseño arquitectónico empleando BIPV.



Fig 1. Ejemplo de casa diseñada empleando BIPV. Tomada de: <https://onyxgreenbuilding.wordpress.com/tag/ceu-university/>

Una de las principales metas en el campo de la BIPV es alcanzar soluciones óptimas a nivel estético, económico y técnico. Asegurando así que todas las nuevas construcciones sean "Edificios de Energía Cero" (ZEB) (2). Para lograr esto, es necesario analizar dos aspectos de gran importancia:

LA NECESIDAD DE UNA NORMATIVIDAD DE EFICIENCIA ENERGÉTICA EN LOS EDIFICIOS FOTOVOLTAICOS

En primera instancia, Para incrementar el rendimiento energético, resulta necesario maximizar la cantidad de radiación solar que incide sobre el generador. Sin embargo, la mayoría de veces lo anterior *no es posible*, debido a factores de arquitectura e ingeniería que intervienen en la construcción. Por ejemplo, en países cerca al ecuador terrestre, las cubiertas de las casas reciben mayor cantidad de irradiación por cada metro cuadrado de superficie, que las fachadas. Por otra parte, el reemplazar un material de construcción de una pared por un generador fotovoltaico, puede resultar económicamente factible. Estos hechos hacen necesario plantear la siguiente cuestión: ¿Hasta qué punto es recomendable implementar la fotovoltaica en cualquier superficie del edificio?

En el año 2009 España se convirtió en uno de los países pioneros en responder a la anterior pregunta, cuando publicó el denominado *Código Técnico de la Edificación (CTE)* (3). En este documento, se ponen límites a las pérdidas ocasionadas por sombreado y orientación del generador fotovoltaico. Esta normativa ha contribuido con mucho éxito a masificar la integración arquitectónica de la fotovoltaica en esa nación. Sin embargo, muy pocos países tienen regulaciones técnicas que permitan optimizar el rendimiento y la eficiencia energética en la BIPV.

Respecto a esto, cabe destacar que a nivel mundial es necesario unificar criterios que permitan el desarrollo de proyectos en conjunto, la transferencia tecnológica de materiales e insumos, adecuar técnicamente los sistemas a cada región, y reducir el impacto ambiental de los residuos.

En el caso de Colombia, se estima que el mercado fotovoltaico vende aproximadamente 300 KWP al año, principalmente a sistemas aislados de la red (4). Si esta cifra se extrapola a los 30 años que lleva el sector en el país, la potencia instalada total sería del orden de 9MWp (5). Esta cifra es muy baja, si se tiene en cuenta los altos niveles de radiación solar disponibles. Actualmente el gobierno nacional se encuentra promoviendo las energías renovables pero, desafortunadamente, aún no hay una normativa técnica que permita regular el desarrollo en el sector. Una situación similar se presenta en la mayoría de los países en Latinoamérica.

En esta investigación se propone una metodología para establecer normas técnicas, que limitan las pérdidas por sombreado y orientación de los sistemas fotovoltaicos en las superficies constructivas. Con esto se contribuye a la sostenibilidad ambiental de las ciudades del futuro.

EL REQUERIMIENTO DE NUEVOS MODELOS QUE FACILITEN EL DISEÑO DE EDIFICIOS FOTOVOLTAICOS

El segundo aspecto de importancia radica en el hecho de que resulta vital predecir *de forma fácil* la cantidad de electricidad que producirá la instalación, de tal forma que se pueda realizar el balance neto de energía. Este cálculo se debe realizar en una de las etapas de diseño del sistema por parte de los ingenieros y arquitectos.

En 1998 la *Comisión Electrotécnica Internacional (IEC)* publicó la Norma Internacional IEC 61724. En este estándar se describen las recomendaciones para el análisis del comportamiento eléctrico de los sistemas fotovoltaicos. Uno de los parámetros característicos lo constituye la energía anual producida, que para Sistemas Fotovoltaicos Conectados a la Red Eléctrica, se puede calcular (6) según la ecuación:

$$E_{PV} = \frac{G_a(\beta, \alpha) \cdot P_{peak} \cdot PR}{G_{STC}} \quad [1]$$

Donde $G_a(\beta,\alpha)$ la irradiación solar anual sobre la superficie del generador, P_{peak} es la potencia pico fotovoltaica instalada, PR el rendimiento anual de la instalación denominado "Performance Ratio" y G_{STC} la irradiancia solar en condiciones estándar de medida, igual a 1 kW/m^2 .

El valor de $G_a(\beta,\alpha)$ se puede obtener fácilmente mediante gráficos del denominado *Factor de Irradiación* o FI (7),(8). Por lo tanto, el problema de calcular la energía eléctrica producida se reduce principalmente a determinar el valor de PR. Pero esta tarea *no ha sido fácil*, debido a que el rendimiento depende de varios factores como la radiación solar disponible en el lugar geográfico de la instalación, el clima, la orientación e inclinación de las superficies utilizadas, el diseño adecuado del sistema y la calidad de los componentes que lo conforman, entre otros. Este hecho *ha dificultado* que los arquitectos puedan realizar sus diseños de forma sencilla, y en la mayoría de casos son los ingenieros los que recurren a software especializado. Como consecuencia, hay un retraso en el desarrollo de la Fotovoltaica Integrada a Edificios (BIPV), con su correspondiente impacto en la sostenibilidad ambiental de las ciudades.

Con el objetivo de resolver el anterior problema, se han propuesto varios métodos para tratar de predecir la influencia de diferentes variables en la cantidad de energía eléctrica generada. Algunos de ellos son analíticos, por ejemplo los empleados por Osterwald (9), Araujo (10) o Green (11); que permiten calcular las pérdidas por temperatura. También se han propuesto otros procedimientos que incluyen más variables, basados en redes neuronales artificiales (12)(13). Sin embargo, la mayoría de estos *son muy tediosos* de implementar, mientras que otros no tienen en cuenta todas las características propias del sistema.

Otra vía que se ha propuesto para resolver el problema es proponer un rendimiento estándar de $\text{PR}=0.75$ para cualquier sistema fotovoltaico (14), lo cual no es adecuado ya que las variables propias del lugar se deben tener en cuenta. Por ejemplo, se han reportado estudios del PR en 8 países, obteniendo valores entre 0.42 y 0.81 (15). Esto es coherente, pues el rendimiento de los módulos fotovoltaicos depende de la temperatura ambiente del lugar. Así mismo, la latitud juega un papel importante, ya que su efecto en la irradiación solar hace que la potencia entregada a la entrada del inversor pueda llegar ser muy baja dentro de ciertos periodos de tiempo, disminuyendo así la eficiencia de conversión DC-AC.

Según lo comentado, la gran cantidad de factores presentes hacen *muy difícil* la predicción del rendimiento de la instalación fotovoltaica integrada en un edificio (BIPV), por lo que se hace necesario implementar un método sencillo que se pueda utilizar por parte de los arquitectos e ingenieros. Esto es muy importante, debido a que muchos países necesitan masificar la energía solar fotovoltaica. En Colombia, por ejemplo, cerca del 52% del territorio nacional está constituido por zonas no interconectadas, es decir, lugares que no tienen acceso al servicio de electricidad a través del Sistema de Interconexión Nacional (16). Así mismo, dentro de las ciudades es aconsejable implementar BIPV con miras a obtener beneficios ambientales y económicos.

En este trabajo se propone una expresión simple y confiable para estimar el PR, que se puede usar en países de bajas latitudes, haciendo el caso de estudio para Colombia.

METODOLOGÍA

METODOLOGÍA PARA LA NORMATIVA DE EFICIENCIA ENERGÉTICA EN EDIFICIOS FOTOVOLTAICOS

El siguiente procedimiento se propuso para establecer los límites de pérdidas por orientación y sombreado para distintas ciudades de Colombia, y puede ser usado para cualquier otro país. Como convención, a cada una de las ciudades del país a estudiar (Colombia), se les nombró como "lugar 2". Así mismo, "lugar 1" hizo mención al país de referencia, en este caso es España, pero puede ser cualquier otro.

Se procedió primeramente a calcular la cantidad de irradiación media anual que recibe una superficie en función de su inclinación y su azimut. Seguidamente se comparó la máxima cantidad incidente en el lugar 2, con la correspondiente en la peor fachada en el lugar 1. Como resultado se obtiene el porcentaje límite de pérdidas debidas a orientación e inclinación por ciudad. Este criterio es de gran utilidad debido a que:

A. No se fijan los límites de forma universal, teniendo en cuenta que el recurso solar es diferente en cada región. Este hecho es importante debido a que iguales porcentajes de radiación global, pueden corresponder a valores muy diferentes de irradiación solar sobre las superficies.

B. El hecho de que se iguale la cantidad de energía solar recibida por cada metro cuadrado, representa que los países que reciben más radiación anual disponen de más variedad de posibilidades de integración arquitectónica. Por el contrario, si se adoptara un porcentaje universal, en países ecuatoriales no sería posible usar ninguna fachada para BIPV (Tomando como referencia a España).

C. Desde el punto de vista económico y ambiental es más beneficioso. Esto se debe a que el hecho de reemplazar materiales constructivos por los módulos fotovoltaicos es más ventajoso en países con mayor cantidad de irradiación anual.

Por otra parte, para hallar los límites de pérdidas por sombreado en el lugar 2 (Colombia), se tuvo en cuenta que la fracción de difusa es diferente que en el lugar 1 (España). Así, el porcentaje límite de pérdidas equivale a una fracción de la irradiación máxima que es físicamente posible perder por sombreado. La idea principal consistió en igualar esa fracción para ambos lugares. Por ejemplo, si en España se puede perder la tercera parte de la radiación máxima posible, en Colombia se mantendrá esa misma fracción.

CÁLCULO DE LAS PÉRDIDAS MÁXIMAS PERMITIDAS POR ORIENTACIÓN E INCLINACIÓN DEL GENERADOR

Para establecer el máximo porcentaje de pérdidas en cada superficie primero se estableció la referencia del 100%, es decir, la irradiación solar anual máxima $G_a(\beta_{opt})$. Una vez obtenida $G_a(\beta_{opt})$ para cada ciudad de Colombia, se procedió a calcular la mínima cantidad de irradiación solar anual $G_{a,MIN}(90,0)$ que puede recibir una fachada en España. Según el CTE, las pérdidas por orientación e inclinación en cualquier superficie destinada a BIPV no pueden superar el 40%. A esta superficie se nombró como la *peor fachada permisible*. Luego esta fachada se "Traslada" a la ciudad de Colombia en cuestión. Por lo tanto, el porcentaje permisible para el lugar 2 queda dado entonces por:

$$L_{\beta,\alpha,MAX,2} = 100 \left(1 - \frac{G_{a,MIN,1}(90,0)}{G_{a,2}(\beta_{opt})} \right) \quad [2]$$

Donde los subíndices 1 y 2 hacen referencia a los lugares 1 y 2, respectivamente.

CÁLCULO LAS PÉRDIDAS MÁXIMAS PERMITIDAS POR SOMBREADO DEL GENERADOR

De forma similar, se calcularon las máximas pérdidas permisibles por sombreado para cada ciudad referencia en Colombia. En España, el CTE pone como límite el 20% para BIPV. Para trasladar el equivalente de éste porcentaje a Colombia, se calculó la fracción equivalente a éste 20%, respecto a la situación de sombreado

permanente. En tal hipotético caso, la radiación dejada de percibir sería igual a la radiación directa $B_a(0)$, más la difusa circunsolar $D_a^c(0)$; ambas medidas sobre superficie horizontal.

Teniendo en cuenta lo anterior, se procedió a calcular la fracción de difusa de las principales ciudades de España. Para esto se utilizaron los datos provenientes del *Atlas de Radiación Solar en España* (17), publicado por la Agencia Estatal de Meteorología (18). Luego se halló el valor promedio del anterior parámetro que representa al país, siendo la fracción restante radiación directa. Seguidamente se procedió a comparar este valor con la máxima estipulada según las tablas de referencia publicadas por el CTE. De esta comparación se dedujeron los valores representativos de $B_a(0)$ y $D_a^c(0)$ para el lugar 1.

Para lo que sigue, se supuso que en el país de referencia dispone de una norma con límites máximos de pérdidas por sombreado $L_{shading,MAX,1}$. La fracción a la que corresponde éste porcentaje, respecto a la irradiación máxima perdida físicamente posible, quedó determinada para el lugar 1 por:

$$f_{MÁX,losses,1} = \frac{L_{shading,MAX,1}}{100\% \left(\frac{B_{a,1}(0) + D_{a,1}^c(0)}{G_{a,1}(0)} \right)} \quad [3]$$

Donde el subíndice 1 indica la irradiación del país de partida, mientras que $L_{shading,MAX,1}$ se tomó como 20%, según lo expuesto por la normativa española.

La fracción de la ecuación [3] se igualó a su equivalente en Colombia. Así, las máximas pérdidas por sombreado para el lugar 2 fueron calculadas mediante:

$$L_{shading,MAX,2} = 100\% \left(\frac{B_{a,2}(0) + D_{a,2}^c(0)}{G_{a,2}(0)} \right) f_{MÁX,losses,1} \quad [4]$$

Donde el subíndice 2 indica la irradiación de cada ciudad de Colombia.

METODOLOGÍA PARA DESARROLLO DEL MODELO DE PRODUCCIÓN ENERGÉTICA FOTOVOLTAICA

El siguiente procedimiento se propuso para hallar una expresión sencilla del PR para países de bajas latitudes, aunque puede ser usado para extender el modelo a otras regiones a nivel mundial, asignando de forma adecuada los parámetros de ajuste a los resultados. Se procedió primeramente a calcular la cantidad de irradiación media anual que recibe una superficie en función de su inclinación y su azimut. Seguidamente se calcularon las pérdidas angulares y por suciedad. Con la cantidad de irradiancia corregida y la temperatura ambiente, se calculó la potencia de entrada en cada módulo fotovoltaico, determinando así las pérdidas por temperatura. Seguidamente, se calcularon las pérdidas en el inversor mediante la ecuación de su curva característica de rendimiento.

A continuación se construyeron diagramas de contorno del PR en función de la inclinación y orientación para cada ciudad. Finalmente, se realizó un análisis cuidadoso de éstos, de tal forma que se encontró una ecuación sencilla que permite reproducir los resultados obtenidos mediante todo el proceso descrito en el párrafo anterior. A continuación se describe de forma detallada el método empleado.

OBTENCIÓN DE DATOS DE IRRADIACIÓN Y TEMPERATURA

El primer paso fue disponer de datos de irradiación solar global para diferentes ciudades del país de Colombia. La fuente para obtener este tipo de información fue el sitio web especializado en proyectos de energía renovable denominado *REScreen International* (19), que cuenta con soporte brindado por 6700 estaciones meteorológicas terrestres y por satélites de la NASA. Como resultado de este paso, se hallaron los 12 valores diarios medios mensuales de la irradiación solar global sobre superficie horizontal $G_{dm}(0)$. Similarmente, los datos de temperatura fueron obtenidos de la página web de la *Organización Meteorológica Mundial* (20), cuya información climatológica global está basada en las medias mensuales de 30 años, entre 1971 y 2000. Así, se obtuvieron los 12 valores medios mensuales de temperatura mínima y máxima de cada ciudad.

CÁLCULO DE LA IRRADIACIÓN SOLAR ANUAL SOBRE SUPERFICIES INCLINADAS EN COLOMBIA

Tomando las cifras de $G_{dm}(0)$ como punto de partida, se procedió a descomponer cada valor en radiación difusa $D_{dm}(0)$ y directa $B_{dm}(0)$. Para esto se tomó en cuenta el hecho descrito por Liu y Jordan (21), según el cual la relación entre el índice de claridad K_{Tm} y la fracción de difusa K_{Dm} es independiente de la latitud. Como dependencia de estos parámetros se tomó la ecuación propuesta por Page (22), válida para latitudes entre 40°N y 40°S. Para calcular la irradiación solar extraterrestre sobre superficie horizontal, se utilizó la expresión propuesta en (23). Así mismo, para el ángulo de declinación solar se utilizó la expresión de Spencer (24). Una vez obtenidas las componentes diarias de la radiación global, $D_{dm}(0)$ y $B_{dm}(0)$, se calcularon sus respectivos valores horarios, $D_h(0)$ y $B_h(0)$. Esto se hizo usando las expresiones propuestas por Collares – Pereira y Rabl (25). El paso siguiente fue calcular la irradiación global horaria sobre la superficie del generador $G_h(\beta, \alpha)$. Para esto se tomó el *modelo de las tres componentes*, que ha demostrado bastante exactitud (26), y establece que la radiación incidente está formada de radiación directa $B_h(\beta, \alpha)$, difusa $D_h(\beta, \alpha)$, y reflejada $R_h(\beta, \alpha)$. El intervalo de tiempo Δt se tomó igual a 0.25h.

Para calcular la componente difusa sobre la superficie inclinada, en la literatura hay más de 20 modelos. Se seleccionó el modelo isotrópico de Hay – Davies (27), debido a que en varios estudios comparativos se destaca por su alta precisión y simplicidad (28)(29)(30)(31). En éste se considera la radiación difusa compuesta por dos partes; una componente circunsolar $D^C(\beta, \alpha)$ que viene directamente del sol, y otra componente isotrópica $D^I(\beta, \alpha)$ proveniente de toda la semiesfera celeste. Para calcular la componente reflejada, o albedo, se asumió que el suelo es horizontal de extensión infinita, y que refleja la luz de forma isotrópica. La reflectividad del suelo, fue tomada de forma general como $\rho=0.2$.

CÁLCULO DE LAS PÉRDIDAS ANGULARES Y POR SUCIEDAD

Aunque se han propuesto varias expresiones para calcular las pérdidas angulares (32)(33)(34), se utilizó el modelo de Martin-Ruiz (35), debido a que reproduce resultados reales (36) y es relativamente simple. Así, la irradiación global fue corregida teniendo en cuenta tanto las pérdidas por suciedad como las angulares.

CÁLCULO DE LAS PÉRDIDAS POR TEMPERATURA

La temperatura ambiente varía a lo largo del día, pero inicialmente se disponía sólo de dos datos: la temperatura media mínima Tam y la máxima TaM. Para tener esto en cuenta, se empleó un modelo que supone lo siguiente (23):

- a. La temperatura ambiente mínima se produce siempre al amanecer, es decir, cuando $\omega = \omega_s$. (ω representa el ángulo horario solar)
- b. La temperatura ambiente máxima tiene lugar dos horas después del mediodía solar, es decir, cuando $\omega = \pi/6$.
- c. A lo largo del día la temperatura ambiente varía de acuerdo con dos semiciclos de funciones coseno, en función del tiempo solar ω .

La temperatura de operación nominal del generador (TNOC) se tomó igual a 46°C, un valor típico emitido por los fabricantes de módulos fotovoltaicos. Con este valor, y la ecuación propuesta por Osterwald (9) se halló la potencia máxima de salida $P_{máx}$. Así, quedaron determinadas las pérdidas instantáneas por temperatura, según la ecuación propuesta por Caamaño (37).

CÁLCULO DE LAS PÉRDIDAS POR CONVERSIÓN DC-AC

Con la potencia hallada en el punto anterior y el modelo propuesto por Schmidt (38), se calculó la eficiencia instantánea del inversor. A continuación se obtuvo la potencia instantánea de salida, quedando determinadas las pérdidas totales de conversión DC-AC.

DETERMINACIÓN DE LOS DEMÁS TIPOS DE PÉRDIDAS

Respecto a los tipos de pérdidas restantes, fueron tomados iguales a los valores promedio reportados en la literatura, (39) (40) (41) (42): Perdidas por diferencias con la potencia nominal del 5%, perdidas por desacople del 3%, las perdidas errores de seguimiento del punto de máxima potencia del 6%, las pérdidas óhmicas del 1%, y las pérdidas por sombreado del 7%.

CÁLCULO DEL RENDIMIENTO GLOBAL DEL SISTEMA - PR

El *performance ratio (PR)* final de la instalación se calculó con la ecuación (1). El procedimiento descrito se repitió de forma cíclica, de tal forma que se obtuvo el valor de PR para cada par de coordenadas (β, α) , de la ciudad en cuestión. La inclinación β se varió entre 0° y 90°, tomando $\Delta\beta=5^\circ$; y la orientación α entre -180° y 180°, tomando $\Delta\alpha=5^\circ$. De esta forma se logró cubrir todas las superficies posibles del edificio fotovoltaico.

Finalmente, el proceso se empleó de nuevo para 16 ciudades de Colombia ubicadas entre latitudes de -4°S y 12°N. Algunas de estas ciudades se muestran en la figura 2.



Fig. 2. Ubicación algunas de las ciudades estudiadas. Imagen utilizada con permiso del IGAC (43).

También se tuvieron en cuenta unas pocas ciudades de Centro América.

RESULTADOS Y DISCUSIÓN

NORMATIVA TÉCNICA DE EFICIENCIA ENERGÉTICA PARA EDIFICIOS FOTOVOLTAICOS

Con el fin de proponer una expresión simple para calcular los límites de pérdidas debidas a orientación e inclinación para cualquier país, se realizó la figura 3. Puede apreciarse que los valores oscilan entre 30% y 60%, dependiendo de la máxima radiación solar disponible del lugar. De acuerdo con esto, para conocer el valor máximo permisible de las pérdidas por este concepto, sólo es necesario ubicar el valor de $G_a(\beta_{opt})$ de la ciudad.

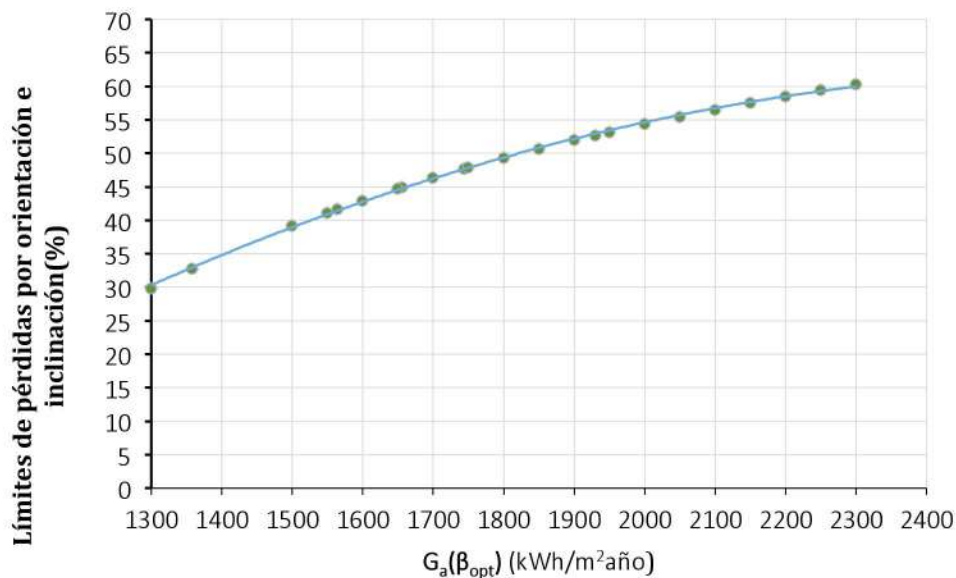


Fig 3. Límites de pérdidas debido a orientación e inclinación, en función de la irradiación solar máxima de la ciudad

Similarmente, para encontrar los límites de pérdidas por sombreado se realizó la figura 4. Se puede apreciar que los valores oscilan entre 10% y 25%, en función de la fracción de radiación difusa del lugar.

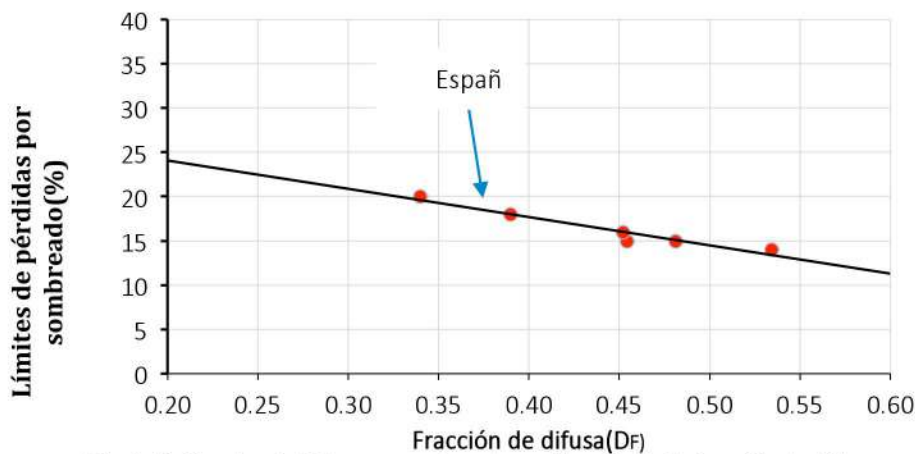


Fig 4. Límites de pérdidas por sombreado, en función de la fracción de difusa

Estas herramientas constituyen la normativa técnica propuesta, y son muy útiles para hallar las máximas pérdidas permitidas debidas a sombreado, orientación e inclinación. Pueden ser usadas para asegurar que el diseño del edificio fotovoltaico es energéticamente eficiente, con tan sólo conocer la fracción de difusa del lugar del proyecto, así como su radiación solar anual máxima.

PÉRDIDAS ANGULARES Y POR SUCIEDAD

Los resultados de las pérdidas angulares para las 16 ciudades de Colombia se consignaron en la tabla 1. Allí se puede ver que los valores mínimos de esta variable oscilan entre 4% y 5%, mientras que los máximos están entre 11% y 15%. Este comportamiento difiere un poco del reportado para algunas ciudades de Europa (35), según el cual las pérdidas máximas eran del 8%, para 90° de inclinación. Esto se puede explicar en el hecho de que en los países ecuatoriales, las fachadas orientadas hacia el sur reciben menos cantidad de radiación que los ubicados en altas latitudes.

Tabla 1. Resultados obtenidos para las pérdidas angulares.

Ciudad	Latitud φ ($^{\circ}$)	Pérdidas angulares mínimas	Pérdidas angulares máximas
Leticia	-4.2	5%	12%
Pasto	1.2	5%	11%
Tumaco	1.8	4%	12%
Popayán	2.5	5%	12%
Neiva	3	5%	12%
Cali	3.6	5%	12%
Villavicencio	4.2	5%	11%
Bogotá	4.7	4%	13%
Manizales	5.1	5%	12%
Medellín	6.2	5%	12%
Barrancabermeja	0.5	4%	14%
Cúcuta	7.9	4%	13%
Montería	8.8	4%	13%
Valledupar	10.5	4%	14%
Barranquilla	10.9	4%	14%
San Andrés	12.6	4%	15%

En la tabla 1 también se observa que hay una tendencia aproximada de aumento de un 1% en las pérdidas máximas, por cada 3° de latitud. Esto es lógico, ya que este tipo de pérdidas se dan para superficies verticales orientadas hacia el norte, las cuales reciben menos cantidad de radiación a medida que aumenta la latitud. Para entender mejor el comportamiento de las pérdidas angulares de superficies orientadas hacia el sur, en función de su ángulo de inclinación, se elaboró la figura 5.

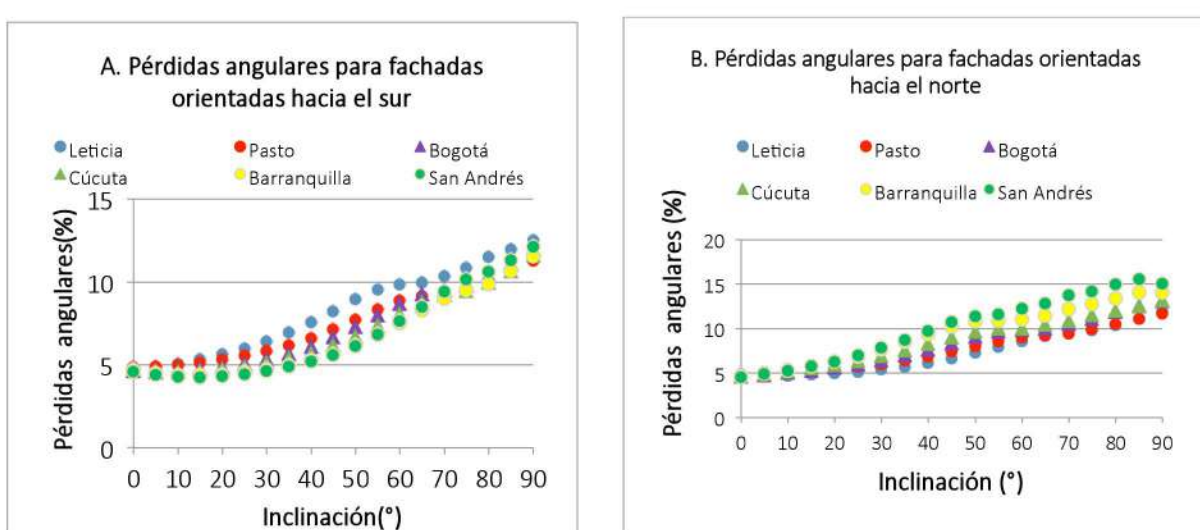


Fig. 5. Perdidas angulares anuales versus ángulo de inclinación, para superficies orientadas hacia: A. el sur. B. el norte

Al observar la figura 5.A, se aprecia que las pérdidas angulares crecen con la inclinación, sin embargo, realmente cada curva presenta un mínimo, que se da para el ángulo óptimo que maximiza la irradiación global anual. Esta tendencia se puede apreciar mejor entre mayor sea la latitud del lugar, en este caso es San Andrés, cuyo mínimo se da aproximadamente a 15° . Para hallar las pérdidas mínimas y máximas en las cubiertas ($0 < \beta < 30^\circ$), se graficó la figura 5.B, que muestra el caso de superficies orientadas hacia el norte. Al contrastar esta con la figura 5.A, se llega a la conclusión de que en las cubiertas se perderá como mínimo el 4% por conceptos angulares. Así mismo, las pérdidas máximas no superan el 8%, cuando el tejado está orientado hacia el norte. Esto es relativamente bueno para el rendimiento final del sistema. El problema ocurre en las fachadas, donde ascienden desde 11% hasta 15%.

En orden de conocer las orientaciones de las fachadas permiten incrementar el rendimiento del sistema fotovoltaico, se graficó la figura 6, donde se muestran las pérdidas angulares en función del azimuth.

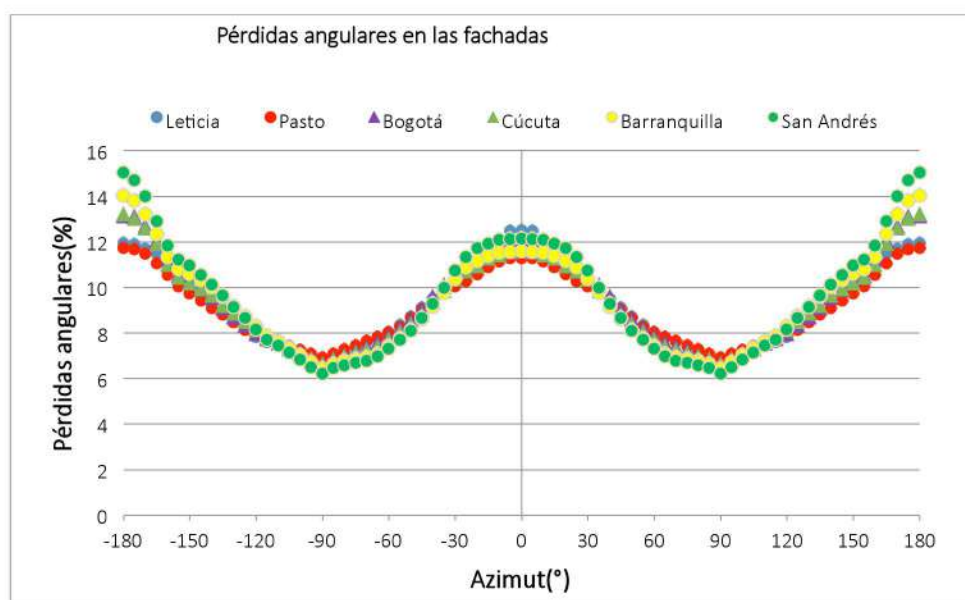


Fig. 6. Perdidas angulares anuales versus ángulo de azimut, para distintos tipos de fachadas.

Se puede observar que las fachadas óptimas son las orientadas hacia el oriente y hacia el oeste, con unas pérdidas angulares entre 6% y 7% para San Andrés y Pasto, respectivamente. La razón de esto es que los rayos solares inciden más perpendicularmente en este tipo de superficies en países cercanos al ecuador terrestre.

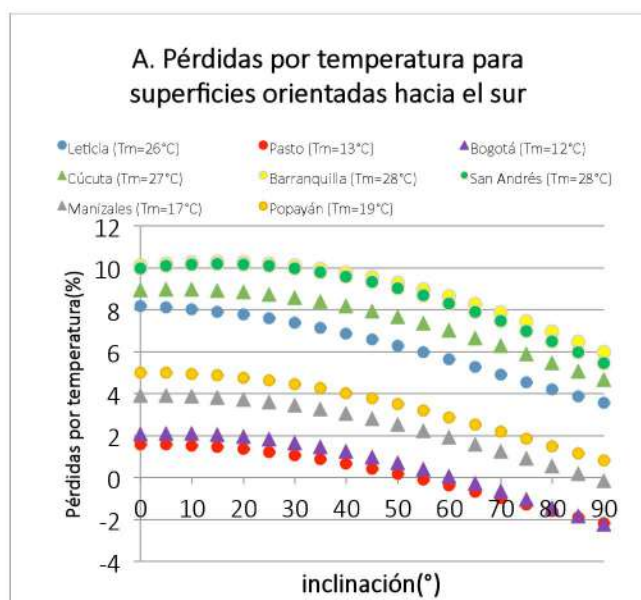
PÉRDIDAS POR TEMPERATURA

Los resultados de las pérdidas por temperatura se consignaron en la tabla 2. Allí se puede ver que los valores mínimos de esta variable oscilan entre -3% y 5%, y se dan para altas inclinaciones. Por otra parte, los máximos oscilan entre 2% y 11%, y se obtienen para superficies poco inclinadas. Estas últimas se encuentran aproximadamente dentro de los rangos esperados (39). También se evidencia que las pérdidas máximas tienen a aumentar en función de la temperatura ambiente promedio, lo cual es lógico. Por otra parte, dentro de cada ciudad las pérdidas no varían más de un 5%, aproximadamente.

Tabla 2. Pérdidas mínimas y máximas por temperatura cada ciudad de Colombia.

Ciudad	Temperatura media Ta (°C)	Pérdidas mínimas	Pérdidas máximas
Bogotá	11,7	-2,9%	2,2%
Pasto	13,3	-2,4%	1,6%
Manizales	16,6	-0,8%	4,0%
Popayán	18,8	0,4%	5,1%
Medellín	22,3	1,8%	6,7%
Cali	24,4	2,6%	6,9%
Tumaco	26,2	3,3%	8,0%
Villavicencio	26,2	3,4%	8,0%
Leticia	26,3	3,5%	8,2%
Cúcuta	27,2	3,8%	9,1%
Barrancabermeja	27,6	4,0%	9,8%
San Andrés	27,6	3,4%	10,2%
Neiva	27,7	4,2%	8,8%
Montería	27,9	4,1%	9,5%
Barranquilla	28,3	4,1%	10,4%
Valledupar	29	4,6%	11,1%

En la figura 7.A se representa la variación de las pérdidas por temperatura, para superficies orientadas hacia el sur. En esta se aprecia que tienen un comportamiento parabólico decreciente, en función de la inclinación. Entre 0° y 20° se pueden asumir constantes, luego disminuyen con la inclinación, a razón de 1% cada 15°. Este decrecimiento se debe a que la irradiación solar anual recibida es menor para superficies más verticales, lo que hace que las células se calienten menos. Por lo anterior, las fachadas presentan los mejores rendimientos por temperatura. Las ciudades de Pasto y Bogotá obtuvieron las menores pérdidas, alrededor del 2% para los tejados, sin embargo, se puede observar que para inclinaciones mayores a 50° se vuelven negativas. Esto implica que se puede obtener un rendimiento final mayor que el teórico, con el simple hecho de utilizar fachadas en esas ciudades.



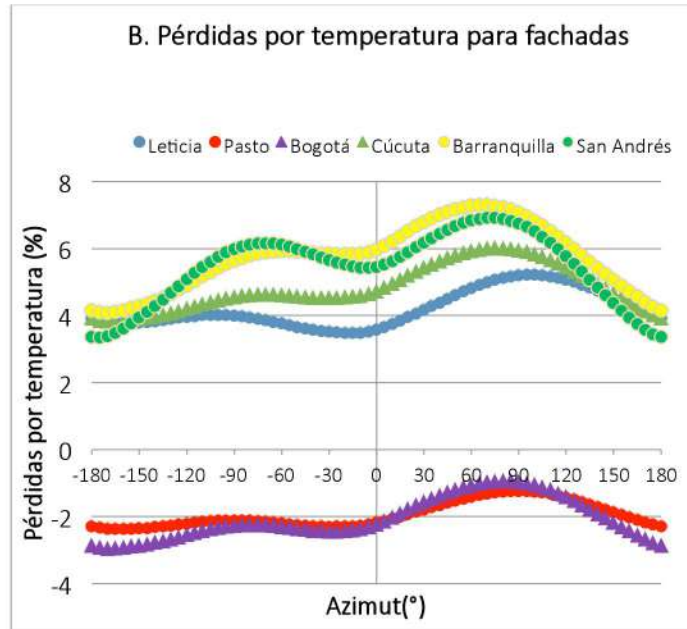


Fig. 7. Perdidas por temperatura anuales versus ángulo de azimut para: A. superficies orientadas hacia el sur. B. Fachadas

Para saber que orientaciones de las fachadas son las óptimas, se graficó la figura 7.B, donde se muestran las pérdidas por temperatura en función del azimut. Se puede observar que las fachadas óptimas son las orientadas hacia el norte, mientras que las orientadas hacia el oeste presentan las mayores pérdidas. La razón de esto es que después del medio día se alcanza la temperatura ambiente máxima, cuando el sol se encuentra hacia el occidente, por lo cual los generadores que apuntan en esa dirección se calientan más.

Con el fin de encontrar una relación matemática entre la temperatura ambiente promedio del lugar y las pérdidas máximas por temperatura, se construyó la figura 8. Esta representa los datos para generadores poco inclinados.

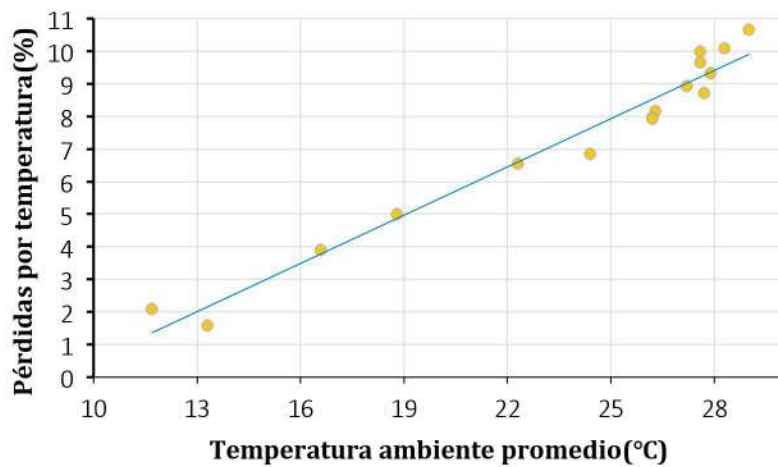


Fig. 8. Pérdidas máximas por temperatura anuales en función de la temperatura ambiente promedio.

Al hacer una regresión lineal, los puntos establecen una relación del tipo ($R^2=0.96$):

$$L_{\text{temperatura, max}}(T_a) = 0.493T_a - 4.405 \quad [5]$$

Esta expresión implica que por cada 2° de aumento en la temperatura ambiente media del lugar, las pérdidas máximas aumentan aproximadamente en un 1%. De esta ecuación se concluye que para una ciudad de temperatura media 9°C no habría pérdidas por este concepto.

Así, se pudo encontrar la relación entre la temperatura de operación equivalente máxima y la temperatura ambiente:

$$TOE_{\max} = 1.12T_a + 15 \quad [6]$$

PÉRDIDAS EN EL INVERSOR

En la tabla 3 se muestran los valores de las pérdidas de conversión DC-AC. Allí se puede ver que su valor mínimo es aproximadamente del 11%, lo que se explica según la elección de los parámetros k_0 , k_1 y k_2 , que caracterizan la curva de eficiencia del inversor. Por otra parte, el máximo está entre 19% y 22%. Esto indica que a medida las superficies se inclinan más y más, las perdidas aumentan hasta llegar a ser el doble.

En la figura 9 se puede ver mejor el anterior comportamiento, para superficies orientadas hacia el sur. Entre $\beta=0^\circ$ hasta $\beta=40^\circ$ se puede considerar que las pérdidas de conversión DC-AC son aproximadamente constantes (11%). Después de esta inclinación tienen a crecer hasta 15% o 20%, dependiendo de la latitud. También se puede apreciar que San Andrés presenta menos pérdidas que Leticia, debido que la cantidad de radiación solar recibida por este tipo de superficies crece en función de la latitud. Por consiguiente, habrá mayores potencias a la entrada del inversor, y mayor eficiencia.

Tabla 3. Pérdidas mínimas y máximas de conversión DC-AC cada ciudad de Colombia.

Ciudad	Temperatura ambiente Ta (°C)	Pérdidas mínimas	Pérdidas máximas
Leticia	-4.2	11.1%	19.9%
Pasto	1.2	11.2%	18.8%
Tumaco	1.8	10.1%	19.1%
Popayán	2.5	11.0%	18.9%
Neiva	3	11.2%	19.9%
Cali	3.6	11.4%	20.0%
Villavicencio	4.2	11.2%	20.4%
Bogotá	4.7	10.8%	18.6%
Manizales	5.1	11.0	19.1%
Medellín	6.2	11.0	19.8%
Barrancabermeja	0.5	10.8%	20.0%
Cúcuta	7.9	10.9%	20.4%
Montería	8.8	10.9%	20.8%
Valledupar	10.5	10.7%	21.3%
Barranquilla	10.9	10.8%	21.4%
San Andrés	12.6	10.7%	21.9%

El comportamiento observado en las pérdidas en el inversor (Figura 9) es similar al exhibido por las pérdidas angulares (figura 5.A). Esto se explica en el hecho de fuerte dependencia de la eficiencia del inversor en función de la potencia de entrada. De acuerdo a esto, para superficies orientadas hacia el norte las pérdidas crecerán con el aumento de la inclinación, más concretamente hasta valores entre 19% y 22%. Similarmente, las fachadas orientadas hacia el este o hacia el oeste presentan menores pérdidas que las demás, alrededor del 13%.

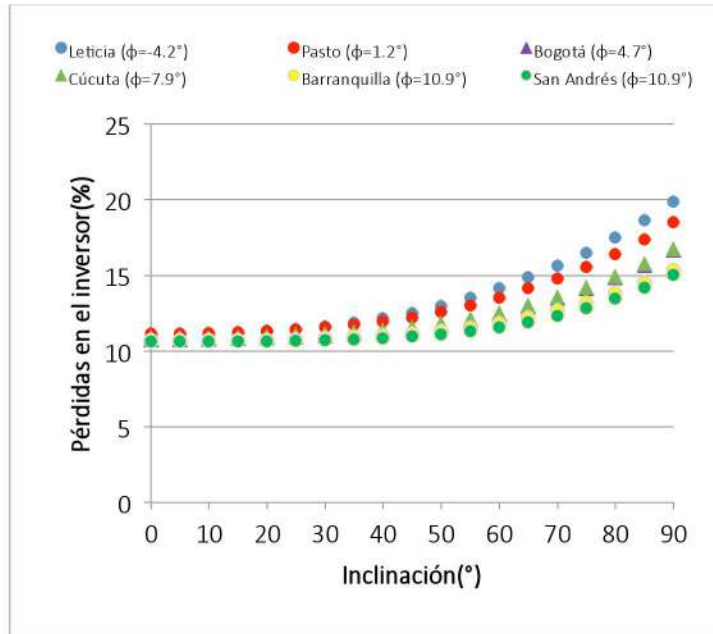


Fig. 9. Pérdidas anuales de conversión contra la inclinación, para superficies orientadas hacia el sur.

RENDIMIENTO DEL SISTEMA

En la tabla 4 se muestran los valores mínimo y máximo del PR, obtenidos para cada ciudad. Los valores están comprendidos entre 0,51 y 0,65. En total, el intervalo de variación fue mayor al 20%, mientras que dentro de cada ciudad puede ser hasta de 15%. Estos resultados van en contra de la práctica usual asignar siempre un mismo valor "estándar" de PR a diferentes localidades o tipos de superficies.

Tabla 4. Performance Ratio mínimo y máximo cada ciudad de Colombia. Los datos representan el comportamiento de un sistema fotovoltaico "promedio".

Ciudad	Average Ta (°C)	PR min	PR max
Bogotá	11,7	0,58	0,650
Pasto	13,3	0,58	0,646
Manizales	16,6	0,56	0,635
Popayán	18,8	0,56	0,628
Medellín	22,3	0,54	0,618
Cali	24,4	0,54	0,611
Tumaco	26,2	0,54	0,608
Villavicencio	26,2	0,54	0,606
Leticia	26,3	0,54	0,606
Cúcuta	27,2	0,53	0,604
Barrancabermeja	27,6	0,53	0,602
San Andrés	27,6	0,51	0,599
Neiva	27,7	0,54	0,602
Montería	27,9	0,53	0,601
Barranquilla	28,3	0,52	0,599
Valledupar	29	0,51	0,597

Principalmente, el PR máximo depende fuertemente de la temperatura ambiente media del lugar, de forma decreciente. Esta tendencia se puede apreciar mejor en la línea de regresión de la figura 10, con un grado de ajuste de $R^2=0.9967$.

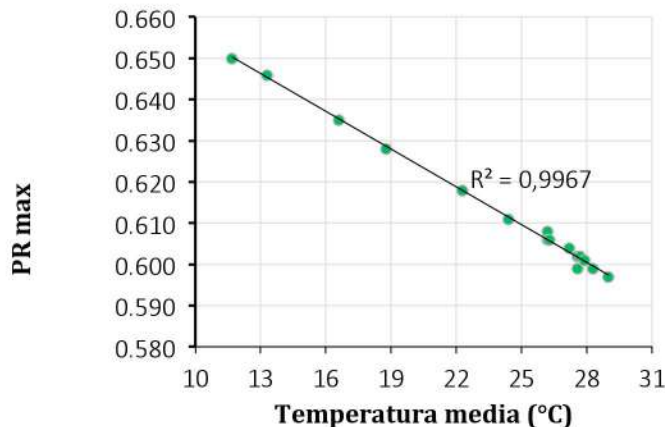


Fig. 10. Rendimiento máximo anual del sistema contra la temperatura ambiente promedio.

La ecuación de la línea recta que representa los datos es:

$$PR_{\max} = 0,686 - 0,0031 \cdot T_a \quad [7]$$

Esta expresión es de gran utilidad ya que permite evaluar el máximo rendimiento del sistema, con tan sólo disponer de la temperatura ambiente de la ciudad.

Los resultados obtenidos en este modelo corresponden a un SFCR promedio, sobre superficies fijas. Pero es posible obtener valores mayores para PR si se asume que el sistema está muy bien diseñado. Teniendo esto, la ecuación [7] puede ser simplificada para fines prácticos, introduciendo una constante k_{sist} que depende del tipo de sistema, así:

$$PR_{\max} = k_{sist} \cdot [1 + \gamma (1,12 \cdot T_a - 10)] \quad [8]$$

Donde T_a es la temperatura ambiente media de la ciudad en °C, y γ es el coeficiente de variación del punto de máxima potencia con la temperatura. Para el silicio cristalino puede usarse $\gamma = -0,0044 \text{ } ^\circ\text{C}^{-1}$.

Esta ecuación reprodujo los resultados obtenidos con una precisión muy alta ($R^2=0,992$). Con el fin de probar la validez de esta expresión en países diferentes a los ecuatoriales, se aisló el término de temperatura, y se calcularon las pérdidas para inclinaciones cercanas a la óptima, así:

$$L_{temperatura,max} = -\gamma (1,12 \cdot T_a - 10) \quad [9]$$

Los resultados obtenidos para algunos sistemas reales monitorizados se muestran en la tabla 5. Así, los valores reportados concuerdan con lo reportado para sistemas fotovoltaicos instalados en casas, por lo cual la expresión [9] tiene validez universal. Sin embargo, es importante recalcar que estas pérdidas podrían ser mayores en el caso de BIPV, si en el diseño final no se tiene en cuenta una adecuada ventilación de los módulos.

Tabla 5. Valores de pérdidas por temperatura para generadores inclinados cerca de su ángulo óptimo.

Ciudad	País	Número de sistemas	Pérdidas medidas	Referencia	Pérdidas calculadas
Tokio	Japón	100	4%	(41)	4%
Dublín	Irlanda	1	0%	(44)	0%
Sukatani	Indonesia	101	8%	(45)	8%

Para estudiar el rango posible del máximo rendimiento del sistema según la ciudad, se construyó la figura 11. En esta, se puede apreciar que un sistema óptimo puede alcanzar valores de PR comprendidos entre 0.74 y 0.81, dependiendo del tipo de ciudad. Bogotá es la ciudad en la que mejor se podría desempeñar el hipotético sistema ($PR_{max}=0,81$), mientras que en Valledupar el rendimiento sería menor ($PR_{max}=0,74$). Sin embargo, para el cálculo de la energía anual producida en la ubicación óptima conviene utilizar los valores de un sistema "promedio".

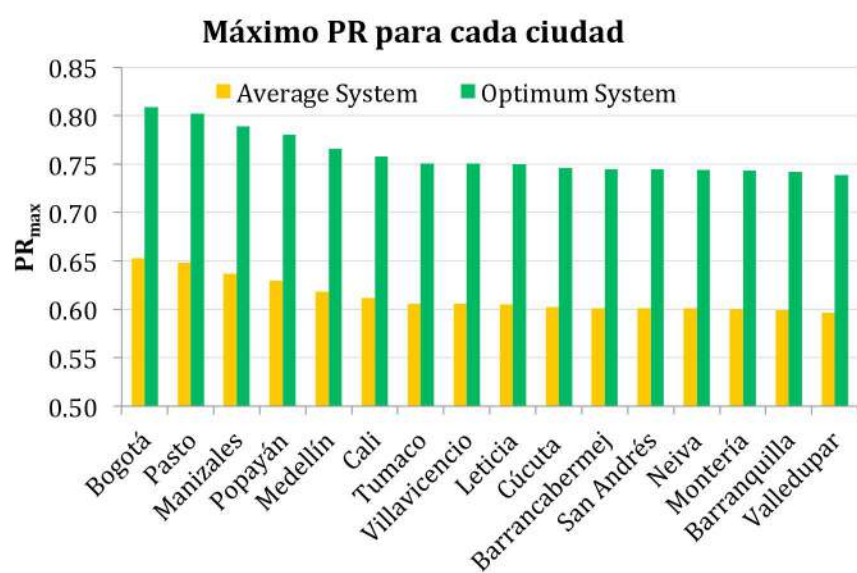


Fig. 11. Rendimiento anual máximo de un sistema, para cada ciudad función del tipo de sistema.

VARIACIÓN DEL PR CON LA INCLINACIÓN Y ORIENTACIÓN

Es importante recordar que la ecuación [8] sirve para calcular el PR en el caso de inclinaciones y orientaciones cercanas a la óptima. Sin embargo, su valor puede disminuir hasta en un 15%, dependiendo del tipo de superficie sobre el cual se ubiquen los módulos. Ese comportamiento implica su correspondiente error en el cálculo de la energía anual producida. Lo anterior se puede dar cuando se trata de integración arquitectónica (BIPV). Teniendo en cuenta esto, se construyeron mapas de contorno del PR en función de la orientación e inclinación para cada ciudad. Algunos de los resultados se exponen para las ciudades de Leticia (Fig. 12), Pasto (Fig. 13), Bogotá (Fig. 14), Cúcuta (Fig. 15), y Barranquilla (Fig. 16).

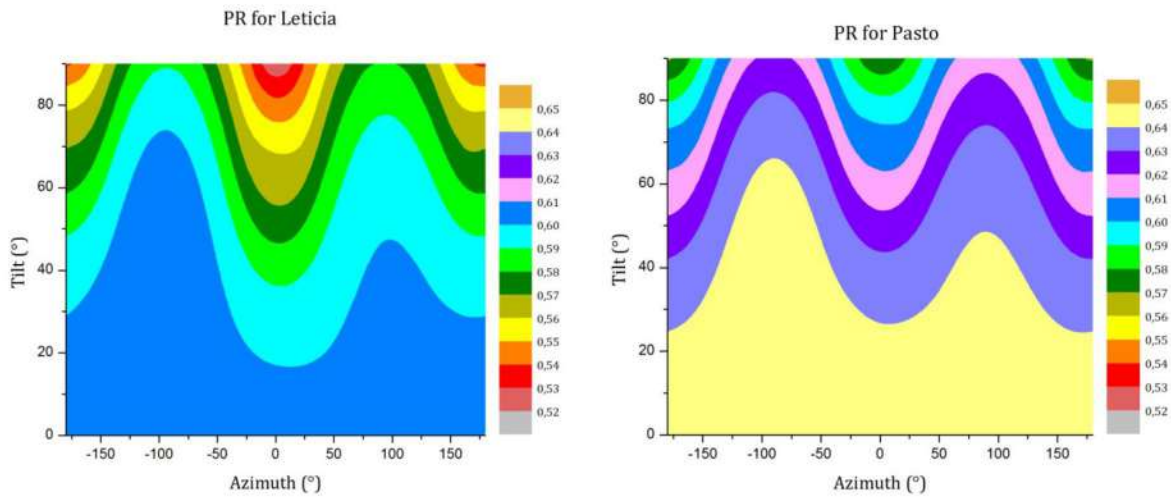


Fig. 12.

Fig. 13.

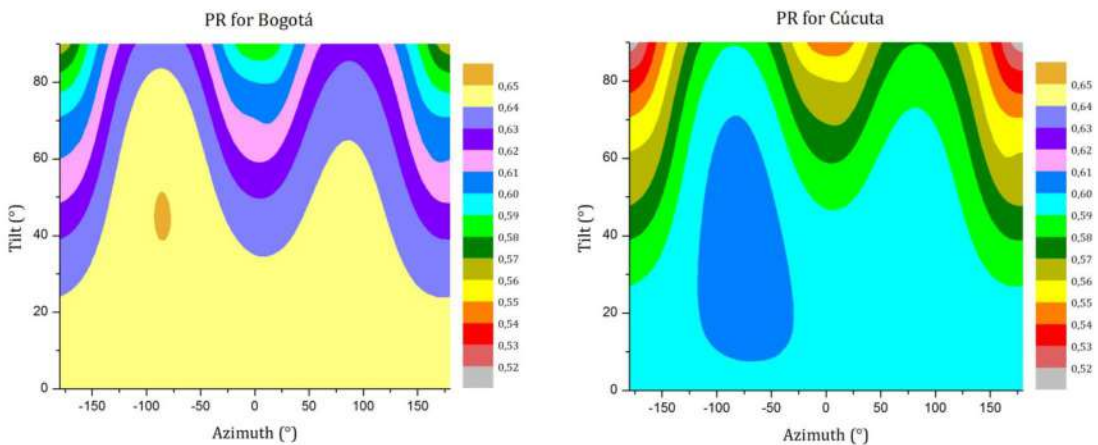


Fig. 14.

Fig. 15.

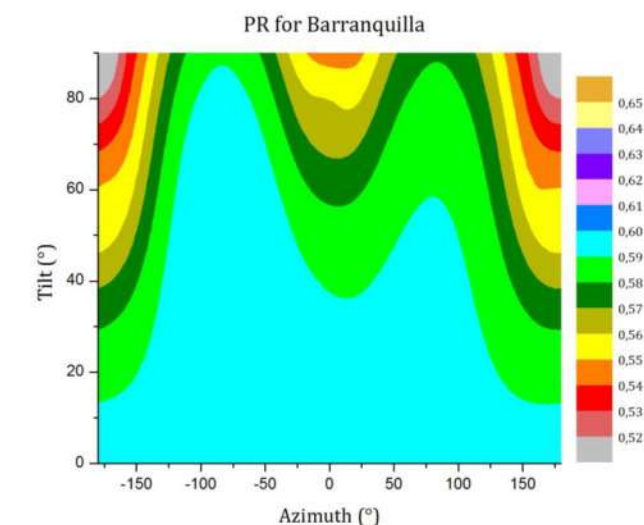


Fig. 16.

En las figuras 12 a 16 se puede apreciar que todas las superficies con inclinaciones menores a 30°, sin importar su orientación, tienen un PR aproximadamente igual al máximo de esa ciudad. Esto implica que para todas las cubiertas se puede tomar $PR=PR_{\max}$.

También se puede observar que en todos los gráficos hay dos picos de rendimiento, para las orientaciones aproximadas de -90° y 90°. Esto se debe a que tanto las pérdidas angulares como las de conversión, son mínimas para superficies orientadas hacia el oeste y hacia el este. También se ve que el pico del PR en $\alpha=-90^\circ$ es mayor que para $\alpha=90^\circ$. La razón para esto es que en las mañanas, cuando el sol se encuentra en esa orientación, la temperatura ambiente es menor, dando como resultado unas menores pérdidas por este concepto.

Por otra parte, en ciudades ubicadas en latitudes negativas, los menores rendimientos se observan para generadores verticales orientados hacia el sur ($\alpha=0^\circ$). Lo opuesto se observa en ciudades ubicadas por encima de la línea del ecuador ($\alpha=180^\circ$). Estos comportamientos son lógicos debido a las altas pérdidas angulares y del inversor en esos casos.

MODELO SIMPLIFICADO PARA CALCULAR EL PR

Todos los gráficos obtenidos en el presente artículo son útiles para hacer un estudio detallado de las pérdidas en un futuro edificio fotovoltaico. En particular, los mapas de contorno expuestos en las figuras 12 a 16 permiten identificar el PR del sistema de forma visual. Pero cada ciudad tiene un mapa de contorno diferente, caracterizado por su temperatura ambiente media y su latitud. Por lo tanto, sería necesario emplear el largo procedimiento descrito cada vez que se quiera predecir el comportamiento de una instalación. En realidad, lo anterior no resulta viable técnicamente cuando se plantea un proyecto fotovoltaico. Esta es la razón por la que muchos diseñadores optan por asignar un "valor estándar" de 0.75 cuando se quiere predecir la energía producida. Pero, como se mostró anteriormente, los valores obtenidos el PR pueden variar con la ciudad y el tipo de superficie, de tal forma que al realizar esta práctica se podría inducir un error *por encima del 45%* en el cálculo de la electricidad anual, en el peor de los casos.

Como propuesta para resolver el problema, se pensó en encontrar una ecuación que se ajustara a los mapas de contorno obtenidos. Razonando de esta forma se encontró que, para un mismo PR, la curva de puntos describe de forma aproximada a una suma de dos funciones gaussianas. La amplitud y el ancho de tales funciones varían con la latitud del lugar. Además, los valores obtenidos para el PR en cada curva de nivel son característicos de la temperatura media del lugar. De acuerdo a esto, se propuso el siguiente modelo para el cálculo del PR:

$$PR = 0,0011 \left(A_1 \cdot e^{-2\left(\frac{\alpha-\alpha_0}{W}\right)^2} + A_2 \cdot e^{-2\left(\frac{\alpha+90}{W}\right)^2} - \beta - 50 \right) + 1,117 \cdot PR_c \quad [10]$$

Donde

$$A_1 = -1,1 \cdot |\varphi| + 60 \quad [11]$$

$$A_2 = -0,1 \cdot |\varphi| + 65 \quad [12]$$

$$W = -1,1 \cdot \varphi + 92 \quad [13]$$

$$\alpha_0 = -1,4 \cdot \varphi + 92 \quad [14]$$

$$PR_c = PR_{\max} + 0,0006 \cdot T_a - 0,017 \quad [15]$$

Siendo β el ángulo de inclinación, α el ángulo de acimut y ϕ la latitud de la ciudad, todos en grados. T_a es la temperatura ambiente media de la ciudad en °C. El procedimiento para emplear la ecuación [10] es el siguiente:

- Se calcula el valor de PR_c según la ecuación [15].
- Se calcula PR mediante la ecuación [10]. Si $PR > PR_c$ entonces se toma como valor de rendimiento $PR = PR_c$. En caso contrario se deja igual al obtenido.

Así, se obtuvo una expresión que necesita sólo 4 parámetros de entrada. Dos de ellos corresponden a la ciudad donde se instalará el sistema fotovoltaico: La temperatura ambiente media T_a , y la latitud ϕ . Los otros dos caracterizan al tipo de superficie del plano del generador: Su ángulo de inclinación β , y la orientación α .

GRADO DE PRECISIÓN DEL MODELO

Con el ánimo de verificar el grado de precisión del modelo, se construyó la figura 17, donde se muestran dos diagramas de contorno del PR, uno realizado mediante el largo y tedioso proceso descrito en la metodología, y el otro calculado mediante la ecuación propuesta, ambos para la ciudad de Bogotá.

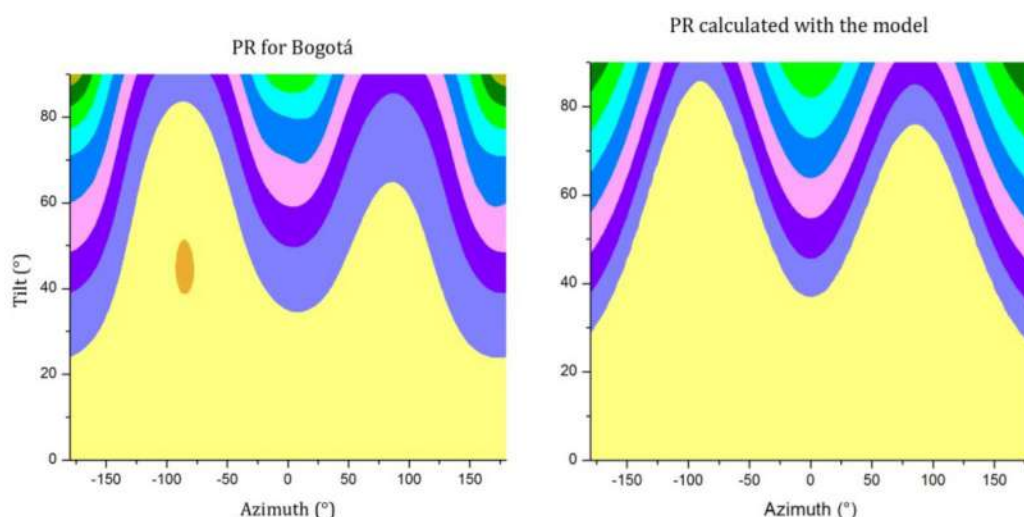


Fig. 17. Contornos del PR para Bogotá, calculado mediante la simulación completa (Izquierda) y mediante el modelo propuesto (Derecha).

Así mismo, la figura 18 representa el porcentaje de error en cada punto del gráfico. Se puede observar como en la mayoría del diagrama el error cometido es menor al 1%. Este error crece levemente con la temperatura y la latitud. Por ejemplo, para Tegucigalpa-Guatemala ($\phi = 14.1$); el error cometido en la mayor parte de los puntos es del 3%. Estos resultados indican el excelente grado de precisión del modelo propuesto, a pesar de su simplicidad.

Finalmente, para tener una idea del trabajo ahorrado al emplear la ecuación [10] para el cálculo del PR, se describe lo siguiente: Para hallar cada punto del diagrama de contorno de la parte izquierda de figura 17 fue necesario emplear más de 40 ecuaciones, en un algoritmo de computador que realizó más de 20.000 operaciones. De forma contraria, en cada punto del gráfico de la derecha de la misma figura sólo se utilizaron dos ecuaciones: la del PR_{max} , Ecuación [8], y la propuesta en nuestro modelo, ecuación [10].

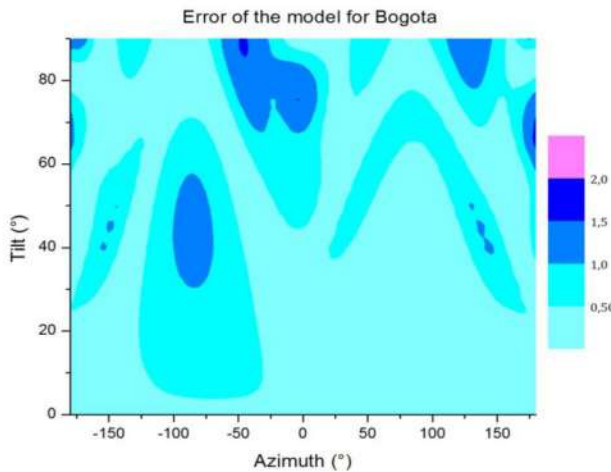


Fig. 18. Porcentaje de error cometido en el modelo propuesto para el PR de Bogotá

CONCLUSIONES

En este trabajo se realizaron grandes aportes para el diseño de edificios fotovoltaicos.

En primera instancia se propuso una normativa técnica a *nivel mundial*, que permite calcular de forma fácil las máximas pérdidas energéticas permitidas por orientación y sombreado. El procedimiento se puede emplear para cualquier lugar del mundo, con tan solo conocer la fracción de difusa y la radiación solar máxima. Esto permitirá tener en cuenta la eficiencia energética del sistema fotovoltaico, en la etapa de diseño arquitectónico del edificio.

También se analizaron detalladamente las posibles pérdidas energéticas que inciden en el rendimiento de un sistema fotovoltaico conectado a red. El procedimiento se hizo para 16 ciudades de Colombia, en todas las inclinaciones y orientaciones posibles del plano del generador. Así mismo, se propuso una ecuación para calcular las pérdidas máximas por temperatura en *cualquier país del mundo*. Esta expresión fue validada mediante datos de sistemas monitorizados reales.

El segundo gran aporte consiste en un modelo simple y validado de predicción de la energía producida por un sistema fotovoltaico, para países de bajas latitudes. Este modelo es de gran valor a nivel mundial, ya que evita el utilizar más de 40 ecuaciones en un algoritmo que realizó más de 20000 operaciones. Las variables de entrada son sólo cuatro: la temperatura ambiente, la latitud de la ciudad, y la orientación e inclinación del generador fotovoltaico.

Esta investigación es un valioso apoyo para los arquitectos e ingenieros de Latinoamérica, ya que facilita de forma considerable el diseño de un edificio fotovoltaico. Con esto se contribuye al desarrollo de la Fotovoltaica Integrada a Edificios (BIPV) en la región, y a la construcción de ciudades ambientalmente sostenibles.

REFERENCIAS

1. Pearce JM. Photovoltaics — a path to sustainable futures. *Futures*. septiembre de 2002;34(7):663-74.
2. Kanders J, Horvat M. Solar Energy as a Design Parameter in Urban Planning. *Energy Procedia*. 2012;30:1143-52.
3. Gobierno de España. Código Técnico de la Edificación – HE5 Ahorro de Energía – Contribución Fotovoltaica Mínima de Energía Eléctrica. 2009.
4. GEC, E JD. El Sector Solar Fotovoltaico en el Caribe Colombiano: Análisis Técnico y de Mercado. *Sci Tech*. 1 de agosto de 2012;2(51):87-91.
5. Rodríguez Murcia H. Desarrollo de la energía solar en Colombia y sus perspectivas. *Rev Ing*. noviembre de 2008;(28):83-9.
6. The International Electrotechnical Commission (IEC). IEC 61724 - 1998, Photovoltaic system performance monitoring - Guidelines for measurement, data exchange and analysis. Multiple. Distributed through American National Standards Institute; 1998.
7. Thomas R. Photovoltaics and Architecture. London: Taylor & Francis; 2012. 169 p.
8. Roberts S, Guariento N. Building Integrated Photovoltaics: A Handbook. Switzerland: Springer; 2009. 175 p.
9. Osterwald CR. Translation of device performance measurements to reference conditions. *Sol Cells*. septiembre de 1986;18(3-4):269-79.
10. Araujo GL, Sánchez E, Martí M. Determination of the two-exponential solar cell equation parameters from empirical data. *Sol Cells*. enero de 1982;5(2):199-204.
11. Green MA. Solar Cells: Operating Principles, Technology and System Applications. University of New South Wales; 1998. 274 p.
12. Almonacid F, Rus C, Pérez PJ, Hontoria L. Estimation of the energy of a PV generator using artificial neural network. *Renew Energy*. diciembre de 2009;34(12):2743-50.
13. Rodrigo P, Rus C, Almonacid F, Pérez-Higueras PJ, Almonacid G. A new method for estimating angular, spectral and low irradiance losses in photovoltaic systems using an artificial neural network model in combination with the Osterwald model. *Sol Energy Mater Sol Cells*. enero de 2012;96:186-94.
14. Markvart T, Castaner L. Practical Handbook of Photovoltaics: Fundamentals and Applications. Elsevier; 2003. 1012 p.
15. Mondol JD, Yohanis Y, Smyth M, Norton B. Long term performance analysis of a grid connected photovoltaic system in Northern Ireland. *Energy Convers Manag*. noviembre de 2006;47(18-19):2925-47.
16. Senado de la República de Colombia. Ley 855 de 2003. Definición de Zonas No Interconectadas al SIN. Ley 855 de 2003 dic 18, 2003.
17. Sancho Ávila JM, Riesco Martín J, Jiménez Alonso C, Sánchez de Cos Escuin MC, Montero Cadalso J, López Bartolomé M. Atlas de Radiación Solar en España [Internet]. Red Radiométrica Nacional, AEMET; 2012 [citado 1 de octubre de 2013]. Recuperado a partir de: <http://www.humboldt.edu/moved/account-moved.php?old=ccat&new=ccat>
18. Agencia Estatal de Meteorología - AEMET. Gobierno de España [Internet]. <http://www.aemet.es>. 2013 [citado 1 de octubre de 2013]. Recuperado a partir de: <http://www.aemet.es>
19. Government of Canada NRC. RETScreen International. [Internet]. <http://www.retscreen.net/>. 2013 [citado 24 de agosto de 2013]. Recuperado a partir de: <http://www.retscreen.net/>
20. Organización Meteorológica Mundial. <http://wwis.aemet.es/>. 2013.
21. Liu BYH, Jordan RC. The interrelationship and characteristic distribution of direct, diffuse and total solar radiation. *Sol Energy*. julio de 1960;4(3):1-19.
22. Page J. The estimation of monthly ea values of daily total short wave radiation on vertical and inclined surfaces from sunshine records for latitudes 40°N–40°S. *Proc UN Conf New Sources Energy*. 1961;4(598):378-90.
23. Luque A, Hegedus S. Handbook of Photovoltaic Science and Engineering. 2.a ed. United Kingdom: Wiley; 2011. 1166 p.
24. Spencer JW. Fourier series representation of the position of the sun. *Search*. 1971;2(5):172.
25. Collares-Pereira M, Rabl A. The average distribution of solar radiation-correlations between diffuse and hemispherical and between daily and hourly insolation values. *Sol Energy*. 1979;22(2):155-64.
26. Haberlin H. Photovoltaics: System Design and Practice. United Kingdom: John Wiley & Sons; 2012. 957 p.
27. Hay JE. Study of Shortwave Radiation on Non-horizontal Surfaces. *Atmospheric Environ Serv*. 1979;Report No 79-12.
28. Denegri MJ, Raaijijk C, Gallegos HG. Evaluación de diferentes modelos utilizados para la estimación de la radiación fotosintéticamente activa en planos inclinados. *Av En Energ Renov Medio Ambiente*. 2012;16:9-15.
29. Noorian AM, Moradi I, Kamali GA. Evaluation of 12 models to estimate hourly diffuse irradiation on inclined surfaces. *Renew Energy*. junio de 2008;33(6):1406-12.

30. Diez-Mediavilla M, de Miguel A, Bilbao J. Measurement and comparison of diffuse solar irradiance models on inclined surfaces in Valladolid (Spain). *Energy Convers Manag.* agosto de 2005;46(13–14):2075-92.
31. Souza AP de, Escobedo JF. Estimates of hourly diffuse radiation on tilted surfaces in Southeast of Brazil. *Int J Renew Energy Res IJER.* 19 de marzo de 2013;3(1):207-21.
32. Preu, R. PV-module reflection losses: Measurement, simulation and influence on energy yield and performance ratio. Thirteenth European Photovoltaic Solar Energy Conference 1995 Proceedings Vol2. 1995. p. 1465-8.
33. Krauter S, Grunow P. Optical Modelling and Simulation of PV Module Encapsulation to Improve Structure and Material Properties for Maximum Energy Yield. Conference Record of the 2006 IEEE 4th World Conference on Photovoltaic Energy Conversion. 2006. p. 2133-7.
34. Engineers AS of H, Refrigerating and Air-Conditioning. ASHRAE Standard Methods of Testing to Determine the Thermal Performance of Solar Collectors. ASHRAE; 1978. 56 p.
35. Martin N, Ruiz JM. Calculation of the PV modules angular losses under field conditions by means of an analytical model. *Sol Energy Mater Sol Cells.* 1 de diciembre de 2001;70(1):25-38.
36. Zang J, Wang Y. Analysis of Computation Model of Particle Deposition on Transmittance for Photovoltaic Panels. *Energy Procedia.* 2011;12:554-9.
37. Caamaño Martín E. Edificios fotovoltaicos conectados a la red eléctrica: caracterización y análisis [Internet] [phd]. E.T.S.I. Telecomunicación (UPM); 1998 [citado 24 de noviembre de 2013]. Recuperado a partir de: <http://oa.upm.es/1322/>
38. Jantsch M, Schmidt H, Schmid. Results on the concerted action on power conditioning and control. 11th European photovoltaic Solar Energy Conference. Montreux; 1992. p. 1589-92.
39. Almonacid F, Rus C, Pérez-Higueras P, Hontoria L. Calculation of the energy provided by a PV generator. Comparative study: Conventional methods vs. artificial neural networks. *Energy.* enero de 2011;36(1):375-84.
40. Baltus CWA, Eikelboom JA, Zolingen RJC. Analytical Monitoring of Losses in PV Systems. 14th European Photovoltaic Solar Energy Conference. Barcelona; 1997.
41. Sugiura T, Yamada T, Nakamura H, Umeya M, Alonso-Abella M, Chenlo F. A model for energy production estimation of PV grid connected systems based on energetic losses and experimental data on site diagnosis. 19th European Photovoltaic Solar Energy Conference. Paris; 2004. p. 2447-50.
43. INSTITUTO GEOGRÁFICO AGUSTÍN CODAZZI - IGAC. [http://www.igac.gov.co/igac.](http://www.igac.gov.co/igac) 2013.
44. Ayompe LM, Duffy A, McCormack SJ, Conlon M. Measured performance of a 1.72 kW rooftop grid connected photovoltaic system in Ireland. *Energy Convers Manag.* febrero de 2011;52(2):816-25.
45. Reinders AHME, Pramusito, Sudradjat A, van Dijk VAP, Mulyadi R, Turkenburg WC. Sukatani revisited: on the performance of nine-year-old solar home systems and street lighting systems in Indonesia. *Renew Sustain Energy Rev.* marzo de 1999;3(1):1-47.



8^a VERSIÓN
PREMIO **GRUPO**
ENERGÍA DE BOGOTÁ
FABIO CHAPARRO

Fundación Grupo Energía de Bogotá, certifica
la participación de Luis Fernando Mulcué
en la categoría de Maestría, con el artículo resumen:

Desarrollo de herramientas para el dimensionamiento y simulación de
sistemas fotovoltaicos en Colombia

en la octava versión del Premio Grupo Energía de Bogotá -
Fabio Chaparro.

Se firma en Bogotá D.C. en el mes de noviembre de 2014.



NATALIA GARCÍA DE CASTRO
DIRECTORA/ FUNDACIÓN
GRUPO ENERGÍA DE BOGOTÁ



GRUPO ENERGÍA
DE BOGOTÁ



FUNDACIÓN
GRUPO ENERGÍA DE BOGOTÁ

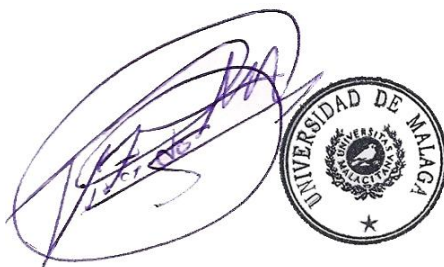
ENERGÍA PARA EL
DESARROLLO
ENERGÍA PARA
LA VIDA



El Vicerrector de Proyectos Estratégicos INFORMA:

Una vez finalizado el proceso de selección para participar como MENTEE/ASESORADO DE LA UNIVERSIDAD DE MÁLAGA en el Programa Internacional de Asesoramiento (IMP) 2016-2017, puesto en marcha por la International Mentorship Foundation for the Advancement of Higher Education (IMFAHE) y en el que participa la Universidad de Málaga, la solicitud realizado por Luis Fernando Mulcue Nieto ha sido SELECCIONADA.

Malaga, 11 de Noviembre de 2016



The image shows a purple ink signature of 'Víctor Fernando Muñoz Martínez' to the left of the university's official circular seal. The seal is black and white, featuring the text 'UNIVERSIDAD DE MÁLAGA' around the perimeter and a central emblem with a figure and a star at the bottom.

Víctor Fernando Muñoz Martínez

Vicerrector de Proyectos Estratégicos

Referencias

- [1] J. Kanters y M. Horvat, «Solar Energy as a Design Parameter in Urban Planning», *Energy Procedia*, vol. 30, pp. 1143-1152, 2012, doi: 10.1016/j.egypro.2012.11.127.
- [2] C. R. Osterwald, «Translation of device performance measurements to reference conditions», *Sol. Cells*, vol. 18, n.º 3-4, pp. 269-279, sep. 1986, doi: 10.1016/0379-6787(86)90126-2.
- [3] G. L. Araujo, E. Sánchez, y M. Martí, «Determination of the two-exponential solar cell equation parameters from empirical data», *Sol. Cells*, vol. 5, n.º 2, pp. 199-204, ene. 1982, doi: 10.1016/0379-6787(82)90027-8.
- [4] M. A. Green, *Solar Cells: Operating Principles, Technology and System Applications*. University of New South Wales, 1998.
- [5] F. Almonacid, C. Rus, P. J. Pérez, y L. Hontoria, «Estimation of the energy of a PV generator using artificial neural network», *Renew. Energy*, vol. 34, n.º 12, pp. 2743-2750, dic. 2009, doi: 10.1016/j.renene.2009.05.020.
- [6] P. Rodrigo, C. Rus, F. Almonacid, P. J. Pérez-Higueras, y G. Almonacid, «A new method for estimating angular, spectral and low irradiance losses in photovoltaic systems using an artificial neural network model in combination with the Osterwald model», *Sol. Energy Mater. Sol. Cells*, vol. 96, pp. 186-194, ene. 2012, doi: 10.1016/j.solmat.2011.09.054.
- [7] T. Markvart y L. Castaner, *Practical Handbook of Photovoltaics: Fundamentals and Applications*. Elsevier, 2003.
- [8] J. D. Mondol, Y. Yohanis, M. Smyth, y B. Norton, «Long term performance analysis of a grid connected photovoltaic system in Northern Ireland», *Energy Convers. Manag.*, vol. 47, n.º 18-19, pp. 2925-2947, nov. 2006, doi: 10.1016/j.enconman.2006.03.026.
- [9] Senado de la República de Colombia, *Ley 855 de 2003. Definición de Zonas No Interconectadas al SIN*. 2003.
- [10] B. Y. H. Liu y R. C. Jordan, «The interrelationship and characteristic distribution of direct, diffuse and total solar radiation», *Sol. Energy*, vol. 4, n.º 3, pp. 1-19, jul. 1960, doi: 10.1016/0038-092X(60)90062-1.
- [11] J. Page, «The estimation of monthly ea values of daily total short wave radiation on vertical and inclined surfaces from sunshine records for latitudes 40°N–40°S», *Proc. UN Conf. New Sources Energy*, vol. 4, n.º 598, pp. 378-390, 1961.
- [12] M. Collares-Pereira y A. Rabl, «The average distribution of solar radiation-correlations between diffuse and hemispherical and between daily and hourly insolation values», *Sol. Energy*, vol. 22, n.º 2, pp. 155-164, 1979, doi: 10.1016/0038-092X(79)90100-2.
- [13] H. Haberlin, *Photovoltaics: System Design and Practice*. United Kingdom: John Wiley & Sons, 2012.
- [14] M. J. Denegri, C. Raaijijk, y H. G. Gallegos, «Evaluación de diferentes modelos utilizados para la estimación de la radiación fotosintéticamente activa en planos inclinados», *Av. En Energ. Renov. Medio Ambiente*, vol. 16, pp. 9-15, 2012.
- [15] A. M. Noorian, I. Moradi, y G. A. Kamali, «Evaluation of 12 models to estimate hourly diffuse irradiation on inclined surfaces», *Renew. Energy*, vol. 33, n.º 6, pp. 1406-1412, jun.

- 2008, doi: 10.1016/j.renene.2007.06.027.
- [16] M. Diez-Mediavilla, A. de Miguel, y J. Bilbao, «Measurement and comparison of diffuse solar irradiance models on inclined surfaces in Valladolid (Spain)», *Energy Convers. Manag.*, vol. 46, n.º 13–14, pp. 2075-2092, ago. 2005, doi: 10.1016/j.enconman.2004.10.023.
- [17] A. P. de Souza y J. F. Escobedo, «Estimates of hourly diffuse radiation on tilted surfaces in Southeast of Brazil», *Int. J. Renew. Energy Res. IJRRER*, vol. 3, n.º 1, pp. 207-221, mar. 2013, Accedido: ago. 23, 2013. [En línea].
- [18] N. Martin y J. M. Ruiz, «Calculation of the PV modules angular losses under field conditions by means of an analytical model», *Sol. Energy Mater. Sol. Cells*, vol. 70, n.º 1, pp. 25-38, dic. 2001, doi: 10.1016/S0927-0248(00)00408-6.
- [19] M. Jantsch, H. Schmidt, y Schmid, «Results on the concerted action on power conditioning and control», en *11th European photovoltaic Solar Energy Conference*, Montreux, 1992, pp. 1589-1592.
- [20] F. Almonacid, C. Rus, P. Pérez-Higueras, y L. Hontoria, «Calculation of the energy provided by a PV generator. Comparative study: Conventional methods vs. artificial neural networks», *Energy*, vol. 36, n.º 1, pp. 375-384, ene. 2011, doi: 10.1016/j.energy.2010.10.028.
- [21] T. Sugiura, T. Yamada, H. Nakamura, M. Umeya, K. Sakuta, y K. Kurokawa, «Measurements, analyses and evaluation of residential PV systems by Japanese monitoring program», *Sol. Energy Mater. Sol. Cells*, vol. 75, n.º 3-4, pp. 767-779, feb. 2003, doi: 10.1016/S0927-0248(02)00132-0.
- [22] L. M. Ayompe, A. Duffy, S. J. McCormack, y M. Conlon, «Measured performance of a 1.72 kW rooftop grid connected photovoltaic system in Ireland», *Energy Convers. Manag.*, vol. 52, n.º 2, pp. 816-825, feb. 2011, doi: 10.1016/j.enconman.2010.08.007.
- [23] A. H. M. E. Reinders, Pramusito, A. Sudradjat, V. A. P. van Dijk, R. Mulyadi, y W. C. Turkenburg, «Sukatani revisited: on the performance of nine-year-old solar home systems and street lighting systems in Indonesia», *Renew. Sustain. Energy Rev.*, vol. 3, n.º 1, pp. 1-47, mar. 1999, doi: 10.1016/S1364-0321(99)00004-0.
- [24] The International Electrotechnical Commission (IEC), «IEC 61724 - 1998, Photovoltaic system performance monitoring - Guidelines for measurement, data exchange and analysis». Multiple. Distributed through American National Standards Institute, 1998.
- [25] Gobierno de España, «Código Técnico de la Edificación – HE5 Ahorro de Energía – Contribución Fotovoltaica Mínima de Energía Eléctrica». 2009.
- [26] N. R. C. Government of Canada, «RETScreen International.», <http://www.retscreen.net/>, ago. 24, 2013. <http://www.retscreen.net/> (accedido ago. 24, 2013).
- [27] J. M. Sancho Ávila, J. Riesco Martín, C. Jiménez Alonso, M. C. Sánchez de Cos Escuin, J. Montero Cadalso, y M. López Bartolomé, «Atlas de Radiación Solar en España», Red Radiométrica Nacional, AEMET, 2012. Accedido: oct. 01, 2013. [En línea]. Disponible en: <http://www.humboldt.edu/moved/account-moved.php?old=ccat&new=ccat>.
- [28] «Agencia Estatal de Meteorología - AEMET. Gobierno de España», <http://www.aemet.es>, 2013. <http://www.aemet.es> (accedido oct. 01, 2013).
- [29] Instituto para la Diversificación y Ahorro de la Energía de España, «Pliego de Condiciones Técnicas de Instalaciones Aisladas de Red (Instalaciones de Energía Solar Fotovoltaica)». 2009, Accedido: ago. 20, 2013. [En línea]. Disponible en: <http://www.idae.es/>.
- [30] R. Thomas, *Photovoltaics and Architecture*. London: Taylor & Francis, 2012.
- [31] D. G. für Sonnenenergie, *Planning and Installing Photovoltaic Systems: A Guide for Installers, Architects and Engineers*. London: Earthscan, 2008.
- [32] S. Roberts y N. Guariento, *Building Integrated Photovoltaics: A Handbook*. Switzerland: Springer, 2009.
- [33] D. K. Prasad y D. M. Snow, *Designing with Solar Power: A Source Book for Building*

- Integrated Photovoltaics (BiPV).* Australia: Images Publishing, 2005.
- [34] P. E. G. J. Kiss, *Building-Integrated Photovoltaic Designs for Commercial and Institutional Structures: A Sourcebook for Architects*. DIANE Publishing.
- [35] J. Cronemberger, E. Caamaño-Martín, y S. V. Sánchez, «Assessing the solar irradiation potential for solar photovoltaic applications in buildings at low latitudes – Making the case for Brazil», *Energy Build.*, vol. 55, pp. 264-272, dic. 2012, doi: 10.1016/j.enbuild.2012.08.044.
- [36] «PVWatts Calculator». <http://pvwatts.nrel.gov/> (accedido jun. 19, 2017).
- [37] «Findeter». pruebas-findeter.nexura.com/ (accedido jun. 03, 2020).
- [38] J. M. Pearce, «Photovoltaics — a path to sustainable futures», *Futures*, vol. 34, n.º 7, pp. 663-674, sep. 2002, doi: 10.1016/S0016-3287(02)00008-3.
- [39] «About the PVSites project». <https://www.pvsites.eu/project/> (accedido jun. 03, 2020).
- [40] «BIPV Markets Analysis and Forecasts 2014-2021». <https://www.reportlinker.com/p02115227/BIPV-Markets-Analysis-and-Forecasts.html> (accedido jun. 03, 2020).
- [41] John. E. Hay, «Study of Shortwave Radiation on Non-horizontal Surfaces», *Atmospheric Environ. Serv.*, vol. Report No 79-12, 1979.
- [42] D. R. Myers, *Solar Radiation: Practical Modeling for Renewable Energy Applications*. pg 58. CRC Press, 2016.
- [43] J. Zang y Y. Wang, «Analysis of Computation Model of Particle Deposition on Transmittance for Photovoltaic Panels», *Energy Procedia*, vol. 12, pp. 554-559, 2011, doi: 10.1016/j.egypro.2011.10.075.
- [44] A. Luque y S. Hegedus, Eds., *Capítulo 20: Energy Collected and Delivered by PV Modules en Handbook of Photovoltaic Science and Engineering.*, 1 edition. Hoboken, NJ: Wiley, 2003.
- [45] A. Luque y S. Hegedus, *Handbook of Photovoltaic Science and Engineering*, 2.ª ed. United Kingdom: Wiley, 2011.
- [46] C. W. A. Baltus, J. A. Eikelboom, y R. J. C. V. Zolingen, «Analytical Monitoring of Losses in PV Systems», en *14th European Photovoltaic Solar Energy Conference*, Barcelona, 1997.
- [47] S. Wittkopf, S. Valliappan, L. Liu, K. S. Ang, y S. C. J. Cheng, «Analytical performance monitoring of a 142.5 kWp grid-connected rooftop BIPV system in Singapore», *Renew. Energy*, vol. 47, pp. 9-20, nov. 2012, doi: 10.1016/j.renene.2012.03.034.
- [48] H. T. Nguyen y J. M. Pearce, «Incorporating shading losses in solar photovoltaic potential assessment at the municipal scale», *Sol. Energy*, vol. 86, n.º 5, pp. 1245-1260, may 2012, doi: 10.1016/j.solener.2012.01.017.
- [49] C. Zomer y R. Rüther, «Simplified method for shading-loss analysis in BIPV systems – part 1: Theoretical study», *Energy Build.*, vol. 141, pp. 69-82, abr. 2017, doi: 10.1016/j.enbuild.2017.02.042.
- [50] A. P. Dobos, «PVWatts Version 5 Manual», National Renewable Energy Lab. (NREL), Golden, CO (United States), NREL/TP-6A20-62641, sep. 2014. doi: 10.2172/1158421.
- [51] E. Caamaño Martín, «Edificios fotovoltaicos conectados a la red eléctrica: caracterización y análisis», phd, E.T.S.I. Telecomunicación (UPM), 1998.
- [52] G. TamizhMani, «Solar ABCs Policy Recommendation: Module Power Rating Requirements». 2011.
- [53] M. Alonso-Abella y F. Chenlo, «A model for energy production estimation of PV grid connected systems based on energetic losses and experimental data on site diagnosis», en *19th European Photovoltaic Solar Energy Conference*, Paris, jun. 2004, pp. 2447-2450.
- [54] J. Leloux, L. Narvarte, y D. Trebosc, «Review of the performance of residential PV systems in France», *Renew. Sustain. Energy Rev.*, vol. 16, n.º 2, pp. 1369-1376, feb. 2012, doi: 10.1016/j.rser.2011.10.018.
- [55] Y. Muñoz, D. Zafra, V. Acevedo, y A. Ospino, «Analysis of energy production with

different photovoltaic technologies in the Colombian geography», *IOP Conf. Ser. Mater. Sci. Eng.*, vol. 59, p. 012012, jun. 2014, doi: 10.1088/1757-899X/59/1/012012.